CERFACS **Scientific Activity Report**

Jan. 2002 – Dec. 2003

Centre Européen de Recherche et de Formation Avancée en Calcul Scientifique

European Center for Research and Advanced Training in Scientific Computing

CERFACS
Scientific Activity Report
Jan. 2002 – Dec. 2003

CERFACS
42, Avenue Gaspard Coriolis, 31057 Toulouse Cedex 1, FRANCE.
Tel. : 33 (0) 561 19 31 31 – Fax : 33 (0) 561 19 30 30
secretar@cerfacs.fr – http://www.cerfacs.fr

Contents

1 Foreword x

2 CERFACS Structure xiv

3 CERFACS Staff xvi

4 CERFACS Wide-Interest Seminars xxii

1 Parallel Algorithms Project 1

1 Introduction (I. S. Duff) 3

2 Dense and Sparse Matrix Computations 7

3 Iterative Methods and Preconditioning 12

4 Qualitative Computing 22

5 Nonlinear Systems and Optimization 27

6 Signal and Image Processing 31

7 Publications 33

2 Computational Fluid Dynamics 37

1 Introduction 39

2 Combustion 41

3 Aerodynamics 65

4 Environmental impact of aviation 81

5 Publications 83

3 Computational Electromagnetism 89

1 Overview Presentation 91

2 Boundary Integral Equations Methods 93

3 Fast Multipole Method in electromagnetic calculations 96

4 Domain decomposition Methods 99

5 Publications 103

4 Climate Modelling and Global Change 105

1 Introduction 107

2 Climate variability and predictability 108

3 Oceanic data assimilation for climate studies and seasonal prediction 115

4 OASIS and PALM couplers and applications 123

5 SMOS Mission 129

6 CERFACS contribution to the MERCATOR project 133

7 Publications 147

5 ENScube Group 153

1 Introduction 155

2 Numerical simulation projects 156

3 Virtual reality projects 159

4 Development of collaborative working solutions 161

6 Computer Support Group 163

1 Introduction 165

2 Architecture and Actions. 166

Appendix : Color illustrations 169

List of Figures

Mensual external hits on CERFACS' Web server during the period 1999-2003 xiv
External hits by domain on CERFACS' Web server during the year 2002 xiv
External hits by domain on CERFACS' Web server during the year 2003 xiv

CERFACS chart as of Dec. 31, 2003 xv

1 Parallel Algorithms Project **1**

6.1 Example of interferometric and GPS graphs (left and right, respectively). The vertices of the first one are the pupil elements of aperture synthesis device (here, 6 telescopes or 6 antennas). The lacking edges correspond, for example, to the baselines for which the modulus of the Fourier transform of the object is in the noise. The vertices of the second are the receivers and the satellites of the GPS device (here 2 receivers and 4 satellites). The signals emitted by a satellite are received by each receiver, hence the lacking edges. The edges shown as thicklines correspond to a spanning tree which can be selected in an arbitrary manner. The edges that do not lie to this tree are referred to are cycle entry edges. Here, their number, n, is equal to 7 for the interferometric graph and to 3 for the GPS graph. 31
6.2 Nearest lattice point problem. In the special case shown here, where n is equal to 2, the lattice is generated by the vectors e_1 and e_2 which are parameters of the problem. Given some point $\widehat{\alpha}$ of $\mathbb{R}^2$, endowed here with the Euclidean inner product, the problem is to find the lattice point α closest to $\widehat{\alpha}$. One then speaks of "integer ambiguity resolution." In most cases encountered in pratice, n is less than or of the order of 100. 32

2 Computational Fluid Dynamics **37**

2.1 Configuration of the flame interaction with a liquid film. 42
2.2 Normalized flame / wall distance (triangle), consumption speed (dashed line) and wall heat flux (solid line) during the flame interaction with a liquid film. 42
2.3 Density field of an underexpanded jet (pressure ratio 7). The inserted picture is the result from Rayleigh Scattering on the same jet obtained by B. Yip et al. 43
2.4 Comparison between initial and converged profiles of species mass fractions. 44
2.5 Two-phase Direct Numerical Simulation of Homogeneous and Isotropic Turbulence: number density field. Left: lagrangian approach; Right: eulerian approach. 46
2.6 Computation of the M88 geometry with evaporating droplets: droplet trajectories.The initial size is 20 μm. 47
2.7 Computation of the M88 geometry with evaporating droplets: equivalence ratio. The initial size is 20 μm. 47
2.8 Computation of the VESTA geometry with a droplet size of 100 μm (left column) and 1 μm (right column).(a): liquid velocity field;(b): number density field;(c):Quasi-Brownian energy field. 48

2.9 Configuration (left). Location of cuts for velocity profiles (right). . . . 51
2.10 Vector and pressure field in central plane (left) and isosurface of low pressure (right). . . . 52
2.11 Cold flow: average axial velocity profiles. Circles: LDV; solid line: LES. . . . 53
2.12 Cold flow; RMS axial velocity profiles. Circles: LDV; solid line: LES. . . . 53
2.13 Reacting flow; mean axial velocity in the central plane. Circles: LDV; solid line: LES. . . 54
2.14 Reacting flow; RMS axial velocity in the central plane. Circles: LDV; solid line: LES. . . 54
2.15 Chamber A: burner (left) and set up for system identification (right). . . . 55
2.16 Chamber A: isosurface of fuel mass fraction and reaction rate in three planes. . . . 55
2.17 Chamber B: burner (left) and combustion chamber (right). . . . 56
2.18 Combustor B: flame shapes (isocontours of temperature T=1000 K) at two instants of the forcing cycle separated by a half period. . . . 56
2.19 Combustor C. Left: geometry: the whole shaded area is meshed and computed. Right: isosurfaces of $Y_{CH4} = 0.1$ and isosurface of temperature $T = 1000$ K. . . . 57
2.20 Acoustic pressure for the 1200 Hz mode. Left: Helmholtz result. Right: LES result. . . . 58
2.21 Isosurfaces of temperature $T = 1000$ K at two instants of the 1200 Hz cycle separated by a half period. The turning mode shapes the flame along a spiral motion. . . . 58
2.22 Left: geometry of the burner (Ecole Centrale Paris). Center: experimental view for stable regime. Right: flashback. . . . 59
2.23 Left: stable lifted flame. Right: flame after flashback. The flame is visualized by an isosurface of reaction rate. . . . 60
2.24 Three-burner combustion chamber of DLR. Left: isosurface of temperature T=1000 K. Right: field of reaction rate in a surface passing through the axis of the three burners. . . . 61
2.25 LES of combustion including CO formation. Left: configuration. Right: CO instantaneous fields in various cuts in the burner. . . . 61
2.26 Isosurfaces of axial vorticity tracing the dilution air jets injected in the main duct. . . . 63

3.1 Isosurfaces of vorticity magnitude showing the global dynamics for the simulation with $\epsilon = 10^{-6}$ for time instants $t/t_{ref} = 10.14$ & 13.46 with $t_{ref} = b_1^2/\Gamma_1$. . . . 66
3.2 Meshes with non coincident interface boundary conditions for a RAE 2822 configuration (left) and mach number isolines (right). . . . 69
3.3 Meshes with non coincident interface boundary conditions for a nozzle configuration (left) and mach number isolines (right). . . . 69
3.4 Two sliding O-meshes of a pitching NACA0012 airfoil (left) and the lift coefficient versus the angle of attack (right). . . . 70
3.5 Sliding meshes of an axisymmetric four-block configuration for a laminar Taylor-Couette flow (left) and time-independent Taylor vortices (right). . . . 71
3.6 AS28 wing, level 2, mesh and mach number contours. . . . 72
3.7 Hierarchy of 3 grids for a RAE 2822 configuration (left) and mach number contours (right). 72
3.8 AS28G aerodynamic coefficients convergence . . . 73
3.9 RAE2822 test-case : iso-Mach number field (left) and pressure coefficient (right) . . . 74
3.10 Error estimation : isosurfaces corresponding to 80% of the maximum error . . . 75
3.11 Automatic polar : RAE Profile . . . 75
3.12 Comparison of the first harmonic of C_p given by elsA unsteady simulation and experimental data . . . 76
3.13 Mach number iso-contours for the MARCO nozzle configuration . . . 77
3.14 Speedup of LussorSca5 on 4 processors of the Compaq Alpha. . . . 79
3.15 CPU time of the function LussorSca before and after optimisation. . . . 79

4.1 Steps involved in the formation and the transformation of gases and particles emitted by the kerosene combustion. . . . 81

4.2 Iso-surface of the vorticity magnitude during the jet/vortex interaction: (a) case 1; (b) case 2. 82

3 Computational Electromagnetism 89

2.1 Impedance curve versus the frequency from measurements, code CESC and code SAPHIR 94
2.2 Size reduction by exploiting symmetries 95

3.1 Configuration antenna–satellite 98

4.1 Decomposition of the cavity 100
4.2 Domain decomposition of the cavity 100
4.3 Coupling a BE and and asymptotic technique 101

4 Climate Modelling and Global Change 105

2.1 **(abcd)** 1949-2001 Winter Sea Level Pressure regimes $[hPa]$ over the North Atlantic sector from NCEP Reanalysis. Shaded areas exceed the 95% confidence level. Contour interval is every $1hPa$. **(ef)** Time history of the occurrence of the NAO and Ridge/GS regimes . The vertical bars indicate the number of months relative to each winter where the given regime is present. Solid line stands for the standardized expansion coefficient of the leading DJF SLP EOF. The dashed line is the NAO index based on Hurrell dataset. 114

3.1 Depth section at the equator of the background error covariance between SSH and temperature (upper left panel), SSH and salinity (upper right panel), and SSH and the zonal component of velocity (lower left panel). 117
3.2 Left panel: vertical profiles of the background-error standard deviations (in $^\circ$C) used in 3D-Var and 4D-Var at the equator at 140°W. The dashed-dotted curve corresponds to the standard deviations specified at the beginning of the assimilation window. In 3D-Var, these are also the effective standard deviations used at all future times within the window. The solid curve corresponds to the effective standard deviations used implicitly in 4D-Var at the end of the 30-day window in a particular cycle of 4D-Var. Right panel: the corresponding profile of the background $|\partial T/\partial z|$ at this location. The values of $|\partial T/\partial z|$ have been multiplied by a factor of ten in order to be plotted with the same horizontal scale as in panel a. 118
3.3 a) Observed climatology. Climatologies from assimilation experiments with the tropical Pacific model using existing and improved formulations of the background error covariances: b) 4D-Var with univariate, flow-independent covariances; c) 3D-Var with univariate, flow-independent covariances; d) 3D-Var with multivariate, flow-dependent covariances. The contour interval is $0.1\mathrm{ms}^{-1}$, and the shaded blue (yellow) regions indicate westward (eastward) currents. 119
3.4 Depth section at the equator of the 1993-99 mean salinity state in the global OPA model (ORCA2) produced from 3D-Var assimilation of *in situ* temperature data. Left panel: 3D-Var with univariate, flow-independent covariances; Right panel: 3D-Var with multivariate, flow-dependent covariances. 120

4.1 The 3D-FGAT method as seen through the PrePALM_MP interface 126

4.2 Total ozone field on March 2nd, 2000, 0 UT : (a) simulated by MOCAGE, without assimilation ; (b) simulated by MOCAGE with assimilation of March 1st, 2000, GOME ozone profiles. (c) Total ozone column relative differences (in %) between the MOCAGE run with assimilation and without assimilation of the GOME ozone profiles. The differences are produced after one day of assimilation, for March 2nd , 2000, at 0 UT. (d) Total ozone column measured by TOMS at local noon on March 1st, 2000. TOMS observations are not assimilated but used as a rough validation of the assimilating algorithm. 127

5.1 Variations of $\|V - \mathbf{G}T_r\|_F$ with $\|T_r\|_E$ for the Tikhonov solution (5.5) with 131

6.1 Schematic representation of the software platform SAM1/SAM2. SAM1 units (1D background error) and SAM2 (3D background error) are respectively shown in dark green and light green. Common units SAM1/SAM2 are bi-color. Two kinds of algorithm (OI or SEEK) are available depending on the activation of units 135

6.2 Barotropic stream function increment (m) from a multivariate SAM-2-v0 analysis 136

6.3 Pacific equatorial undercurrent : in the left panel, the yearly mean of the zonal velocity field at the equator in POG-04 experiment, in the right panel, the zonal velocity field issued from hydrological data CTD/ADCP data, (Johnson et al, Oct. 2001). 143

6.4 Eddy Kinetic Energy computed over the third year of the POG-04 experiment. 143

5 ENScube Group 153

2.1 Multisite collaborative review between N'S^3 group and its industrial partners thanks to the N'S3 solution 157

6 Computer Support Group 163

2.1 CERFACS' computing resources 166

2.2 Performance ration between Alpha 1 Ghz and Itanium Processor 167

Appendix : Color illustrations 169

iii Convergence behaviour of GMRES and SQMR with various fast multipole calcultations. . 171

iv Reconstruction of an airplane 171

v Shape deformation of a structural mode 172

vi A340 MSR1 configuration. 172

vii CERFACS prediction of the Niño3 temperature anomaly peak of late 1997 (in red) along with other models results. 173

viii Seasonal prediction one month in advance of Niño3 and season-averaged indices of surface temperature, as produced by the CERFACS system. 173

ix **(a)** Changes in regime residence frequency (in %) between the present climate and the four time-slice scenarios of the late 21st century as simulated by the variable resolution ARPEGE AGCM. **(b)** Changes in regime residence frequency (in %) between the control integration (GHG fixed at their 1950 values), the present and future climate (given by the 1950-2000 and 2060-2099 periods of the two transient scenarios, respectively) as simulated by the ARPEGE-OPA CGCM. The black arrows indicate the range of uncertainty due to internal atmospheric variability as given by one standard deviation of the within-ensemble variability. 174

x Ranked Probability Skill Scores of winter temperature predictions over Europe one month in advance; CERFACS is in black. 175
xi Path and concentration of lagrangian particles released through the air supply 175
xii Flow simulation around a hypersonic missile - Mach number field 176
xiii 3D visualization of CFD results in the N'S^3 group Reality Centre 176
xiv Visit of the Airbus STAR virtual mock-up 176

Foreword

Welcome to this two-year issue of the CERFACS Scientific Activity Report.

What have been the major scientific achievements of these past two years? Reading through the report will hopefully provide the reader with very many answers to this question, but let me just select a few results for each team as an appetizer:

Parallel Algorithms
Many tools were successfully developed by the team:

- an algorithm for parallel distributed dense symmetric direct solvers, which requires only half of the memory required by more standard ScalaPack routines, has been proposed and integrated in the electromagnetic solver code;
- the best-student-paper prize was awarded to Julien Langou at the Copper Mountain 2002 meeting, for his work on the Gram-Schmidt algorithm. This has an application both to iterative linear solvers and eigenvalue solvers;
- the GMRES public domain package was downloaded for the 1000th time in 2003, showing the great worldwide interest in such a tool.

As a way to better disseminate these and other results, as well as keeping on working on new issues, the sparse days and grid-computing workshop was organized in Saint-Girons during June 2003, attracting 80 participants, mainly from Europe and USA, including representatives from all the CERFACS' shareholders. In the field of signal processing it has been shown that phase-closure imaging and differential GPS do share a common mathematical structure, opening new ways for improving GPS.

Computational Fluid Dynamics
While all the earlier NSMB functionalities were being transferred to elsA, this latter code, developed cooperatively with ONERA, was intensively tuned during the second part of 2002, providing a factor of 3 gain in computer efficiency. As a result, elsA was chosen by Airbus as their structured code for all their national establishments.
Coupling techniques, originating in the so-called PALM software developed at CERFACS for data-assimilation, were successfully applied to study flutter phenomena.
Wake vortices studies reached a mature phase, so that they can now be applied to study the physico-chemical behaviour of pollutants in aircraft wakes, allowing new projects to start in the field of environmental impacts.
Very significant progress has been made in the development of simulation methods for turbulent combustion. Let us just mention a few ”world-premières” in this field:

- a 2.5 10^6 dof[1] calculation of combustion within a complete industrial burner was performed during the 2002 Stanford Summer Program;

[1] Degrees of freedom

- a 5 10^6 dof calculation of a 3-burner combustion chamber using the LES[2] technique was performed during 2003, requiring the efficient use of 128 processors.

Other developments deal with the first LES calculation of 2-phase flow combustion for real industrial geometries, and with the remote visualization of very large fields (5 to 10 million dof) computed remotely at CINES in Montpellier.
As a result, the AVBP code is now recognized as the main French code for unsteady combustion and is deployed by many national and international groups, as well as in industrial laboratories.

Computational Electromagnetism
Spectral preconditioners developed by the "Parallel algorithms" group were used in boundary-element solvers for Maxwell's equations, allowing the solution of problems which were otherwise out of reach, as, e.g., simulation of a complete aircraft.
Fast multipole techniques were applied to real-world problems, like the interaction between an antenna and the satellite, or the shape-reconstruction of objects from the knowledge only of their RCS[3]. Domain-decomposition methods were successfully used for simulating the effects of cavities, of interest for stealth technologies.

Climate Modelling and Global Change
Earlier studies, dealing with the relationships between the structure of the surface temperature field in the North-Atlantic ocean and the climate in Europe a few months later, have been further developed, allowing a method for predicting the winter North-Atlantic Oscillation (NAO) index with a 6-month time lead. The prototype system for seasonal-climate prediction was tested against a number of other systems within the framework of a European program: it showed very comparable good skills. Emphasis was also put on the data assimilation part of the system, with the aim of including either improved 3-dimensional or 4-dimensional versions of the so-called variational methods.
Data assimilation methods were also applied to other problems, like the modelling of the properties of aging structures, with very promising results. This opens new avenues for data assimilation.
The MERCATOR group successfully provided the fully-tested Atlantic ocean model at $1/15^{th}$ degree resolution, which is now used operationally every week (since January 8, 2003) for providing oceanic forecasting at this high resolution (the so-called PSY2 system). The development of a global, medium-resolution ($1/4^{th}$ degree) model was simultaneously started.
The development of the SMOS[4] simulator progressed significantly, with three methods being proposed for the regularization of the inverse problem.

Technology Transfer
The so-called N'S'[3] solutions, including the package for collaborative working, have been used for applications in a number of different industrial domains. They are now ready to be transferred to a new commercial company, to be created soon.

Computing resources
CERFACS' main computer has been upgraded to a 40-processor configuration, with a 80 Gflop/s peak. This system has been complemented by 2 cluster configurations (16 Gflop/s and 24 Gflop/s).

CERFACS scientific production is still high:

- the number of high-standard publications, i.e. in internationally-refereed journals, is 61, a number very close to the mean rate of 30 publications per year;

[2]Large Eddy Simulation
[3]Radar Cross Section
[4]SMOS, Soil Moisture and Ocean Salinity, an ESA satellite mission foreseen for launch in 2005

- CERFACS' researchers have produced yearly more than 100 technical reports, book chapters, papers in conference proceedings ;
- they are active in training new researchers, with 13 Ph. D. theses being awarded over the period, and with 1 ”Habilitations Diriger des Recherches” (HDR) over the same period.
- they have also very actively developed applied research, with a total of approximately 65 grants per year being held over the period, approximately 15-20 of them coming from the European Commission through its various programmes, and the rest, of the order of 40-50, being awarded by other funding agencies and/or industrial partners ;
- CERFACS web site is still experiencing rapid development, with the number of monthly hits by external visitors increasing from 200,000 in early 2002 to almost 350,000 towards the end of the period (see Fig.1), demonstrating CERFACS steadily-improving attraction. Another interesting feature can be seen in Fig.3, where the ”Climate” activities are those that are the most attractive to external visitors (this does not come as a surprise!), while the ”Parallel Algorithms” and the ”CFD” teams are those with the second-largest number of accesses;
- let us also finally mention that CERFACS wide-interest seminars have attracted high-level and well-known external scientists (see below).

At the end of 2003, the number of people working at CERFACS was 91.3 (full-time equivalent) scientists (see Tables ii to ix), with a global budget close to 6.1 M.

I sincerely hope that you will have some time to read through the detailed activity reports of the teams, and that you will find there enough interest to pursue your collaboration with us, or to initiate some new ones.

Enjoy your reading.

Jean-Claude ANDRÉ
CERFACS Director

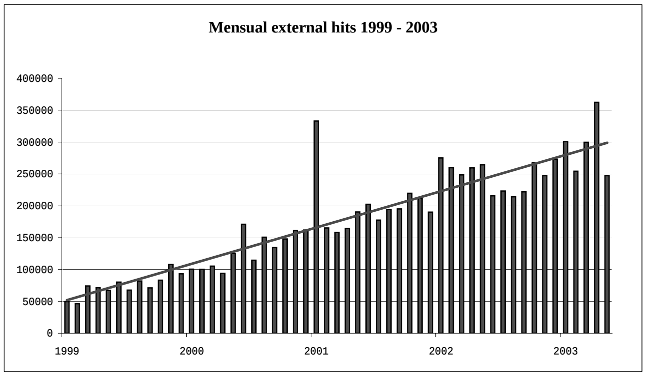

Figure 1: Mensual external hits on CERFACS' Web server during the period 1999-2003

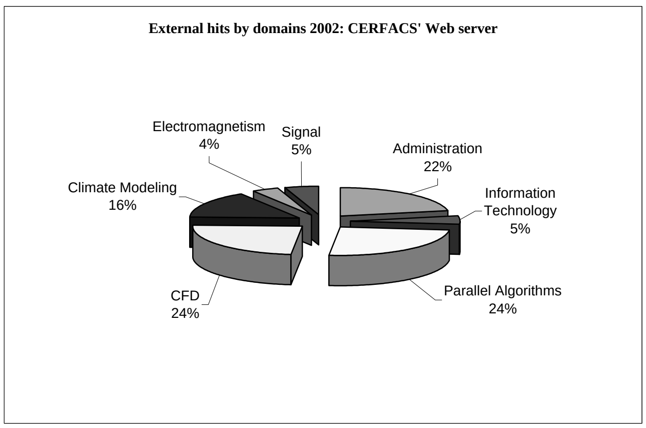

Figure 2: External hits by domain on CERFACS' Web server during the year 2002

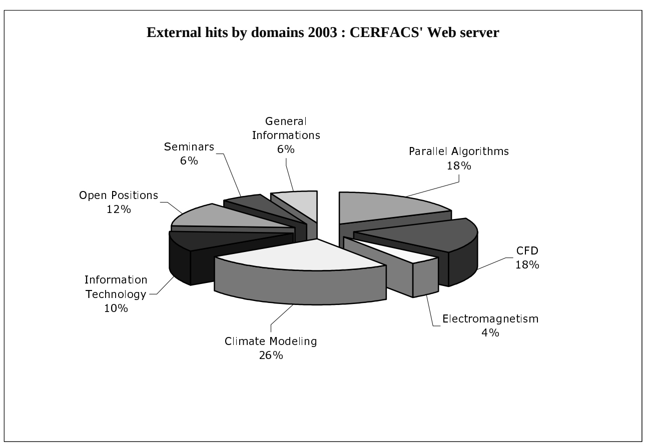

Figure 3: External hits by domain on CERFACS' Web server during the year 2003

CERFACS Structure

As a ”Société Civile” CERFACS is governed by two bodies. Firstly, the ”Conseil de Gérance”, composed of only 4 managers (in French, ”Gérants”) nominated by the 4 shareholders (see table i), follows quite closely the CERFACS activities and the financial aspects. It met 9 times during the period (25 January 2002, 3 April 2002, 26 June 2002, 11 September 2002, 20 December 2002, 2 April 2003, 9 July 2003, 5 September 2003 and 17 December 2003). Secondly the Board of Governors (in French ”Assemblée des Associés”), composed of representatives of CERFACS shareholders and of 3 invited personalities, including the Chairman of the Scientific Council. It met 4 times during the period (12 February 2002, 4 October 2002, 30 January 2003 and 25 September 2003).

CERFACS Scientific Council met for the sixth and seventh times, on 21 June 2002 and 16 June 2003, under the chairmanship of Prof. Jean-François MINSTER.

The general organization of CERFACS is depicted in the CERFACS chart, where the two support groups (Administration and Computing) are shown together with the other teams.

EUROPEAN AERONAUTIC DEFENCE AND SPACE COMPANY (EADS)	22 %
CENTRE NATIONAL D'ÉTUDES SPATIALES (CNES)	26 %
ÉLECTRICITÉ DE FRANCE	26 %
MÉTÉO-FRANCE	26 %

Table i: Table of Société Civile Shareholders.
(Note : On January 1st, 2004, SNECMA Group joined CERFACS as its fifth shareholder)

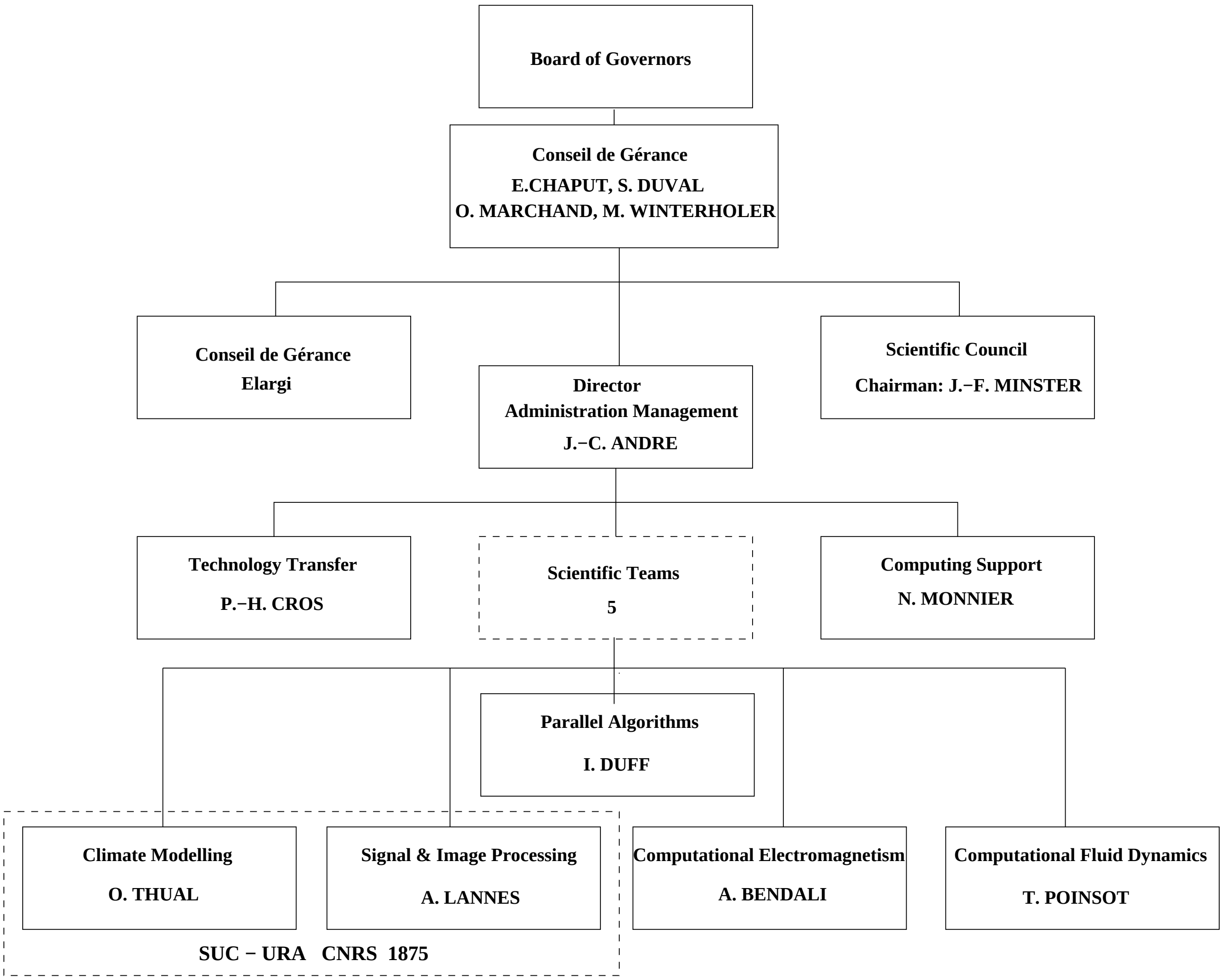

CERFACS chart as of Dec. 31, 2003

CERFACS Staff

The staff of the scientific teams and of the computing support group, consisting of, on December 31, 2003, a total of 102 scientists and technical staff (7 project and group leaders, 17 senior researchers, 10 post-doctoral fellows, 34 PhD students, 22 engineers and 2 technicians, 3 CNRS employees and 7 long-duration visitors of various origins) is shown in Tables ii to ix.

NAME	POSITION	PERIOD
DUFF	Project Leader	1988/11
CHATELIN	Group leader	1988/09
GIRAUD	Senior	1993/10
GRATTON	Senior	2002/07
VAN GIJZEN	Senior	2002/02
CARPENTIERI	Post Doc	2003/01
LOGHIN	Post Doc	2002/10
MESKAUSKAS	Post Doc	2000/03-2002/03
TRAVIESAS	Post Doc	2000/10-2002/06
BABOULIN	Ph.D student Student	2003/09 2003/02-2003/07
LANGOU	Ph.D student	1999/10-2003/09
MARTIN	Ph.D student	2001/10
RIOUAL	Ph.D student	1999/01-2002/04
SONGKLOD	Ph.D student	2002/07
VOEMEL	Ph.D student	1999/10-2003/09
PRALET	Ph.D student Student	2002/09 2002/02-2002/07
DELMAS	Student	2003/07-2003/10
DORE	Student	2002/06-2002/08
DURDOS	Student	2002/06-2002/09
HALUITTE	Student	2002/06-2002/08
LACOURT	Student	2003/02-2003/09
LEAL	Student	2002/06-2002/09
ORBAN	Engineer Ph.D student	2001/09-2002/01 1997/10-2001/09
AHMADNASAB	Visitor	2003/08

Table ii: List of members of the PARALLEL ALGORITHMS project.

NAME	POSITION	PERIOD
POINSOT	Project Leader	1992/09
CHEVALIER	Senior	1999/11
CUENOT	Senior	1996/10
DARRACQ	Senior	1999/04-2002/08
JOUHAUD	Senior	2001/10
MONTAGNAC	Senior	2000/11
BARTON	Post Doc	2002/09
CELIC	Post Doc	2003/09
DULOUE	Post Doc	2001/09-2003/08
ESCRIVA	Post Doc	2001/11-2003/08
GRONDIN	Post Doc	2000/03-2002/03
GUILHEM	Post Doc	2001/03-2002/09
HANSS	Post Doc	2003/04
KNIKKER	Post Doc	2002/03-2002/10
LAPORTE	Post Doc Ph.D student	2002/01-2002/08 1998/09-2001/12
MOET	Post Doc Ph.D student	2003/04 1999/12-2003/03
PUIGT	Post Doc	2001/10-2003/04
SAUDREAU	Post Doc	2002/04
VAROQUIE	Post Doc	2003/01
ARTAL	Ph.D student	2002/11
AUFFRAY	Ph.D student	2003/10
BENOIT	Ph.D student	2001/10
BOHBOT	Ph.D student	1998/09-2002/03
BOILEAU	Ph.D student Student	2003/10 2003/02-2003/08
DABIREAU	Ph.D student	1999/09-2002/12
DAUPTAIN	Ph.D student Student	2002/10 2002/02-2002/09
DELBOVE	Ph.D student	2001/10
DESOUTTER	Ph.D student Student	2003/10 2003/02-2003/09
DEVESA	Ph.D student	2003/10
GIAUQUE	Ph.D student Engineer	2003/09 2003/03-2003/08
KAUFMANN	Ph.D student	2000/09-2003/12
KOZUCH	Ph.D student	1998/09-2002/06
LARTIGUE	Ph.D student	2000/10-2003/12
MARTIN	Ph.D student Engineer	2002/05 2000/10-2002/04
MASSOL	Ph.D student	2000/10-2003/05
MOSSA	Ph.D student	2001/10
PASCAUD	Ph.D student Student	2002/10 2002/02-2002/08

Table iii: List of members of the COMPUTATIONAL FLUID DYNAMICS project (1/2).

PRIERE	Ph.D student	2001/10
RIBER	Ph.D student Student	2003/10 2003/02-2003/09
ROUX	Ph.D student Student	2003/10 2003/03-2003/09
SCHMITT	Ph.D student	2002/03
SELLE	Ph.D student	2000/09
SENGISSEN	Ph.D student Student	2002/10 2002/03-2002/08
SOULERES	Ph.D student	1999/10-2002/10
STAFFELBACH	Ph.D student Student	2002/10 2002/03-2002/09
THOBOIS	Ph.D student	2002/10
TOUSSAINT	Ph.D student Student	2002/10 2002/03-2002/08
TRUFFIN	Ph.D student	2001/09
BOUSSUGE	Research Engineer	2002/02
CHAMPAGNEUX	Research Engineer	1997/11
SOMMERER	Research Engineer Engineer	2002/04 2000/10-2002/03
DENEVE	Engineer	2003/03
FONTAINE	Engineer Student	2002/10-2003/05 2002/04-2002/08
GICQUEL	Engineer Post Doc	2003/04 2001/05-2003/01
MARGERIT	Engineer	2003/10
PAOLI	Engineer Post Doc	2003/05-2003-06 2001/04-2003/04
PASCAL-JENNY	Engineer	2001/03-2002/08
PHAM	Engineer	2002/11-2003/05
PIRAS	Engineer	2001/03-2002/09
GARCIA MARTINEZ	Engineer	2002/03-2003/08
AIT-ABDELLAH	Student	2002/03-2002/08
LE DAUPHIN	Student	2002/03-2002/08
LIZARAZU	Student	2002/02-2002/08
LOERCHER	Student	2003/03-2003/09
RENAUD	Student	2002/06-2002/08
RUE	Student	2002/03-2002/09
SAULNIER	Student	2002/02-2002/09
YERLY	Student	2003/03-2003/08
MULLER	Visitor	1997/11
NICOUD	Visitor	2001/10
RIZZI	Visitor	1987/10
SCHONFELD	Visitor	2001/01

List of members of the COMPUTATIONAL FLUID DYNAMICS project (2/2).

NAME	POSITION	PERIOD
THUAL	Project Leader	1991/09
ROGEL	Senior	1998/10
TERRAY	Senior	1992/10
WEAVER	Senior	1999/11
DE COETLOGON	Post Doc	2003/04-2003/09
DELON	Post Doc	2000/10-2002/09
MACHU	Post Doc	2000/11-2002/10
MASSART	Post Doc Ph.D student	2002/12 1999/11-2002/11
CAMINADE	Ph.D student Student	2003/10 2003/02-2003/06
CIBOT	Ph.D student	2001/08
DREVILLON	Ph.D student	1998/09-2002/06
JOUZEAU	Ph.D student	2001/10-2003/09
RICCI	Ph.D student	2001/01
BUIS	Research Engineer Engineer	2003/01 2000/08-2002/12
DECLAT	Research Engineer	2001/08
MAISONNAVE	Research Engineer	2000/12
MOREL	Research Engineer	2000/03
PIACENTINI	Research Engineer	1996/10-2003/02
VALCKE	Research Engineer	1997/02
BARRIQUAND	Engineer	2003/12
DAGET	Engineer	2003/11
MAYNARD	Engineer	2003/12
BENTICHA	Student	2003/06-2003/08
CHAPELON	Student	2003/01-2003/03
CILLY	Student	2003/06-2003/08
DANIEL	Student	2002/06-2002/09
DELCOURT	Student	2002/04-2002/08
DEMORY	Student	2003/02-2003/08
DION	Student	2002/06-2002/09
DRISS	Student	2003/02-2003/06
ELAKKRAOUI	Student	2003/01-2003/03
FENIEYS	Student	2002/07-2002/08
FROUVELLE	Student	2003/06-2003/08
JAUFFREY	Student	2003/01-2003/06
KORABI	Student	2003/02-2003/06
MONTEILLET	Student	2003/06-2003/09
PANNEKOUCHE	Student	2003/01-2003/03
PAUSE	Student	2002/02-2002/07
GACON	Visitor	2003/04
CASSOU	CNRS	2002/11

Table iv: List of members of the CLIMATE MODELLING & GLOBAL CHANGE project.

NAME	POSITION	PERIOD
FLEURY	Senior	2001/03
SIEFRIDT	Senior	2000/01
TRANCHANT	Senior	2001/07
LELLOUCHE	Senior Post Doc	2002/10 2000/09-2002/09
REMY	Senior Post Doc	2003/12 2001/11-2003/11
GARRIC	Post Doc	2003/03
BOURDALLE-BADIE	Research Engineer	2001/01
DERVAL	Research Engineer Engineer	2003/07 2002/04-2003/06
DRILLET	Research Engineer	1999/03
DAGET	Engineer Student	2002/11-2003/04 2002/02-2002/06
BESSIERES	Student	2002/07-2002/08

Table v: List of members of the MERCATOR group.

NAME	POSITION	PERIOD
BENDALI	Project Leader	1996/01
FARES	Senior	1992/06
MILLOT	Senior	1995/11
BARTOLI	Senior Research Engineer	2003/02 2000/02
BALLIN	Ph.D.student	2002/03
BOUBENDIR	Ph.D.student	1997/01-2002/06
ZERBIB	Ph.D.student	2002/10
DODU	Engineer	2002/02-2002/12
AITMENSOUR	Student	2002/04-2002/07
LAGES	Student	2002/06-2002/09
SILVA	Student	2003/06-2003/07
COLLINO	Visitor	1994/04

Table vi: List of members of the COMPUTATIONAL ELECTROMAGNETISM project.

NAME	POSITION	PERIOD
LANNES	Project Leader	1994/01
PICARD	Ph.D student	2001/10
ANTERRIEU	CNRS	1993/07
RAMILLIEN	CNRS	2001/02-2002/09

Table vii: List of members of the SIGNAL & IMAGE PROCESSING project.

NAME	POSITION	PERIOD
CROS	Project leader	1997/04
CROUZET	Engineer	2002/02-2002/09
JONVILLE	Engineer	2000/10
MOINAT	Engineer	2000/03
MEDARD	Student	2003/05-2003/06

Table viii: List of members of the TECHNOLOGY TRANSFER group.

NAME	POSITION	PERIOD
MONNIER	Project Leader	1996/12
D'AST	Engineer	1996/10
LAPORTE	Engineer	1988/04
DEJEAN	Technician	1990/11
FLEURY	Technician	1999/10
ARAIA	Student	2003/04-2003/07
DURAND	Student	2003/03-2003/06
KONCEWICZ	Student	2003/02-2003/02
MALARTIC	Student	2003/02-2003/09
MUDRY	Student	2002/06-2002/08
PIGNOT	Student	2003/06-2003/10

Table ix: List of members of the COMPUTER SUPPORT group.

CERFACS Wide-Interest Seminars

Franoise Chaitin-Chatelin (CERFACS) : *About the Creation of Numbers Randomness and Crativity in Mathematics.* (Feb. 13, 2002)

Martin Van Gijzen (CERFACS) : *Computational Ocean Acoustics: Do Finite Element Models have a future?* (Feb. 27, 2002)

Alain Blanchard (Observatoire Midi-Pyrénées): *L'apport des observations du fond de rayonnement cosmologique.* (May 15, 2002)

Philippe Pebay (Sandia National Laboratories, USA) : *IM-EX multistage time-integrators for low Mach number reacting flows.* (June 7, 2002)

Richard C. J. Sommerville (University of California, USA) : *Recent Progress in Cloud-Radiation Interactions in Climate.* (June 27, 2002)

W. C. Reynolds (Stanford, USA) : *The Stanford ASCI Gas Turbine Engine Simulation Program.* (July 5, 2002)

Mathieu Rouault (University of Cape Town, South Africa) : *Droughts and Floods in Southern Africa : Role of Global and Local Ocean-Atmosphere Interactions.* (Nov. 5, 2002)

Franois-Xavier Roux (ONERA, Paris VI) : *Une approche algébrique générale pour les méthodes de résolution par sous-domaines.* (Dec. 4, 2002)

Fabien Esdourubail (INTEL): *INTEL et le Calcul Scientifique : Etat des lieux et développements.* (Feb. 11, 2003)

Philippe Mirabel (Université Louis Pasteur de Strasbourg) : *Formation de particules dans le sillage des avions.* (March 26, 2003)

Patrick Monfray (LEGOS) : *Evolution de la modélisation en biogéochimie marine.* (May 27, 2003)

Emmanuel Romagnoli (ID-IMAG) : *Batch Scheduler pour la gestion de ressources hétérogènes.* (June 2, 2003)

Franois Bouttier (CNRM/GMAP Météo-France) : *The AROME project issues for Fine-Scale atmospheric data assimilation.* (June 27, 2003)

Paul D. Roonney (University of Southern California, USA) : *Premixed flame ignition by transient plasma discharges.* (Sep. 8, 2003)

Eric Guilyardi (IPSL/LSCE and University of Reading, UK) : *PRISM and ENES : a European Approach to Earth System Modeling.* (Sep. 26, 2003)

Per Christian Hansen (Technical University of Denmark) : *Inverse Accoustic Problems : Sound and source reconstruction.* (Oct. 14, 2003)

Daniel Cariolle (Météo-France/CERFACS) : *The environmental effects of aviation.* (Nov. 20, 2003)

Jean-Michel Tanguy & Jean-Marie Carrière (SCHAPI) : *Flood early warning in France.* (Dec. 15, 2003)

1

Parallel Algorithms Project

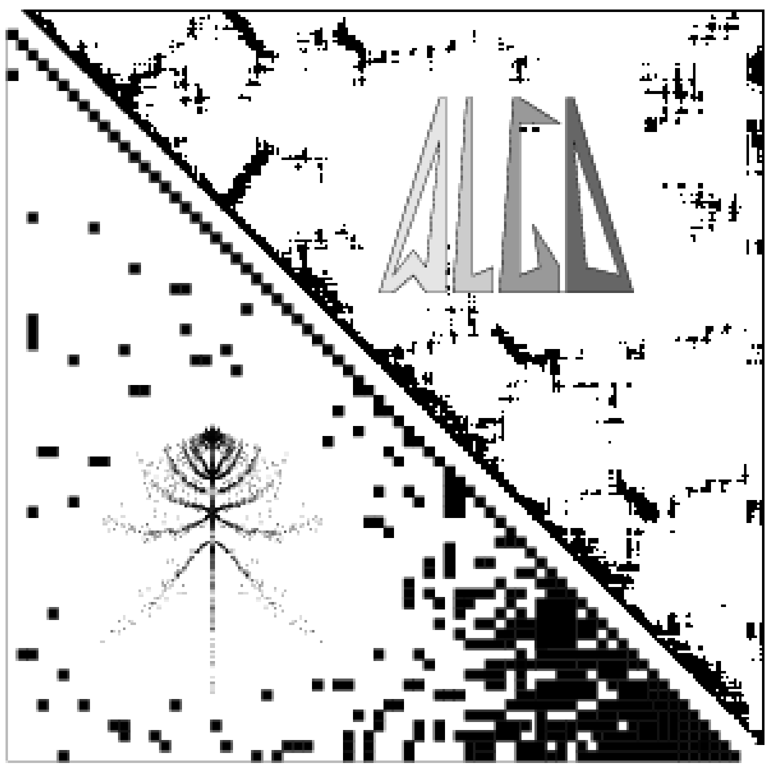

1 Introduction

Iain S. Duff
The research programme conducted by the Parallel Algorithms Project combines the excitement of basic research discoveries with their use in the solution of large-scale problems in science and engineering in academic research, commerce, and industry. We are concerned both with underlying mathematical and computational science research, the development of new techniques and algorithms, and their implementation on a range of high performance computing platforms.

The description of our activities is presented in several subsections, but this is only to give a structure to the report rather than to indicate any compartmentalization in the work of the Project. Indeed one of the strengths of the Parallel Algorithms Project is that members of the Team work very much in consultation with each other so that there is considerable overlap and cross-fertilization between the areas demarcated in the subsequent pages. This cross-fertilization extends to formal and informal collaboration with other teams at CERFACS, the shareholders of CERFACS, and research groups and end users elsewhere. In fact, it is very interesting to me how much the research directions of the Project are increasingly influenced by problems from the partners.

Members of the Team very much play their full part in the wider academic and research community. They are involved in Programme Committees for major conferences, are editors and referees for frontline journals, and are involved in research and evaluation committees. These activities both help CERFACS to contribute to the scientific life of France, Europe and the world while at the same time maintaining the visibility of CERFACS within these communities. Some measure of the visibility of CERFACS can be found from the number of accesses to the Algo Web pages.

Our main approach in the direct solution of sparse equations continues to be the multifrontal technique originally pioneered at Harwell in the early 1980s. During this last period we have further developed the MUMPS package in conjunction with our colleagues at ENSEEIHT, INRIA-Lyon, and Bergen. The release currently being distributed is Version 4.3.2. The main improvements over the last two years have been the incorporation of new ordering and scheduling strategies and the availability of a complex version. The code continues to be downloaded on a daily basis by researchers throughout the world. The complex version has been accessed extensively and used in many applications, particularly in electromagnetics.

At the level of international efforts for standards in numerical linear algebra, we have been very involved in the development of a new standard for the Basic Linear Algebra Subprograms (or BLAS) coordinated through the BLAST Technical Forum. I am delighted to say that the new standard appeared in 2002 as two special issues of the journal “High Performance Computing Applications”. One of our main roles was the development of the Fortran 95 instantiation of the Sparse BLAS. This code is now accepted as an ACM TOMS algorithm and is available from the relevant pages of netlib. We also report on the start of the three-year ACI-GRID Project with ENSEEIHT and others on developing a Grid based expert site for sparse matrices called GRID-Tlse.

We have been involved in pursuing a deep analysis and understanding of the Gram-Schmidt orthogonalization process both at a theoretical and an implementational level. In particular, a new theoretical result has been obtained that proves that the computed orthogonal factors are accurate in the sense that their norm is bounded by a quantity close to one. Julien Langou received an award for the best student paper for this work at the Copper Mountain meeting in April 2002.

Although iterative methods remove many of the bottlenecks of direct approaches, particularly regarding memory, it is now well established that they can only be used in the solution of really challenging problems if the system is preconditioned to create a new system more amenable to the iterative solver. During this last period, we have continued our work on developing such preconditioners, including two-level schemes that effectively and explicitly remove error components in a subspace spanned by eigenvectors corresponding to small eigenvalues of the already preconditioned system. The use of such a two-level spectral scheme has proved very powerful in the solution of very large problems in electromagnetics, including the industry standard COBRA test problem. The notion of two-level schemes has also been implemented within a two level multigrid scheme for solving general unsymmetric problems and an examination comparing various ways of using spectral information has been conducted. An inner-outer scheme involving FGMRES at the outer level has been successfully combined with fast multipole software to solve very large electromagnetics problems efficiently. The development of domain decomposition techniques in solving semiconductor device modelling problems was the subject of joint work with INRIA and was the topic of one of our PhD dissertations. Work has continued on analysing and experimenting with inner-outer iterations, in particular with consolidating the initial discoveries at CERFACS with more recent theoretical analysis by other groups. The GMRES and FGMRES codes that were discussed in a previous activity report have been further developed and continue to be available through the CERFACS web and have attracted over 1000 downloads, some from important establishments including partners of CERFACS. The technical papers describing these codes are the most popular ones for Web page access.

The main area of interest for the Qualitative Computing Group concerns a deep understanding of the influence of finite-precision computation on complex scientific numerical applications. The use of inner-outer iteration has continued in quite different applications. In Krylov methods where we have shown that reduced accuracy for the inner iteration can be accepted as the outer iteration converges; and in the power method where the accuracy needs to increase as the outer iteration proceeds. Solvers based on the former have been implemented in the ASTER code of EDF, while those based on the latter were incorporated into a neutronics code. A nested approach using flexible Krylov methods has been investigated in a system involving global ocean circulation. The application of homotopic deviations include the analysis of parameterised quadratic eigenproblems in computational acoustics and the study of Krylov type methods. A joint project with the NS^3-group has resulted in the development of tools for studying large deviations.

A major focus of our work on nonlinear systems and optimization has been in joint work with the PALM Project and the Climate Modelling and Global Change Group on data assimilation. We are particularly involved in a study of solution techniques for linear least-squares computations that lie at the heart of their algorithms and have established that one of the major algorithms used by the climate community is Gauss-Newton. This insight has led to the consideration of more powerful schemes. We have also examined regularization techniques for the solution of rank-deficient least-squares problems in synthetic aperture imaging applications from signal processing. The work on the solution of large scale dense least-squares problems using an out-of-core factorization of the normal equations matrix has resulted in a code that is competitive with ScaLAPACK but only requires half the storage.

I am pleased to include a section by André Lannes (6.1). Although not in the Parallel Algorithms Team, he certainly is producing excellent work quite in sympathy with the interests of several people in the Group. This section discusses aspects of phase closure imaging and differential GPS that involve use of the Moore-Penrose pseudo-inverse in their analysis.

The Parallel Algorithms Project is heavily involved in the Advanced Training aspects of CERFACS' mission. We ran internal training courses for new recruits to all Projects at CERFACS to give them a basic understanding of high performance computing and numerical libraries. This course was also open to the shareholders of CERFACS. We are also involved in training through the “stagiaire” system and feel that this is extremely useful to young scientists and engineers in both their training and their career choice. It can also help us to focus our research efforts and thus can benefit the work of the Team. A win-win situation. Members of the Team have assisted in many lecture courses at other centres, including ENSICA, INPT, Météo, Toulouse 1 and INSA. Four PhD theses were completed during the reporting period, among which Bruno Carpentieri was awarded the Léopold Lescande prize for the best INPT thesis.

Our list of visitors is a veritable who’s who of numerical analysts, including many distinguished scientists from Europe and the United States. We have included a list of the visitors at the end of this introduction. Four of our visitors stayed for a reasonably long period. These were: Julian Hall (sparse matrices and linear programming), Shane Mulligan (numerical solution of 3-dimensional PDEs), Marielba Rojas (optimization), and Masha Sosonkina (iterative solvers). In addition to inviting some of our visitors to give seminars, some of which are of general interest to other teams, we also run a series of “internal seminars” that are primarily for Team members to learn about each other’s work and are also a good forum for young researchers to hone their presentational skills. At the beginning of 2003, Martin van Gijzen accepted the baton for running the CERFACS wide interest seminars and has run a very active and energetic programme in support of these more general seminars.

We held two major meetings that attracted several people from around the world. In June 2002, we were able to take advantage of our visitors to design a very interesting and exciting programme that attracted nearly 50 participants from not only outside Toulouse but also outside France. Some researchers from the partners of CERFACS also participated. In 2003, we expanded this annual “Sparse Day” to a three-day meeting on “Sparse matrices and grid computing” that we held in St Girons, Ariège. This “St Girons Deux” meeting attracted 83 participants from 12 countries that included many world recognized researchers in sparse matrices and in grid computing, which theme was chosen because of our involvement in the GRID-Tlse Project supported by the ACI-Grid initiative.

I am very pleased to record that, over the reporting period, we have continued our involvement in joint research projects with shareholders and with other teams at CERFACS. We are represented in the CCT of CNES on orbitography and have developed a strong collaboration with them in the parallel distributed generation of normal equations and their subsequent Choleski factorization for applications in geodesy. We have two projects with EADS on preconditioning techniques in electromagnetics and a sponsored PhD on the study of iterative solution techniques for multiple right-hand sides. One of the stagiaires worked on an EADS project for implementing a dense out-of-core direct solver. We completed a contract with EDF to incorporate our strategies on inner-outer iteration within their ASTER code. We have had detailed discussions with EDF on parallel linear solvers. Our work on the optimization and linear algebraic aspects of data assimilation has been of great interest to and the subject of some discussions with Météo-France. We are involved in the training programme for the Mastere, organized by ENM. Our main collaboration with INRIA reached a major milestone with the successful defence of a PhD on domain decomposition techniques in semiconductor device modelling. We help the other Projects at CERFACS at all levels from the “over-a-coffee” consultancy to more major collaborations. These include advice on the elsA code (see CFD chapter) and many aspects of algorithms and error analysis with TSI. We now have a strong and growing collaboration with the Climate Modelling and Global Change Team on aspects of data assimilation and have co-hosted a visit of a researcher from Belgium with the PALM Project of that Group. We are involved in close collaborations over linear solvers in electromagnetic codes with the EMC team. We have also interacted with the CSG group on issues concerning new computer chips and technologies.

As a postscript, I should record my thanks to my three seniors, Luc Giraud, Serge Gratton, and Martin van Gijzen, for doing all the hard work to ensure the smooth running of the Team.

Visitors to Parallel Algorithm Project in 2002-2003

In alphabetical order, our visitors in the years 2002-2003 included:
YANNIS ALIFERIS (Université de Nice-Sophia Antipolis, France), GUILLAUME ALLÉON (EADS-CCR, France), PATRICK AMESTOY (ENSEEIHT-IRIT, France), MARIO ARIOLI (CLRC-Rutherford Appleton Laboratory, UK), MICHELE BENZI (Emory University, USA), OLIVIER BESSON (Université de Neuchâtel, Switzerland), AKE BJÖRCK (Linkoping University, Sweden), PETTER BJÖRSTAD (University of Bergen), MATTHIAS BOLLHOEFER (TU Berlin, Germany), ERIK BOMAN (Sandia National Labs, USA), DORON CHEN (Tel-Aviv University, Israel), FILOMENA D'ALMEIDA (Universidade do Porto, Portugal), TIM DAVIS (University of Florida, USA), JACK DONGARRA (University of Tennessee, USA), FRÉDÉRIC DESPREZ (INRIA/LIP-ENS, France), ABDELLATIF EL GHAZI (Université Mohammed V, Rabat, Morocco), JASPER VAN DEN ESHOF (University of Utrecht, Netherlands), ENRIC FONTDECABA (Industrias de Optica S.A., Spain), CRISTIAN GATU (Université de Neuchâtel, Switzerland), JOHN GILBERT (Xerox Parc, USA), GENE GOLUB (Stanford University, USA), IVAN GRAHAM (University of Bath, UK), NICKY GRAVES GREGORY (University of Brighton, UK), LAURA GRIGORI (Lawrence Berkeley National Laboratory, USA), ABDOU GUERMOUCHE (LIP-ENS, France), PHILIPPE GUILLAUME (INSA, France), JULIAN HALL (University of Edinburgh, UK), PER CHRISTIAN HANSEN (Technical University of Denmark), HUSSEIN HOTEIT (INRIA/IRISA, France), ALAIN HUARD (INSA, France), ABDERRAZAK ILAHI (Facult des Sciences de Gabès, Tunisia), ERRICOS KONTOGHIORGHES (Université de Neuchâtel, Switzerland), JACKO KOSTER (Parallab, BCCS, Bergen, Norway), FELIX KWOK (McGill University, Montreal, Quebec, Canada), JEAN-YVES L'EXCELLENT (INRIA/LIP-ENS, France), SÉBASTIEN LACROIX (IFP, France), ALEXANDRE LE BLANC (University of Artois, France), JOHN LEWIS (The Boeing Company, USA), SHERRY LI (Lawrence Berkeley National Laboratory, Berkeley, CA, USA), PIERRE MARECHAL (Université de Montpellier II), OSNI MARQUES (Lawrence Berkeley National Laboratory, USA), JOSÉ MAS MARI (Universitat Politecnica de Valencia ETSE Agrunoms, Spain), AMERICO MARROCCO (INRIA-Rocquencourt, France), GÉRARD MEURANT (CEA, France), SHANE MULLIGAN (Dublin Institute of Technology, Dublin, Ireland), NANCY NICHOLS (University of Reading, UK), ESMOND NG (Lawrence Berkeley National Laboratory, Berkeley, CA, USA), SUELY OLIVEIRA (The University of Iowa, USA), FRANÇOIS PELLEGRINI (LaBRI, France), BERNARD PHILIPPE (INRIA/IRISA, France), SERGE PIPERNO (CERMICS/INRIA, France), ALEX POTHEN (Old Dominion University, Norfolk VA, USA), ROLDAN POZO (NIST, USA), PIERRE RAMET (LaBRI, France), MARIELBA ROJAS (Wake Forest University, Winston-Salem, USA), JEAN ROMAN (INRIA Futurs, LaBRI, Talence, France), DANIEL RUIZ (ENSEEIHT, France), YOUSEF SAAD (University of Minnesota, USA), ROBERT SCHEICHL (University of Bath, UK), STEFAN SCHNEIDER (Technische Universitaet Dresden, Germany), JENNIFER SCOTT (Rutherford Appleton Laboratory, UK), GERARD SLEIJPEN (University of Utrecht, Netherlands), ANNICK SARTENAER (The University of Namur, Belgium), MICHAEL SAUNDERS (Stanford University, USA), MASHA SOSONKINA (Ames Laboratory/DOE Iowa State University, USA), GUILLAUME SYLVAND (EADS-CCR and CERMICS/INRIA, France), WEI-PAI TANG (The Boeing Company, Seattle, USA), PHILIPPE TOINT (The University of Namur, Belgium), SIVAN TOLEDO (Tel-Aviv University, Israel), HENRY TUFO (University of Colorado at Boulder, USA), MIROSLAV TŮMA (Academy of Sciences of the Czech Rep., Prague, Czech Republic), JEAN TSHIMANGA (The University of Namur, Belgium), MARINA VIDRASCU (INRIA-Rocquencourt, France).

2 Dense and Sparse Matrix Computations

2.1 Rank-revealing and incremental norm estimation (I. S. Duff and C. Vömel)

We have developed an incremental approach to 2-norm estimation for triangular matrices which is important for the detection of ill-conditioning, one of the basic problems arising in the numerical solution of linear systems. Applications of our scheme include the calculation of forward error bounds based on the condition number, robust pivot selection criteria and rank-revealing factorizations, in particular, when *inverse* factors arise in the factorization. In [2], we introduced such a scheme applicable for both dense and sparse matrices which can arise for example from a QR, a Cholesky or a LU factorization. If the explicit inverse of a triangular factor is available, as in the case of an implicit version of the LU factorization, we can relate our results to incremental condition estimation (ICE) presented in [1]. Incremental norm estimation (INE) extends directly from the dense to the sparse case without needing the modifications that are necessary for the sparse version of ICE. INE can be applied to complement ICE, since the product of the two estimates gives an estimate for the matrix condition number. Furthermore, when applied to matrix inverses, INE can be used as the basis of a rank-revealing factorization. The quality of our results on standard test cases is constantly high and demonstrates the general reliability of our scheme [ALG7].

[1] C. H. Bischof, (1990), Incremental Condition Estimation, *SIAM J. Matrix Analysis and Applications*, **11**, 312–322.

[2] I. S. Duff and C. Vömel, (2000), Incremental Norm Estimation for Dense and Sparse Matrices, Tech. Rep. TR/PA/00/83, CERFACS, Toulouse, France. Preliminary version of the article published in BIT, Numerical Mathematics, Volume 42, Issue 2 (June 2002), pp. 300–322.

2.2 Development of kernels for sparse numerical linear algebra (I. S. Duff and C. Vömel)

It is with great pleasure that we can report on the release during this current year of the new Basic Linear Algebra Subprogram (BLAS) Standard developed and defined by the BLAS Technical Forum [3]. This involved many extensions to the earlier standards, including new functionalities, mixed precision BLAS, and sparse BLAS. A technical description of these can be found in [ALG4]. Our main contribution to this effort was in the design, implementation, and testing of the sparse BLAS.

The design of the sparse BLAS is discussed in the paper [ALG8]. This consists of a set of kernels providing basic operations for sparse matrices and vectors, including the multiplication of a dense vector or a set of dense vectors by a sparse matrix. A principal goal of the Sparse BLAS standard is to aid in the development of iterative solvers for large sparse linear systems by specifying interfaces for a high-level description of vector and matrix operations for the algorithm developer while leaving enough freedom for vendors to provide the most efficient implementation of the underlying algorithms for their specific architectures.

The Sparse BLAS standard defines interfaces and bindings for the three target languages: C, Fortran 77 and Fortran 95. Our Fortran 95 implementation is intended as a reference model for the Sparse BLAS. The design is based on the idea of matrix handles so that the user need not be concerned with the details of the underlying storage schemes. It is envisaged that these kernels will be widely used in the solution of sparse equations by iterative methods. The software implementation has been published as TOMS algorithm [ALG6].

[3] BLAS Technical Forum, (2002), Special Issue: On Basic Linear Algebra Subprograms Technical BLAST Forum Standard -I and II, *The International Journal of High Performance Computing Applications*, **16**.

2.3 Development of the MUMPS package for solving sparse linear systems on distributed memory computers (P. R. Amestoy, C. Bousquet, C. Daniel and I. S. Duff)

We were fortunate to have three stagiaires working on the MUMPS Project principally supervised by Patrick Amestoy of ENSEEIHT-IRIT. They were working from the base of Version 4.1 of the MUMPS package [5] and they performed some preliminary work that has proved of assistance for the development of Version 4.2 of MUMPS that was released at the end of 2002.

The work performed at ENSEEIHT-IRIT by Gregoire Richard [ALG65] concerned coupling and testing other ordering packages within MUMPS. This was important since we had already observed that different orderings can have a significant effect on the performance of the code in terms of work, memory and parallelism. Version 4.1 had only one integrated ordering (AMD) and an interface to other orderings through acceptance of a input permutation. In Version 4.2, several orderings are more tightly coupled to the package.

The work of Caroline Bousquet and Christophe Daniel [ALG38] concerned the development of a much requested complex version (that now exists in Version 4.2) and the design and development of a rigorous test deck for the code, an essential tool for the verification and development of any package, particularly one so large and complicated as the MUMPS package.

This work together with that described in Sections 2.4 and 2.7 has been very important for the future development of the MUMPS package and, in particular, for the Version 4.2 release.

[4] P. R. Amestoy, I. S. Duff, J.-Y. L'Excellent, and J. Koster, (2001), A fully asynchronous multifrontal solver using distributed dynamic scheduling, *SIAM J. Matrix Analysis and Applications*, **23**, 15–41.

2.4 Candidate-based dynamic scheduling for a distributed direct linear solver (P. R. Amestoy, I. S. Duff and C. Vömel)

The asynchronous distributed memory multifrontal solver MUMPS [5, 34] can be described by a computational graph in the form of a tree (the so-called *assembly tree*) where the computation at a node of the tree is equivalent to several steps of Gaussian elimination on a dense submatrix (the *frontal matrix*) and the remaining Schur complement from this partial factorization (the so-called *contribution block*) is sent to the parent of the node of the tree and is summed (or *assembled*) with contribution blocks from other children and data from the original matrix to form another frontal matrix at the parent. MUMPS exploits both the parallelism inherent in the tree (by processing independent branches in parallel) as well as parallelism within tree nodes with a large enough contribution block. A master process is assigned to the node to factorize the pivot block and this in turn distributes the work of generating the contribution block to a set of slave processes that are assigned dynamically during the numerical factorization.

While the *master* processor of each node in the tree (i.e. the one that is responsible for the factorization of the block of fully summed variables) is chosen during the analysis phase, the *slaves* for the parallel update of large contribution blocks are only chosen during the factorization phase. This dynamic task scheduling takes place in order to balance the work load of the processors at run time. Problems can arise if too much freedom is offered to the dynamic scheduling. If every processor is a candidate for a slave then, on each processor, enough workspace has to be reserved during the analysis phase for the corresponding computational tasks. However, during the factorization, typically not all processors are actually needed as slaves (and, on a large number of processors, only a very few are needed), so the prediction of the required workspace will be overestimated. Thus the size of the problems that can be solved is reduced unnecessarily because of this difference between the prediction and allocation of memory in the analysis phase and the memory actually used during the factorization.

With the concept of *candidate processors* it is possible to address this issue. The concept originates in an algorithm presented in [7] and extends efficiently to MUMPS. For each node that requires slaves to be chosen dynamically during the factorization because of the size of its contribution block, we introduce a limited set of processors from which the slaves can be selected. While the master previously chose slaves from among all less loaded processors, the freedom of the dynamic scheduling can be reduced so that the slaves are only chosen from the candidates. This effectively allows us to exclude all non-candidates from the estimation of workspace during the analysis phase and leads to a more realistic prediction of workspace needed. Furthermore, the candidate concept allows us to better structure the computation since we can explicitly restrict the choice of the slaves to a certain group of processors and enforce a 'subtree-to-subcube' mapping principle.

Our new approach significantly improves the scalability of the solver in terms of execution time and storage. By comparison with the previous version of MUMPS, we demonstrate the efficiency and the scalability of the new algorithm on up to 512 processors. Our test cases include matrices from regular 3D grids and irregular ones from real-life applications [ALG34].

[5] P. R. Amestoy, I. S. Duff, J.-Y. L'Excellent, and J. Koster, (2001), A fully asynchronous multifrontal solver using distributed dynamic scheduling, *SIAM J. Matrix Analysis and Applications*, **23**, 15–41.

[6] P. R. Amestoy, I. S. Duff, J.-Y. L'Excellent, and X. S. Li, (2001), Analysis, Tuning and Comparison of Two General Sparse Solvers for Distributed Memory Computers, *ACM Trans. Math. Softw.*, **27**, 388–421.

[7] A. Pothen and C. Sun, (1993), A Mapping Algorithm for Parallel Sparse Cholesky Factorization, *SIAM J. Scientific Computing*, **14(5)**, 1253–1257.

2.5 Symmetric weighted matching and application to indefinite multifrontal solvers (I. S. Duff and S. Pralet)

We study techniques for scaling and choosing pivots when using multifrontal methods in the LDL^T factorization of symmetric indefinite matrices where L is a lower triangular matrix and D is a block diagonal matrix with 1×1 and 2×2 blocks.

For the LU factorization of a matrix A, `MC64` [9] can be used to get a maximum weighted matching so that the corresponding permutation will place large entries on the diagonal. The matrix can then be scaled so that diagonal entries have modulus one and off-diagonals have modulus less than or equal to one. This has been found to greatly improve the numerical stability of the subsequent LU factorization.

If, however, `MC64` is applied to a symmetric matrix the resulting permutation will not normally preserve symmetry. We examine ways in which `MC64` can be used while still preserving symmetry. Then an ordering (for example, AMD [8]) can be computed on the permuted matrix to get a symmetric permutation in order to decrease the fill-in in the factors.

We use our "symmetric" `MC64` preprocessing with two symmetric multifrontal codes `MA47` [10] and `MA57` [11] to validate our preprocessing heuristics on real test problems.

[8] P. R. Amestoy, T. A. Davis, and I. S. Duff, (1996), An approximate minimum degree ordering algorithm, **17**, 886–905.

[9] I. S. Duff and J. Koster, (1999), The design and use of algorithms for permuting large entries to the diagonal of sparse matrices, **20**, 889–901.

[10] I. S. Duff and J. K. Reid, (1994), MA47, a Fortran code for direct solution of sparse symmetric indefinite structured systems of linear equations, Tech. Rep. (to appear).

[11] I. S. Duff, (2002), MA57 - A new code for the solution of sparse symmetric definite and indefinite systems, technical report RAL-TR-2002-024, Rutherford Appleton Laboratory.

2.6 Unsymmetric orderings using a constrained Markowitz scheme (P. R. Amestoy, X. S. Li and S. Pralet)

We consider the LU factorization of a sparse unsymmetric matrix A based on a three-phase approach (analysis, factorization, solve). The analysis phase transforms A into $\bar{A}$ with better properties for sparse factorization. It exploits the structural information to reduce the fill-ins in the LU factors and exploits the numerical information to reduce the amount of numerical pivoting needed during factorization. Two separate passes are commonly used for these two objectives. Firstly, scaling and maximum transversal algorithms are used to transform A into A_1 with large entries on the diagonal. Secondly, a symmetric fill-reducing ordering, which preserves the large diagonal, is used to permute A_1 into A_2 so that the factors of A_2 are sparser than those of A_1. Note that during factorization, numerical instabilities can still occur and will be handled either by partial pivoting resulting in extra fill-in in the factor matrices or by static pivoting resulting in a potentially less accurate factorization.
During analysis, the numerical treatment requires the fill-reducing ordering to be symmetric, and the structural phase does not have numerical information to correct any wrong numerical decisions. To avoid these two drawbacks, we present an approach which mixes the numerical and structural phases. Based on a numerical pre-treatment of the matrix we build at each step k of the elimination a set of numerically acceptable pivots, referred to as matrix C^k that may contain off-diagonal entries. We then compute an unsymmetric ordering taking into account both the structure of A and the numerical information in C^k.

2.7 Adapting a parallel sparse direct solver to architectures with clusters of SMPs (P. R. Amestoy, I. S. Duff, S. Pralet and C. Vömel)

In the context of the direct solution of general sparse linear systems, we consider the problem of task scheduling on clusters of SMPs. Our main target type of computer architecture can be defined as a so called two-level architecture. Each level is composed of a set of identical processors sharing a common memory (that is, is an SMP node). The work in [ALG34] implicitly assumed that our target computer was a distributed memory computer with uniform memory access and uniform cost of communication. We show the limitations of this approach on machine with two-level architecture and we indicate how we can remedy these limitations in [ALG3]. Our modifications of the algorithms affect both the symbolic factorization and the numerical factorization phase. Our experiments on the IBM SP from CINES (Montpellier) with 16 processors per SMP node and up to 128 processors show that we can significantly reduce both the amount of inter-node communication and the factorization time. The algorithms have been integrated into Version 4.3 of `MUMPS`.

2.8 The Grid-TLSE project (P. R. Amestoy, M. Buvry, M. Daydé, I.S. Duff, L. Giraud, J. Y. L'Excellent, M. Pantel and C. Puglisi)

In the context of large sparse calculations, we are involved as one of the leading partners of a ACI-Grid project (funded by the French Ministry of Research from December 2002 until November 2005). This project will use the grid at several levels. It will add new services on the Grid and use the grid capabilities to implement these services. The main services will be mainly twofold:

- provide the users with automatic expertise on sparse direct solvers using matrices either from the data base or provided by the user (a natural follow up step will be to extend this to iterative solvers).
- make available to the scientific community a set of test problems through a data base. The set of examples will grow dynamically as Grid users submit new problems that are integrated within the data set.

A prototype developed in 2003 was opened to the industrial partners that are the end-users (CEA, CNES, EADS, EDF, IFP). The specification phase is still ongoing, it is conducted jointly with ENSEEIHT and involves other academic Labs (LABRI, Bordeaux; INRIA-ENS, Lyon) as well as industrial partners. More information on the project can be found from the URL: `http://www.enseeiht.fr/lima/tlse`

3 Iterative Methods and Preconditioning

3.1 A robust criterion for modified Gram-Schmidt with selective reorthogonalization (L. Giraud and J. Langou)

In this work we investigate a new criterion for selective reorthogonalization in the modified Gram-Schmidt algorithm that is referred to as the L-criterion.. This criterion depends on a single parameter L. When L is chosen smaller than 1 (e.g. $L = 0.99$), for numerically nonsingular matrices, this criterion is able to realize the compromise between saving useless reorthogonalization and giving a set of computed vectors that are orthogonal up to machine precision level. We study its behaviour in the presence of rounding errors. We give some counter-examples which prove that the standard criteria might fail. Through numerical experiments, we illustrate that our new criterion seems also suitable for the classical Gram-Schmidt algorithm. More details on this work can be found in [ALG55, ALG56].

3.2 On the round-off error analysis of the iterated classical Gram-Schmidt algorithm (L. Giraud, J. Langou and M. Rozložník)

In this work we analyse the numerical behaviour of the classical Gram-Schmidt algorithm with one iterative refinement/reorthogonalization step. Assuming numerical nonsingularity of the matrix we prove that two steps of the Classical Gram-Schmidt process are enough for preserving the orthogonality of the computed vectors close to machine-precision level. We give a rounding error analysis and relate our results to the approach used in the Kahan-Parlett [14] "twice is enough" algorithm as well as to results given by Abdelmalek, Daniel et al [12], Hoffmann [13] and others.
More details on this work can be found in [ALG60]

[12] W. Daniel, W. B. Gragg, L. Kaufman, and G. W. Stewart, (1976), Reorthogonalization and stable algorithms for updating the Gram-Schmidt QR factorization, *Math. Comp.*, **30**, 772–795.

[13] W. Hoffmann, (1989), Iterative algorithms for Gram-Schmidt orthogonalization, *Computing*, **41**, 335–348.

[14] B. N. Parlett, (1980), *The Symmetric Eigenvalue Problem*, Prentice-Hall, Englewood Cliffs, NJ.

3.3 A reorthogonalization procedure for the modified Gram–Schmidt algorithm based on a rank k update (L. Giraud, S. Gratton and J. Langou)

The modified Gram–Schmidt algorithm is a well-known and widely used procedure to orthogonalize the column vectors of a matrix. When applied to ill-conditioned matrices in floating-point arithmetic, the orthogonality among the computed vectors may be lost. In this work, we propose an *a posteriori* reorthogonalization technique based on a rank k update of the computed vectors. The set of vectors built is orthogonal up to machine precision assuming a large enough k is chosen. Moreover, we show that the rank of the update can be tuned to monitor the orthogonality quality. We illustrate the efficiency of this approach

in the framework of the GMRES-Seed technique for the solution of an unsymmetric linear system with multiple right-hand sides. In particular, we report experiments on numerical simulations in electromagnetic applications where such problems arise.
A complete description of this work is available in [ALG58, ALG30]

3.4 A class of spectral two-level preconditioners (B. Carpentieri, I. S. Duff and L. Giraud)

It is well known that the convergence of Krylov methods for solving linear systems often depends to a large extent on the eigenvalue distribution. In many cases, it is observed that “removing” the smallest eigenvalues can greatly improve the convergence. Several techniques have been proposed in the past few years that attempt to tackle this problem. The proposed approaches can be split into two main families depending on whether the scheme enlarges the generated Krylov space or adaptively updates the preconditioner. In this work, we follow the second approach and propose a class of preconditioners both for unsymmetric and for symmetric linear systems that can also be adapted for symmetric positive definite problems. We effectively solve the preconditioned system exactly in the low dimensional space associated with the smallest eigenvalues and use this to update the preconditioned residual. This update results in shifting eigenvalues from close to the origin to near to one for the new preconditioner. This is ideal when there are only a few eigenvalues near the origin while all the others are close to one because the updated preconditioned system becomes close to the identity. We illustrate the performance of our method through extensive numerical experiments on a set of general linear systems.
More details are available in [ALG39] as well as examples on two different applications in [ALG29, ALG31]. Finally, we refer to Section 3.7 for the use of this technique for large electromagnetic simulations.

3.5 Two grid spectral preconditioning for general sparse linear systems (B. Carpentieri, L. Giraud and S. Gratton)

Multigrid methods are among the fastest techniques to solve a linear system $Ax = b$ arising from the discretization of a partial differential equation. The core of the multigrid algorithms is a two-grid procedure that is applied recursively. The basic idea of the two-grid solver is :

1. given x_0, perform a few (μ_1) steps of a basic stationary method of the form $x^{(k+1)} = (I-MA)x^{(k)} + g$ to compute x^{μ_1}. This step is referred to as the pre-smoothing.

2. project the residual $r = b - Ax^{\mu_1}$ on a coarse space using a restriction operator R and solve the linear system $RAPe = Rr$, where P is the prolongation operator.

3. prolongate the error in the fine space and update $x = x^{\mu_1} + Pe$.

4. perform few (μ_2) steps of a basic stationary method of the form $x^{(k+1)} = (I - MA)x^{(k)} + g$ to compute x^{μ_2}. This step is referred to as the post-smoothing.

5. If x_2^{μ} is accurate enough stop, else $x_0 = x^{\mu_2}$, go to Step 1.

The smoother iterations aim at reducing the high frequencies of the error (ie the components of the error in the space spanned by the vectors associated with the largest eigenvectors of A). The restriction operator and consequently the coarse space is chosen so that this space contains the low frequency of the error (i.e. the components associated with the smallest eigenvalues). In classical multigrid, the coarse space is not defined explicitly through the knowledge of the eigencomponents but by the selection of a space that is expected to capture them. The scheme presented above is a multiplicative algorithm [16] but additive variants [17] also exist.

In this work, we exploit the idea of the two-grid method to design additive and multiplicative preconditioners for general linear systems. We explicitly define the coarse space by computing the eigenvectors V associated with the smallest eigenvalues of MA (that is, the components of the error that are not damped efficiently by the smoother). In that context, the prolongation operator is $P = V$. We show that our preconditioners shift the smallest eigenvalues of MA to one and tend to cluster those that were already in the neighbourhood of one closer to one. We illustrate the performance of our method through numerical experiments on a set of general linear systems, both symmetric and positive definite and unsymmetric. Finally, we consider a case study of a non-overlapping domain decomposition method of semiconductor device modelling for the solution of the drift-diffusion equations.

A more detail description of these approaches as well as their numerical behaviour on a range of standard test problems is available in [15]

[15] B. Carpentieri, L. Giraud, and S. Gratton, (2004), Two-grid spectral preconditioning for general sparse linear systems, Tech. Rep. In preparation, CERFACS, Toulouse, France.

[16] W. Hackbusch, (1985), *Multigrid methods and applications.*, Springer-Verlag.

[17] R. S. Tuminaro, (1992), A highly parallel multigrid-like method for the solution of the Euler equations, *SIAM J. Scientific and Statistical Computing*, **13**, 88–100.

3.6 A comparative study of iterative solvers exploiting spectral information for SPD systems (L. Giraud, D. Ruiz and A. Touhami)

When solving the Symmetric Positive Definite (SPD) linear system $\mathbf{Ax} = \mathbf{b}$ with the Conjugate Gradient (CG) method, the smallest eigenvalues of the matrix A often slow down the convergence. This observation is still of course true when a preconditioner is used and some additional techniques can be investigated to improve the convergence rate of CG on the preconditioned system. Several techniques have been proposed in the literature that either consists of updating the preconditioner or enforcing CG to work in the orthogonal complement to the invariant subspace associated with small eigenvalues. In this work, we compare the numerical efficiency and computational complexity of the techniques presented in [18, ALG5, 20, 21, 22]. A more detail description of these approaches as well as their numerical behaviour on a range of standard test problems is available in [19].

[18] M. Arioli and D. Ruiz, (2002), A Chebyshev-based two-stage iterative method as an alternative to the direct solution of linear systems, Tech. Rep. RAL-TR-2002-021, Rutherford Appleton Laboratory, Atlas Center, Didcot, Oxfordshire, OX11 0QX, England.

[19] L. Giraud, D. Ruiz, and A. Touhami, (2004), A comparative study of iterative solvers exploiting spectral information for SPD systems, Tech. Rep. In preparation, CERFACS, Toulouse, France.

[20] R. Nabben and C. Vuik, (2003), A comparison of deflation and coarse grid correction applied to porous media flow, Tech. Rep. Report 03-10, Delft University of Technology, Department of Applied Mathematical Analysis.

[21] R. Nicolaides, (1987), Deflation of conjugate gradients with applications to boundary value problems, *SIAM J. Numerical Analysis*, **24**, 355–365.

[22] Y. Saad, M. Yeung, J. Erhel, and F. Guyomarc'h, (2000), A deflated version of the conjugate gradient algorithm, *SIAM J. Scientific Computing*, **21**, 1909–1926.

3.7 Using spectral low rank preconditioners for large electromagnetic calculations (I. S. Duff, L. Giraud, J. Langou and E. Martin)

For solving large dense complex linear systems that arise in electromagnetic calculations, we perform experiments using a general purpose spectral low rank update preconditioner [ALG5] in the context of the GMRES method preconditioned by an approximate inverse preconditioner [23]. The goal of the spectral preconditioner is to improve the convergence properties by shifting by one the smallest eigenvalues of the original preconditioned system.
Numerical experiments have been performed on parallel distributed memory computers, using a Fast Multipole code [31], to illustrate the efficiency of this technique on large and challenging real–life industrial problems. More details on this work are available in [ALG51].

[23] G. Alléon, M. Benzi, and L. Giraud, (1997), Sparse Approximate Inverse Preconditioning for Dense Linear Systems Arising in Computational Electromagnetics, *Numerical Algorithms*, **16**, 1–15.

[24] G. Sylvand, (2002), *Résolution Itérative de Formulation Intégrale pour Helmholtz 3D : Applications de la Méthode Multipôle à des Problèmes de Grande Taille*, PhD thesis, Ecole Nationale des Ponts et Chaussées.

3.8 Stopping criteria in finite element methods (M. Arioli, D. Loghin and A. J. Wathen)

This work [ALG37] extends the results of Arioli [26, 25] on stopping criteria for iterative solution methods for linear finite element problems to the case of nonsymmetric positive-definite problems. We show that the residual measured in the norm induced by the symmetric part of the inverse of the system matrix is relevant to convergence in a finite element context. We then use Krylov solvers to provide alternative ways of calculating or estimating this quantity and present numerical experiments which validate our criteria. This work is expected to continue in 2004 with generalizations to the case of finite element discretizations of systems of PDEs.

[25] M. Arioli, E. Noulard, and A. Russo, (2001), Stopping criteria for iterative methods: applications to PDEs, *Calcolo*, **38**, 97–112.

[26] M. Arioli, (2000), A Stopping Criterion for the Conjugate Gradient Algorithm in a Finite Element Method Framework, Tech. Rep. IAN-1179, Istituto di Analisi Numerica, Pavia.

3.9 Efficient iterative methods for non-Newtonian fluid flows (D. Loghin)

Discretizations of non-Newtonian flow models lead to large nonlinear block systems of equations the solution of which is usually sought through an iterative approach. Standard techniques suggested and analysed in the literature involve splittings of the block systems which lead to fixed-point iterations which generally are slow to converge. One example is that of the three-fields Stokes problem which arises in the solution of Oldroyd-B models via nonlinear schemes explicit in the nonlinear terms. The slow convergence of the explicit nonlinear scheme is compounded here by the aforementioned sluggish convergence of the splittings employed to solve the resulting linear systems. In this work, we present an approach based on the use of the structure of the underlying system of PDEs to construct a preconditioner for the solution of the global system via a Krylov method. In particular, we use block-triangular preconditioners coupled with GMRES to construct efficient and mesh-independent solution algorithms for mixed finite element

discretizations of our problems. While the usual drawback associated with this approach is the need to approximate a Schur complement of the global matrix, in the case of the three-fields Stokes problem this Schur complement is readily available as a scaled mass matrix, not unlike that arising in the solution of the standard Stokes problem for Newtonian flow.
This work was included in the presentation given at the Workshop on Solution Methods for Saddle-Point Problems in Santa Fe. The work is presented in detail in a report which is currently being written [27].

[27] D. Loghin, (2004), Efficient iterative methods for non-Newtonian fluid flows, Technical Report.

3.10 Adaptive preconditioners for Newton-Krylov methods (D. Loghin, D. Ruiz and A. Touhami)

The use of preconditioned Newton-Krylov methods has become a mandatory choice for the solution of large nonlinear systems of equations. In many situations the available preconditioners are sub-optimal, due to the changing nature of the linearized operator. This the case, for instance, for quasi-Newton methods where the Jacobian (and its preconditioner) are kept fixed at each non-linear iteration, with the rate of convergence usually degraded from quadratic to linear. Updated Jacobians, on the other hand require updated preconditioners, which may not be readily available. In this work, we introduce an adaptive preconditioning technique based on the Krylov subspace information generated at previous steps in the nonlinear iteration. In particular, we use to advantage a deflation technique suggested by Reichel, Calvetti and Golub for restarted GMRES to enhance existing preconditioners with information about (almost) invariant subspaces constructed by GMRES at previous stages in the nonlinear iteration. We provide guidelines on the choice of invariant-subspace bases used in the construction of our preconditioner and demonstrate the improved performance on various test problems. We also describe an efficient implementation of our approach in the case of augmented systems arising from CFD modelling. This work has been contributed to the Copper Mountain Conference on Iterative Methods [28].

[28] D. Loghin, D. Ruiz, and A. Touhami, (2004), Adaptive preconditioners for Newton-Krylov methods, tech. rep., CERFACS.

3.11 Using symmetric Krylov solvers for solving electromagnetic problems using a fast multipole code (R. Durdos, L. Giraud and J. Langou)

In this work we investigate the use of symmetric QMR [30] for the solution of symmetric dense linear systems arising from electromagnetic applications. Symmetric QMR (SQMR) is a hybrid version of QMR that benefits from the symmetry of the matrix so dividing by two the cost compared to QMR. The advantage over solvers like GMRES is that SQMR uses a short term recurrence and therefore requires only a few vectors to be stored while the number of dot products is also considerably reduced. The main drawback is an observed delay in the convergence due in general to a loss of orthogonality among the computed vectors. In our experiments, the matrix-vector products are performed using a fast multipole code [31] with three different formulations. Even though, in exact arithmetic, the dense matrix is symmetric, the use of floating-point arithmetic combined with the approximations made in the three implementations of the fast multipole method deteriorate this property. We therefore end up by using a non-symmetric matrix-vector product in a symmetric solver. In Figure iii in the appendix, we plot the backward error as a function of the iterations for three formulations of the multipole expansion (denoted by fmm1, fmm2 and fmm3) and two different arithmetics (i.e. single or double precision). These experiments indicate that SQMR converges well down to a level that is related to the symmetry of the computed matrix (only accessible through mat-vec product); this latter also greatly influences the rate of convergence. The better the symmetry is, the better the convergence. In Figure iii in the appendix, we also plot the convergence of GMRES as a reference. When the matrix is nearly symmetric, the behaviour of SQMR is close to that of GMRES. SQMR, which is very appropriate for those problems when the matrix is fully assembled [29], may also be applied with the multipole method but requires careful implementation to maintain the symmetry of the multipole expansion. Finally, preliminary experiments on small problems have been conducted to embed SQMR in flexible FQMR [32] iterations. The behaviour of the resulting inner-outer procedure is rather disappointing and does not exhibit the nice convergence observed with its counterpart based on GMRES [ALG40]. More details on this work can be found in [ALG52, ALG30].

[29] B. Carpentieri, I. Duff, L. Giraud, and M. M. monga Made, (2001), Sparse symmetric preconditioners for dense linear systems in electromagnetism, Technical Report TR/PA/01/35, CERFACS, Toulouse, France. Preliminary version of a paper to appear in Numerical Linear Algebra with Applications.

[30] R. W. Freund and N. M. Nachtigal, (1994), An implementation of the QMR method based on coupled two-term recurrences, *SIAM J. Scientific Computing*, **15(2)**, 313–337.

[31] G. Sylvand, (2002), *La Méthode Multipôle rapide en Electromagnétisme : Performances, Parallélisation, Applications*, PhD thesis, Ecole Nationale des Ponts et Chaussées.

[32] D. B. Szyld and J. A. Vogel, (2001), A Flexible Quasi-Minimal Residual Method with Inexact Preconditioning, *SIAM J. Scientific Computing*, **23**, 363–380.

3.12 Combining fast multipole techniques and approximate inverse preconditioners for large calculations in electromagnetism (B. Carpentieri, I.S. Duff, L. Giraud and G. Sylvand)

The boundary element method has become a popular tool for the solution of Maxwell's equations in electromagnetism. From a linear algebra point of view, this leads to the solution of large dense complex linear systems where the unknowns are associated with the edges of the mesh defined on the surface of the illuminated object. In this paper, we address the iterative solution of these linear systems via preconditioned Krylov solvers. Our primary focus is on the design of an efficient parallelizable preconditioner. In that respect, we consider an approximate inverse method based on the Frobenius-norm minimization. The preconditioner is constructed from a sparse approximation of the dense coefficient matrix, and the patterns both for the preconditioner and for the coefficient matrix are computed *a priori* using geometric information from the mesh. We describe how such a preconditioner can be naturally implemented in a parallel code that implements the multipole technique for the matrix-vector product calculation. We investigate the numerical scalability of our preconditioner on realistic industrial test problems and show that it exhibits some limitations on very large problems of size close to one million unknowns. To improve its robustness on those large problems we propose an embedded iterative scheme that combines nested GMRES solvers with different fast multipole computations. We show through extensive numerical experiments that this new scheme is extremely robust at affordable memory and CPU costs for the solution of very large and challenging problems. More details can be found in [ALG40].

3.13 Domain decomposition methods in semiconductor device modelling (L. Giraud, J.-C. Rioual and A. Marrocco)

The numerical simulation of semiconductor devices is extremely demanding in term of computational time because it involves complex embedded numerical schemes. At the kernel of these schemes is the solution of very ill-conditioned large linear systems. In this work, we investigate the effects of the various

ingredients of our hybrid iterative schemes that play a central role in the robustness of those solvers when they are embedded in other numerical schemes. On a set of bidimensional unstructured mixed finite-element problems representative of large semiconductor simulations, we perform a fair and detailed comparison between parallel iterative and parallel direct linear solvers. We show that iterative solvers can be robust enough to solve the very challenging linear systems that appear in those simulations. This study greatly benefits from and makes intensive use of MUMPS [33, 34].
A complete description of this work is available in [ALG62, ALG31].

[33] P. R. Amestoy, I. S. Duff, J. Koster, and J.-Y. L'Excellent, (2001), A Fully Asynchronous Multifrontal Solver Using Distributed Dynamic Scheduling, *SIAM Journal on Matrix Analysis and Applications*, **23**, 15–41.

[34] P. R. Amestoy, I. S. Duff, J.-Y. L'Excellent, and X. S. Li, (2001), Analysis, Tuning and Comparison of Two General Sparse Solvers for Distributed Memory Computers, *ACM Transactions on Mathematical Software*, **27**, 388–421.

3.14 Parallel algebraic preconditioners for the solution of Schur complement systems (L. Giraud and S. Mulligan)

Domain decomposition methods are a natural way to parallelize the numerical solution of elliptic partial differential equations for 2D and 3D problems. In this study we consider the parallel solution of a standard finite element discretisation of 3D elliptic problems. The method used is a preconditioned conjugate-gradient solver following [35] on the Schur complement system for the interface unknowns. An additive Schwarz preconditioner is computed which consists of the local assembled Schur complements for each subdomain. These schur complements are computed using the MUMPS [36] package. We also used a sparsified version of this preconditioner, where elements whose relative magnitudes are below a certain tolerance are dropped; this typically results in Cholesky factors that retain only about 10% of the original dense factors.
The methods were implemented on an IBM SP by assigning each sub-domain to a single process and using MPI for the parallel communication. The numerical results have been obtained for a number of model problems, including problems with variable and discontinuous coefficients. The results indicate a good parallel scalability of these methods for 3D problems, in that the convergence rate is not seriously degraded as the number of domains increases. Further tests are being carried out, including comparisons with a direct solver and results will be documented.

[35] L. M. Carvalho, L. Giraud, and G. Meurant, (2001), Local preconditioners for two-level non-overlapping domain decomposition methods, *Numerical Linear Algebra with Applications*, **8**, 207–227.

[36] J.-Y. L. P.R. Amestoy, I.S. Duff and J. Koster, (2003), MUltifrontal Massively Parallel Solver (MUMPS Version 4.3) Users' guide. http://www.cerfacs.fr/algor/Softs/index.html.

3.15 Some complementary investigations in inner-outer iterations (V. Frayssé, L. Giraud and S. Gratton)

Embedded iterative linear solvers are more and more often used in Linear Algebra. An important issue is how to tune the level of accuracy of the inner solver to guarantee the convergence of the outer solver at the best global cost. As a first step towards the challenging goal of controlling embedded linear solvers, inexact Krylov methods are used as a model of inner-outer iterations with an external Krylov scheme. This work aims at completing the pioneering work described in the reports [52, 53] in order to address the symmetric and positive definite situation with Conjugate Gradients as well as further investigate other Krylov methods than GMRES. Various new relaxation strategies have also been considered that are based on polynomials of

the residual norm, while only experiments with the residual norm were reported in the earlier work. Finally the bibliography of the previous paper has been updated to include recent theoretical studies [39, 40] that attempt to explain the observed phenomenon. We notice that these studies were motivated by the earlier version of our work.
The experiments have been integrated into the revised version of [52] submitted to the *SIAM Journal of Matrix Analysis and Applications*.

[37] A. Bouras and V. Frayssé, (2000), A relaxation strategy for inexact matrix-vector products for Krylov methods, Tech. Rep. TR/PA/00/15.

[38] A. Bouras, V. Frayssé, and L. Giraud, (2000), A relaxation strategy for inner-outer linear solvers in domain decomposition methods, Tech. Rep. TR/PA/00/17.

[39] V. Simoncini and D. Szyld, (2002), Theory of Inexact Krylov Subspace Methods and Applications to Scientific Computing, tech. rep., Temple University Report. To appear in SIAM SISC, 2003.

[40] G. L. G. Sleijpen and J. van den Eshof, (2002), Inexact Krylov subspace methods for linear systems, preprint 1224, Dep. Math., University Utrecht.

3.16 A set of GMRES routines for real and complex arithmetics on high performance computers (V. Frayssé, L. Giraud, S. Gratton and J. Langou)

Because the CERFACS public domain GMRES package has become fairly widely used (more than 1000 downloads since December 1997 from all over the world) we decide to make a major release in order to take into account the recent update of the BLAS standard [ALG4] and to introduce a few new features. One of these enables the user to avoid an extra matrix-vector product at each restart. This is of interest when the matrix-vector product is expensive such as in our applications in electromagnatism using a Fast Multipole expansion (see Section 3.7) and in non-overlapping domain decomposition (see Section 3.13).
The associated User's guide [ALG54] has been updated and supersedes [42]. In this report, we describe the implementations of the GMRES algorithm for both real and complex, and single and double precision arithmetics that are suitable for serial, shared memory and distributed memory computers. For the sake of portability, simplicity, flexibility and efficiency the GMRES solvers have been implemented in Fortran 77 using the reverse communication mechanism for the matrix-vector product, the preconditioning and the dot product computations. For distributed memory computation, several orthogonalization procedures have been implemented to reduce the cost of the dot product calculation, that is a well-known efficiency bottleneck for the Krylov methods. Finally, various stopping criteria based on normwise backward error are available.

[41] L. S. Blackford, J. Demmel, J. Dongarra, I. S. Duff, S. Hammarling, G. Henry, M. Heroux, L. Kaufman, A. Lumsdaine, A. Petitet, R. Pozo, K. Remington, and R. C. Whaley, (2002), An updated set of Basic Linear Algebra Subprograms (BLAS), *ACM Transactions on Mathematical Software (TOMS)*, **28**, 135–151.

[42] V. Frayssé, L. Giraud, and S. Gratton, (1997), A Set of GMRES Routines for Real and Complex Arithmetics, Technical Report TR/PA/97/49.

3.17 Combining MPI and OpenMP: application to a finite-element program for acoustics (L. Giraud and M. van Gijzen)

Finite-Element programs are usually parallelized either at a low level by exploiting fine-grain loop parallelism or at a much higher level by exploiting the coarse grain parallelism of a mesh splitting in

a domain decomposition type approach. On clusters of Symmetric Multi-Processors (SMP's) these two approaches can be combined by, on the one hand mapping separate subdomains onto separate nodes, and on the other hand exploiting the loop parallelism within a node.
Following the work described in [ALG13], we have made a combined fine grain/coarse grain parallel implementation of the vectorized, Finite-Element program SIMPLE for ocean-acoustic simulations. We have used OpenMP to parallelize the vectorized loops and MPI to implement communication between nodes.
When solving the linear system, the coarse grain parallelism based on domain decomposition techniques degrades the numerical properties of the preconditioner when the number of subdomains is increased because of the lack of a global mechanism in the preconditioner. As a result, iterative methods like the Conjugate Gradient method take more iterations as the number of subdomains increases. The combination of OpenMP and MPI is of particular interest for reducing the adverse effect of the domain decomposition on the preconditioner. By using OpenMP within each subdomain handled by the nodes, and MPI between the nodes, the number of subdomains can be reduced from the number of processors to the number of nodes. Consequently, the undesired numerical deterioration is alleviated while keeping the number of processors involved in the calculation unchanged. This highlights a situation where mixing Open-MP and MPI enables us to find a satisfactory trade-off between the efficiency of the numerical scheme and the efficiency of the parallel implementation. More details can be found in [ALG57].

3.18 Two level parallelism in a stream-function model for global ocean circulation (M. van Gijzen)

In ocean modelling, it is customary to split the ocean flow into a 2D depth-averaged part, and the 3D deviations from it. The 2D part can be formulated in terms of a stream-function, which simplifies the governing partial differential equations. However, in this formulation additional contour integral conditions around continents are needed. These conditions destroy the structure in the matrix that results after discretisation and pose difficulties to parallelisation. In [ALG70] we describe how the continent boundary conditions can be treated in a parallel setting by taking into account the land points in the calculations. We have implemented our ideas in the model described in [43]. By far the computationally most expensive part of a model calculation is the solution of a linear system of equations. Our iterative solution technique combines loop-level parallelism with a domain decomposition method. The communication between subdomains is implemented with MPI and the loop-level parallelism with OpenMP. Realistic numerical experiments on a cluster of bi-processor PC's using field data show superlinear performance, which can be attributed to a better use of the cache memory. Moreover, the performance of the mixed OpenMP/MPI method is noticeably better than for a pure MPI approach.

[43] M. B. van Gijzen, C. B. Vreugdenhil, and H. Oksuzoglu, (1998), The finite element discretization for stream-function problems on multiply connected domains, *J. Comput. Phys.*, **140**, 30–46.

3.19 Efficient CFD calculations on clusters of SMPs (J. F. Boussuge, S. Champagneux, G. Chevalier, L. Giraud, F. Loercher and M. Montagnac)

Based on our experience on high performance scientific platforms and their associated programming techniques [ALG13] we have studied how the code elsA [44] can efficiently exploit clusters of SMPs. In particular, we investigate techniques that avoid some of the penalizing effects of the memory hierarchy (cache or TLB) and also combine MPI and Open-MP in the context of this multi-block solver. The results of this work will be presented at the forthcoming ECCOMAS 2004 conference.

[44] L. Cambier and M. Gazaix, (2002), elsA: an efficient object-oriented solution to CFD complexity, In *40th AIAA Aerospace Science Meeting & Exhibit, Reno*, AIAA Paper 2002-0108, 14–17.

3.20 Experiments on sparse matrix partitioning (S. Riyavong)

We have undertaken experiments to determine the comparative quality of four graph partitioners: PaToH [45, 46], hMeTiS [49], Mondriaan [50], and Monet [48] with application to sparse matrix partitioning. A large selection of application-driven matrices from the Rutherford-Boeing Collection [51] are partitioned and then permuted so that the resulting form exhibits block structures. This form is useful for implementing sparse matrix-vector multiplication in a parallel computing environment where each block will be assigned to a single computing node. The details will be given in a working note.

[45] U. V. Çatalyürek and C. Aykanat, (1999), Hypergraph-partitioning-based decomposition for parallel sparse-matrix vector multiplication, *IEEE Transaction on Parallel and Distributioned Systems*, **10**, 673–693.

[46] U. V. Çatalyürek and C. Aykanat, (2002), PaToH: Partitioning Tools for Hypergraphs. The manual, http://www.cs.umd.edu/umit/software.htm.

[47] I. S. Duff, R. G. Grimes, and J. G. Lewis, (1997), The Rutherford-Boeing Sparse Matrix Collection, Tech. Rep. TR/PA/97/36, CERFACS, Toulouse, France. Also Technical Report RAL-TR-97-031 from Rutherford Appleton Laboratory and Technical Report ISSTECH-97-017 from Boeing Information & Support Services.

[48] Y. F. Hu, K. C. F. Maguire, and R. J. Blake, (2000), A multilevel unsymmetric matrix ordering algorithm for parallel process simulation, *Computers and Chemical Engineering*, **23**, 1631–1647.

[49] G. Karypis and V. Kumar, (1998), hMeTiS: A Hypergraph Partitioning Package version 1.5.3. The manual, http://www-users.cs.umn.edu/ Karypis/metis/hmetis.

[50] B. Vastenhouw and R. H. Bisseling, (2002), A two-dimensional data distribution method for parallel sparse matrix-vector multiplication, preprint 1238, Utrecht University.

3.21 Experiments on parallel matrix-vector products (S. Riyavong)

We designed and implemented a data structure appropriate for computing the matrix-vector product efficiently on distributed computing environments using MPI. Experiments with GMRES [ALG54] have been performed with sparse matrices selected from the Rutherford-Boeing Collection [51]. Numerical results on a COMPAQ and a cluster of PCs show a satisfactory performance and scalability. The details are given in the working note [ALG66].

[51] I. S. Duff, R. G. Grimes, and J. G. Lewis, (1997), The Rutherford-Boeing Sparse Matrix Collection, Tech. Rep. TR/PA/97/36, CERFACS, Toulouse, France. Also Technical Report RAL-TR-97-031 from Rutherford Appleton Laboratory and Technical Report ISSTECH-97-017 from Boeing Information & Support Services.

4 Qualitative Computing

Françoise Chaitin-Chatelin

The work of the Qualitative Computing Group is a collaborative effort to assess the validity of computer simulations. The central question is to give meaning to computer results which are seemingly wrong such as in chaotic computations. This goal can be reached by discovering the laws of computation which govern finite-precision computations in the neighbourhood of singularities.

Some of these laws are now well understood. For example, one can cite i) the role of the normwise backward error to assess the reliability of numerical software in finite precision, ii) the role of nonnormality which makes approximated singularities appear much closer than they are in exact arithmetic.

A number of fundamental laws have been discovered, which are the focus of attention for the Group. These laws concern in particular:

a) *inexact computing* and the associated homotopic deviation theory as a fruitful framework to understand approximate numerical methods, in exact arithmetic,

b) the unreasonable robustness of Krylov-type methods to perturbations in the data,

c) the (underestimated) role of Geometry in Scientific Computing.

Our research and understanding is vitally nourished by work on practical numerical software applications in Physics and Technology, which come from CERFACS partners. We review below the work accomplished in 2003 in five related areas.

4.1 Inner-outer iterations (F. Chaitin-Chatelin, G.L.G. Sleijpen, J. van den Eshof and M. van Gijzen)

There are classes of problems for which the matrix-vector product is a time consuming operation because an expensive approximation method is required to compute it to a given accuracy. Obviously, the more accurately the matrix-vector product is computed the more expensive or time consuming the overall process becomes. The question of how to control the accuracy of the matrix-vector product if the outer loop is a Krylov method has been extensively investigated at CERFACS [52, 53]. This work has led to the development of so called *relaxation strategies* in which the accuracy to which the matrix-vector multiplication is computed is reduced when the process comes closer to the solution. These results have attracted the attention of several other groups [55, 56].

The relaxation strategies have been proved to be an effective tool for various problems, see for example [54] for an industrial application. Typically a reduction in computing time between 20% and 50% can be obtained. In order to obtain a further reduction we have studied, in collaboration with the Numerical Mathematics group at the University of Utrecht, the combination of a relaxation strategy with so called flexible Krylov methods for the solution of linear systems of equations. A flexible Krylov subspace method allows a variable preconditioner. The preconditioning operation can for such a method be performed by applying a Krylov method like GMRES. In the preconditioning operation, GMRES only has to yield an approximate solution of the system, so at this level only a low accuracy is required. In such a nested Krylov

method, a relaxation strategy can be employed both at the outer level (the flexible Krylov method) and at the inner level (the preconditioning operation performed with GMRES).
We have analysed this nested approach for several flexible Krylov methods. We have experimentally verified the efficiency of this computational scheme with a Schur complement system that arises in the modelling of global ocean circulation. If we solve this system with GMRES we gain a factor of two by applying a relaxation strategy. If we combine this with a nested GMRES method (FGMRES or GMRESR) we gain an additional factor of five, thus yielding an overall improvement of performance of a factor of ten. The results are reported in [ALG68].

[52] A. Bouras and V. Frayssé, (2000), A relaxation strategy for inexact matrix-vector products for Krylov methods, Technical Report TR/PA/00/15, CERFACS, Toulouse, France. Submitted to SIAM Journal in Matrix Analysis and Applications.

[53] A. Bouras, V. Frayssé, and L. Giraud, (2000), A relaxation strategy for inner-outer linear solvers in domain decomposition methods, Technical Report TR/PA/00/17, CERFACS, Toulouse, France.

[54] F. Chaitin-Chatelin and T. M. skauskas, (2001), Inner-Outer ierations for mode solvers in structural mechanics: application to the Code Aster, Tech. Rep. TR/PA/01/85, CERFACS, Toulouse, France.

[55] V. Simoncini and D. B. Szyld, (2003), Theory of Inexact Krylov Subspace Methods and Applications to Scientific Computing, *SIAM J. Sci. Comput.*, **25**, 454–477.

[56] J. van den Eshof and G. L. G. Sleijpen, (2002), Inexact Krylov subspace methods for linear systems, Preprint 1224, Dep. Math., University Utrecht, Utrecht, the Netherlands. Submitted.

4.2 Inexact computing and homotopic deviation (F. Chaitin-Chatelin and M. van Gijzen)

To study the robustness of approximation methods to large perturbations, it is useful to consider the linear coupling $\mathbf{A} + t\mathbf{E}$, where $\mathbf{A}, \mathbf{E} \in \mathbb{C}^{n\times n}$ and the parameter $t \in \mathbb{C}$.
The variation of the spectrum of linear operators and matrices under the influence of one or several parameters has long been an active domain of research, giving rise to the elegant analytic/algebraic spectral theory initiated by Puiseux. The case of a linear dependence on a parameter $t \in \mathbb{C}$, of the form $\mathbf{A}(t) = \mathbf{A} + t\mathbf{E}$ has been particularly studied [62, 63, 64]. See also [57, 58, 66].
In the 1990's, there has been a renewed interest for the topic amongst numerical analysts, coming form the widespread availability of graphical tools, as exemplified by Trefethen [67], Simoncini [66], and Chaitin-Chatelin and co-workers [59, 61, 60]. In particular, the easy access to plots of parameterised computed spectra of matrices make it possible to explore computationally the spectral maps $t \to \lambda(t) \in \sigma(\mathbf{A}(t))$, the spectrum of $\mathbf{A}(t)$, that is the set of eigenvalues of $\mathbf{A}(t)$. They are the singularities of the resolvent field $z \to \mathbf{R}(t, z) = (\mathbf{A} + t\mathbf{E} - z\mathbf{I})^{-1}$
For any $t \in \mathbb{C}$, $\mathbf{R}(t, z)$ is defined for all z in the resolvent set $re(\mathbf{A}) = \mathbb{C}\backslash\sigma(\mathbf{A})$, as long as z is not an eigenvalue of $\mathbf{A}(t) = \mathbf{A} + t\mathbf{E}$. The analyticity of $t \to \mathbf{R}(t, z)$ is guaranteed for $|t| < 1/\rho(\mathbf{E}(\mathbf{A} - z\mathbf{I})^{-1})$, where $\rho(.)$ denotes the spectral radius. What can be said beyond, for $|t| \geq 1/\rho(\mathbf{E}(\mathbf{A} - z\mathbf{I})^{-1})$?
We exclude the degenerate case where $\sigma(\mathbf{A}(t)) = \sigma(\mathbf{A})\ \forall t \in \mathbb{C}$. Then there are at most n different matrices $\mathbf{A}(t_i), i = 1, \cdots, n$, such that $z \in \sigma(\mathbf{A}(t_i))$ for any z in $re(\mathbf{A})$: $\mathbf{R}(t, z)$ exists for almost all $t \in \mathbb{C}$. The connection between z and t which makes $\mathbf{R}(t, z)$ singular is central in our investigation.
When $\mathbf{E}$ is regular, $\lim_{|t|\to\infty} \mathbf{R}(t, z) = 0$ and for all n eigenvalues $\lambda(t)$ of $\mathbf{A}(t), |\lambda(t)| \to \infty$. However, when $\mathbf{E}$ has rank r, $1 \leq r < n$, two new phenomena occur. Firstly, when $\lim_{|t|\to\infty} \mathbf{R}(t, z) = \mathbf{R}(\infty, z)$ exists, it is *nonzero* and *computable* in *closed form*. Secondly, certain eigenvalues $\lambda(t)$ may remain at a finite distance in the limit of $|t| \to \infty$. Among the points in $re(\mathbf{A})$ where $\mathbf{R}(\infty, z)$ does not exist, there are finitely many *kernel* points which are the limit of $\lambda(t)$ as $|t| \to \infty$. Moreover, it is possible that among these kernel points there exist *critical* ones for which z cannot be an eigenvalue of $\mathbf{A}(t)$ for any finite t. At a critical point, the resolvent $\mathbf{R}(t, z)$ is a polynomial in t of degree $\delta \leq r$.

The properties of $\mathbf{R}(t,z)$ and of $\sigma(\mathbf{A}(t))$ in the limit $|t| \to \infty$ depend on the Jordan and Frobenius structures of $0 \in \sigma(\mathbf{E})$. An account of the complete theory of Homotopic Deviation is in [ALG46, ALG47, ALG48].

Homotopic Deviation is a specialized version of more general problems in Matrix and Linear Operator Theory, usually analysed by analytic spectral theory, which often puts a limit to $|t|\|\mathbf{E}\|$, or by algebraic geometry on the spectral variety $(t,z) \to det(\mathbf{A}+t\mathbf{E}-z\mathbf{I}) = 0$, where (t,z) describe $\mathbb{C}^2$. A third approach for such problems, stimulated by linear systems theory, consists of the theory of (nonmonic) matrix polynomials.
In Homotopic Deviation theory, we specifically look beyond analyticity in t, for $|t|$ large enough. Our tools are elementary linear algebra, based on the Jordan structure of $0 \in \sigma(\mathbf{E})$. The rank deficient matrix $\mathbf{E}$ is called the $deviation$, and the term "perturbation" covers the case where $|t|\|\mathbf{E}\|$ is limited, $\mathbf{E}$ being possibly of full rank. Our work provides an elementary analysis for $z, t \in \bar{\mathbb{C}} = \mathbb{C} \cup \infty$ of singular perturbation theory for matrices, since $\mathbf{E}$ is singular in the case of interest. To the best of our knowledge, the study of $\mathbf{R}(t,z)$ and $\lambda(t)$ as $|t| \to \infty$ has been, so far, scattered in the literature. We believe that the notion of kernel/critical points is new [ALG48].
The elementary approach of Homotopic Deviation is driven by algorithmic considerations arising from the Sherman-Morrison formula. The key role of the structure of $0 \in \sigma(\mathbf{E})$ emerges naturally from the computational perspective; see [ALG48] for an application to Arnoldi's algorithm, where $\mathbf{E}$ is nilpotent (see also 4.4). Homotopic Deviation tries to make the best use of the extreme simplicity of the matrix setting to present results which are specific to the $linear$ coupling $\mathbf{A}(t) = \mathbf{A} + t\mathbf{E}$, leading to computational insight for numerical software. The following two articles present two different applications of homotopic deviation.

[57] R. Alam and S. Bora, (2003), Effect of linear perturbation on spectra of matrices, *Linear Algebra and its Applications*, **368**, 329–342.

[58] R. Alam and S. Bora, (2003), Stability of eigenvalues and spectral decompositions under linear perturbation, *Linear Algebra and its Applications*, **364**, 189–211.

[59] F. Chaitin-Chatelin and V. Frayssé, (1996), *Lectures on Finite Precision Computations*, SIAM, Philadelphia.

[60] F. Chaitin-Chatelin and E. Traviesas, (2001), Homotopic perturbation - Unfolding the field of singularities of a matrix by a complex parameter: a global geometric approach, Technical Report TR/PA/01/84, CERFACS, Toulouse, France.

[61] F. Chaitin-Chatelin, V. Toumazou, and E. Traviesas, (2000), Accuracy assessment for eigencomputations: variety of backward errors and pseudospectra, *Linear Algebra and its Applications*, **309**, 73–83.

[62] F. Chatelin, (1983), *Spectral approximation of linear operators*, Academic Press, New York.

[63] F. Chatelin, (1988), *Valeurs propres de matrices*, Masson, Paris.

[64] F. Chatelin, (1993), *Eigenvalues of matrices*, Wiley, Chichester. enlarged translation of *Valeurs propres de matrices*, F. Chaitin-Chatelin, 1988, Masson, Paris.

[65] M. Ochmann and F. Mechel, (2002), Analytical and Numerical Methods in Acoustics, In *Formulas of Acoustics*, F. Mechel, ed., Springer Verlag.

[66] V. Simoncini, (1999), Remarks on nonlinear spectral perturbation, *BIT*, **39**, 350–365.

[67] L. N. Trefethen, (1997), Pseudospectra of linear operators, *SIAM Review*, **39**, 383–406.

4.3 Quadratic eigenproblems, an example in computational acoustics (F. Chaitin-Chatelin and M. van Gijzen)

In the basic Homotopic Deviation the matrix $\mathbf{A} + t\mathbf{E} - z\mathbf{I}$ depends linearly on the parameters t and z. The analysis can be extended straightforwardly to a polynomial dependence in z. For example, the quadratic case $z^2\mathbf{M}+zt\mathbf{C}+\mathbf{K}$, where $\mathbf{M}$ is regular, is treated in [ALG43, 68] for a problem arising in computational acoustics. It concerns the discrete wave equation with an impeding boundary condition controlled by the complex impedance ζ [69]. The condition becomes Neumann (resp. Dirichlet) as $|\zeta| \to \infty$ (resp 0) [70]. The homotopy parameter t is taken to be $t = 1/\zeta$. The Homotopic Deviation theory, combined with the properties of the continuous wave equation allows us to give the *kernel points* in *closed form* as eigenvalues of the discrete Dirichlet problem. We also specify which of them are *critical*. We are able to prove that the degree δ of the polynomial $\mathbf{R}(t, z)$ is $\delta = 1$ for the critical points. Ample numerical illustrations are provided in [ALG43, 68].

[68] F. Chaitin-Chatelin and M. B. van Gijzen, (2004), Homotopic Deviation with an application to Computational Acoustics, Technical Report TR/PA/04/05, CERFACS, Toulouse, France. Submitted.

[69] M. V. Gijzen, (1999), The parallel computation of the smallest eigenpair of an acoustic problem with damping, *Int. J. Numer.Meth. Engng.*, **45**, 765–777.

[70] M. Ochmann and F. Mechel, (2002), Analytical and Numerical Methods in Acoustics, In *Formulas of Acoustics*, F. Mechel, ed., Springer Verlag.

4.4 Robustness of Krylov type methods (F. Chaitin-Chatelin and M. van Gijzen)

We approach this question by considering an iterative Krylov method as an inner–outer iteration. The outer loop modifies the starting vector for the construction of the Krylov basis. The inner loop is a direct method which consists of an incomplete Arnoldi decomposition of size $k << n$ [72, 71]. To study the dynamics of this 2-level algorithm, we perform a homotopic deviation of the matrix of order $k+1$

$$\mathbf{B} = \begin{pmatrix} \mathbf{H_k} & \mathbf{u} \\ 0 & a \end{pmatrix},$$

such that

$$\mathbf{H}_{k+1} = \begin{pmatrix} \mathbf{H_k} & \mathbf{u} \\ 0 \; h_{k+1,k} & a \end{pmatrix}.$$

The homotopy parameter is $h = h_{k+1,k} \in \mathbb{C}$ and the deviation matrix is $\mathbf{E} = \mathbf{e}_{k+1}\mathbf{e}_k^T$. $\mathbf{E}$ is nilpotent ($\mathbf{E}^2 = 0$), with $\sigma(\mathbf{E}) = \{(0^1)^{k-1}, (0^2)\}$. For k fixed, $1 < k < n$, we set $\mathbf{H}^- = \mathbf{H}_{k-1}, \mathbf{H} = \mathbf{H}_k, \mathbf{H}^+ = \mathbf{H}_{k+1}$. The three matrices represent the sections of order $k-1, k, k+1$ for the Hessenberg matrix constructed from $\mathbf{A}$ by the iterative Arnoldi process.
A complete analysis of $h \mapsto \{(\mathbf{H}^+ - z\mathbf{I})^{-1}, \sigma(\mathbf{H}^+)\}$ is performed in [ALG47]. This is the first step in our study. The second step will relate the algebraic properties present in the inner loop to the quality of the convergence of the outer loop [73].

[71] F. Chaitin-Chatelin, E. Traviesas, and L. Plantié, (2000), Understanding Krylov methods in finite precision, Tech. Rep. TR/PA/00/40, CERFACS, Toulouse, France. Also in Proceedings of the Second Conference on Numerical Analysis and Applications, Rousse, Bulgaria, Springer, pp. 187–197.

[72] F. Chaitin-Chatelin, (2000), Comprendre les méthodes de Krylov en précision finie : le programme du Groupe Qualitative Computing au CERFACS, Technical Report TR/PA/00/11, CERFACS.

[73] F. Chaitin-Chatelin, (2004), Robustness of Krylov type methods, Technical Report, CERFACS, Toulouse, France. In preparation.

4.5 Geometric aspects of computing (F. Chaitin-Chatelin)

In conventional scientific computing, the four arithmetic operations (+, -, $\times$, /) are usually defined on scalars or real numbers, that is 1D vectors. Linear algebra is performed on matrices and vectors of

potentially very large dimension, but the numbers themselves are either real scalars (1 dimension) or complex scalars (2 dimensions). Hypercomplex scalars are usually not used in numerical linear algebra. However, it is known since the days of Hamilton and Graves that one can multiply and divide real vectors of dimension 2^k, $k = 0, 1, 2, \ldots$, which define algebras of hypercomplex numbers. This requires introducing an additional geometric operation, the conjugation. These five operations define the arithmetic-geometric core of nature's computation. For example, the laws of classical mechanics and of Maxwell's electromagnetism can be written most efficiently by using products of quaternions, which are 4D vectors. The real component can be interpreted as time and the three imaginary components as space [74, ALG45].
The first four real hypercomplex algebras A_k, which are isometric, are well known: $A_0 = \mathbb{R}, A_1 = \mathbb{C}, A_2 = \mathbb{H}$ (quaternions) and $A_3 = \mathbb{G}$ (octonions). By comparison the corresponding four binary algebras B_k on $\mathbb{Z}_2 = \{0, 1\}$ are hardly known [ALG50, ALG45, ALG44]. $B_1 \sim \mathbb{Z}_4$ is given an important interpretation related to quantum computing on qu-bits (i.e. quantum bits): the logical gate $\sqrt{\mathbf{not}}$ is a rotation of angle $\pi/2$ [ALG45].
Real hypercomplex algebras A_k are studied in [ALG49] in the light of the dominant role of multiplication over addition, which is experienced in ”real life” scientific computing - See the fundamental Borel-Newcomb paradox about the role of the first digit of a number chosen at random [ALG50]. This leads to the study of the hypercomplex exponential on A_k, for $k \geq 2$. The Euler identity $e^{2ik\pi} = 1$ for $k \in \mathbb{Z}$ is extended to Pythagorean triples $(n, m, q) \in \mathbb{N}^*$ such that $n^2 + m^2 = q^2$, in order to insure the commutativity $e^{x+y} = e^x \times e^y = e^y \times e^x$ for a given $x \in Im\ A_k, y \in Im\ A_k$. For $k \geq 4$, the presence of zero divisors allows us to have commutativity in continuous and finite modes at the same time. By comparison, for $k = 2$ (quaternions) or 3 (octonions) the two modes are mutually exclusive [ALG49].

[74] F. Chaitin-Chatelin, (1999), The computing power of Geometry, In *Numerical Analysis 1999*, D. Griffiths and G. Watson, eds., CRC Press LCC, 83–92. also Cerfacs Report TR/PA/99/24.

5 Nonlinear Systems and Optimization

5.1 Out-of-core solvers for large dense linear least squares (M. Baboulin, L. Giraud and S. Gratton)

The long term objective of our work is to design a least-squares solver with out-of-core capabilities to tackle very large problems on distributed memory computers with two features that will make the code original compared with exisiting public domain software [76, 77]:

1. computation of some parts of the covariance matrix $\left(A^T A\right)^{-1}$,
2. possibility of carrying out incremental solutions, i.e. of updating the solution after appending a set of rows to A and b.

For the sake of the numerical robustness of the code, we plan to use orthogonal transformations. However, we decided to start with a normal equation implementation of the code because we believe that this first step will enable us to become more familiar with some aspects of out-of-core solvers such as the efficient use of I/O systems on various platforms.
So far we have designed a parallel code that computes the upper-triangular part of the normal equation matrix $A^T A$ and the right-hand side $A^T b$, mixing OpenMP and MPI. A sustained Megaflops rate close to the peak performance on each processor has been obtained on various architectures including an IBM Regatta and a quadri-processor Itanium II.
We have also developed a parallel distributed implementation of a linear solver for large-scale applications involving real symmetric or complex symmetric non Hermitian dense systems. The main advantage of this routine is that it performs a Cholesky factorization by requiring half the storage needed by the standard parallel libraries ScaLAPACK or PLAPACK. Our solver uses a left-looking algorithm and a one-dimensional block-cyclic column data distribution but gives similar Megaflops performance when applied to problems that can be solved on moderately parallel computers with up to 32 processors. Experiments and performance comparison with ScaLAPACK on our target applications are presented in [75]. These applications arise from the Earth's gravity field recovery and computational electromagnetics.
However, it is also necessary to assess the normal equation approach and, in this respect, we are investigating the use of a condition number estimate in our Cholesky algorithm.

[75] M. Baboulin, L. Giraud, and S. Gratton, (In preparation), A parallel distributed solver for large dense symmetric systems: applications to geodesy and electromagnetism problems, tech. rep., CERFACS, Toulouse, France.

[76] L. S. Blackford, J. Choi, A. Cleary, E. D'Azevedo, J. Demmel, I. Dhillon, J. Dongarra, S. Hammarling, G. Henry, A. Petitet, K. Stanley, D. Walker, and R. C. Whaley., (1997), *ScaLAPACK Users' Guide*, SIAM.

[77] R. A. V. de Geijn, (1997), *Using PLAPACK*, The MIT Press.

5.2 Iterative techniques in variational data assimilation (L. Giraud, S. Gratton and A. T. Weaver)

In this work, we intend to develop and study algorithms for nonlinear least-squares, with a particular focus on large-scale data assimilation problems arising in oceanography. In the framework of an ocean incremental variational assimilation algorithm [83], we define the nonlinear functional J by

$$J(x_0) = \frac{1}{2}(x_0 - x_b)^T B^{-1}(x_0 - x_b) + \frac{1}{2}\sum_{i=0}^{N} \left(\mathcal{H}_i(x(t_i)) - y_i\right)^T R_i^{-1} \left(\mathcal{H}_i(x(t_i)) - y_i\right),$$

where $x(t) = \mathcal{M}(t, t_0)(x_0)$, and the operators $\mathcal{H}$ and $\mathcal{M}(t, t_0)$ are nonlinear. The functional J can be rewritten as a nonlinear least-squares problem $\min_{x_0} \|F(x_0)\|$. This property is exploited in operational data assimilation systems, since J is usually minimized using an inexact Gauss-Newton algorithm named "Incremental 4D-Var algorithm". The target applications are problems for which the size of the unknown vector x_0 is typically several millions : the only viable methods to solve the linear least squares arising in the Gauss-Newton are Conjugate Gradient type iterative method such as CGNE, CGLS, or LSQR [78, 79, 81] algorithm.

A study of the convergence properties of inexact Gauss-Newton is carried out in [80]. We consider the case where the Jacobian of the function F is perturbed. We derive a convergence result for the inexact algorithm, and show the relevance of this analysis in a test case where the data are assimilated in a one-dimensional shallow water system representing the flow of a fluid over an obstacle in the absence of rotation. A key parameter to understand the behaviour of the Inexact Gauss-Newton algorithm is the order of magnitude of F at the optimum, which is also an indicator of the level of noise in the data assimilation system. In the numerical experiments, the exact Jacobian is obtained using an automatic differentiation technique, the inexact one is obtained by solving a linearized shallow water equation using a semi-implicit semi-Lagrangian discretization scheme.
In ocean data assimilation, the computational cost of some of the matrix-vector evaluations is extremely high. In that respect, re-orthogonalization strategies in CG or LSQR become effective and affordable. Such techniques have already been used in other applications occurring in structural mechanics [82], and numerical weather forecasting [79]. In this work, we have considered an extension of these techniques that improve the convergence of Conjugate Gradient type algorithms when a sequence of slowly varying linear least-squares problems are considered.

[78] A. Bjorck, T. Elfving, and Z. Strakos, (1998), Stability of conjugate gradient and Lanczos methods for linear least squares problems, *SIAM J. Matrix Anal. Appl.*, **19**, 720–736.

[79] M. Fisher, (1998), Minimization Algorithms for Variational Data Assimilation, In *Proc. ECMWF Seminar "Recent Developments in Numerical Methods for Atmospheric Modelling", 7-11 Sept. 1998*, 364–385.

[80] A. S. Lawless, S. Gratton, and N. K. Nichols, (2004), An investigation of incremental 4D-Var using non-tangent linear models, tech. rep. In préparation.

[81] C. C. Paige and M. A. Saunders, (1982), Algorithm 583; LSQR: Sparse linear equations and least-squares problems, *ACM TOMS*, **8(2)**, 195–209.

[82] F. X. Roux, (1990), Acceleration of the outer conjugate gradient by reorthogonalisation for a Domain Decomposition Method for structural analysis problems, In *Proc. of the third international symposium on Domain Decomposition Methods*, SIAM.

[83] A. T. Weaver, J. Vialard, and D. L. T. Anderson, (2003), Three- and four-dimensional variational assimilation with a general circulation model of the tropical Pacific Ocean. Part 1: formulation, internal diagnostics and consistency checks, *Monthly Weather Review*, **131**, 1360–1378.

5.3 Techniques for the regularisation of discrete rank-deficient least-squares problems (E. Anterrieu and S. Gratton)

The solution of least-squares problems, with a very ill-conditioned coefficient matrix, is likely to be contaminated by many error sources, such as rounding errors or noise in the data.

However, for some applications, the solution can be stabilized by introducing appropriate a priori information, which takes for instance the form of a penalty added to the least-squares criterion in the Tikhonov regularization.
We compare three regularization strategies, S_1, S_2 and S_3, on an inverse problem arising in the reconstruction of the brightness temperature by a band-limited space-borne instrument in the framework of the SMOS (Soil Moisture and Ocean Salinity) project. Our formulation leads to an under-determined linear least-squares problem, where the coefficient matrix and the right-hand side are both complex, but whose solution should be real because of the physical properties of the problem. In Strategy S_1 the *real* solution of minimum norm is computed using a decomplexification of the problem and an SVD on a real matrix. Strategy S_2 [84, 85] makes use of the band property to give a full rank linear least-squares problem in real arithmetic that is solved using orthogonal transformations. The third strategy S_3 is based on a truncated singular value decomposition. These strategies are compared using simulated data that are perturbed using a zero mean Gaussian noise whose covariance is obtained from a physical model of the instrument. It follows [85, 86] from the simulations that S_2 and S_3 are superior to S_1 in the sense that the perturbations on the solution resulting from perturbations of the data are smaller for S_2 and S_3 than for S_1. To confirm these results, we have performed a first order analysis. One of the contributions of this work is the derivation of a first order analysis and of an expected condition number [87, p.136] for the truncated SVD solution.

[84] E. Anterrieu, (2003), A resolving matrix approach for synthetic aperture imaging radiometers. Submitted to IEEE Transaction on Geoscience and Remote Sensing.

[85] S. G. E. Anterrieu and B. Picard, (2003), Inverse problem in remote sensing by aperture synthesis imaging. Accepted in TS, the french journal of signal processing.

[86] S. G. E. Anterrieu and B. Picard, (2003), Self characterization of modelling parameters for Synthetic Aperture Imaging Radiometers, Toulouse (France), 3052–3054. Proc. International Geoscience And Remote Sensing Symposium (IGARSS'03).

[87] N. J. Higham, (2002), *Accuracy and Stability of Numerical Algorithms*, Society for Industrial and Applied Mathematics, Philadelphia, PA, USA, second ed.

5.4 Algorithmic and computational techniques for solving large scale sparse linear programming problems using the revised simplex method (J. Hall)

Based on my experience with asynchronous variants of the revised simplex method, I developed at CERFACS SYNPLEX-MI, a strategy for exploiting parallelism within the revised simplex method when using minor iterations of the standard simplex method. When implemented in parallel on a shared memory multiprocessor, this synchronous algorithm should address the two major drawbacks of the asynchronous algorithms which I have implemented previously. Limited experiments carried out on the CERFACS 32-processor SGI Origin 2000 machine suggest that one potential limitation of parallel revised simplex algorithms on shared memory machines will not restrict the performance of SYNPLEX-MI.

The phenomenon of hyper-sparsity in the context of linear systems of equations occurs when the solution (for a sparse right-hand-side) is sparse. Given a decomposition of the matrix as a product of elementary (Gauss-Jordan) elimination matrices, in the presence of hyper-sparsity the Gilbert-Peierls algorithm is commonly used to determine which very small subset of these elementary matrices needs to be applied. Whilst at CERFACS, I implemented the Gilbert-Peierls algorithm for use in the context of the revised simplex method for linear programming. This led to the development of specialist variants of the algorithm which are better adapted to this context.

The branch-and-price algorithm for solving (Mixed)-Integer Programming (MILP) problems requires each of several small MILP sub-problems to be solved (using traditional branch-and-bound) many times. Each instance of a given MILP problem differs only in the coefficients of the objective. The branch-and-bound trees for a given MILP sub-problem are very similar in each instance and, typically, the optimal solution to a node from the previous instance remains optimal. Huge computational savings can be made if the cost of solving each node is reduced to checking optimality of the previous solution and, if necessary, performing the few simplex iterations to obtain the optimal solution. This requires very close integration of the branch-and-bound and LP solvers. I have developed data structure manipulation routines for my revised simplex solver so that this can be achieved. Based on experience so far and expected further efficiency gains, we predict that, for our practical problems of interest, the resulting branch-and-price solver will be orders of magnitude faster than a leading commercial MILP solver.

6 Signal and Image Processing

6.1 Phase Closure Imaging and Differential GPS - Local minima of related objective functionals (A. Lannes)

As recently established by the signal team, the nearest lattice point problems arising in Phase Closure Imaging (PCI) and in Differential GPS (DGPS) share a common feature. Their statement appeals to elementary notions of algebraic graph theory: vertices, edges, spanning trees, cycles, related spaces and operators. In both cases, the original data are defined on the edges of the graph to be considered (see Figure 6.1). These data are biased by differences between unknown terms that take their values on the vertices of the graph: phase shifts in interferometry and clock offsets in GPS. The effective data are then closure terms in the sense of Kirchhoff: the sums of the original data on the directed edges of the n cycles defined by the choice of a spanning tree (see Figure 6.1). Clearly, the closure data are not biased. The original phase data are defined modulo 2π in interferometry, or modulo the carrier wavelengths in GPS. The "closure integers" involved in the related nearest lattice point problems (see Figure 6.2) are associated with these cycles.

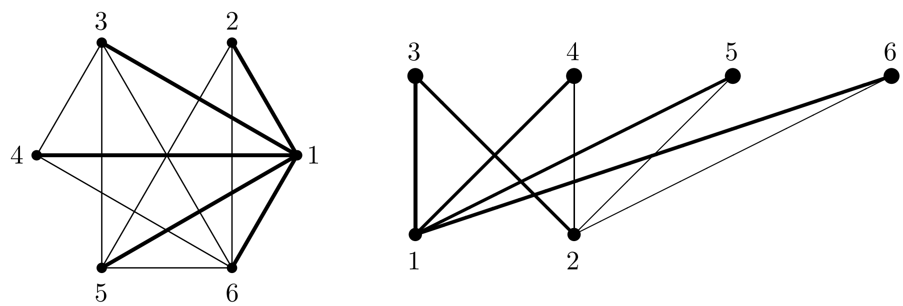

Figure 6.1: Example of interferometric and GPS graphs (left and right, respectively). The vertices of the first one are the pupil elements of aperture synthesis device (here, 6 telescopes or 6 antennas). The lacking edges correspond, for example, to the baselines for which the modulus of the Fourier transform of the object is in the noise. The vertices of the second are the receivers and the satellites of the GPS device (here 2 receivers and 4 satellites). The signals emitted by a satellite are received by each receiver, hence the lacking edges. The edges shown as thicklines correspond to a spanning tree which can be selected in an arbitrary manner. The edges that do not lie to this tree are referred to are cycle entry edges. Here, their number, n, is equal to 7 for the interferometric graph and to 3 for the GPS graph.

The PCI and DGPS spinoffs of this approach are presented below. They essentially derive from the fact that the Moore-Penrose pseudo-inverse of the closure operator is basically involved in the related analysis. Indeed, via this pseudo-inverse, it is possible to have access to the phase residuals associated with the secondary minima of the objective functional to be minimized [88, 89].

6.1.1 Phase Closure Imaging

In radio imaging and optical interferometry, the phase calibration problem is usually stated and solved at the level of the complex amplitudes, i.e., in more technical terms, at the chord level. Then, the only way

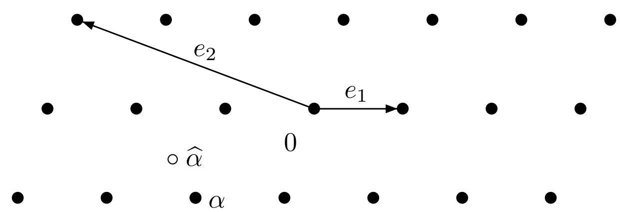

Figure 6.2: Nearest lattice point problem. In the special case shown here, where n is equal to 2, the lattice is generated by the vectors e_1 and e_2 which are parameters of the problem. Given some point $\widehat{\alpha}$ of $\mathbb{R}^2$, endowed here with the Euclidean inner product, the problem is to find the lattice point α closest to $\widehat{\alpha}$. One then speaks of "integer ambiguity resolution." In most cases encountered in pratice, n is less than or of the order of 100.

to be convinced that the solution is unique (or not) is to initialize the corresponding nonlinear optimization procedures in a random manner. This uncertain approach can be avoided by stating and analyzing the problem at the level of the phases, i.e., at the arc level. This essentially derives from the fact that the minima of the phase calibration functional (the arc functional) can be determined, in a systematic manner, by resolving a related integer ambiguity problem (see Figure 6.2). As expected, a minimum of the arc functional is often associated with a minimum of the chord functional. In the framework of the analysis developed at CERFACS, these "significant minima," and the related instabilities, can easily be identified [ALG19, 89, ALG20]. From a practical point of view, the arc approach is also preferable. Indeed, in most situations encountered in practice, the solution of the problem is then simply obtained by solving a linear equation.

6.1.2 Differential GPS

The fact that the standard deviations of the original GPS phase data are small against the carrier wavelengths suggests that a certain constraint should be imposed on the integers involved in the original phase equations. In the framework of the dual algebraic approach developed at CERFACS [ALG17] a related objective functional is then introduced. This single-epoch DGPS functional, f, depends only on a set of real variables: the variable of physical interest β (position, ionospheric DGPS terms), and the clock offset bias ϕ. In the corresponding optimization problem, each minimum of $f(\beta, \phi)$ proves to be associated with some point of the DGPS ambiguity lattice $\mathbb{Z}^n$ (see Figure 6.2). These points are the points of $\mathbb{Z}^n$ contained in some bounded convex subset of $\mathbb{R}^n$. The properties of this "minima confinement set" have been thoroughly analyzed [ALG18, 88]. In the process of finding a reliable physical solution for the optimal DGPS ambiguity point, it is crucial to identify the epochs for which the reference physical modelling is not acceptable. As indicated in [ALG18, 88], the CERFACS approach suggests that new data validation criteria should be considered.

[88] A. Lannes, (2003), Local minima of the single-epoch DGPS objectif functional. Data validation tests, *submitted to the Journal of Geodesy*.

[89] A. Lannes, (2003), Phase calibration minimizers, *submitted to IEEE Transactions on Image Processing*.

7 Publications

7.1 Journal Publications

[ALG1] P. R. Amestoy, I. S. Duff, J.-Y. L'Excellent, and X. S. Li, (2003), Impact of the implementation of MPI point-to-point communications on the performance of two general sparse solvers, *Parallel Computing*, **29**, 833–847.

[ALG2] P. R. Amestoy, I. S. Duff, S. Pralet, and C. Vömel, (2003), Adapting a parallel sparse direct solver to architectures with clusters of SMPs, *Parallel Computing*, **29**, 1645–1668.

[ALG3] P. R. Amestoy, I. S. Duff, S. Pralet, and C. Vömel, (2003), Adapting a parallel sparse direct solver to architectures with clusters of SMPs, *Parallel Computing*, **29**, 1645–1668.

[ALG4] L. S. Blackford, J. Demmel, J. Dongarra, I. S. Duff, S. Hammarling, G. Henry, M. Heroux, L. Kaufman, A. Lumsdaine, A. Petitet, R. Pozo, K. Remington, and R. C. Whaley, (2002), An updated set of Basic Linear Algebra Subprograms (BLAS), *ACM Trans. Math. Softw.*, **28**, 135–151.

[ALG5] B. Carpentieri, I. S. Duff, and L. Giraud, (2003), A class of spectral two-level preconditioners, *SIAM J. Scientific Computing*, **25**, 749–765.

[ALG6] I. S. Duff and C. Vömel, (2002), Algorithm 818: A Reference Model Implementation of the Sparse BLAS in Fortran 95, *ACM Trans. Math. Softw.*, **28(2)**, 268–283. Implementation available from URL: http://www.netlib.org/netlib/toms/818.

[ALG7] I. S. Duff and C. Vömel, (2002), Incremental Norm Estimation for Dense and Sparse Matrices, *BIT*, **42(2)**, 300–322.

[ALG8] I. S. Duff, M. A. Heroux, and R. Pozo, (2002), An Overview of the Sparse Basic Linear Algebra Subprograms: the New Standard from the BLAS Technical Forum, *ACM Trans. Math. Softw.*, **28**, 239–267.

[ALG9] H. C. Elman, D. Loghin, and A. J. Wathen, (2003), Preconditioning techniques for Newton's method for the incompressible Navier–Stokes equations, *BIT*, **in press**.

[ALG10] L. Giraud and J. Langou, (2002), When modified Gram-Schmidt generates a well-conditioned set of vectors, *IMA Journal of Numerical Analysis*, **22(4)**, 521–528.

[ALG11] L. Giraud and J. Langou, (2003), Robust selective Gram-Schmidt reorthogonalization, *SIAM J. Scientific Computing*, **25**, 417–441.

[ALG12] L. Giraud, F. G. Vasquez, and R. S. Tuminaro, (2003), Grid transfer operators for highly variable coefficient problems in two-level non-overlapping domain decomposition methods, *Numerical Linear Algebra with Applications*, **10**, 467–484.

[ALG13] L. Giraud, (2002), Combining shared and distributed memory programming models on clusters of symmetric multiprocessors: some basic promising experiments, *International Journal of High Performance Computing Applications*, **16(4)**, 425–430.

[ALG14] N. I. M. Gould, D. Orban, and P. L. Toint, (2003), CUTEr, a Constrained and Unconstrained Testing Environment, revisited, *ACM Transactions on Mathematical Software*, **vol. 29**.

[ALG15] N. I. M. Gould, D. Orban, A. Sartenaer, and P. L. Toint, (2002), Componentwise fast convergence in the solution of full-rank systems of nonlinear equations, *Mathematical Programming Serie B*, **92**, 481–508.

[ALG16] D. Kay, D. Loghin, and A. J. Wathen, (2002), A preconditioner for the Steady-State Navier-Stokes equations, *SIAM J. Scientific Computing*, **24**, 237–256.

[ALG17] A. Lannes and S. Durand, (2003), Dual algebraic formulation of differential GPS, *Journal of Geodesy*, **77**, 22–29.

[ALG18] A. Lannes, (2003), Constrained minima of the single-epoch DGPS objectif functional. Integrity tests, In *2003 Int. Symp. on GPS/GNSS (Tokyo)*, 255–261.

[ALG19] A. Lannes, (2003), Instabilités de calibration de phase, *C. R. Acad. Sci. Paris, Physique série IV*, 725–730.

[ALG20] A. Lannes, (2003), Phase closure imaging, *Advances in Imaging and Electron Physics*, **126**, 287–327.

[ALG21] D. Laurichesse, S. Gratton, F. Mercier, T. Tournier, and J. Berthias, (Summer 2003), Use of GNSS-based pseudo-acceleration measurements and orbital constraints to initialize spaceborne receiver orbit solutions, *Navigation Journal*, **36**, 455–469.

[ALG22] D. Loghin and A. J. Wathen, (2002), Schur complement preconditioners for the Navier–Stokes equations, *Int. J. Num. Meth. in Fluids*, **40**, 403–412.

[ALG23] D. Loghin and A. J. Wathen, (2003), Schur complement preconditioning for elliptic systems of partial differential equations, *Numerical Linear Algebra with Applications*, **10**, 423–443.

[ALG24] D. Orban and S. J. Wright, (2002), Properties of the Log-Barrier Function on Degenerate Nonlinear Programs, *Mathematics of Operations Research*, **27**, 585–613.

[ALG25] J. Rahola and S. Tissari, (2002), Iterative solution of dense linear systems arising from the electrostatic integral equation in MEG, *Physics in Medicine and Biology*, **47**, 961–975.

[ALG26] M. Rojas and D. C. Sorensen, (2002), A trust-region approach to the regularization of large-scale discrete ill-posed problems, *SIAM J. Scientific Computing*, **26**, 1843–1861.

[ALG27] M. Rojas and T. Steihaug, (2002), An interior-point trust-region-based method for large-scale nonnegative regularization, *Inverse Problems*, **18**, 1291–1307.

[ALG28] S. Tissari and J. Rahola, (2003), Error analysis of a new Galerkin method to solve the forward problem in MEG and EEG using the boundary element method, *Computer Methods and Programs in Biomedicine*, **72**, 209–222.

7.2 Theses

[ALG29] B. Carpentieri, (2002), *Sparse preconditioners for dense complex linear systems in electromagnetic applications*, Ph.D. dissertation, INPT. TH/PA/02/48.

[ALG30] J. Langou, (2003), *Iterative methods for solving linear systems with multiple right hand sides.*, Ph.D. dissertation, INSA Toulouse. TH/PA/03/24.

[ALG31] J.-C. Rioual, (2002), *Solving linear systems for semiconductor device simulations on parallel distributed computers*, Ph.D. dissertation, INPT. TH/PA/02/49.

[ALG32] C. Vömel, (2003), *Contributions to research in high performance scientific computing for sparse matrices.*, Ph.D. dissertation, INPT. TH/PA/03/26.

7.3 Technical Reports

[ALG33] G. Alléon, B. Carpentieri, I. S. Duff, L. Giraud, J. Langou, E. Martin, and G. Sylvand, (2003), Efficient parallel iterative solvers for the solution of large dense linear systems arising from the boundary element method in electromagnetism, Technical Report TR/PA/03/65, CERFACS, Toulouse, France. Preliminary version of the paper published electronically in the proceedings of the international conference on supercomputing in nuclear application, Paris, 2003.

[ALG34] P. R. Amestoy, I. S. Duff, and C. Vömel, (2002), Task scheduling in an asynchronous distributed memory multifrontal solver, Technical Report TR/PA/02/105, CERFACS, Toulouse, France.

[ALG35] P. R. Amestoy, I. S. Duff, J. Y. L'Excellent, and X. S. Li, (2003), Impact of the implementation of MPI point-to-point communications on the performance of two general sparse solvers, Technical Report TR/PA/03/14, CERFACS, Toulouse, France. Various versions have appeared as technical reports RT/APO/01/4 from ENSEEIHT-IRIT, Toulouse, RR-4372 from INRIA, Lyon, and LBNL-48968 from Lawrence Berkeley National Laboratory, California. Preliminary version of the article published in Parallel Computing, vol. 29, nber 7, pp 833-847, 2003.

[ALG36] P. R. Amestoy, I. S. Duff, S. Pralet, and C. Vömel, (2003), Adapting a parallel sparse direct solver to SMP architectures, Technical Report TR/PA/03/05, CERFACS, Toulouse, France. Preliminary version of the article published in Parallel Computing, special issue on Parallel and Distributed Scientific and Engineering Computing, vol. 29, nber 11-12, pp 1645-1668, 2003.

[ALG37] M. Arioli, D. Loghin, and A. J. Wathen, (2003), Stopping criteria for iterations in finite element methods, Technical Report TR/PA/03/21, CERFACS, Toulouse, France.

[ALG38] C. Bousquet and C. Daniel, (2002), Complex version and validation of MUMPS, Multifrontal Massively Parallel Solver, Working Notes WN/PA/02/34, CERFACS, Toulouse, France. Mémoire de Maîtrise Ingénierie Mathématique, UPS III.

[ALG39] B. Carpentieri, I. S. Duff, and L. Giraud, (2002), A class of spectral two-level preconditioners, Technical Report TR/PA/02/55, CERFACS, Toulouse, France. Preliminary version of the article published in SIAM Journal on Scientific Computing, vol. 25, nber 2, pp. 749-765, 2003.

[ALG40] B. Carpentieri, I. S. Duff, L. Giraud, and G. Sylvand, (2003), Combining fast multipole techniques and an approximate inverse preconditioner for large parallel electromagnetics calculations, Technical Report TR/PA/03/77, CERFACS, Toulouse, France.

[ALG41] F. Chaitin-Chatelin and E. Traviesas, (2002), PRECISE and the reliability of Numerical Software, Technical Report TR/PA/02/57, CERFACS, Toulouse, France. To appear in Handbook of Computation, Bo Einarsson ed., SIAM Philadelphia.

[ALG42] F. Chaitin-Chatelin and E. Traviesas, (2002), Qualitative Computing, Technical Report TR/PA/02/58, CERFACS, Toulouse, France. To appear in Handbook of Computation, Bo Einarsson ed., SIAM Philadelphia.

[ALG43] F. Chaitin-Chatelin and M. B. van Gijzen, (2003), Homotopic deviation: an example in acoustics, Technical Report TR/PA/03/04, CERFACS, Toulouse, France. Submitted to LAAp.

[ALG44] F. Chaitin-Chatelin and A. N. Zaoui, (2002), Hypercomputation in $\{0,1\}$, Technical Report TR/PA/02/73, CERFACS, Toulouse, France.

[ALG45] F. Chaitin-Chatelin, T. M. skauskas, and A. N. Zaoui, (2002), Hypercomplex division in the presence of zero divisors on $\mathbb{R}$ and $\mathbb{Z}_2$, Technical Report TR/PA/02/29, CERFACS, Toulouse, France.

[ALG46] F. Chaitin-Chatelin, (2002), About Singularities in Inexact Computing, Technical Report TR/PA/02/106, CERFACS, Toulouse, France.

[ALG47] F. Chaitin-Chatelin, (2003), The arnoldi method in the light of homotopic deviation theory, Technical Report TR/PA/03/15, CERFACS, Toulouse, France.

[ALG48] F. Chaitin-Chatelin, (2003), Computing beyond analyticity. Matrix algorithms in inexact and uncertain computing, Technical Report TR/PA/03/110, CERFACS, Toulouse, France.

[ALG49] F. Chaitin-Chatelin, (2003), Elements of hypercomputations on $\mathbb{R}$ and $\mathbb{Z}_2$ with the Dickson-Albert inductive process, Technical Report TR/PA/03/34, CERFACS, Toulouse, France.

[ALG50] F. Chaitin-Chatelin, (2003), On a recursive hierarchy for numbers algorithmically emerging from processing binary sequences, Technical Report TR/PA/03/08, CERFACS, Toulouse, France.

[ALG51] I. S. Duff, L. Giraud, J. Langou, and E. Martin, (2003), Using spectral low rank preconditioners for large electromagnetic calculations, Technical Report TR/PA/03/95, CERFACS, Toulouse, France.

[ALG52] R. Durdos, (2002), Krylov solvers for large symmetric dense complex linear systems in electromagnetism: some numerical experiments, Working Notes WN/PA/02/97, CERFACS, Toulouse, France.

[ALG53] H. C. Elman, D. Loghin, and A. J. Wathen, (2003), Preconditioning techniques for Newton's method for the incompressible Navier–Stokes equations, Technical Report TR/PA/03/31, CERFACS, Toulouse, France. Preliminary version of the paper to appear in BIT.

[ALG54] V. Frayssé, L. Giraud, S. Gratton, and J. Langou, (2003), A Set of GMRES routines for real and complex arithmetics on high performance computers, Technical Report TR/PA/03/03, CERFACS, Toulouse, France.

[ALG55] L. Giraud and J. Langou, (2002), Another proof for modified Gram-Schmidt with reorthogonalization, Working Notes WN/PA/02/53, CERFACS, Toulouse, France.

[ALG56] L. Giraud and J. Langou, (2002), Robust selective Gram-Schmidt reorthogonalization, Technical Report TR/PA/02/52, CERFACS, Toulouse, France. Preliminary version of the paper to appear in SIAM SISC.

[ALG57] L. Giraud and M. B. van Gijzen, (2002), Large scale acoustic simulations on clusters of SMPs, Technical Report TR/PA/02/116, CERFACS, Toulouse, France. To appear in the proceedings of the IMSE2002 conference.

[ALG58] L. Giraud, S. Gratton, and J. Langou, (2003), A reorthogonalization procedure for modified Gram–Schmidt algorithm based on a rank–k update, Technical Report TR/PA/03/11, CERFACS, Toulouse, France. Preliminary version of the paper to appear in SIAM SIMAX.

[ALG59] L. Giraud, J. Langou, and M. Rozložník, (2003), On the loss of orthogonality in the Gram-Schmidt orthogonalization process, Technical Report TR/PA/03/25, CERFACS, Toulouse, France. Preliminary version of the paper to appear in Computer and Mathematics with Applications.

[ALG60] L. Giraud, J. Langou, and M. Rozložník, (2002), On the round-off error analysis of the Gram-Schmidt algorithm with reorthogonalization, Technical Report TR/PA/02/33, CERFACS, Toulouse, France.

[ALG61] L. Giraud, A. Marrocco, and J.-C. Rioual, (2002), Iterative versus direct parallel substructuring methods in semiconductor device modeling, Technical Report TR/PA/02/114, CERFACS, Toulouse, France.

[ALG62] L. Giraud, A. Marrocco, and J.-C. Rioual, (2002), Iterative versus direct parallel substructuring methods in semiconductor device modeling, Technical Report TR/PA/02/114, CERFACS, Toulouse, France. Submitted.

[ALG63] N. I. M. Gould, D. Orban, and P. L. Toint, (2002), General CUTEr documentation, Technical Report TR/PA/02/13, CERFACS, Toulouse, France.

[ALG64] N. I. M. Gould, D. Orban, and P. L. Toint, (2002), General SifDec documentation, Technical Report TR/PA/02/14, CERFACS, Toulouse, France.

[ALG65] G. Richard, (2002), Coupling MUMPS and ordering software, Working Notes WN/PA/02/24, CERFACS, Toulouse, France.

[ALG66] S. Riyavong, (2003), Experiments on parallel matrix-vector product, Working Notes WN/PA/03/127, CERFACS, Toulouse, France.

[ALG67] S. Riyavong, (2003), Experiments on sparse matrix partitioning, Working Notes WN/PA/03/32, CERFACS, Toulouse, France.

[ALG68] J. van den Eshof, G. L. G. Sleijpen, and M. B. van Gijzen, (2003), Relaxation strategies for nested Krylov methods, Technical Report TR/PA/03/27, CERFACS, Toulouse, France.

[ALG69] M. B. van Gijzen, (2003), Two level parallelism in a stream-function model for global ocean circulation, Technical Report TR/PA/03/09, CERFACS, Toulouse, France. Preliminary version of the paper published in the proceedings of Euro-Par2003, Lecture Notes in Computer Science 2790, pp. 820-829, 2003.

[ALG70] M. B. van Gijzen, (2003), Two level parallelism in a stream-function model for global ocean circulation, In *Euro-Par 2003 Parallel Processing*, H. Hellwagner, ed., Berlin, Springer-Verlag, 820–829.

2

Computational Fluid Dynamics

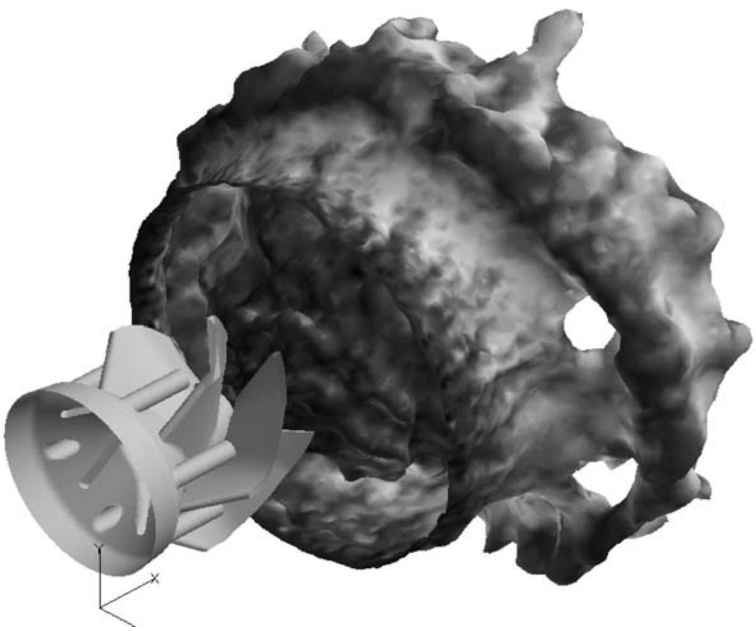

1 Introduction

Thierry Poinsot

The objective of the CFD team is to develop and apply high-performance new generation codes for fluid mechanics applications. The activities of the CFD team have been organized for 2002 and 2003 in two main groups:

- *Aerodynamics (supervision: G. Chevalier).* Developing advanced simulation codes for aerodynamics applications in Europe is now the central theme of this group. The code NSMB which had been the center of developments at CERFACS until 2000 and was the production code of Airbus Toulouse has been progressively replaced in 2002 by the new software elsA developed by ONERA with a strong participation of CERFACS. In 2003, NSMB has been completely stopped at CERFACS and all efforts focus now on elsA and its future developments.

- *Combustion.* The LES (Large Eddy Simulation) tool of CERFACS (AVBP) has become the standard tool for LES of reacting flows at many places in Europe (CNRS laboratories, ONERA centers, Universities in Spain or Germany, etc). Another important change took place: Institut Français du Pétrole is now developing AVBP jointly with CERFACS. Industrial partners (SNECMA, Turbomeca, Siemens, Alstom) have continued their collaboration with CERFACS to increase AVBP capabilities and validate it in multiple cases. In certain cases, the industrial use of LES has already been tested (at SNECMA or TURBOMECA) opening a new area for reacting flow computations in industry.

The aerodynamics and combustion activities are described in the next sections. General remarks are listed below:

- Even though code developments are an important part of the team work, the core of this activity remains research in fluid mechanics as evidenced by the number of publications (which has increased in 2003) and by the reputation of the team. Obviously, the focus of this academic work has shifted from fundamentals studies in turbulence or in laminar flames towards more complex topics: unsteady flows, fluid structure interaction, coupled phenomena, optimization, acoustic / combustion instabilities, two-phase reacting flows. This academic level is one of the keys explaining the present results of the CFD team. It also explains why outside experts join CERFACS as consultants to be able to find codes in which they can test new concepts: Pr Nicoud (Montpellier) or Pr Sagaut (Paris VI) for example are now collaborating routinely to CERFACS work. The quality of the research produced by CERFACS was also recognized in 2003 through the Grand Prix de l'Académie des Sciences for T. Poinsot, jointly with D. Veynante, and the PhD prize in aerodynamics of Académie des Sciences, Belles Lettres et Inscriptions de Toulouse for Dr F. Laporte.

- A significant part of the activity of the CFD team continues to be supported by European contracts. The 5th PCRD contracts on wake vortices (C Wake, S Wake, Wakenet 2, Awiator), LES of combustion in gas turbines (Icleac, Preccinsta, Molecules, Fuelchief, Desire), atmospheric pollution (Stopp) are being continued and expanded through 6th PCRD programmes (Fluistcom, Timecop, Lessco2) confirming the efficiency of the team at the European level.

- The team gathers now more than 40 people but less than 10 of these are at CERFACS on a permanent basis. All others spend 2 to 3 years at CERFACS and leave so that CERFACS continues to provide multiple high-level experts for industry: EADS in Paris, CORYS in Grenoble, Siemens in Regensburg, Airbus-F, Airbus-D and CEA.
- The new topics started in 2000 or 2001 (such as two-phase flows or aerodyamics with elsA) have expanded very rapidly: 7 scientists are now working full time on two phase flow (supervision: Dr Cuenot) and more than 10 are working on elsA. Such rapid evolutions require a high level of adaptability from the whole team. In 2003, other new topics have also appeared such as fluid structure interaction with combustion, optimization for reacting flows, aircraft impact on environment (supervision: D. Cariolle) suggesting that the team will adjust again in the near future.
- The collaboration with laboratories keeps increasing. In the field of combustion, AVBP is now used in France at IMF Toulouse, Ecole Centrale Paris, IRPHE, ONERA Paris, ONERA Toulouse and Institut Français du Pétrole. Multiple joint papers have been written with foreign universities (Netherlands, Germany) where experiments are performed and for which CERFACS performs LES. This collaborative European work is typical of the present research of the team. The CRCT ('Centre de Recherche sur la Combustion Turbulente') is very active: annual CRCT meetings gather more than 40 scientists. Outside Europe, CERFACS continues to collaborate with the Center of Turbulence Research: 4 CERFACS scientists participated to the CTR Summer Program in 2002 and one of our scientist is presently at Stanford for a year before coming back to CERFACS to work on aircraft impact in 2004.
- Formation is still an important part of the team's activity: in 2002 and 2003, 15 trainees will have spent periods of six months at CERFACS to learn CFD. The PhD program is also increasing with 17 PhD students working in the team in 2003. Formation also takes other forms: in the case of industry, CERFACS has received trainees working for industry (SNECMA), for laboratories (IRPHE, Ecole Centrale de Paris, Ecole des Mines d'Albi) for periods of one to four weeks to teach them how to use CERFACS codes. Another ambitious project was started by sending a senior of the team for six months in 2003 to Turbomeca in Pau. Here formation worked both ways: he has shown the use of AVBP to Turbomeca and has learned the basis of the work of helicopter gas turbine designers. Recently, CERFACS has participated to the training of Airbus users of elsA with ONERA.

2 Combustion

The increasing needs of society in the field of reacting flows (for energy production and transport as well as for reduced pollution and increased safety) and the lack of experienced groups in numerical combustion have generated an increasing activity of combustion research at CERFACS. This includes:

- Fundamental research in combustion: flame dynamics, chemistry, interaction with walls, Direct Numerical Simulation
- Development of tools which can be applied to industrial problems: RANS (Reynolds Averaged Navier Stokes) and LES (Large Eddy Simulation) codes.

These two aspects must be balanced to fulfill the task of the team. The academic part, for example, is necessary to maintain a high level of expertise. Interestingly, funding has been found even for these fundamental aspects and multiple contracts cover such 'basic' combustion phenomena at CERFACS. These studies are described in Section 2.1. The LES of two phase flows which is the fastest growing activity in the team is described in Section 2.2 while the unsteady combustion work (in gaseous flows) is presented in Section 2.3. Finally, Section 2.4 describes the software engineering tasks needed to make all large LES studies at CERFACS possible: optimisation, parallelization, visualization, etc. Many of these tasks require intense collaboration with national computing centers such as CINES or IDRIS.

2.1 Basic phenomena

The study of basic phenomena in combustion is an essential part of the activity of the team. It feeds its scientific expertise which is a solid basis for the other activities. During the last three years, a number of different subjects have been investigated that are either generic or more focused on a specific topic:

- Flame-wall interaction and wall heat flux in rocket engines
- Stratified combustion modelling
- Autoignition in diffusion layers
- Interaction of a flame with a liquid fuel film on a wall
- Structure and ignition of supersonic coaxial jets
- Propagation of laminar two-phase flames
- Reduced chemistry

These studies all aim at improving our understanding of the mechanisms that controll turbulent flames from ignition to extinction. The results are either used to improve the modelling in CFD simulations or directly applied to industrial applications, as for example the use of the maximal wall heat flux obtained in the flame-wall interaction study to help the design of the engine. We develop below four selected topics, that illustrate the present activity.

2.1.1 Interaction of flame with liquid fuel on a wall (G. Deroutter, B. Cuenot, C. Habchi)

The interaction between walls and flames is a critical issue in the design of many modern combustion systems: in gas turbines, Lean Premixed Prevaporized (LPP) technologies often lead to the coexistence of liquid films on combustor walls and of flames (for example during flashback). In piston engines, Direct Injection (DI) techniques can create fuel films on the piston or on the cylinder walls: these films burn at later times, interacting with the flame in a complex manner which is not understood or modelled at the present time. The consequences are an increased emission of pollutant species, lower performance and shorter life time of the engine.

The problem of flame wall interaction with a liquid film is a dual problem in which the temperature profile must be solved simultaneously in the gas and in the liquid film. While a DNS (Direct Numerical Simulation) code (NTMIX) is used for the gas phase problem, the resolution of the temperature field in the liquid film is done with an integral method in which the temperature profiles are assumed to be polynomial functions of the spatial coordinate.

First computations of a monodimensional premixed flame interacting with a liquid film have been

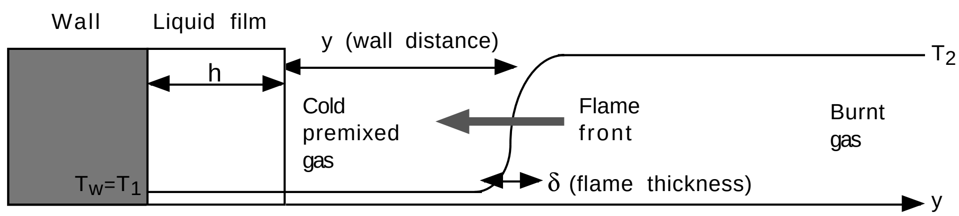

Figure 2.1: Configuration of the flame interaction with a liquid film.

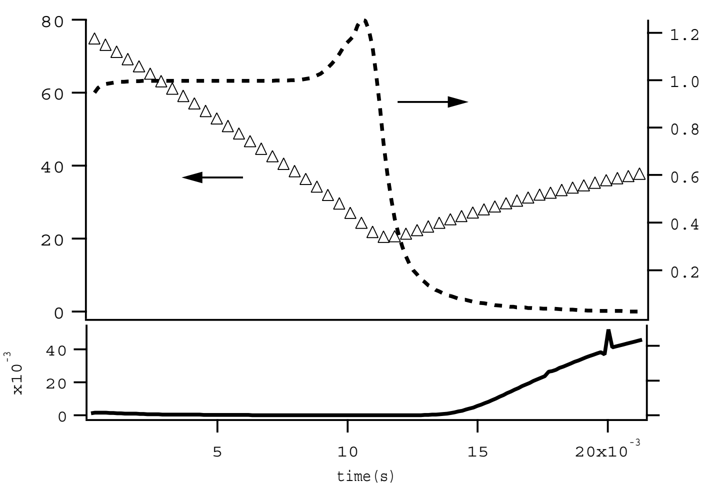

Figure 2.2: Normalized flame / wall distance (triangle), consumption speed (dashed line) and wall heat flux (solid line) during the flame interaction with a liquid film.

performed (Fig. 2.1). The results show that the evaporation of the liquid film changes the equivalence ratio in front of the flame and modifies its propagation. Typical results are shown on Fig. 2.2 where the distance between the flame and the liquid surface, the flame speed and the heat flux to the wall have been plotted. It appears that the flame does not approach the film surface as close as a dry wall and that it is quenched by an excess of fuel and not because of heat loss. As a consequence the heat flux to the wall stays much lower than in the case of interaction with a dry wall. This project is continued through a thesis in collaboration with IFP.

2.1.2 Ignition and structure of supersonic coaxial jets (A. Dauptain, B. Cuenot)

Rocket engines technology raises very basic combustion problems. This is the case for the ignition of the VINCI combustor that operates at very low ambiant pressures (almost vacuum). The high pressure ratio between the injectors and the chamber leads to supersonic flow with high compressibility. This raises the problem of mixing and ignition of the two initially separated reactants (H2 and O2). Indeed, the underexpanded jets that come out of the injectors have a particular structure with slip lines, weak and strong shocks. The very strong shear at the envelope of the jet prevents mixing (see Fig. 2.3). Mixing is mostly due to the turbulence that develops behind the first strong shock.
Simulations of underexpanded jets at high pressure ratios have been performed with the AVBP code, using a particular numerical treatment of the thin interfaces (slip lines and shocks). The thermodynamic conditions correspond to the igniter jet. An example is shown Fig. 2.3 where the density field of a jet at pressure ratio 7 is plotted. For comparison a visualisation of the same jet obtained in the laboratory (B. Yip et al, 2003, private communication) is inserted, demonstrating the performance of the code on this configuration.
The next step is to study H2-O2 autoignition in this configuration and to perform simulations with two jets: the igniter and an H2/O2 injector of the first row of injectors. This project is going on within a thesis supported by SNECMA Moteurs Fusée.

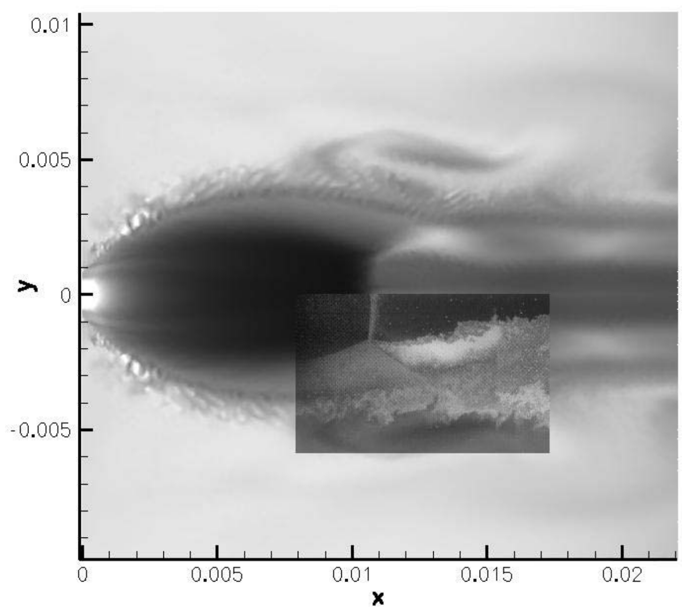

Figure 2.3: Density field of an underexpanded jet (pressure ratio 7). The inserted picture is the result from Rayleigh Scattering on the same jet obtained by B. Yip et al.

2.1.3 Propagation of laminar two-phase flames (B. Cuenot, M. Boileau, S. Pascaud)

The development of the two-phase flow solver AVBP-TPF for combustion applications requires to master the physics and behaviors of two-phase laminar flames. Depending on the thermodynamic conditions, droplet size, fuel characteristics and chemistry, different classes of two-phase flames may be encountered: either all droplets evaporate before burning and combustion occurs in a pure gaseous phase, or evaporation is not complete in front of the flame and droplet burning occurs. The simplest case where all the liquid fuel is first vaporized before burning through a premixed flame in a purely gaseous zone, has the great advantage to present an analytical solution, that can be used as a reference solution to validate the computation.

As an example, the flame presented in this section burns ethanol C_2H_5OH, with a laminar flame speed of $0.42\ m.s^{-1}$. This value is used to initialize the velocity profile in order to keep the flame front steady. Fig. 2.4 shows the comparison between the computed solution and the analytical solution of the mass fraction profiles. The agreement is very good.

This shows that the mechanisms of two-phase flames are understood and that the AVBP-TPF code is able to compute such flames. The relative facility to calculate two-phase burning flows is one of the advantage of the Eulerian formulation for the dispersed phase used in AVBP-TPF, compared to a Lagrangian formulation.

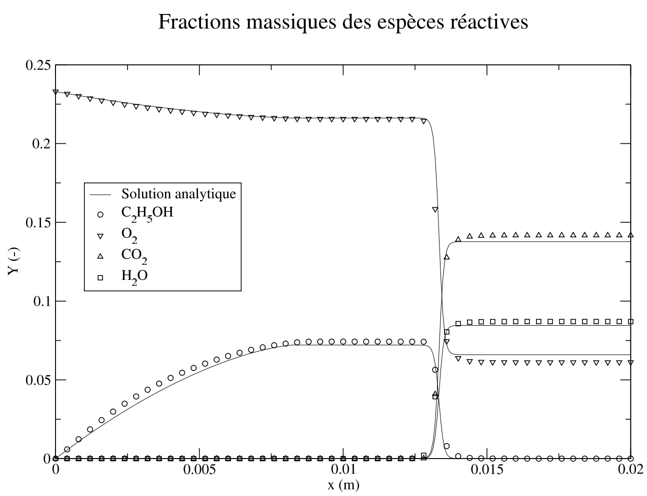

Figure 2.4: Comparison between initial and converged profiles of species mass fractions.

2.1.4 Reduced chemistry (K. Truffin, T. Poinsot)

Chemical kinetics are one of the controlling factors in all combustion applications. Although the chemistry of most fuels is known the accurate description of the chemical kinetics in practical computations still remains a problem. This is due to the complexity of the available chemical kinetic schemes which add many variables to the system and drastically increase its stiffness.
To address this problem, the team has developed a strategy for chemistry reduction based on the following statements:

- the reduced chemistry must guarantee a certain number of flame characteristics (flame speed and thickness at least)
- the reduced chemistry must decrease the stiffness of the full scheme
- the reduced chemistry must minimize the number of added variables

Such reduced schemes are built either with an empirical method, in which the chemical species and reactions are chosen and the reaction constants fitted to match flame characteristics or in a more systematic way using an optimisation code (EPORCK) based on a genetic algorithm. The obtained reduced schemes are usually valid on a restricted range of parameters but have the advantage of a very easy implementation.

2.2 LES of two phase reacting flows

Most industrial combustors burn liquid fuel, that goes through an injector producing a spray of droplets of varying size and velocity. The presence of liquid droplets in the burner strongly influences its behavior: the turbulence field is modified, liquid films may form on the walls and evaporation occurs before (or while) burning, leading to a non-homogeneous gaseous fuel field. All these effects have to be taken into account in the simulations of combustion chambers and a project has been launched in 2000 to develop a two-phase flow solver based on AVBP.

2.2.1 Numerical Approach (J.-B. Mossa, B. Cuenot, S. Pascaud, A. Kaufmann, O. Simonin)

There are two classes of numerical methods to compute two-phase flows:

- The lagrangian approach calculates the trajectories of the inclusions (bubbles or droplets), including models for rupture or coalescence, evaporation, etc ...The main advantage of this approach is that the system of equations describing the dispersed phase is relatively easy to write. On the other hand the coupling between a discrete system and a continuous phase raises some delicate questions. In typical combustion applications the number of droplets that are simultaneously present in a system is very large. This number may be reduced by a stochastic approach, in which the set of droplets is interpreted as a statistical sampling of the dispersed phase. However the minimum number of samples remains high to reach a reasonable accuracy, as required by LES simulations. One of the main difficulties of lagrangian methods is therefore to compute efficiently (through vectoral or parallel algorithms) a large number of trajectories.
- In the eulerian approach, the dispersed phase is viewed as a continuous phase and described by continuous fields of variables. This allows to benefit from the same numerical algorithm as used for the gaseous phase (in particular the parallelism can be directly extended) and to facilitate the coupling between the two phases. In this approach the system of equations for the dispersed phase is obtained from the individual droplet equations through an averaging operation. This leads classically to unclosed non-linear terms for which models must be developed and validated.

In the AVBP-TPF project, the eulerian approach has been chosen for its implementation facility. It has also demonstrated less difficulties than the lagrangian approach in flame computations. Note that the lagrangian approach is also investigated, mainly in terms of computing efficiency and parallel algorithms development. The project is made of two parts:

- Models development: as mentioned above, the eulerian approach requires models for some unclosed terms in the equations, related to the small-scale movement of the droplets.

- Code development and validation: the code AVBP-TPF has been developed on the basis of AVBP-5.1, under the control of CVS and with a quality procedure.

2.2.2 Modelling aspects (B. Cuenot, E. Riber, A. Kaufmann, O. Simonin)

Modelling aspects have been addressed in the framework of a collaboration with O. Simonin (IMFT) [CFD33]. The most needed model for computations to be stable and meaningful is the so-called ”Quasi-Brownian Model” (QBM). This model is developed to take into account the small scale uncorrelated movement (called the Quasi-Brownian movement) of the droplets, droped during the averaging operation. This small scale movement plays an essential role in the larger scale droplet dynamics, to some extent similar to the small scale turbulent movement of the gas. For intermediate Stokes numbers (around 1), the omission of the Quasi-Brownian movement leads to excessive segregation and high compressibility effects. A conservation equation has been derived for the Quasi-Brownian energy, including transport terms, source and sink terms and a diffusion-like term. Validation with DNS of decreasing homogeneous isotropic turbulence has shown that the QBM is able to capture qualitatively the overall droplet behavior and dynamics (see Fig. 2.5). However the use of this model in the framework of LES is still an open question.

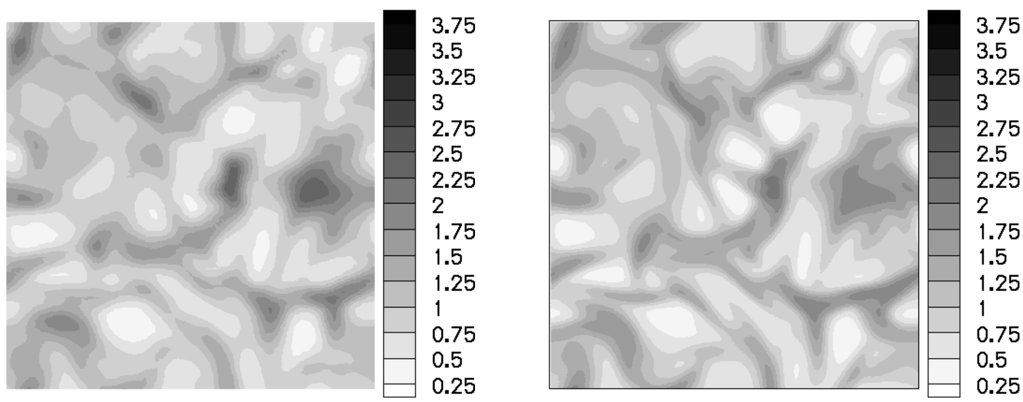

Figure 2.5: Two-phase Direct Numerical Simulation of Homogeneous and Isotropic Turbulence: number density field. Left: lagrangian approach; Right: eulerian approach.

2.2.3 Applications (S. Pascaud, J.-B. Mossa, B. Cuenot, T. Poinsot)

Two applications have been computed with the first version of AVBP-TPF. Both are gas turbines combustion chambers. One is the M88 chamber used on the ”Rafale” aircraft. The other application is the chamber of the VESTA, designed by Turbomeca. The geometry, as well as inlet and operating conditions have been supplied by the industrial partner.
For the M88 case, calculations with evaporation have been performed. Fig. 2.6 shows droplet trajectories and evaporation. It appears that evaporation is almost completed in the dilution zone (where the flame is usually located). The associated fuel vapor field is displayed in Fig. 2.7 in terms of equivalence ratio. As expected the resulting fresh gas mixture is strongly inhomogeneous. This will have an important impact on the turbulent flame propagation and modelling.
To see the impact of the Stokes number, the VESTA chamber has been computed with two different droplet sizes. In the case of 1 μm droplets, the Stokes number is very small and the velocity field of the dispersed

phase is similar to the gaseous velocity field (Fig. 2.8a). The droplet number density field shows that the droplets have not enough inertia to go through the strong dilution jets and concentrate in the area close to the injector (Fig. 2.8b). The associated Quasi-Brownian energy field shows that the small size droplets have no uncorrelated movement: the Quasi-Brownian energy is depleted below the default value (used in the purely gaseous regions) (Fig. 2.8c). This is in accordance with the fact that the movement of these droplets is fully correlated with the gaseous velocity field.
The results are quite different for 100 μm droplets, as shown in Fig. 2.8a to Fig. 2.8c. The droplets have too much inertia to be significantly affected by the gaseous velocity field and go through the chamber along ballistic trajectories. This also shows on the droplets velocity field and on the Quasi-Brownian energy field, where the high maximum level illustrates the strong uncorrelated movement.

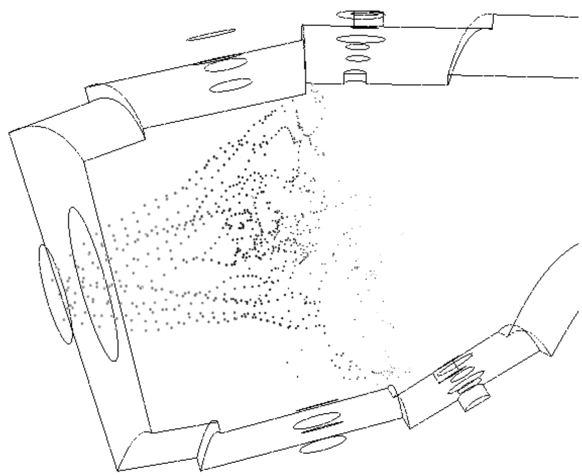

Figure 2.6: Computation of the M88 geometry with evaporating droplets: droplet trajectories.The initial size is 20 μm.

Figure 2.7: Computation of the M88 geometry with evaporating droplets: equivalence ratio. The initial size is 20 μm.

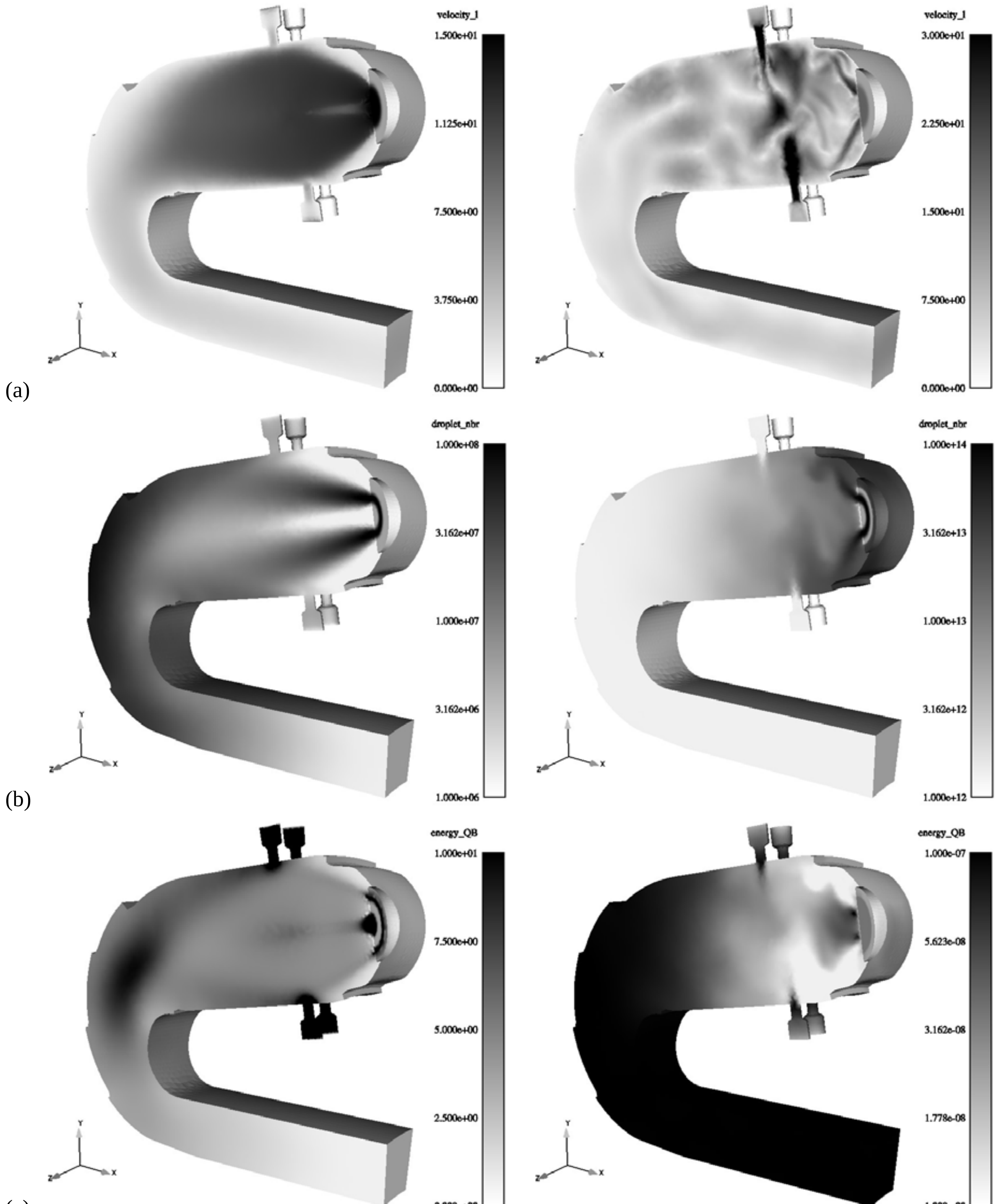

Figure 2.8: Computation of the VESTA geometry with a droplet size of 100 μm (left column) and 1 μm (right column).(a): liquid velocity field;(b): number density field;(c):Quasi-Brownian energy field.

2.3 LES of unsteady combustion

2.3.1 Unsteady combustion studies using LES and acoustic tools (Y. Sommerer, T. Poinsot)

Since 2000, Large Eddy Simulations (LES) have changed the way scientists investigate turbulent combustion and especially combustion instability phenomena. This evolution has been strong at CERFACS in particular in 2002 and 2003 where fifteen different configurations have been simultaneously under study using the LES code AVBP. Table 2.1 presents some examples of the various test cases which were studied: usually, these configurations were tested experimentally at the same time elsewhere in Europe, providing CERFACS with a unique data base for validation of the AVBP code.

Name of laboratory	Type of geometry	Type of flame/flow
Ecole Centrale Paris (EU project ICLEAC)	Dump combustor (backward facing steps)	Lifted turbulent diffusion burner
University of Poitiers (ORACLES)	Dump combustor (rectangular section)	Partially premixed turbulent burner
University of Twente (EU project DESIRE)	Circular swirling with central hub	Diffusion turbulent burner
Ecole Centrale Paris	Backward facing step	Laminar acoustically forced flame
Karlsruhe University (ITS)	Double swirler (rectangular chamber)	Partially premixed turbulent burner
Karlsruhe University (EBI)	Double swirler (circular chamber)	Acoustically forced premixed turbulent burner
Ecole Centrale Paris (COS)	Circular swirling with premixing tube	Lean premixed turbulent burner (with flashback)
Ecole Centrale Paris (EU project FUELCHIEF)	Double stage circular	Staged partially premixed turbulent burner
Ecole Centrale Paris and DLR	Split conic shape	Staged partially premixed turbulent burner
Alstom Daetwill	Backward facing steps	Reheat turbulent burner
SNECMA	Double swirler	Lean premixed gas turbine (LPP) injector
DLR (EU project PRECCINSTA)	Circular swirler with hole injection	Partially premixed turbulent burner
ONERA (EU project MOLECULES)	Jets in cross flow in a tube	Dilution jet mixing
Bochum University	Jets in cross flow in a planar channel	Mixing enhancement

Table 2.1: Examples of configurations investigated with LES in 2002 / 2003 (gaseous reactants).

As a result, several joint papers have been submitted in 2003: LES of jets in cross flow with Bochum University [1], LES of partially premixed flames in gas turbine burners with Karlsruhe (ITS) and Siemens [2], acoustic forcing of gas turbine burners with Karlsruhe EBI and Siemens [3], cold and hot flow validation of LES in swirled burners with DLR [4], system identification for turbulent diffusion flames with Ecole Centrale Paris [5].

LES alone is not sufficient to understand turbulent combustion in confined chambers: theory and experiments show that acoustics play a very important role in many cases, especially in triggering combustion instabilities. Therefore writing acoustic codes allows to describe the structure of acoustic

modes in combustion chambers and their coupling with combustion is required: this is done at CERFACS and discussed in Section 2.3.3.3 and 2.3.3.4.
Many instabilities are caused by insufficient mixing between fuel and combustion air. More generally, mixing in combustors is essential for efficiency and pollution reduction: LES is used at CERFACS to study mixing and methods to enhance mixing for fuel injection or for dilution jets (Section 2.3.3.10).

[1] C. Prière and L.Y.M. Gicquel and A. Kaufmann and W. Krebs and T. Poinsot. LES of mixing enhancement : LES predictions of mixing enhancement for jets in cross-flows. Submitted to Journal of Turbulence, 2004.
[2] L. Selle and G. Lartigue and T. Poinsot and R. Koch and K.-U. Schildmacher and W. Krebs and P. Kaufmann and D. Veynante. Compressible Large-Eddy Simulation of turbulent combustion in complex geometry on unstructured meshes. In press, Combustion ands Flame, 2004.
[3] A. Giauque and L. Selle and T. Poinsot and H. Buechner and A. Kaufmann and W. Krebs. System identification of a large scale swirled premixed combustor using LES and comparison to measurements. Submitted in Journal of Turbulence, 2004.
[4] G. Lartigue and S. Roux and L. Benoit and T. Poinsot and U. Meier and C. Bérat. Studies of unsteady cold and reacting flow in a swirled combustor using experiments, acoustics analysis and Large Eddy Simulations. Submitted in Combustion and Flame, 2004.
[5] Truffin K., Varoquié, Veynante D. and Poinsot T. Large Eddy Simulations of the unsteady response of partially premixed flames. Submitted to Combustion and Flame, 2004.

2.3.2 Submodels used for LES at CERFACS (T. Poinsot, L. Gicquel, D. Veynante)

The efficiency of the LES tool developed by CERFACS jointly with Institut Francais du Pétrole is a compromise between precision and complexity: all submodels for turbulence, boundary conditions, turbulence / flame interaction, ignition, flame wall interaction, etc, are chosen to offer homogeneous performance and implementation costs which are compatible with the use of a compressible explicit solver on very large grids and large number of processors. Most models have been already published by CERFACS and are described in the literature.
The DTF (Dynamically Thickened Flame) model initially written by [1] continues to perform very well in the new configurations and has been extended to partially premixed and diffusion flames (see validations in Section 2.3.3). Many test cases of Table 2.1 could be categorized as diffusion flames in which the fuel (methane or propane) is injected through holes inside the chamber. However results show that these flames are usually lifted with significant mixing upstream of the flame, so that very few diffusion flamelets are found.
An important submodel is the chemical scheme: initially many computations with the DTF model were performed with one step schemes; two-step and four-step schemes are now being developed and the DTF model has been modified to accomodate these multistep schemes. The construction of these schemes is performed by comparing their results on simple laminar premixed flames and using genetic algorithm techniques developed to fit the results of the reduced schemes with the data obtained with full schemes. This was done in 2003 for methane, propane and heptane. These schemes are also being extended to include NOx and CO.
In 2002 and 2003 CERFACS has continued working on boundary conditions and acoustic wave management of boundaries for flame computations. In [CFD9] it is shown that the behavior of a forced flame depended strongly on the method used to pulsate the inlet of the computational domain: methods based on characteristics are well suited to such computations but need some modifications. In 2003 the 'non reflecting' character of these methods has been analyzed and correct scalings for relaxation coefficients on non reflecting boundaries have been proposed [2]. During the 2002 CTR Summer Program at Stanford another specific point was analyzed: how to initialize a reacting LES or in other words, how to ignite combustion in a LES computation ? This is an important point because LES codes are much more sensitive

to 'perturbations' than RANS codes, especially those created by ignition. It is also a field of future studies in which the ignition phase of a combustor will be investigated. In [CFD37] is derived a procedure to ignite a LES which is now used as a standard tool.

[1] O. Colin, F. Ducros, D. Veynante, and T. Poinsot. A thickened flame model for Large Eddy Simulations of turbulent premixed combustion. Physics of Fluids, 12(7):1843-1863, 2000.
[2] L. Selle, F. Nicoud, and T. Poinsot. The actual impedance of non-reflecting boundary conditions: implications for the computation of resonators. In press AIAA Journal, 1-21, 2004.

2.3.3 Typical examples

The following examples do not cover all unsteady combustion studies of CERFACS in 2002 and 2003 but present typical results and recent advances. The first example (Section 2.3.3.1) is used to show the accuracy of LES when it is compared to experimental data. Section 2.3.3.2 shows examples of pulsated flames: the first one is a turbulent diffusion flame, the second example is a premixed swirled flame in a large gas turbine burner and the last example is a new burner dedicated to fluid structure interaction studies during combustion oscillations. The third section shows the importance of acoustics and demonstrates the power of using LES and acoustic analysis together (Section 2.3.3.3). New theoretical methods required to study the budget of acoustic energy in an oscillating burner are simultaneously being developed (Section 2.3.3.4). For the first time in 2003, LES was used to compute flashback in a burner built at Ecole Centrale Paris: results are summarized in Section 2.3.3.5. Section 2.3.3.6 presents a very large LES performed at the French Super Computing Center CINES for a combustion chamber equipped with three burners. The implementation of schemes which can predict pollutant formation is another important topic discussed in Section 2.3.3.7. The specific issue of coupling RANS and LES for reacting flows has been studied for EDF since January 2003 and is discussed in Section 2.3.3.8. One example of LES in a very high-speed reacting flow is presented in Section 2.3.3.9. Finally, examples of mixing studies (between fuel and air or between dilution jets and burnt gases) are described in Section 2.3.3.10.

2.3.3.1 A small gas turbine burner (S. Roux, T. Poinsot, G. Lartigue)

The first example shows the accuracy of LES by comparing LES velocity fields with and without combustion with measurements performed at DLR. The burner is a swirled premixed injector (Fig. 2.9) where swirl is produced by tangential injection downstream of a plenum. A central hub is used to stabilize the flame. Experiments include velocity measurements for the cold flow as well as a study of various combustion regimes. The dimensions of the combustion chamber are 86 mm $\times$ 86 mm $\times$ 110 mm.

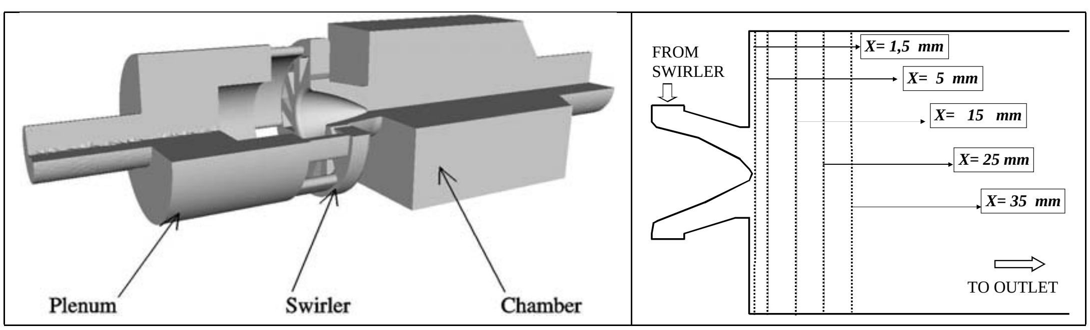

Figure 2.9: Configuration (left). Location of cuts for velocity profiles (right).

For this chamber the critical question of boundary conditions is avoided by extending the computational domain upstream and downstream of the chamber : the swirlers and the plenum are fully meshed and

computed. The mesh includes even a part of the outside atmosphere (not shown on Fig. 2.9 for visibility) to avoid having to specify a boundary condition at the chamber outlet. The expected precision in terms of acoustic waves interacting with the outlet of the chamber is much improved since this section is not a boundary condition but a part of the computational domain.
Swirled flows are very sensitive to an hydrodynamic instability called PVC (Precessing Vortex Core). This mode which induces a rotation of the axis of the recirculation zone is captured by LES (Fig. 2.10) particularly well in the non reacting case.

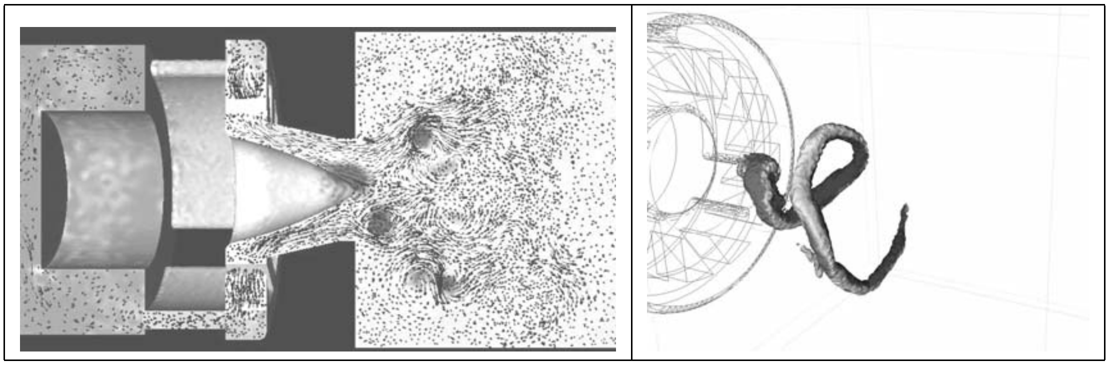

Figure 2.10: Vector and pressure field in central plane (left) and isosurface of low pressure (right).

For nonreacting flow the LES and experimental profiles are compared at various sections of the combustion chamber (Fig. 2.9) for average axial (Fig. 2.11) and RMS axial (Fig. 2.12) velocities. Azimuthal velocities are predicted with the same accuracy. All mean and RMS velocity profiles are correctly predicted. Considering that this computation has no boundary condition which can be tuned to fit the velocity profiles this confirms the predictive capacity of LES in such swirling flows which are well known to be difficult for RANS. A large central recirculation zone (evidenced through negative values of the mean axial velocity) is formed on the chamber axis. This recirculation zone begins at x=2 mm downstream of the central hub and is not yet closed at x=35mm. The large values of RMS velocities on the axis in Fig. 2.12 are due to the PVC.
With combustion LES also performs very well. For an equivalence ratio of 0.75, an air flow rate of 12 g/s and a thermal power of 27 kW, the velocity fields are presented in Fig. 2.13 (mean axial velocity), 2.14 (RMS axial velocity). The overall agreement between mean LES results and experimental data is outstanding. LES also shows that the PVC is damped when combustion starts.

2.3.3.2 System identification of turbulent burners (<u>K. Truffin</u>, <u>A. Sengissen</u>, <u>T. Poinsot</u>, <u>B. Varoquié</u>, L. Selle)

This section presents examples of forced turbulent flames. Forcing is a normal procedure in the investigation of combustors stability. Burners are forced in order to examine their response to acoustic waves entering the air inlet. This type of analysis, called system identification can be performed experimentally or numerically using LES. But the cost of such experiments is very high and LES are presently being developed to try to replace experiments for this task.
At CERFACS, three studies of this type were performed in 2003:

- Chamber A: forced response of a turbulent diffusion flame in a rectangular propane / air burner. This burner is installed in Ecole Centrale Paris (ICLEAC EC project).
- Chamber B: forced response of a large scale industrial gas turbine mounted in a square cross section chamber in Karlsruhe University.

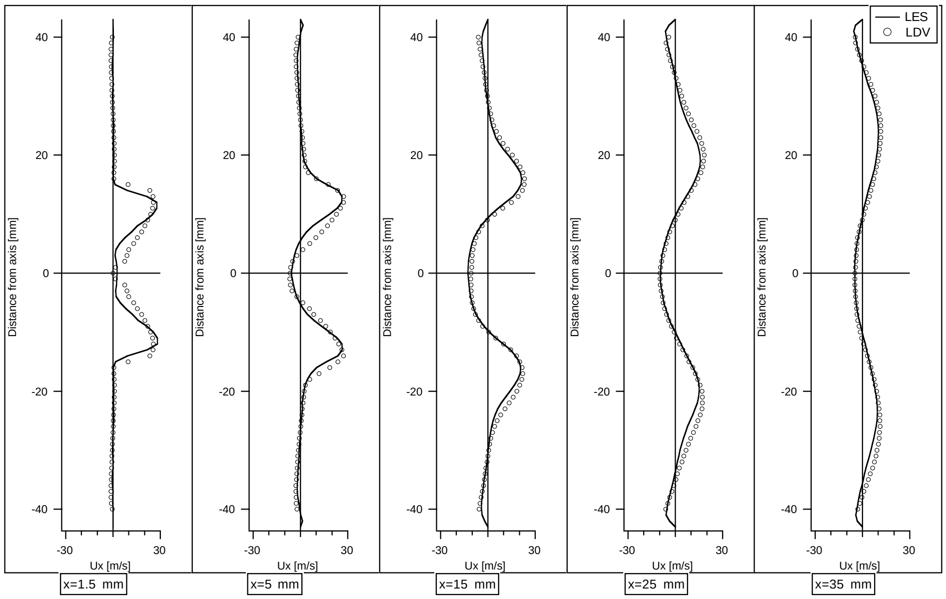

Figure 2.11: Cold flow: average axial velocity profiles. Circles: LDV; solid line: LES.

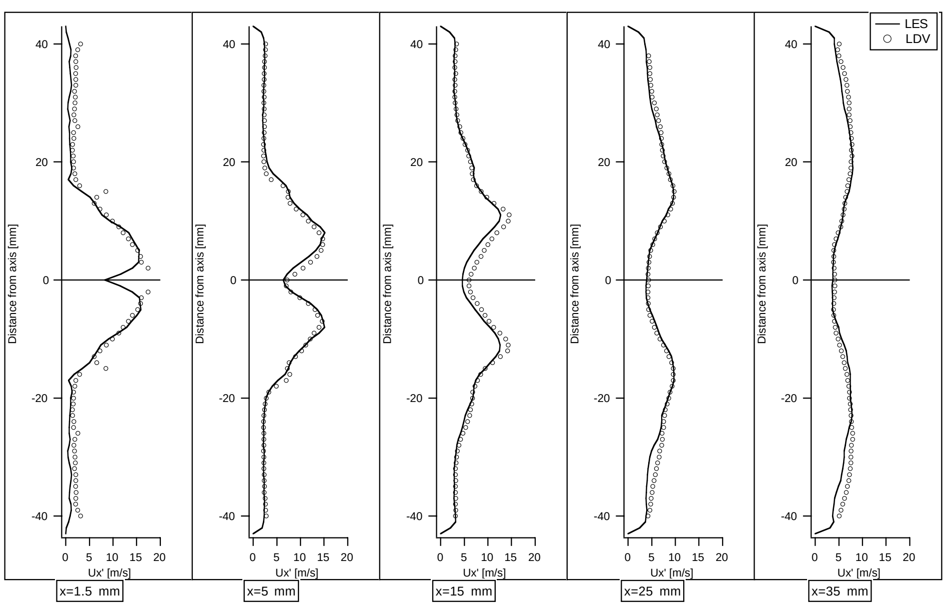

Figure 2.12: Cold flow; RMS axial velocity profiles. Circles: LDV; solid line: LES.

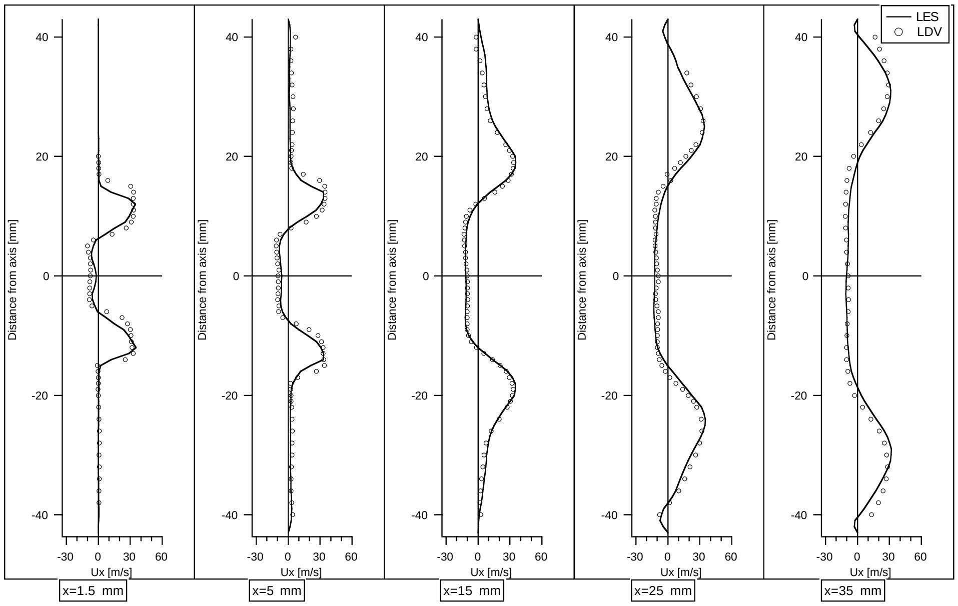

Figure 2.13: Reacting flow; mean axial velocity in the central plane. Circles: LDV; solid line: LES.

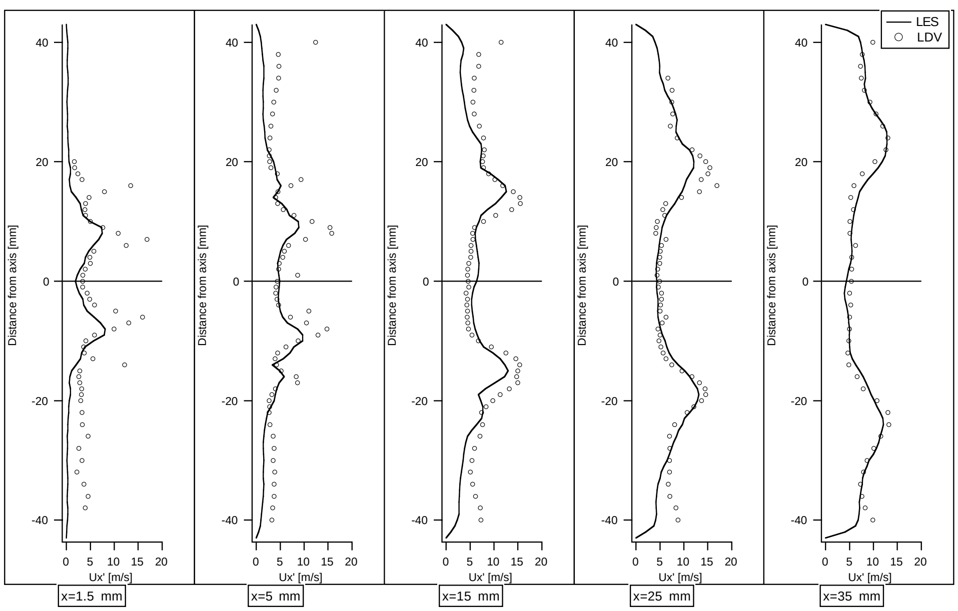

Figure 2.14: Reacting flow; RMS axial velocity in the central plane. Circles: LDV; solid line: LES.

- Chamber C: a new experiment built atTwente Univ. in the DESIRE EC project. For this last burner, multiple innovations will take place: the computation will include both mixing from the methane jets and the combustion in the chamber. All LES and measurements will be performed to address the issue of fluid structure interaction during combustion oscillations.

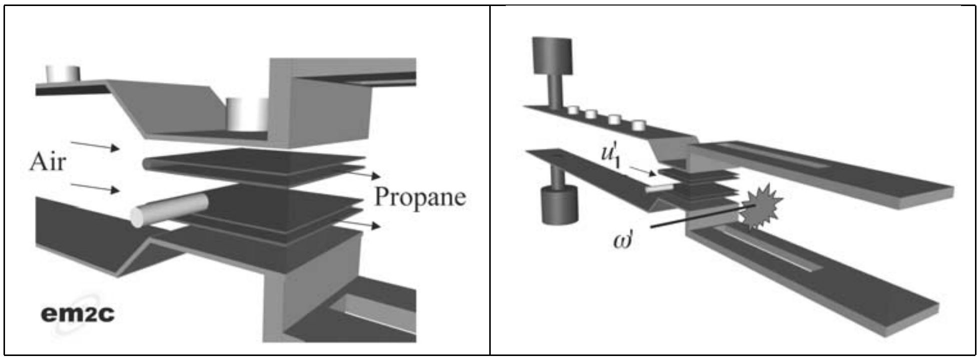

Figure 2.15: Chamber A: burner (left) and set up for system identification (right).

The geometry of burner A is displayed in Fig. 2.15. Loudspeakers produce the acoustic excitation u' at the chamber inlet. A photomultiplier measures the resulting unsteady heat release ω'. The transfer function between u' and ω' is used in acoustic codes to predict the burner stability (Section 2.3.3.3). A typical view of the flame for Chamber A is given in Fig. 2.16. Note that the flame is very long: it does not swirl and is lifted from the injectors. The comparison with the experimental results of Ecole Centrale is promising [1].

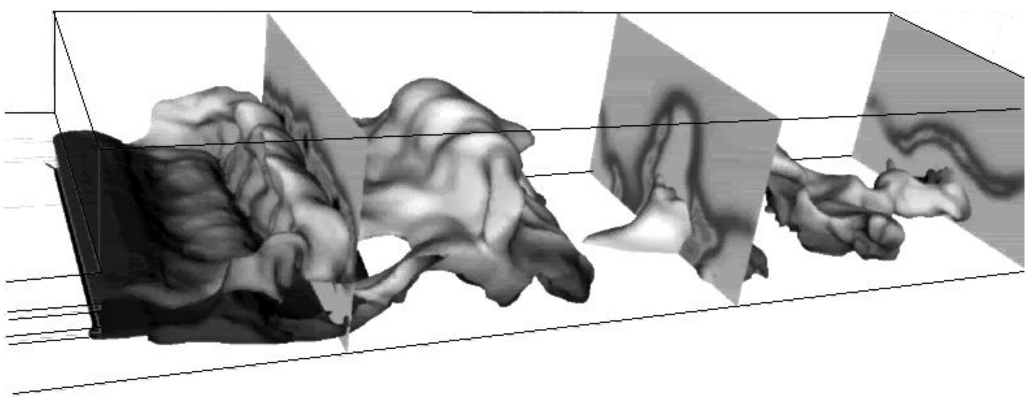

Figure 2.16: Chamber A: isosurface of fuel mass fraction and reaction rate in three planes.

For chamber B, a much larger burner is used. This burner is also swirled and reaches a power up to 800 kW. It is installed in two different institutes in Karlsruhe, either in a square (ITS) or a circular (EBI) combustion chamber depending on the type of experimentation.
Fig. 2.17 shows the main features of the burner in which this identification by acoustic forcing is performed: a central axial swirler (colored in dark) is used to inject and swirl a mixture of natural gas and preheated air. The main part of the combustion air as well as fuel is injected by the diagonal swirler through holes located on both sides of the vanes in order to achieve swirling. Perfectly mixed gases enter the diagonal swirler while pure air enters the axial swirler: the flame inside the chamber is in a partially premixed regime.

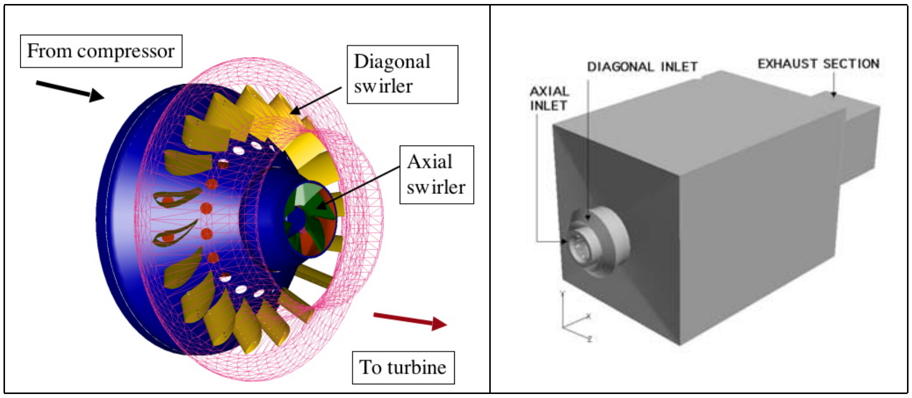

Figure 2.17: Chamber B: burner (left) and combustion chamber (right).

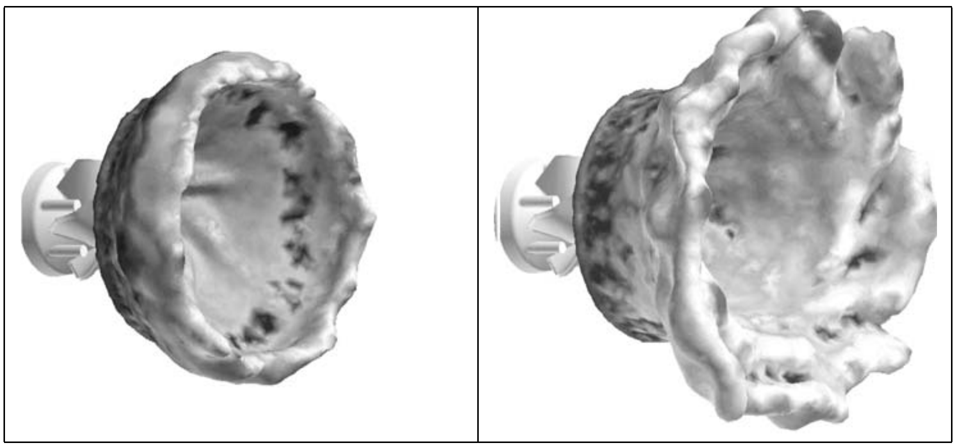

Figure 2.18: Combustor B: flame shapes (isocontours of temperature T=1000 K) at two instants of the forcing cycle separated by a half period.

This burner has been analyzed in detail in [2], but only the pulsated results [3] are presented here: for this study, the flame is pulsated at various frequencies by modulating the inlet velocity. Results are compared to experiments performed at EBI Karlsruhe. For a pulsation at 120 Hz Fig. 2.18 shows two extreme positions of the flame front during one cycle. The inlet pulsation leads to very large excursions of the flame shape and area so that the total heat release is also oscillating. This response is the building block of acoustic solvers that predict the stability of combustors (see Section 2.3.3.3).
The geometry of burner C is displayed in Fig. 2.19: for this flame the computation must include both mixing from the four methane jets with air and combustion in the chamber. This burner is not yet built but LES has already been used for its design: one of the conclusions is that the geometry of Fig. 2.19 would have led to flashback (see Section 2.3.3.5) and had to be modified before final construction. The walls of the combustion chamber are equipped with accelerometers to measure the structure vibrations and to correlate them with the pressure and heat release oscillations inside the combustor.

[1] K. Truffin, B. Varoqui, D. Veynante, T. Poinsot, and L. Lacas. Large eddy simulations and experimental characterization of the unsteady response of partially premixed flames. Submitted for publication to Combustion and flame, 2004.

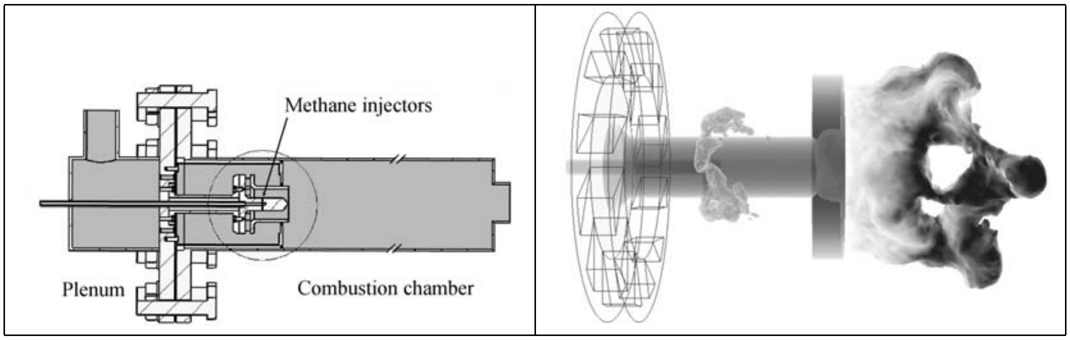

Figure 2.19: Combustor C. Left: geometry: the whole shaded area is meshed and computed. Right: isosurfaces of $Y_{CH4} = 0.1$ and isosurface of temperature $T = 1000$ K.

[2] L. Selle. Simulation aux grandes échelles des interactions flamme/acoustique dans un écoulement vrillé. PhD thesis, Institut National Polytechnique de Toulouse, 2004.
[3] A. Giauque and L. Selle and T. Poinsot and H. Buechner and A. Kaufmann and W. Krebs. System identification of a large scale swirled premixed combustor using LES and comparison to measurements. Submitted in Journal of Turbulence, 2004.

2.3.3.3 Acoustic tools development. Application to high-frequency modes (L. Benoit, T. Poinsot, A. Kaufmann, F. Nicoud)

The importance of acoustics in combustion has been the subject of a long controversy in which certain authors argued that acoustics could be neglected both experimentally and numerically. Most recent experimental and numerical results actually confirm that acoustics are essential phenomena for turbulent confined flames. To understand confined flames, developing acoustic codes which can solve the wave equation in complex geometries for reacting flows is therefore a necessary step. CERFACS is developing such tools [1].

The first tool called Soundtube is able to provide the low-frequency longitudinal resonant modes in a network of interconnected ducts with variable sections and temperatures. This tool has been installed at SNECMA and EDF. The second tool is a full three-dimensional Helmholtz solver. This Helmholtz solver (called AVSP) provides the solution of the Helmholtz equation in the frequency domain and is coupled to the LES code AVBP: they use the same grids; the mean temperature and mass fraction fields required by AVSP (to know the sound speed) and the flame transfer function (to know the acoustic / flame coupling, see Section 2.3.3.2) are provided by AVBP.

Low frequency modes are not the only evident product of flame / acoustics interactions. Higher order acoustic modes of the chamber can also interact with the flame front. These modes are more difficult to understand than low-frequency oscillations and the joint usage of LES and Helmholtz solvers offers a new and powerful approach for such phenomena as shown in this section for a turning mode in the combustor of Fig. 2.17. In the LES, this combustor exhibits a natural unstable mode at 1200 Hz which is visible in the wall pressure traces. The structure of this mode can be visualized by plotting the p' amplitude on the walls of the chamber (Fig. 2.20 right). Even though the data is slightly noisy because of insufficient sampling, a clear mode structure appears.

When the Helmholtz solver is applied to this geometry, it also exhibits two transverse eigenmodes (the (1,1,0) and the (1,0,1) modes) at the same frequency 1220 Hz which can be combined into a turning mode. This turning mode rotates around the axis of the combustion chamber. The resulting average structure is displayed in Fig. 2.20 (left): obviously it perfectly matches the structure measured in the LES: the 1200 Hz

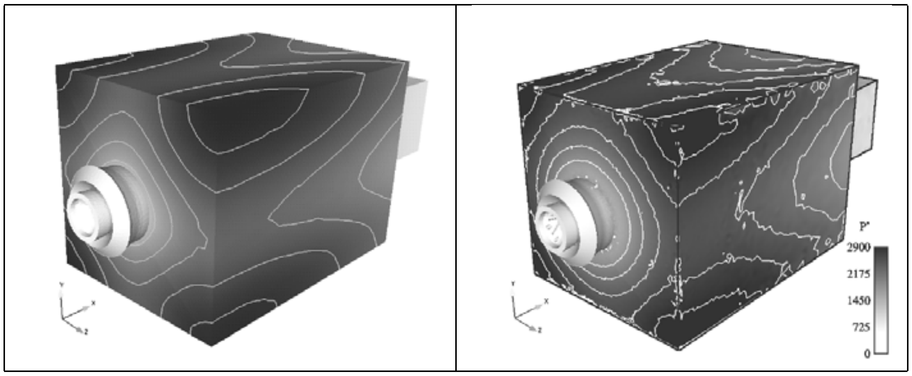

Figure 2.20: Acoustic pressure for the 1200 Hz mode. Left: Helmholtz result. Right: LES result.

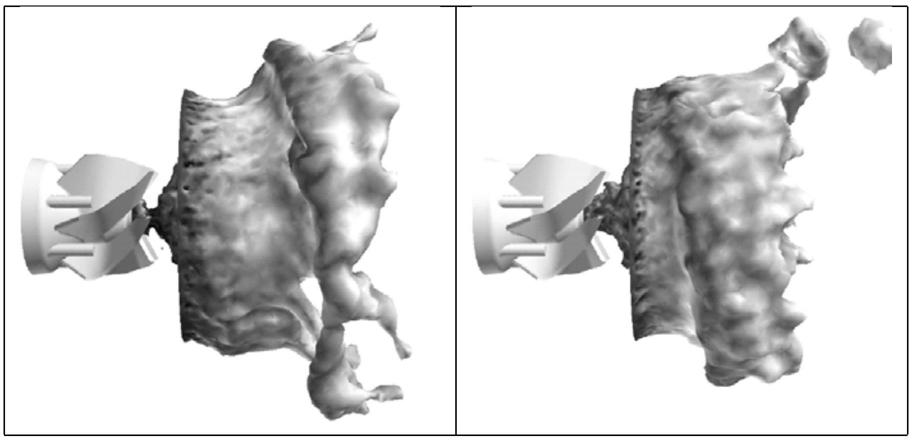

Figure 2.21: Isosurfaces of temperature $T = 1000$ K at two instants of the 1200 Hz cycle separated by a half period. The turning mode shapes the flame along a spiral motion.

mode seen in the LES is a turning mode which is a linear combination of the (1,0,1) and (1,1,0) modes. This turning mode has a direct effect on the flame topology. Fig. 2.21 shows the flame shape at two instants during one 1200 Hz cycle (phase $\pi/2$ and $3\pi/2$): the acoustic velocity induced by the turning mode at the lips of the diagonal swirler creates a helicoidal perturbation which is convected downstream and slices flame elements when it reaches the flame extremities.

[1] A. Kaufmann. Towards Eulerian-Eulerian large eddy simulation of reactive two phase flow. PhD thesis, Institut National Polytechnique de Toulouse, 2004.

2.3.3.4 Acoustic / combustion coupling tools: the acoustic energy equation (C. Martin, T. Poinsot, F. Nicoud)

A key issue to control combustion oscillations is to understand them. At the moment, no one can predict at the design stage whether a given combustor will oscillate. If and when it oscillates, measurements and computations sometimes give indications of the reasons of the problem but it is usually by then too late. Being able to predict these phenomena requires the development of a new approach in which LES and acoustics are coupled. Section 2.3.3.3 has shown how acoustic codes were developed at CERFACS. In parallel, new theoretical tools must be built: one of them is a method to examine all terms in the acoustic energy equation e_1 [1] which controls the evolution of acoustic perturbations:

$$\frac{\partial e_1}{\partial t} = s_1 - \nabla \cdot (p_1 \vec{u}_1) \quad \text{with} \quad e_1 = \frac{1}{2}\rho_0 u_1^2 + \frac{1}{2}\frac{p_1^2}{\rho_0 c_0^2} \quad \text{and} \quad s_1 = \frac{(\gamma - 1)}{\gamma p_0} p_1 \dot{\omega}_T^1 \tag{2.1}$$

where the ^{0} subscript refers to mean quantities and the ^{1} to acoustic values.
If integrated over the whole volume V of the combustor bounded by the surface A, it yields:

$$\frac{d}{dt}\int_V e_1 dV = \int_V s_1 dV - \int_A p_1 \vec{u}_1.\vec{n} dA \tag{2.2}$$

where $\vec{n}$ is the surface normal vector. This surface consists of walls or of inlet / outlet sections. The RHS source term $\int_V s_1 dV$ corresponds to the well-known Rayleigh criterion and is the source of the oscillations. But there are other terms like acoustic fluxes on outlets and inlets $\int_A p_1 \vec{u}_1.\vec{n} dA$ which also have a very strong effect on the instabilities: these terms can not be measured experimentally and most studies consider only the term they can quantify (the Rayleigh term) which is clearly just a small part of the problem. LES offers a new approach by giving access to all terms of Eq. (2.2). A full closure of the acoustic energy equation using LES equation is tested for the first time in [1]. Preliminary results are very promising: the budget equation for acoustic energy seems to be closed reasonably well so that individual terms can now be examined. This has been done for the burner installed in Ecole Centrale Paris.

[1] T. Poinsot and D. Veynante, (2001), Theoretical and numerical combustion, R.T. Edwards Ed., Chapter 8, 473 pp.

2.3.3.5 LES of flashback in swirled burners (Y. Sommerer, T. Poinsot, J.-P. Légier, D. Galley, D. Veynante)

Flashback is one of the phenomena of high concern for the new generation of lean premixed gas turbine burners: by improving mixing upstream of the combustion chamber (see Section 2.3.3.10), many devices used to reduce pollution by increasing mixing can also create the possibility for the flames to propagate upstream of their normal stabilization zone, thereby risking the destruction of the injector or a part of it. Certain gas turbines manufacturers already imagine future robust designs which would resist a temporary flashback and recover without failure. Being able to predict flashback is therefore a key issue for modern numerical combustion. It is also a challenge for modelling because, during flashback, the flame regime changes considerably from partially premixed to almost purely non premixed flames. The duration of the flashback event can also be long (of the order of a second) requiring significant computing power.

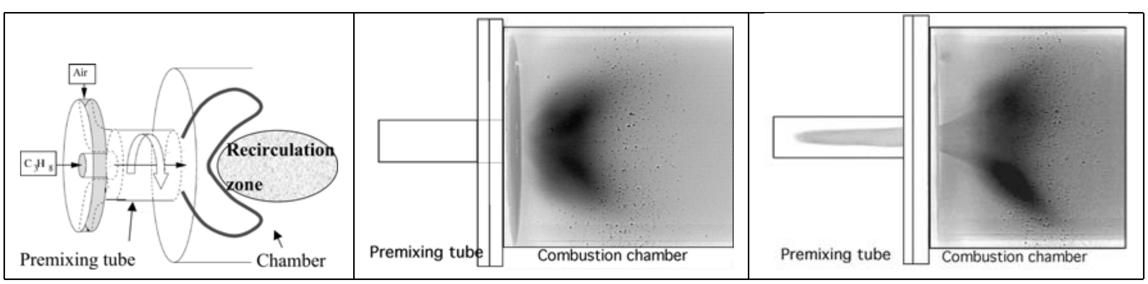

Figure 2.22: Left: geometry of the burner (Ecole Centrale Paris). Center: experimental view for stable regime. Right: flashback.

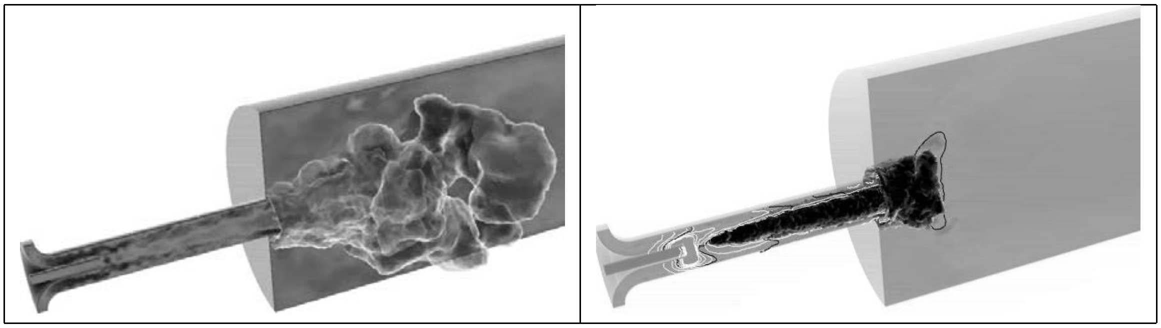

Figure 2.23: Left: stable lifted flame. Right: flame after flashback. The flame is visualized by an isosurface of reaction rate.

CERFACS has worked on flashback in Lean Premixed Prevaporized burners since 1999 [1] and these studies have been continued since then. The experimental validation is performed in Ecole Centrale (PhD of D. Galley) in a special chamber in which premixing tube and combustion chamber are transparent in order to observe the flame flashback. Fig. 2.22 shows the geometry (left) and the two extreme regimes which can be observed: either the flame starts in the combustion chamber (where it should: Fig. 2.22 center) or it starts in the premixing tube (Fig. 2.22 right). Here flashback is obtained by simply reducing the air flow rate. The whole flashback evolution can be studied using LES (Fig. 2.23). The limits where flashback is obtained experimentally are qualitatively recovered by LES but a major problem arises: hysteresis. For the same regime, the flame can be either lifted or flash backed depending on the history of the ignition and stabilization procedure: increasing or decreasing the equivalence ratio to go from point A to point B for example can lead to two different flows at point B. This point is being investigated with LES and experiments. This configuration will also be run for two-phase flow combustion in 2004.

[1] J.-P. Lgier. Simulations numriques des instabilits de combustion dans les foyers aronautiques. PhD thesis, Institut National Polytechnique de Toulouse, 2001.

2.3.3.6 Multiburner computations (G. Staffelbach, T. Poinsot)

Most academic studies of combustion in gas turbines are performed using a gas turbine burner and installing it into a laboratory combustion chamber. However real gas turbines use 16 to 24 burners installed in the same annular chamber. In such situations strong coupling may occur between burners: in regions where the issuing flames from neighbouring burners meet, strong turbulence and heat release can take place and lead to instabilities which cannot be obtained in single burners configurations. CERFACS is studying a chamber equipped with three burners, which is the largest LES computation ever performed with combustion in such a geometry (5 million cells). It requires typically 64 to 128 processors to run efficiently. Fig. 2.24 shows an isosurface of temperature (left) and a snapshot of the reaction rate in a surface passing through the three burners axis (right). The flows issuing from the burners interact and the flames influence each other. The next studies will focus on comparison with experimental data that will be obtained in 2004 at DLR.

2.3.3.7 Prediction of pollutant formation with LES (P. Schmitt, T. Poinsot, D. Veynante, N. Dioc)

A natural extension of the CERFACS LES tools is to predict the formation of pollutants. This can be done in the framework of the Thickened Flame model even though few developments have been done up to now. As an example, LES to predict CO levels are performed : Fig. 2.25 shows the geometry of the burner and a typical instantaneous field of CO. This swirled burner uses a cone cut in two parts and shifted to create a lateral swirling air injection. Fuel (methane) is injected laterally by small holes. In the computation

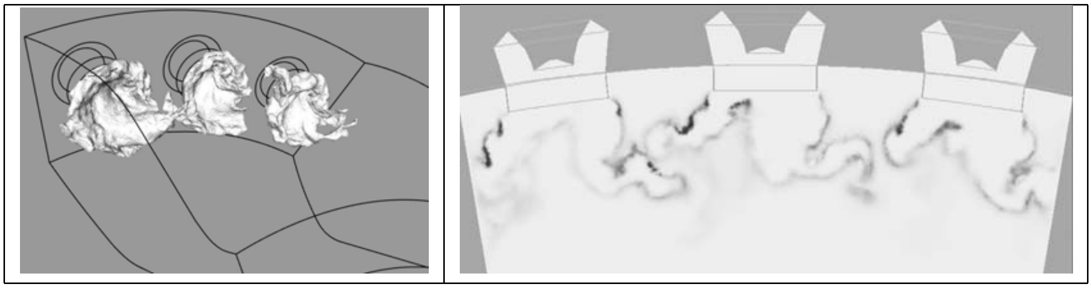

Figure 2.24: Three-burner combustion chamber of DLR. Left: isosurface of temperature T=1000 K. Right: field of reaction rate in a surface passing through the axis of the three burners.

mixing and combustion are handled simultaneously using the DTF model and a two-step chemical scheme. The experimental results corresponding to this burner will be provided in 2004 by Ecole Centrale Paris (at atmospheric pressure) and DLR (at high pressure).

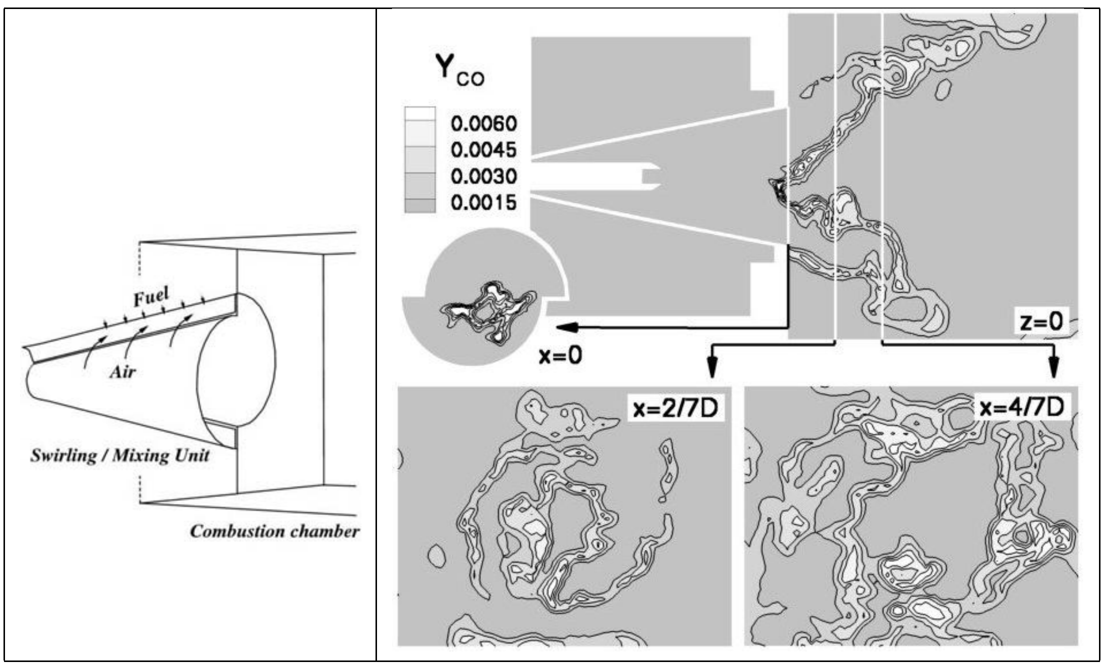

Figure 2.25: LES of combustion including CO formation. Left: configuration. Right: CO instantaneous fields in various cuts in the burner.

2.3.3.8 Coupling RANS and LES for reacting flows (M. Saudreau, B. Varoquié, T. Poinsot)

A usual question about LES is its computing cost. CERFACS' experience is that the cost is low especially on modern parallel computers once an initial solution is available. Obtaining such a first solution rapidly is the central problem. One way to do this is to compute the flow with a RANS (Reynolds Averaged Navier Stokes) solver and to use this solution to initialize the LES code. This issue is studied in collaboration with EDF in the case of the Oracles rig developed at Poitiers. Various coupling solutions between Saturne (the EDF RANS code) and AVBP are being investigated. The main difficulty is that there are significant differences between a RANS solution and an initial LES field: how to reconstruct the LES data from the averaged RANS data raises a variety of fundamental issues which are now being examined.

2.3.3.9 LES for high speed reacting flows (B. Varoquié, T. Poinsot, R. Knikker)

Certain innovative combustion concepts require the study of the combustion of gaseous fuels in high speed hot air (typically a few hundreds of m/s): a first classical lean burner preheats the air and this hot air is then sent to a reheat burner in which methane is injected and autoignites rapidly. Combustion in this reheat burner is very different from low-speed combustion due to the very high injection velocities. Understanding unsteady combustion in reheat burners is therefore a priority for developments. This field of applications is also totally new for LES: in such flows, autoignition is the key process for flame stabilization. CERFACS has worked on such a combustor [1] to investigate chemical schemes adapted to such flames, the feasability of LES and the stability of burners based on this reheat approach.
An essential difference between LES for classical and reheat burners is the importance of chemistry: in reheat burners, autoignition is the main factor controlling the flame position while flame propagation plays the same role in low-speed burners. To understand these mechanisms and to construct a chemical scheme suited to LES of reheat burners, the first part of the study was devoted to the computation of the ignition between a hot air layer and a cold fuel jet. This basic problem contains all the phenomena present in the real combustor except turbulence: the fuel and the air must mix before ignition can start but this mixing also lowers the local temperature, slows the chemical reactions down and delays autoignition. The results are described in [CFD10].

[1] B. Varoquié, C. Martin and T. Poinsot. Large eddy simulation of auto-ignition in gas turbines with sequential combustion. Contract report CR/CFD/04/19, 2004.

2.3.3.10 Mixing studies (C. Prière, L. Gicquel, T. Poinsot)

Being able to mix fuel and air efficiently is a key issue in multiple combustion problems: insufficient mixing leads to high pollution levels and stability problems while too fast mixing can cause flashback and endanger the safety of the burner. CERFACS has investigated the mixing of fuel jets with air, the effects of mixing enhancement devices and the mixing of dilution jets with burnt gases using LES. These numerical studies were accompanied by experiments performed at Univ. Bochum and ONERA Toulouse.
Fig. 2.26 shows a result where 8 dilution jets are injected into a central duct. The full configuration is computed and no assumption is used on the symmetry of the flow. The comparison with the PIV results of ONERA Toulouse is excellent.

2.4 Software engineering

Y. Sommerer, M. Garcia

The production of so many LES at CERFACS raises a number of questions in terms of software engineering. The development of AVBP and of all the other tools surrounding AVBP is done using the most modern methods. This includes:

- Source management: AVBP is developed jointly at Institut Francais du Pétrole and CERFACS but is used at many other institutions in Europe. Source management is performed only at CERFACS: typically two versions are produced and tagged every year using CVS. Regular meetings take place between IFP and CERFACS to define the evolution of versions.
- CTEA are elementary test cases (convection, diffusion, time advancement) which are run on a weekly basis automatically at night and compare versions during their modifications.

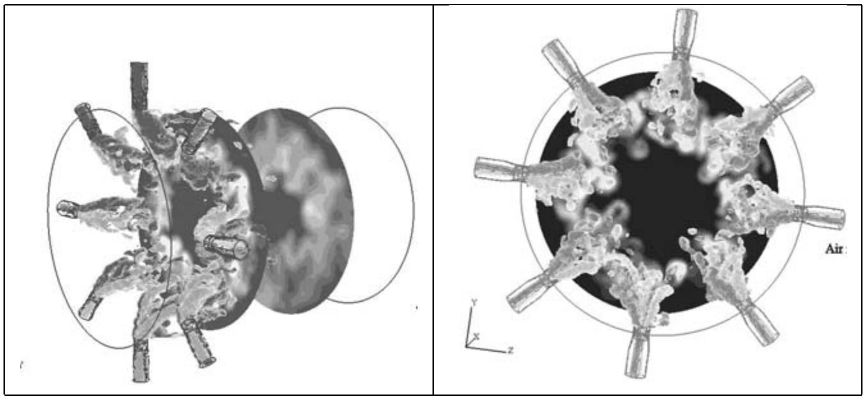

Figure 2.26: Isosurfaces of axial vorticity tracing the dilution air jets injected in the main duct.

- Quality Program Forms (QPF): QPFs are more complete tests of the code which are performed every six months to ensure non regression of versions. QPFs include laminar flames, tubes, homogeneous turbulence, shear layers, acoustic waves, Karmann street, etc.
- Web user page: all documentation related to AVBP is summarized on a specific web page which can be accessed by all users and developers. The web site contains the handbooks, a page to report problems, a user's guide, various tutorials, all QPFs of all versions, reports and PhDs directly linked to AVBP, etc.
- Optimization and parallelization: most present platforms for high-performance computing use parallel codes and AVBP follows the same path. This puts constraints on the algorithms used for LES. For example, in the field of two-phase flows, using Euler Euler formulations instead of Euler Lagrange is typically dictated partly by computer architecture considerations (Section 2.2).
- Visualization: LES generates large data fields but conversely to RANS, LES generates many such fields to retain the unsteady character of the flow. A typical LES can create 200 snapshots on a 2 million points grid. Transporting such fields and storing them becomes difficult. CERFACS has introduced different solutions for this: (1) special tools have been created to reduce the size of data fields (by using coarser grids) in order to transport them back to the user and visualizing the results in a degraded but faster mode (2) experimentations performed with CINES on remote visualization with OpenGL Vizserver: data remains at CINES and is processed on a specific SGI machine and only pictures are transferred in real time to the user. The hardware and software needed for this as well as the results obtained for AVBP data are described in [1] (see also 2.5 of the Computer Support Group chapter). They have also been presented in the specialized press by SGI.
- More generally CERFACS continues to collaborate intensively with the French national super computing centers CINES and IDRIS but also with CEA to develop high performance computing for reacting flows on parallel computers. AVBP or NTMIX are used to benchmark machines for CINES and IDRIS for example. Regular meetings offer opportunities to CERFACS users to discuss the evolutions of the computing centers. This collaboration also extends to the USA: in 2002, Pr W.C. Reynolds, head of the ASCI project at Stanford (which is devoted to computations of combustion in gas turbines on massively parallel machines) came to CERFACS to present the results of the project. In 2003, a very special program took place between CINES and CERFACS: in this 'extreme combustion' project, very large LES were performed (up to 8 million points) to demonstrate the present limits of existing platforms. Interestingly, results have matched what CERFACS scientists have already observed at Stanford in 2002 during the summer program: the present limits have been

found to be essentially at the preprocessing and postprocessing levels. Generating very large hybrid grids (more than 8 million points) and partitioning them for parallel computers for example is a key problem at the present time.

[1] N. Monnier and Y. Sommerer. Utilisation déportée du serveur de visualisation du CINES. In La Gazette du CINES, 2-5, Montpellier, France, 2003.

3 Aerodynamics

In the field of aerodynamics and fluid dynamics modelling the objectives of the Group are:

- The development of reliable, efficient and accurate predictive CFD softwares for their use in industrial environment,
- The numerical investigation of complex flow physics making use of high-performance computing.

The Group develops physical models to study flow fields in and around complex geometries. These models must be implemented in efficient solvers to be tested and used. These models and CFD tools are to be eventually used by both research laboratories and industrial users.
Formerly, CERFACS worked in an European consortium for the development of NSMB solver (Navier Stokes Multi Blocks). Since 2000, the bulk of development work has switched to elsA. elsA (ensemble logiciel Aérodynamique) is an ONERA project, to redesign Navier Stokes simulation methods and algorithm in an Object Oriented framework. CERFACS and ONERA have signed in March 2001 an official agreement for the joint development of elsA. The last two years have seen the completion of the switch over process from NSMB to elsA both for development and applications. Moreover, during the 2002-2003 timeframe, the elsA project has passed successfully two major milestones :

- Intensive optimisation of the code during the fall of 2002 led to the choice of elsA for the common multi bloc structured code for trans european entities of Airbus.
- In the fall of 2003 elsA entered production for design studies at Airbus France. The software is also distributed at other Airbus locations and CERFACS participated with ONERA to the user and developper training sessions organized for DLR and other Airbus users.

In the near future the work with elsA will proceed in collaboration with ONERA and with EADS and SNECMA. Lately, CERFACS has been invited by ONERA and DLR to participate to their internal project on a common architecture platform. CERFACS should take a part in the European integrated project OPERA (Open CFD Alliance Enabler for Revolutionary Aerodynamics and Collaborative Design, to be submitted in the second call of the 6th PCRD). These two actions should ensure that in the future the operating CFD platforms at CERFACS will be among the best in Europe and that the developments will be shared across a large user base.
During that period of transition and strengthening of the CFD platform, the applications and modeling work went on with an emphasis on unsteady simulations: LES and zonal approach of hybrid turbulence simulation, LES and wall laws for thermal applications.
The Wake Vortex activities sustained a high rate of research and publications and have seen the successful completion of two PhDs.

The Group works in collaboration with:

- Industrials : Airbus - F, Airbus - D, SNECMA Moteurs and BAE Systems.
- Research : DLR (emerging through MIRACLE), UCL, IRPHE, IMFT, Paris VI (P. Sagaut) and Montpellier (B. Mohammadi/F. Nicoud).

3.1 Modelling

3.1.1 Wake vortex simulation (H. Moet)

CERFACS has developed a strong expertise on the topic of wake vortex dynamics, which is now widely recognized in the scientific community. Numerous studies have been conducted investigating the stability of different vortex systems, by means of Direct Numerical Simulations (DNS) or Large-Eddy Simulations (LES). These studies are both a means of characterizing the wake of an aircraft in the near-field and a way to determine the decay in the far-field, which is important in predicting the behaviour of the wake of a large transport aircraft. CERFACS investigates wake vortex dynamics through a collaboration with Airbus-Deutschland and CNRS-IRPHE and CERFACS is also active in the framework of European programs such as AWIATOR (FP5).

CERFACS has been involved in studying the unstable behaviour of a four-vortex system ([CFD73]). The particular four-vortex system appears to be unstable with respect to two- and three-dimensional perturbations. The intrinsic dynamics of the system will lead to the development of instabilities with a range of different wavelengths (very short wavelength/elliptic instability, $\lambda_i = \mathcal{O}(r_{core})$ or short wavelength/Crouch-type instability, $\lambda_i = \mathcal{O}(b)$) which amplify rapidly within the inner vortices. The development of the instability occurring in the four-vortex system is simulated by means of DNS simulations. The global dynamics are illustrated by isosurfaces of vorticity magnitude in terms of the nondimensional time, $t^* = t/t_{ref}$ with $t_{ref} = b_1^2/\Gamma_1$. Figure 3.1 shows that the inner vortices ($t^* = 10.14$) experience the amplification of the forced mode k_p which corresponds to the wavelength λ_{Crouch} of the Crouch-type instability for a four-vortex system. In the nonlinear regime, the secondary vortices experience

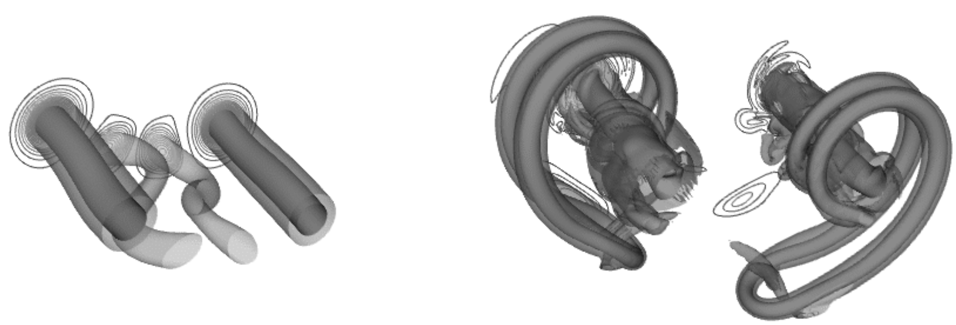

$t^* = 10.14$ $t^* = 13.46$

Figure 3.1: Isosurfaces of vorticity magnitude showing the global dynamics for the simulation with $\epsilon = 10^{-6}$ for time instants $t/t_{ref} = 10.14$ & 13.46 with $t_{ref} = b_1^2/\Gamma_1$.

large-scale deformations, eventually reconnect, which leads to the formation of so called ”omega loops” ($t^* = 13.46$).

The phenomena caused by the generation and propagation of pressure waves in vortex cores have also been investigated, by following the DNS and LES approach ([CFD24]). The propagation of pressure waves is responsible for the generation of axial velocity, which under certain conditions lead to the development of helical instabilities and the abrupt change of flow topology in the vortex core. The dynamics involved may explain vortex bursting and end effect, which are phenomena observed in smoke visualisation of real aircraft wakes as well as in small-scale experiments that are not well understood.

Numerous analyses have been made of the effect of external (atmospheric) turbulence on the stability and decay of vortex systems composed of a single vortex or a pair of counter-rotating vortices ([CFD7], [CFD24]).

3.1.2 Unsteady turbulence modelling

3.1.2.1 LES in elsA software (J.-C. Jouhaud, J.-F. Boussuge, X. Toussaint, P. Sagaut)

Since 2002, the Group develops LES within the elsA software using experience on AVBP, NTMIX and NSMB codes. Even if this leading-edge CFD technology can not yet be applied to complex aeronautical configurations (despite increasing computer capacities along with underlying numerical methods, grid techniques and models), it can play a major role in external aerodynamics when combined with wall functions and U-RANS models (hybridization between U-RANS and LES methods: DES, VLES ...).

In order to obtain an efficient LES tool, different Sub-Grid Models (Smagorinsly, Selective Smagorinsky, WALE, FSF), weakly dissipative schemes with skew-symmetric form that minimizes aliasing error (derivations of classical Jameson scheme) and adapted post-treatments (average quantities, RMS quantities ...) have been implemented in elsA. At the same time, QPF (Quality Programme Forms) have been elaborated to validate the developments and to ensure the integrity of LES with the production of elsA versions. Actually four test-cases are daily used: the turbulent channel flow, the free turbulence decaying in a periodic box, the temporal flat plate and the convection of a vortex in a periodic box.

3.1.2.2 Hybrid U-RANS/LES methods (X. Toussaint, J.-C. Jouhaud, P. Sagaut)

The Group is involved in a leading-edge project concerning the development of hybrid LES/U-RANS methods (application to the buffeting phenomenon [CFD98], elsA software). Hybrid methods, combining precision/low cost computations, could push further away the actual limits of unsteady computations. To develop this topic, the Group recently submitted a FP'6 Research Training Network involving seven European research centers having activities in unsteady turbulence modelling: CERFACS-Toulouse, CEA-Grenoble, UPMC-Paris, EPFL-Lausanne, LSTM-Erlangen, CSIC-Zaragoza and UNINA-Naples.

3.1.2.3 Wall laws for heat exchanges (A. Devesa, J.-C. Jouhaud, F. Nicoud)

At the end of 2003, the Group started 'wall laws' activities for U-RANS/LES models. The aim of these activities is to equip the CEA Trio_U code (designed for 3D thermo hydraulics handling structured and unstructured meshes) with wall laws adapted to heat exchanges in anisothermal configurations. The target applications will concern the nuclear reactor safety.

3.1.3 Statistical turbulence models (A. Celic)

During the last quarter of 2003, implementation of a new variant of Durbin's k, ϵ, v^2, f turbulence model into elsA has been tackled. This activity is aimed at further improving elsA's predictive performance for heat transfers at walls in aerodynamic flows. Typical applications envisaged are impinging jet flows or ventilation of aircraft systems.
Compared to classical employed turbulence models like the k, ω model of Wilcox [1] or the k, ϵ model of Jones and Launder [2], the original k, ϵ, v^2, f model has proved superior predictive performance for wall heat transfers. Yet, its numerical application is non-trivial since the boundary-value problem is ill-posed. To solve this difficulty, a modified version of Durbin's model [3] was chosen to be implemented into elsA. This new variant promises higher numerical robustness while preserving all favorable predictive properties of the original model.

In addition to boundary-condition issues, the implementation of the model equations into elsA was identified as a key challenge. On the one hand, the model's equations for k, ϵ and v^2 constitute classical turbulence transport equation and are therefore straightforward to implement into the existing design of elsA. On the other hand, f represents the non-local character of redistribution terms in the transport equations of the Reynolds-stresses. To capture this non-local property, f is modeled by an elliptic equation and, hence, requires a separate treatment in elsA. This entails more elaborate implementation design and coding than a classical transport-equation model. Suggestions have been made to master this task with a minimum change in the present code structure of elsA.

[1] C. D. Wilcox, (1998), Turbulence Modeling for CFD, DWC Industries, La Cañada 2nd Ed.
[2] W. P. Jones and B. E. Launder, (1972), The Prediction of Laminarization with a Two-Equation Model of Turbulence, International Journal of Heat and Mass Transfer, 15, 301-314.
[3] P. A. Durbin, (1991), Near-Wall Turbulence Closure Modeling Without "Damping Functions", Theoretical and Computational Fluid Dynamics, 3, 1-13.

3.1.4 Hypersonic (G. Chevalier, M. Duloué)

The simulation of hypersonic flows with chemical unequilibrium was the last study conducted on the former Multi Bloc structured code NSMB developped in an European consortium [CFD60]. That work was performed for the EADS Launch Vehicule division. The task was dedicated to the simulation of hypersonic flows with chemichal desiquilibrium. The work started for inviscid flows and proceeded with laminar viscous flows. For the latter case, catalitic, and semicatalitic boundary conditions were implemented. That work gave very interesting and motivating results. In the meantime the AAM team has completely switched CFD codes from NSMB to elsA, and that development appeared as too costly to report in elsA on our own ressources. That work has been integrated and transmitted to the maintainer of NSMB, and is now stopped for the time beeing in CERFACS.

3.2 Numerical aerodynamics

3.2.1 Meshing Techniques

Grid generation is a crucial problem for the computation of complex aircraft configurations using a body fitted structured code. Furthermore, due to the data management of structured grids, the local refinements around the geometry and special flow regions (boundary layers, stagnation lines, wakes) tend to spread through the whole domain even in zones where gradients are expected to be weak. This can lead to very large grids, especially for complex geometries. Two approaches can reduce this drawback:

i) conservative non coincident interface boundary condition;

ii) automatic mesh refinement.

CERFACS develops and maintains those techniques to help Airbus in reducing simulation turn-around times and in improving the flow accuracy. Those two meshing techniques have been implemented and validated in the elsA software.

3.2.1.1 Conservative non coincident interface boundary condition (M. Montagnac)

The purpose is to develop an efficient way to simplify the grid generation and to deal with complex configurations using moderately sized grids. In that technique also called patched grid technique, two domains must have a common interface, or adjacent interface, but grid points of both interfaces do not have to be at the same location or coincident. Grid lines through the interface may be not continuous. This approach prevents mesh points from spreading from a block to others.

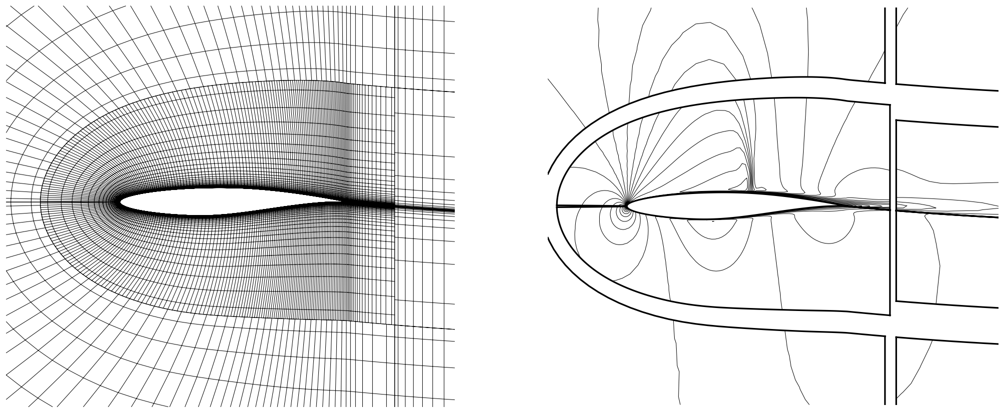

Figure 3.2: Meshes with non coincident interface boundary conditions for a RAE 2822 configuration (left) and mach number isolines (right).

A more restrictive technique than the previous one is the conservative near-matching interface boundary condition. Two domains must also have an adjacent interface but grid points of both interfaces must match in a periodic way.

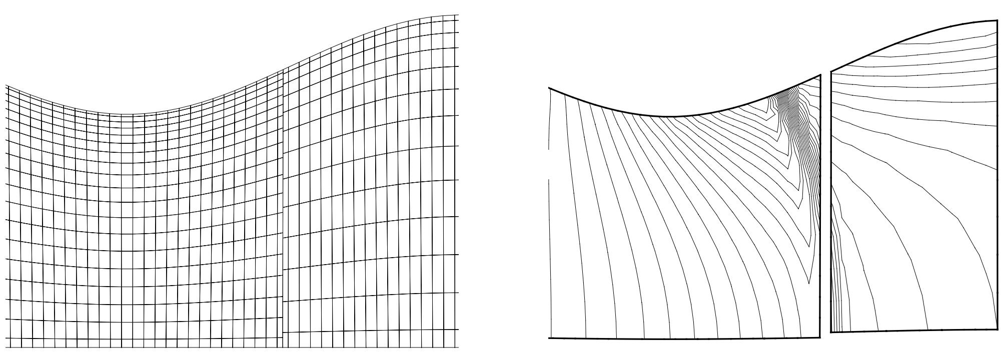

Figure 3.3: Meshes with non coincident interface boundary conditions for a nozzle configuration (left) and mach number isolines (right).

In the elsA software, those two methods are implemented differently for CPU performance and memory requirement issues and they are both fully operational in sequential and parallel modes.

Those techniques are compatible with all spatial numerical schemes, all time marching methods, multigrid acceleration convergence techniques and all turbulence models. Important efforts have been carried out in order to maintain good CPU performances on both scalar and vector computers as well as in a parallel mode.

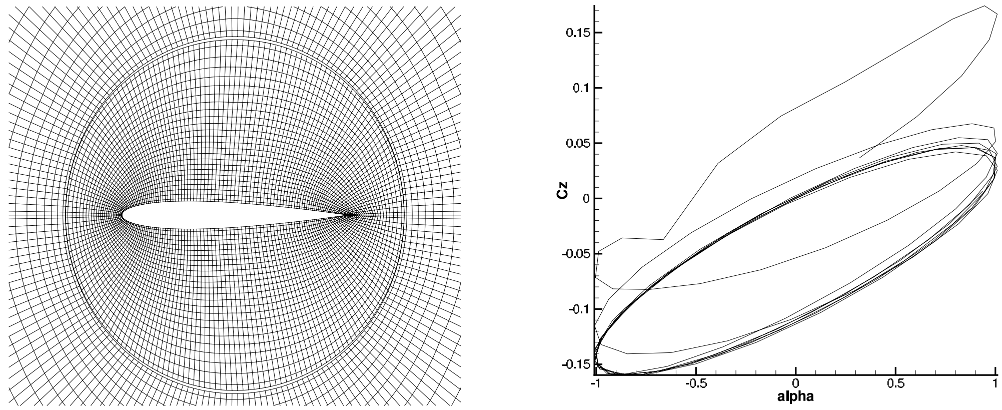

Figure 3.4: Two sliding O-meshes of a pitching NACA0012 airfoil (left) and the lift coefficient versus the angle of attack (right).

Fig. 3.2 shows the 2D turbulent transonic flow around the RAE 2822 airfoil computed with the RANS $k - w$ turbulence model at $M_\infty = 0.73$ and 2.79 degree angle of attack. The Euler flow across a nozzle configuration is shown on Fig. 3.3.
The non coincident interface boundary condition is the core of the sliding mesh option. This functionality is important in turbo machine activities, in rotor-stator interactions or in aerodynamics around advanced high-speed propellers for aeroelastic analysis. The actuator disk boundary condition often used to model a propeller can then be replaced by the mesh of a propeller itself.
The first test case is a 2D transonic Euler flow around a pitching NACA0012 airfoil at $M_\infty = 0.796$. Fig. 3.4 shows two O-meshes with the inner one oscillating in a harmonic motion with an amplitude of 1.01 degree and a frequency of 0.202. It also shows the limit cycle in the evolution of the C_z aerodynamic coefficient that appears after a short transitional period.
The second test case is a laminar Taylor-Couette configuration at $R_e = 80$ with an internal moving cylinder and an outer immobile cylinder. The configuration is decomposed in four meshes with two domains for each cylinder. One domain of each is shown on Fig. 3.5 as well as the four time-independent Taylor vortices splitted by the sliding boundaries.

3.2.1.2 Adaptive Mesh Refinement (M. Montagnac, J.-C. Jouhaud)

Another approach to handle complex configurations with a reasonable number of grid points is to enrich a basic coarse mesh by means of a hierarchical structure of grids, that is to say to use an Adaptive Mesh Refinement (AMR) strategy [CFD1]. Areas of interest (shocks, boundary layers, wake vortices,...) are dectected using physical sensors and are refined to build new blocks. Then, multigrid techniques can be applied on these grids.
The mesh adaptation is currently performed outside the flow solver with the Airbus GAME software. Extension of this method to turbulent flows has been introduced in the elsA software with the development of the local multigrid technique [CFD68]. The AS28 wing (Fig. 3.6) in a transonic Euler flow at $M_\infty = 0.80$ and 2.2 degree angle of attack and the RAE 2822 airfoil case (Fig. 3.7) in a turbulent transonic configuration with the RANS $k - w$ turbulence model at $M_\infty = 0.73$ and 2.79 degree angle of attack, have demonstrated the efficiency of that AMR technique [1].

[1] J.-C. Jouhaud, M. Montagnac and L. Tourette. Multigrid adaptive mesh refinement for structured meshes for 3D aerodynamic design. Submitted in International Journal of Numerical Methods in Fluids, 2003.

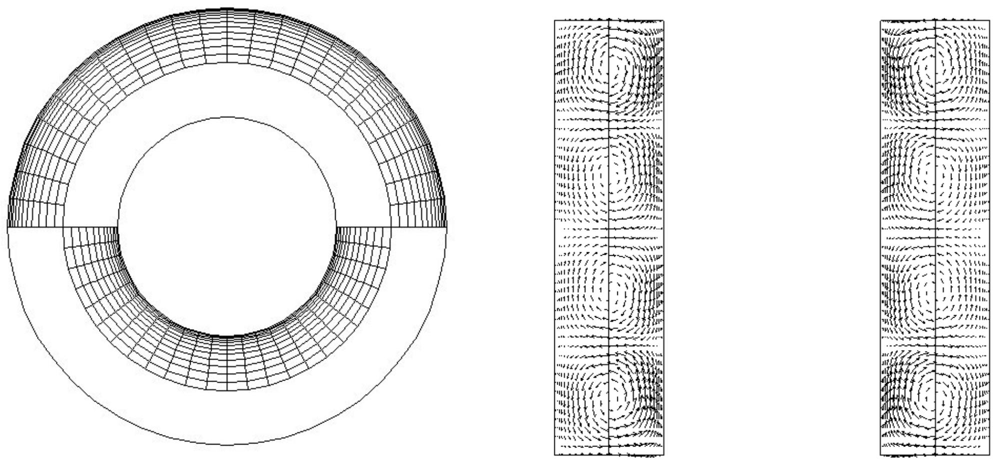

Figure 3.5: Sliding meshes of an axisymmetric four-block configuration for a laminar Taylor-Couette flow (left) and time-independent Taylor vortices (right).

3.2.2 Aerodynamic Data Models

The so-called “Données Aérodynamiques” (DA) characterize the global aerodynamic behavior of an aircraft in all its flight envelope. These data are essential to qualify Performances (flight dynamics, aircraft dimensioning (sploilers, high-lift devices, jacks ...)), Flight Qualities (low and high speeds) and Loads (particularly for airframe integration) of aircrafts. The current competing environment imposes to supply these data as soon as possible in the design cycle, as often as possible, with an increased precision and for a controlled cost.
The improvement in precision requires the use of simulation tools by engineers implied in the production of DA. The exploration of a rather broad flight envelope led to a significant volume of calculations whereas the effort related to wind tunnel or flight testing tends to be reduced. To preserve acceptable production costs of DA, it is necessary to reduce the restoration time of CFD calculations while improving their precision.
One of the aims of this project is consequently to enrich the ”Model” engineers toolbox by adding efficient and robust complex CFD methods. These aspects of speed and precision of numerical simulations are addressed during the preliminary work (first phase) of this program between AIRBUS FRANCE, ONERA. CERFACS, within the framework of its commitment in the elsA software development, has joined this step while bringing in its experience and its know-how. CERFACS’s commitment in the first phase of this program (from january 2003 to december 2004) relates to generic aspects, primarily dedicated to the improvement of the elsA software [CFD43], [CFD44].
Three working directions are considered :

- Algorithmic performances (improvement of the FAS (Full Approximation Scheme) multigrid algorithm within the framework of wall functions usage)
- Precision (verification and validation of wall functions, low speed preconditioning, extension of the AMR strategy and patch grids connectivities to wall functions)
- Automation and Pre/Post processing (complete polar calculations, convergence analysis)

Among these directions, the following tasks are already completed or still under progress.

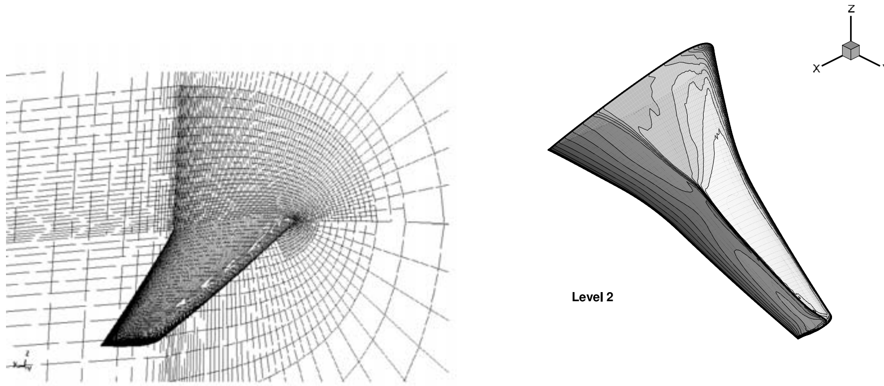

Figure 3.6: AS28 wing, level 2, mesh and mach number contours.

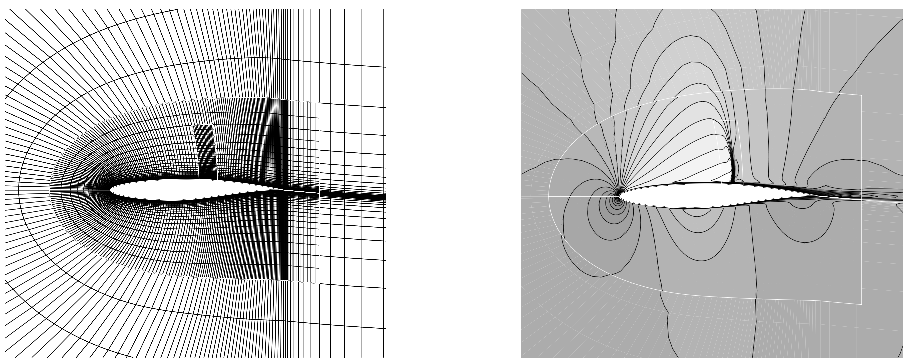

Figure 3.7: Hierarchy of 3 grids for a RAE 2822 configuration (left) and mach number contours (right).

3.2.2.1 Anisotropic multigrid (J.-F. Boussuge)

For steady CFD problems, multigrid algorithms are some of the fastest and most adaptable ways of solving a system of partial differential equations on a fixed grid. elsA uses the Full Aproximation Storage multigrid scheme which has been developped for a full coarsening strategy (this means that the mesh is coarsened isotropically). It implies, that for a given multiblock configuration, the global multigrid level which drives the convergence is fully determined by the dimension of the most constraining boundary conditions. Moreover, for anisotropic problems as including notably external viscous flows, the mesh used to accurately resolve the physics presents an anisotropic refinement. An isotropic coarsening of such a mesh can deteriorate the convergence rate of multigrid.

To overcome the problems quoted above, multigrid methods are much more efficient if coarsening is done anisotropically. This permits to increase the global multigrid level for configurations with different multigrid block levels and to reduce the cell aspect ratio near the wall and the associated numerical stiffness for anisotropic refinement.

CERFACS has extended the standard FAS to anisotropic formulation and this development has been

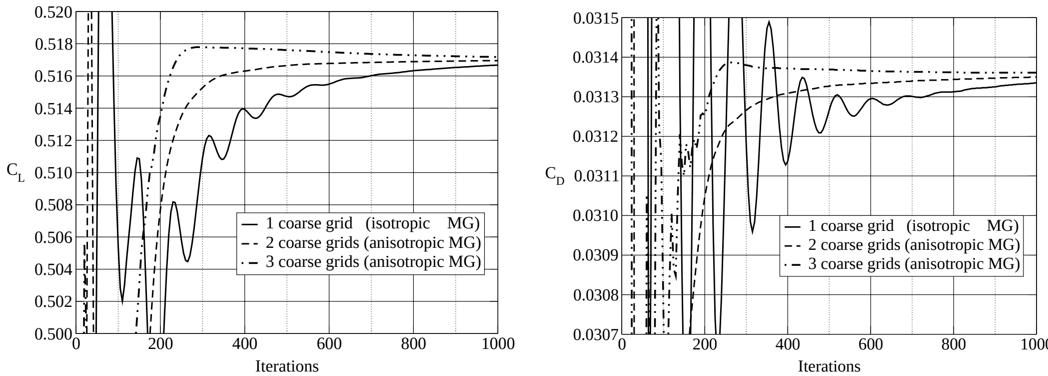

Figure 3.8: AS28G aerodynamic coefficients convergence

successfully validated on two industrial test cases given by AIRBUS (see Fig. 3.8 for the AS28G configuration).

3.2.2.2 Wall functions (N. Denève, G. Puigt)

As part of the effort for time restoration's reduction of high Reynolds number RANS simulations, wall functions appear as an unavoidable way to assess. Indeed, such wall functions both participate to the problem's size reduction since their use implies a lower resolution effort and also to the problem's stiffness reduction because of the replacement of the no-slip condition at walls. Moreover, their use sometimes alleviates the grid dependency of turbulence models. Wall functions are based on the statement that, provided that certain assumptions are verified among which the flow is attached, the internal zone's structure of the boundary layer is independant of the flow in its external zone. A self-similarity velocity profile can be exhibited for the logarithmic region and the linear viscous sub-layer.
The implementation of a specific kind of wall functions [CFD42] developped in the framework of this project is based on the approximation that the distance between the real wall and the location where boundary conditions should be applied is neglected. This approach differs from the initial wall functions of the elsA software based on an apriori agglomeration of near-wall cells of a low Reynolds grid that include the linear and logarithmic zones. Advantages of this method consist of grid generation and reusability of all available algorithms [1]. To evaluate this implementation, some computations have been realized on the RAE2822 test-case. Fig. 3.9 presents a comparison between the pressure coefficient obtained with a low-Reynolds approach (use of a no-slip boundary condition and of an adapted mesh : $y^+ \leq 1.$, 89010 nodes) and the one obtained with the implemented wall functions approach (on a coarser mesh : 55890 nodes and $y^+ \in [30, 130]$). The results are shown to match correctly.

[1] S. Champagneux, J.-F. Boussuge, N. Denève, G. Hanss. Contribution au DTP Modles de Donnes Arodynamiques - Rapport d'avancement un an. Contract Report, CR/CFD/04/15, 2004.

3.2.2.3 Error estimations (G. Hanss)

The quality of a numerical solution with respect to the mesh on which it has been obtained can be assessed by an *a posteriori* error estimation. This post-processing analysis give us a mean to quantify the incertainty of the solution, and could provide us with a criteria for a local mesh adaptation process. An error estimate is expected to give information about the accuracy of the method, therefore it should estimate the absolute

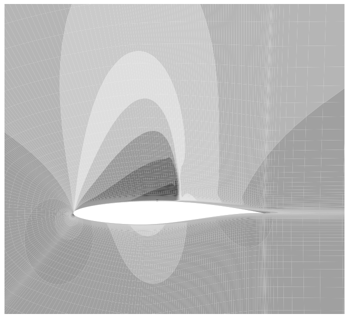

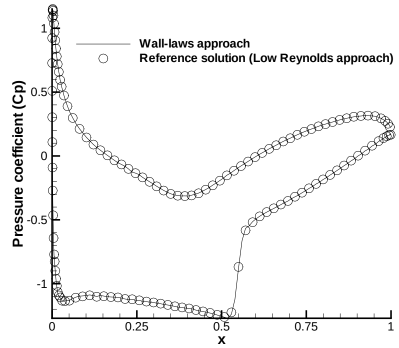

Figure 3.9: RAE2822 test-case : iso-Mach number field (left) and pressure coefficient (right)

error level as well as the distribution of the error throughout the domain.
Two estimators have been implemented in elsA: the first one (Richardson extrapolation) is based on the analysis of the numerical solution in terms of the Taylor series expansion. An approximation of the leading term in the truncation error is deduced from solutions on two meshes with different cell sizes. Hence this method naturally couples with the use of multigrid acceleration techniques, where solutions on grids with different cell size are already available. One drawbacks is the fact that Richardson extrapolation assumes that spacing in each direction scales with h. This is valid only for geometrically similar control volumes. If the control volumes of two meshes are not similar in shape, the extrapolation accuracy decreases. The second estimator implemented in elsA is a Residual error estimate. This estimator measures the disprepancy between the model equations to be solved and the discretized ones.
The following example presents the typical result on a 3D configuration. Fig. 3.10 presents isosurfaces corresponding to 80% of the maximum error throughout the field for the ONERA M6 Wing in a transonic, turbulent flow ($M_\infty = 0.84$, angle of attack $\alpha = 3.06°$). As expected, the maximum errors are found in the lambda shock, leading and trailing edges and the wing tip. Both estimators have proven a capability to predict the region of maximum error either by using the L_2 and L_∞ norms or by using the field extraction. They can also highlight problems in the flow like bad boundary conditions or mesh irregularities. These capabilities could be use for an *a posteriori* analysis of the simulation but also as criteria in a mesh adaptation process as proposed in further studies.

3.2.2.4 Automatic polar curve (G. Hanss)

The evaluation of polar data (Pressure vs Incidence for example) still constitutes a significant investment in terms of resources and know-how. Indeed, because of its non-linear nature, it is necessary to optimize the number of calculations. Generally, one evaluates three points of polar in the linear zone and approximately five in the non-linear one. Today, the total cost of a polar is of the order of the number of points to evaluate because the user computes several independant steady simulations for each flight point.
To minimize this cost, an automatic sequence of stationary calculations has been implemented. Each simulation is initialized with the solution of the previous flight point. The user is offered the possibility to choose the number of flight points and the condition of these points (angle of attack, slip angle, mach number, ...).

The solution proposed here presents several advantages:

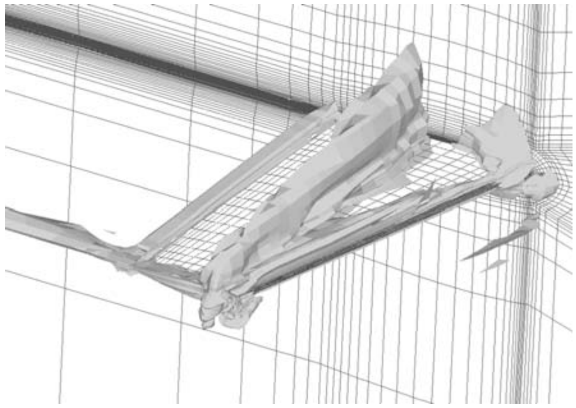

Figure 3.10: Error estimation : isosurfaces corresponding to 80% of the maximum error

- each simulation of a flight point is initialized with the results from the nearest flight point, which should enable the simulation to converge more quickly,
- since it is fully implemented in the core source and not in the Python interface, it is possible to fully use the parallelism already implemented in elsA,
- on the output side, elsA provides a polar curve with each flight point, and a polar curve caracterizing the evolution during the steady calculation (Fig. 3.11), thus allowing the user ”to reconsider” flight points which did not converge perfectly.

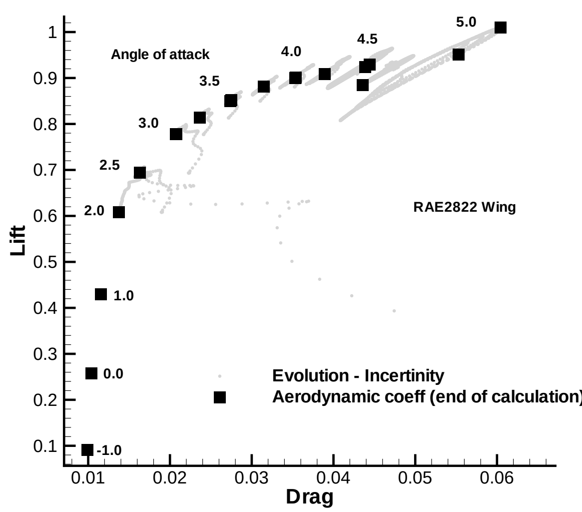

Figure 3.11: Automatic polar : RAE Profile

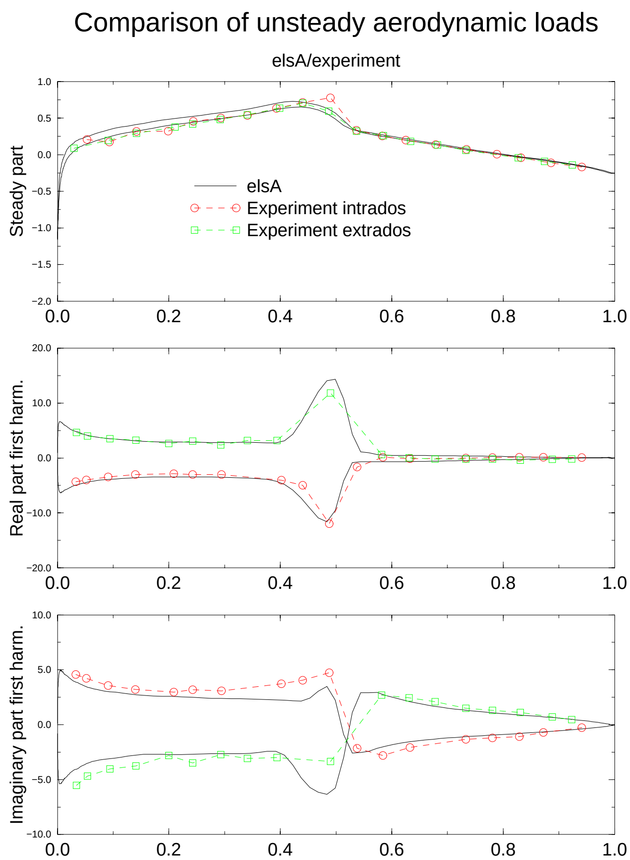

Figure 3.12: Comparison of the first harmonic of C_p given by elsA unsteady simulation and experimental data

3.2.3 Fluid-structure interaction (J. Delbove, G. Chevalier)

The field of aeroelasticity encompasses the interaction of aerodynamic, elastic, and inertia forces acting on a flight vehicle. It had become recognized as an important part of the aircraft design process. CFD emerged as a practical technique for numerically solving the partial differential equations of fluid flow in the compressible flow regimes. The first area of interest is the static fluid-structure interaction. The shapes of the wings of an aircraft in steady flight condition are deformed by the constraint of aerodynamic loads. CERFACS, in collaboration with Airbus, has developed an algorithm which, for a given flexibility matrix representing the wings structure and a set of flight conditions, computes the deformed shape of the wings and the fluid flow. It implies that a robust mesh deformation algorithm must be available in elsA. A first algorithm in this type has been successfully developed (see Fig. v in the appendix for an example of mesh deformation). The second area of interest is unsteady simulation. Efficient numerical methods have been developed in order to enable unsteady simulation with elsA. Direct industrial application is flutter prediction. Flutter is a destructive fluid-structure interaction due to a transfer of energy from the fluid to the aircraft structure. It is characterized by a growing oscillation which can lead to the destruction of the aircraft. It can be predicted either with the use of unsteady aerodynamic loads provided by unsteady simulations (see Fig. 3.12 for an example of the results given by an unsteady simulation), or with a direct temporal fluid structure simulation. The increasing accuracy and efficiency of high performance computing favor the simulation of the temporal response of the nonlinear aeroelastic system.

3.2.4 Codes coupling (F. Loercher, J. Delbove)

In the framework of internal collaborations and in-house software's development and valorisation, the Group has conducted some coupling experiments with the PALM software (see the "Climate and Modelling and Global" chapter). Two types of simple coupling have been achieved : aeroelasticity with elsA and a simple in-house Computational Structural Mechanics (CSM) code and coupling elsA with aerodynamic analysis tools for on-the-fly post-processing. These assessments have shown that PALM is relevant, easy to use and efficient for these applications.

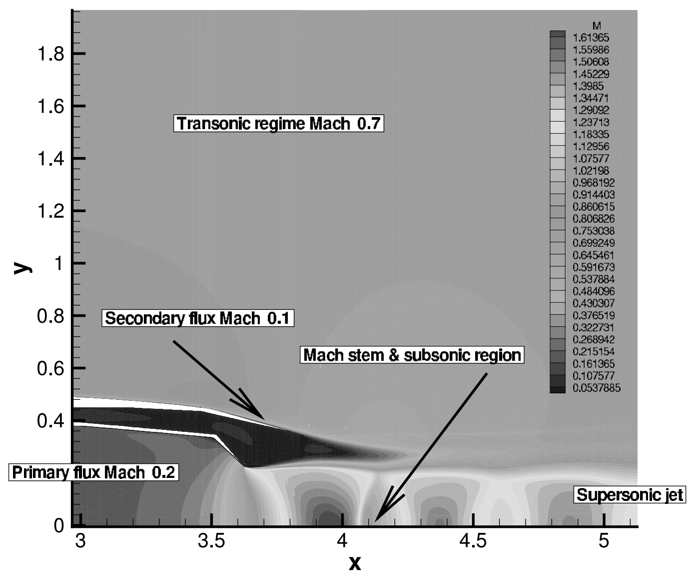

Figure 3.13: Mach number iso-contours for the MARCO nozzle configuration

3.2.5 Treatment of axisymetric configurations (S. Champagneux, M. Fontaine)

A rigorous and effective two-dimensional method for the specific treatment of axisymetric configurations has been implemented in the elsA software [CFD44]. This method offers an alternative to the three-dimensional one that was initialy available and previously used. The main drawback of the original approach was the CPU penalty due to the mandatory 3D numerical treatement despite the intrinsically 2D configuration. Moreover, the need for specific boundary conditions and the definition of an arbitrary azimuthal angle are case-dependent procedures which have limited scientific interest.
A finite volume consistent approach relying on the addition of an extra source term and a metric modification has been implemented and verified for several steady test cases (incompressible laminar and turbulent Poiseuille flows, laminar hypersonic blunt body flow). Finally, the MARCO configuration (a ventilated nozzle from SNECMA-moteurs, Fig. 3.13) where flow conditions lead to an under-expanded

jet is computed with this approach. A speed-up factor of three is obtained concerning the CPU time for convergence and obtained results agree with those provided by SNECMA-moteurs.

3.2.6 Prediction of dynamic derivatives of full aircraft including large winglets (D. Margerit, S. Champagneux, G. Chevalier)

CERFACS also studied the influence of large winglets on aerodynamics characteristics of the wing, and more precisely the use of advanced CFD computation to determine such characteristics through the use of the elsA and Arbitrary Lagrangian Eulerian (ALE) techniques.
α-effect (incidence) and pitching effect (q-effect) computations have been validated on the M6 wing geometry. Values of quasi-static derivatives $\partial Cz/\partial\alpha$ and $\partial Cz/\partial q$ are in good agreement with previous results. Full multi-grid, grid sequencing and solution continuation are used in order to accelerate convergence to steady state solutions.
Invicid (Euler) computations of $\partial Cz/\partial\alpha$ and $\partial Cz/\partial q$ were performed for a coarse grid of the A340 MSR1 geometry (see Fig. vi in the appendix). The process of transforming the Euler A340 grid to a NS (viscous) one is also done. This work will go on with NS computations and large/standard winglets comparisons.

3.3 Software engineering

3.3.1 Open MP (F. Loercher, S. Champagneux, L. Giraud)

A possible parallelisation with OpenMP in elsA has two major advantages to the existing MPI parallelisation:

- The number of processors used could be chosen independantly of the number of blocks.
- With less blocks used, the global numerical behaviour improves.

In this work a strategy to parallelize elsA efficiently with OpenMP has been elaborated in collaboration with the ”Parallel Algorithms” team. Some of the most CPU-time consuming functions (the Lussor-functions and the OperGradIntGF.for) have already been parallelized. Fig. 3.14 shows the acceleration for the LussorSca5 on the Compaq Alpha server of CERFACS as a function of meshsize.

3.3.2 Management and support (M. Montagnac, J.-F. Boussuge, S. Champagneux)

Tasks related to software management and code engineering are of the primary importance in both a research and industrial working environnement. CERFACS' industrial partners require high turnaround time response, reliability and robustness among many other aspects. Furthermore, CERFACS researchers also ask for simplicity in coding, for code clarity and for a highly-tunable code.
Those requests are reflected in the activities of the aerodynamics group. The elsA software comes along with procedures to enhance productivity in a multi-user and multi-platform environment: validation database, unitary test cases, cvs management tools, software quality program, documentation, training.
Common works include the development of new features, the re-engineering of designs, the improvement of verification and validation databases, the contribution to debugging and to quality reviews and the writing of user's, developer's and theoretical manuals.
Portability tests, optimization and benchmarking actions are also frequent activities to ensure the reliability and the efficiency of the code and to enable smooth transitions whenever industrial partners renew their computing facilities.

Finally, researchers at CERFACS can take advantage of the industrial environment delivered by Airbus and installed by the team members on CERFACS computers. That enables a real synergy between the two partners.

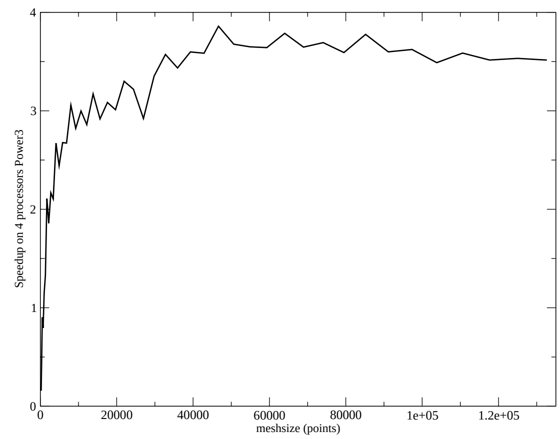

Figure 3.14: Speedup of LussorSca5 on 4 processors of the Compaq Alpha.

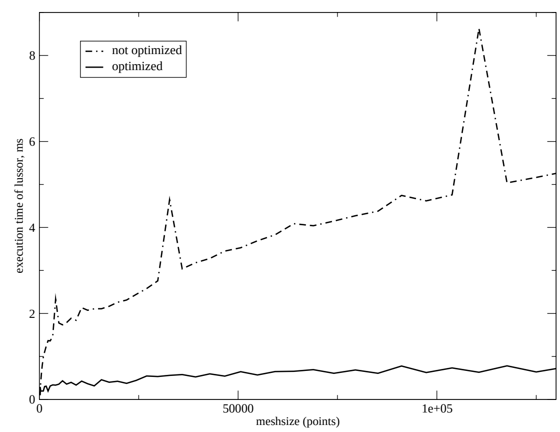

Figure 3.15: CPU time of the function LussorSca before and after optimisation.

3.3.3 Parallelism with MPI (M. Montagnac, J.-F. Boussuge, S. Champagneux)

Since 2002, CERFACS is involved in an ONERA project called ParelsA to parallelize elsA. Unitary test cases were developed to check the implementation of the MPI message passing library so as to ensure the portability of the code. A re-engineering of some aspects in the design has been proposed to reduce the number of synchronous communications and the size of messages. A first insight of that work can be seen in the following numbers. In a four processor calculation with 2 domains in each one, the speedup went from 2.86 in the initial version of the code to 3.55 in an enhanced version. Even better results are expected in the near future. Asynchronous communications are also under investigations.

Those high performance computing activities are carried out with the CERFACS computing facilities but also with supercomputers from the French national center CINES.

3.3.4 Code performance (M. Montagnac, J.-F. Boussuge, S. Champagneux)

As part of CERFACS's continuous effort for performance optimisation of its softwares, specific actions have been conducted. For instance, CERFACS has participated to a benchmark between several European Multi-block codes (NSMB, FLOWer, RANS-MB, etc ...) during automn and winter 2002 in the framework of a rationalisation process conducted within Airbus. CERFACS has contributed to gain an averaged speed-up of three for elsA for a relevant range of industrial configurations on vector architectures such as NEC SX series and FUJITSU VPP series. This has finally lead to the selection of the elsA software as the single MB structured simulation tool across all Airbus sites in Europe. CERFACS is now focusing on SMP's architectures.

Most of the latest high-performance computers have a superscalar architecture. As elsA was initially optimized for vector-computers, a significant gain of performance can be achieved by optimizing the code for scalar machines without changing the numerical behaviour.

In collaboration with the "Parallel Algorithms" team and SMP vendors such as IBM, some optimisation strategies have been examinated in the context of elsA: changing of array-structure, blocking, prefetch Stream optimisation, and changing of loop order. The appearance of significant CPU-time peaks has been explained and methods to avoid them have been found. Fig. 3.15 shows the impact of the optimisation for a very CPU time consuming function, LussorSca.

4 Environmental impact of aviation

D. Cariolle

Aircraft emissions can have an impact on atmospheric chemistry and on the radiative balance of the atmosphere. Emissions of nitrogen oxides and the formation of ice particles within contrails perturb the natural chemical cycles and lead to ozone production or destruction depending on local air mass composition and insolation. These ozone perturbations along with the emissions of CO2, water vapour and ice particles formation, soot particles, sulphuric aerosols from the burning kerosene give an additional contribution to the greenhouse forcing. The most recent evaluations of those effects show the existence of a amplification factor of about 3 for greenhouse potential factor from aircraft emission: a molecule of CO2 emitted from a jet airplane is a factor of 3 more efficient for greenhouse forcing than a similar molecule emitted at ground level.

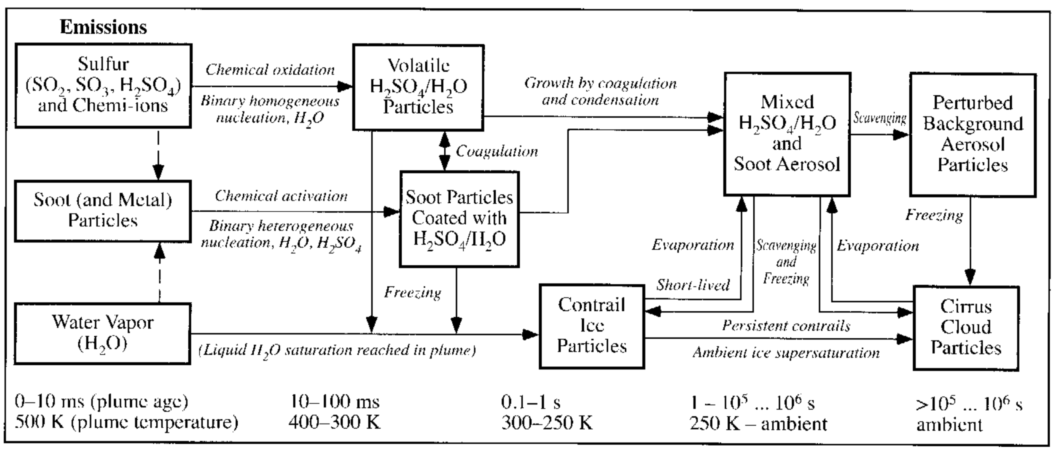

Figure 4.1: Steps involved in the formation and the transformation of gases and particles emitted by the kerosene combustion.

Given the exponential increase of the air traffic it is anticipated that the aircraft emissions will double by year 2020 compared to present. The air traffic would then be a major player of the climate change. There is no doubt that in future negotiation processes for the limitation of greenhouse gaz emissions aviation sources will be a central issue. It is therefore important that the regulations that could be imposed on aviation be based on well-sound scientific studies.
As this thematic was recognised as an important issue for the CERFACS shareholders and for the ministry of transportation (which has the administrative supervision of Météo-France), it was decided to settle a new project ”aviation and the environment” within the CERFACS and CNRM teams. Starting in September 2003, the project is aimed at coordinating the work between the two teams, whose expertise in the field is internationally recognise.

The main scientific objective of the project is to better quantify the chemical and radiative atmospheric impacts of aviation at the various scales from the aircraft near field to the global atmosphere. An integrated evaluation of the different steps that involve the emission transformations must be performed, from the species generation within the combustion chambers, their chemical transformation within the airplane generated vortices, their vertical and horizontal dilution during contrail and track formation to the formation of corridors by the fleets and their transport by the general circulation of the atmosphere. At each of those steps the chemical and radiative atmospheric perturbations must be assessed. This will be done using a hierarchy of numerical models, AVBP and NTMIX from CERFACS and Méso-NHC, Arpège (1D and 3D) and MOCAGE from CNRM.

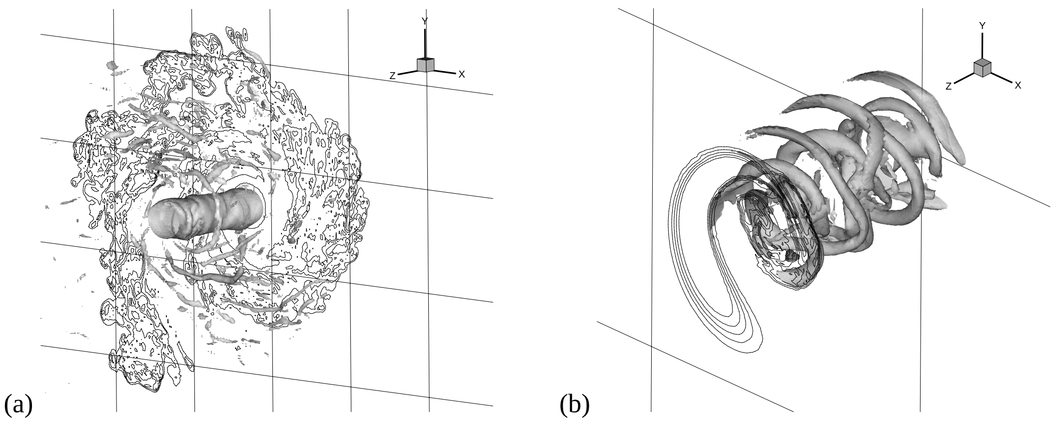

Figure 4.2: Iso-surface of the vorticity magnitude during the jet/vortex interaction: (a) case 1; (b) case 2.

As this project was launched in autumn 2003, it has not generated specific results yet. However, R. Paoli actually at Stanford/Ames, has recently made simulations of contrail formations with various initial size distribution for emitted particles by the jet with growing characteristics varying according to a simplified microphysical model for ice particle nucleation.

Two simulations of the jet/vortex interaction were analyzed, as discussed in detail in Paoli et al. [CFD36, CFD15]. In the first case (see Fig. 4.2a), typical conditions of cruise flight, the jet and the vortex were sufficiently well separated in order to study initially the jet dynamics before considering its interaction with the vortex. The results show that dynamics and mixing are both controlled by the jet diffusion and its entrainment around the vortex core. In the second case (see Fig. 4.2b), the jet partially blowed into the vortex core, making the flow similar to a Batchelor vortex. The strong perturbations injected into the core caused an instability of the system which was continuously fed by the jet elements wrapping around the core. This leads to a strong decay of angular momentum and diffusion of the core. Global mixing properties, such as plume area and global mixedness evolutions, were analyzed and two applications to environmental problems were finally discussed. As the distribution of ice particles are predicted in those simulations, they will be used for 1D radiative model (used within the Arpege model) calculations to be performed in 2004.

Several responses to various calls for proposals have been prepared, anticipating that such funding will give support to the project for the next four years.

Fig. 4.1 Chart showing the steps involved in the formation and the transformation of gases and particles emitted by the kerosene combustion. Those various paths of transformation must be taken into account in microphysic models that predict particle formation and must be coupled to dynamical and radiative models covering a large range of time and geographical scale.

5 Publications

5.1 Journal Publications

[CFD1] A. Benkenida, J. Bohbot, and J.-C. Jouhaud, (2002), Patched grid and adaptive mesh refinement strategies for Vorticies transport calculation, *International Journal of Numerical Methods in Fluids*, **40**, 855–873.

[CFD2] B. Caruelle and F. Ducros, (2003), Detached-eddy simulations of attached and detached boundary layers, *International Journal of Computational Fluid Dynamics*, **17**, 433–451.

[CFD3] F. Dabireau, B. Cuenot, O. Vermorel, and T. Poinsot, (2003), Interaction of H2/O2 flames with inert walls, *Combustion and Flame*, **135**, 123–133.

[CFD4] A. Delataillade, F. Dabireau, B. Cuenot, and T. Poinsot, (2002), Flame/wall interaction and maximum heat wall fluxes, *Proc. of the Combustion Institute*, **29**, 775–780.

[CFD5] F. Ducros, (2003), LESFOIL Investigation, *in Notes on Numerical Fluid Mechanics and multidisciplinary design*, *Springer*, **83**, 105–118.

[CFD6] T. Gerz, F. Holzaepfel, and D. Darracq, (2002), Commercial aircraft wake vortices, *Progress in Aerospace Sciences*, **38**, 181–274.

[CFD7] F. Holzaepfel, T. Hofbauer, D. Darracq, H. Moet, F. Garnier, and G. Ferreira, (2003), Analysis of Wake Vortex decay mechanisms in the atmosphere, *Aerospace Science and Technology*, **7**, 263–275.

[CFD8] C. Jimenez, B. Cuenot, T. Poinsot, and D. Haworth, (2002), Numerical simulation and modeling for lean stratified propane-air flames, *Combustion and Flame*, **128**, 1–21.

[CFD9] A. Kaufmann, F. Nicoud, and T. Poinsot, (2002), Flow forcing techniques for numerical simulation of combustion instabilities, *Combustion and Flame*, **131**, 371–385.

[CFD10] R. Knikker, A. Dauptain, B. Cuenot, and T. Poinsot, (2003), Comparison of computational methodologies for ignition in diffusion layers, *Combustion Science and Technology*, **175**, 1783–1806.

[CFD11] A. Kourta, (2003), Instability of channel flow with fluid injection and parietal vortex shedding, *Computing and Fluids*, **33**, 155–178.

[CFD12] F. Laporte and T. Leweke, (2002), Elliptic Instability of Counter-Rotating Vortices: Experiment and Direct Numerical Simulation, *AIAA Journal*, **40**, 2483–2494.

[CFD13] D. Le and F. Laporte, (2002), Theoretical predictions for the elliptical instability in a two-vortex flow, *Journal of Fluid Mechanics*, **471**, 169–201.

[CFD14] F. Nicoud and T. Schönfeld, (2002), Integral Boundary Conditions for Unsteady Biomedical CFD Applications, *International Journal of Numerical Methods in Fluids*, **40, Issue 3-4**, 457–465.

[CFD15] R. Paoli, F. Laporte, B. Cuenot, and T. Poinsot, (2003), Dynamics and mixing in jet/vortex interactions, *Physics of Fluids*, **15**, 1843–1850.

[CFD16] T. Poinsot, T. Kestens, and F. Nicoud, (2002), Using Computational Fluid Dynamics to Study Flow Control, *Computational Methods for Control Applications*, **16**, 327–346.

[CFD17] R. Struijs, G. Jonville, D. Darracq, and R. Heinrich, (2003), Inviscid Computation of Effect of Wake Vortices on a Scale-Model Airplane, *Journal of Aircraft*, **40**, 100–109.

[CFD18] B. Varoquié, J. Légier, F. Lacas, D. Veynante, and T. Poinsot, (2002), Experimental analysis and Large Eddy Simulation to determine the response of non-premixed flame submitted to acoustic forcing, *Proc. of the Combustion Institute*, **29**, 1965–1970.

[CFD19] J. Vos, A. Rizzi, D. Darracq, and E. Hirschel, (2003), Navier-Stokes Solvers in European Aircraft Design, *Progress in Aeronautic Sciences*, **38**, 601–699.

5.2 Theses

[CFD20] J. Bohbot, (2002), *Simulation numérique d' écoulements transsoniques autour de voilures mobiles et analyse aéroelastique du flottement des sections d' ailes - TH/CFD/02/31*, PhD thesis, Ecole Nationale Supèrieure des Arts et Métiers.

[CFD21] F. Dabireau, (2002), *Etudes des transferts de chaleur aux parois dans les moteurs-fusées - TH/CFD/02/120*, PhD thesis, Institut National Polytechnique de Toulouse.

[CFD22] L. Kozuch, (2002), *Etude de l'écoulement dans une turbomachine axiale transsonique en présence ou non d'une distorsion amont. Validation d'un outil de simulation et analyse instationnaire - TH/CFD/02/54*, PhD thesis, Ecole Centrale de Lyon.

[CFD23] F. Laporte, (2002), *Simulation numérique appliquée à la caractérisation et aux instabilités des tourbillons de sillage d'avions de transport - TH/CFD/02/50*, PhD thesis, Institut National Polytechnique de Toulouse.

[CFD24] H. Moet, (2003), *Simulation numérique du comportement des tourbillons de sillage dans l'atmosphère - TH/CFD/03/40*, PhD thesis, INPT.

[CFD25] T. Soulères, (2003), *Simulations des grandes échelles d'écoulements dans des géométries fixes et mobiles : Application aux moteurs à pistons - TH/CFD/03/17*, PhD thesis, Institut National Polytechnique de Toulouse.

5.3 Conference Proceedings and Book Chapters

[CFD26] J. Bohbot and J.-C. Jouhaud, (2002), Coupled Patched Grid /AMR Meshing Technics for Transonic Aircraft Design, In *40th AIAA Aerospace Sciences Meeting and Exhibit*, Reno, USA, AIAA Paper 2002–0546.

[CFD27] B. Cuenot and R. Paoli, (2003), Modélisation de l'impact environnemental d'une flotte d'aéronefs, In *35ème Congrés National d'Analyse Numérique*, La Grande Motte, France, Universit de Montpellier 2, mathématiques, 1–13.

[CFD28] B. Cuenot, C. Jimenez, and T. Poinsot, (2002), Direct Numerical Simulation of turbulent partially premixed flames, In *Ninth Conference (Int.) on Numerical Combustion*, SIAM, ed., Sorrento, Italy, 177–178.

[CFD29] F. Dabireau, O. Vermorel, B. Cuenot, and T. Poinsot, (2002), Flame wall interaction of an H2/O2 flame, In *12th International Heat Transfer Conference*, Grenoble, France.

[CFD30] F. Garnier, G. Ferreira, A. Brasseur, R. Paoli, and B. Cuenot, (2003), Dispersion and growing of ice particles in a turbulent exhauts plume, In *European Conference onAviation, Atmosphere and Climate*, Friedrichshafen, Germany, 1–6.

[CFD31] D. Joseph, P. Coelho, B. Cuenot, and H. El, (2003), Application of the discrete ordinates method to grey media in complex geometries using unstructured meshes, In *EUROTHERM73 on Computational Thermal Radiation in Participating Media*, D. L. P. Lybaert V. Feldheim and N. Seluk, eds., Facult Polytechnique de Mons, Belgium, EUROTHERM, 97–106.

[CFD32] A. Kaufmann, O. Simonin, J. Helie, and B. Cuenot, (2003), Dynamics and Dispersion in 3D unsteady Eulerian-Eulerian Simulations of Two-Phase Flows, In *International Conference on Supercomputing in Nuclear Applications*, Palais des Congrs, Paris, France.

[CFD33] A. Kaufmann, O. Simonin, T. Poinsot, and J. Helie, (2002), Dynamics and Dispersion in Eulerian-Eulerian DNS of Two Phase Flow, In *Proceeding of the Summer Program*, Center for Turbulence Research, NASA AMES/Stanford University, USA, 381–392.

[CFD34] N. Monnier and Y. Sommerer, (2003), Utilisation déportée du serveur de visualisation du CINES, In *La Gazette du CINES*, CINES, ed., Montpellier, France, 1–4.

[CFD35] N. Monnier and Y. Sommerer, (2003), Visualisation et Post-Traitement distance - prsent lors de la confrence ”SGI Technologie Forum, In *SGI Technologie Forum*, Toulouse, France, 1–17.

[CFD36] R. Paoli, J. Helie, T. Poinsot, and S. Ghosal, (2002), Contrail formation in aircraft wakes using Large Eddy Simulations, In *Proceeding of the Summer program*, Center for Turbulence Research, NASA AMES/Stanford University, USA, 229–241.

[CFD37] L. Selle, G. Lartigue, T. Poinsot, A. Kaufmann, W. Krebs, and D. Veynante, (2002), Large Eddy Simulation of turbulent combustion for gas turbines with reduced chemistry, In *Proceeding of the Summer program*, Center for Turbulence Research, NASA AMES/Stanford University, USA, 333–344.

[CFD38] K. Truffin, B. Varoquié, and T. Poinsot, (2003), Measurements of transfer functions in reacting flows using Large Eddy Simulations, In *Tenth International Congress on Sound and Vibration,*, Stockholm, Sweden, 785–793.

5.4 Technical Reports

[CFD39] M. Aït-Abdellah, (2002), AVBP's optimisation, Rapport de stage de dernière année Ingénieur WN/CFD/02/87, CERFACS.

[CFD40] L. Artal, (2003), Modélisation des flux de chaleur stationnaires pour un mélange multi -espèce avec transfert de masse la paroi, Contract report CR/CFD/03/115, CERFACS.

[CFD41] M. Boileau, (2003), Simulation numérique de la combustion diphasique, Rapport de stage DEA energetique et transferts WN/CFD/03/73, CERFACS.

[CFD42] S. Champagneux, J.-F. Boussuge, and N. Denève, (2003), Rapport d'avancement six mois / DTP Modèles de Données Aérodynamiques, Tech. Rep. CR/CFD/03/129, CERFACS.

[CFD43] S. Champagneux, (2003), Rapport d'avancement six mois / DTP Modèles de Données Aérodynamiques, Tech. Rep. CR/CFD/03/132, CERFACS.

[CFD44] S. Champagneux, (2003), Une formulation axisymétrique bidimensionnelle pour elsA - contract report for SNECMA, Tech. Rep. CR/CFD/03/132, CERFACS.

[CFD45] F. Cheuret, (2003), Acoustique de la chambre de combustion avec sa cavité excitatrice, Tech. Rep. TR/CFD/03/50, CERFACS.

[CFD46] B. Cuenot and R. Paoli, (2002), Rapport COS: Modélisation de l'impact climatique d'une flotte d'aéronefs incluant le concept européen d'avions supersoniques. Contribution du CERFACS : Dynamique et mélange dans une configuration simple d'interaction jet/tourbillon, Tech. Rep. CR/CFD/02/112, CERFACS.

[CFD47] B. Cuenot, L. Benoit, S. Pascaud, J.-B. Mossa, E. Riber, and M. Boileau, (2002), Rapport PRC - Année 1, Contract report CR/CFD/02/129, CERFACS.

[CFD48] B. Cuenot, L. Benoit, K. Truffin, J.-B. Mossa, S. Pascaud, E. Riber, and M. Boileau, (2003), RAPPORT PRC - Année 2, Contract report CR/CFD/03/120, CERFACS.

[CFD49] B. Cuenot, A. Delataillade, F. Dabireau, and T. Poinsot, (2002), Interaction Flamme-Paroi. Rapport final du contrat SNECMA, Rapport contractuel CR/CFD/02/61, CERFACS.

[CFD50] B. Cuenot, C. Jimenez, and T. Poinsot, (2003), GLEVEL Deliverable 6, Contract report CR/CFD/03/22, CERFACS.

[CFD51] B. Cuenot, (2002), STOPP - Second progress report, Contract Report CR/CFD/02/30, CERFACS.

[CFD52] B. Cuenot, (2003), STOPP - 3rd Annual Progress Report, contractual report CR/CFD/03/19, CERFACS.

[CFD53] B. Cuenot, (2003), STOPP Final Report, Contract Report CR/CFD/03/102, CERFACS.

[CFD54] A. Dauptain, (2002), Allumage des moteurs fusées cryotechniques, Rapport DEA WN/CFD/02/89, CERFACS.

[CFD55] A. Dauptain, (2002), Cryotechnic rocket engine ignition, Rapport ENSEEIHT WN/CFD/02/60, CERFACS.

[CFD56] A. Dauptain, (2003), Cryotechnic Rocket Engines Ignition - CIFRE contract 1st biannual report, Rapport Industriel CR/CFD/03/99, CERFACS.

[CFD57] A. Dauptain, (2003), Simulation aux grandes échelles d'un jet sonique sous détendu, Rapport Industriel CR/CFD/03/100, CERFACS.

[CFD58] A. Dauptain, (2003), Underexpanded Jet AVBP Simulations, Industrial report CR/CFD/03/98, CERFACS.

[CFD59] G. Desoutter, (2003), Etude numérique de la propagation d'une flamme sous l'influence d'un film liquide de carburant sur la paroi, rapport master ingenieur WN/CFD/03/82, CERFACS.

[CFD60] M. Duloué, (2003), Rapport de fin d' étude de l'implémentation des équations de Navier-Stokes en déséquilibre chimique dans le code NSMB, Contract report CR/CFD/03/60, CERFACS.

[CFD61] M. Fontaine, (2002), Accélération de convergence des algorithmes de résolution des problèmes d'aérodynamique stationnaire, Rapport de stage DEA WN/CFD/02/85, CERFACS.

[CFD62] M. Fontaine, (2003), Implémentation et validation de fonctionalités axisymétriques dans le code elsA, Contract report CR/CFD/03/105, CERFACS.

[CFD63] M. Garcia, (2003), Analysis of precision differences observed for the AVBP code, Tech. Rep. TR/CFD/03/84, CERFACS.

[CFD64] F. Garnier, B. Cuenot, and P. Mirabel, (2003), Dispersion turbulente et modélisation microphysique des effluents dans le sillage proche d'un avion supersonique, Tech. Rep. CR/CFD/03/131, ONERA/CERFACS.

[CFD65] L. Gicquel and C. Prière, (2002), Simulations of jet in cross flow using LES, Contract Report CR/CFD/02/7, CERFACS.

[CFD66] L. Gicquel, C. Prière, and T. Poinsot, (2003), Intermediate report on LES computations of jets in cross flow, Contract report CR/CFD/03/107, CERFACS.

[CFD67] L. Gicquel, C. Prière, and T. Poinsot, (2003), Workshop on AVBP, Contract Report CR/CFD/03/109, CERFACS.

[CFD68] J. Jouhaud and M. Montagnac, (2002), AMR multigrille K-eps : Une méthode d'adaptation de maillages pour les écoulements turbulents, Rapport contractuel CR/CFD/02/18, CERFACS.

[CFD69] R. Knikker, (2002), Numerical Study of the auto-ignition delay in the second stage of the ALSTOM SEQ-burner, Contract report CR/CFD/02/118, CERFACS.

[CFD70] D. Lizarazu, (2002), Mise en oeuvre de lois de paroi dans le code structure ELSA, Rapport de stage DEA - Ecole MATMECA, Université Bordeaux 1 WN/CFD/02/66, CERFACS.

[CFD71] F. Loercher, (2003), Optimisation d'un code numérique pour des machines scalaires et parallélisation avec OpenMP et MPI, Technical report TR/CFD/03/104, CERFACS.

[CFD72] H. Moet, (2003), Synthesis and design recommendations : synthesis and low vortex design, Contract report CR/CFD/03/101, CERFACS.

[CFD73] H. Moet, (2003), Three-dimensional instability mechanism in a four-vortex system - Benchmark computations, Rapport contractuel AWIATOR CR/CFD/03/89, CERFACS.

[CFD74] H. Moet, (2003), Wake Vortex behaviour in the atmosphere, modeling and validation - SWAKE : WP1R, Rapport contractuel CR/CFD/03/41, CERFACS.

[CFD75] R. Paoli, F. Laporte, B. Cuenot, and T. Poinsot, (2002), Dynamics and mixing in a simple configuration of Jet/Vortex interaction, Tech. Rep. TR/CFD/02/95, CERFACS.

[CFD76] R. Paoli, (2002), Dynamics and mixing in jet/vortex interactions : STOPP Final Report, Final Contract Report CR/CFD/02/103, CERFACS.

[CFD77] J. Pascal, (2002), Implémentation du modèle K-eps-v2-f dans le code ELSA, rapport contractuel AIRBUS/CERFACS CR/CFD/02/92, CERFACS.

[CFD78] S. Pascaud, B. Cuenot, and T. Poinsot, (2003), Réalisation d'un maillage et mise en place d'un calcul AVBP sur foyer M88, Contract report CR/CFD/03/112, CERFACS.

[CFD79] S. Pascaud, (2002), Etude monophasique et diphasique des flammes laminaires monodimensionnelles, Rapport DEA - INP TOULOUSE WN/CFD/02/78, CERFACS.

[CFD80] S. Pascaud, (2002), Etude monophasique et diphasique des flammes laminaires monodimensionnelles, Rapport d'Ingenieur WN/CFD/02/62, CERFACS.

[CFD81] C.-T. Pham, (2003), Contribution CERFACS au DTP Optimisation, June CR/CFD/03/43, CERFACS.

[CFD82] C. Prière, L. Gicquel, and T. Poinsot, (2002), Large Eddy Simulations of Opposed Jets In Cross Flow, Contract report CR/CFD/02/121, CERFACS.

[CFD83] G. Puigt, (2003), Numerical study of wake vortices of the F11 aircraft model : Effects of differential flap setting on wake vortices, Contract report CR/CFD/03/6, CERFACS.

[CFD84] E. Renaud, (2002), Validation du logiciel ELSA pour la prédiction des dérivées dynamiques sur des surfaces portantes, Rapport technique 2eme année Ingénieur TR/CFD/02/88, CERFACS.

[CFD85] E. Riber, (2003), Modélisation et calcul de jets diphasiques, Rapport de DEA WN/CFD/03/74, CERFACS.

[CFD86] E. Riber, (2003), Rapport de fin d' études - PFE, Tech. Rep. WN/CFD/03/72, CERFACS.

[CFD87] S. Roux, L. GIcquel, U. Meier, and C. Bérat, (2003), Experimental and Numerical Investigation of Self-Excited Combustion Oscillations in a Scaled Gas Turbine Combustor - submitted to the New Challenges in Aerospace Technology and Maintenance Conference 2004 to be held in February 2004 at Singapore, Tech. Rep. CR/CFD/03/122, CERFACS.

[CFD88] S. Roux, (2003), Calcul du mélange air-méthane dans un injecteur de turbine gaz par simulation des grandes échelles, Rapport de stage DEA WN/CFD/03/75, CERFACS.

[CFD89] F. Rue, (2002), Projet COS, Tech. Rep. WN/CFD/02/68, CERFACS.

[CFD90] M. Saudreau and H. Moet, (2003), Effect of design modifications to Airbus-type aircraft wing on wake evolution - C-Wake Report, Contract report CR/CFD/03/35, CERFACS.

[CFD91] C. Saulnier, (2002), Analyse théorique et simulation numérique d'une flamme monodimensionnelle laminaire diphasique, rapport de stage WN/CFD/02/64, CERFACS.

[CFD92] T. Schönfeld, J.-D. Müller, and R. Martin, (2003), Projet N3S NATUR : Synthèse sur la fonctionnalité maillage hybride pour la CFD, Contract report CR/CFD/03/62, CERFACS.

[CFD93] T. Schönfeld, (2003), Synthèse sur la fonctionnalité maillage hybride pour la CFD, Contract report CR/CFD/03/116, CERFACS.

[CFD94] A. Sengissen, (2002), Simulation numérique du couplage fluide/structure : application aux turbines à gaz industrielles, Rapport de stage WN/CFD/02/83, CERFACS.

[CFD95] Y. Sommerer, F. Nicoud, and T. Poinsot, (2003), Simulations aux grandes échelles de la combustion instationnaire dans les systèmes partiellement prémélangés pauvres, Contract report CR/CFD/03/118, CERFACS.

[CFD96] Y. Sommerer, F. Nicoud, J. Légier, T. Pasutto, and T. Poinsot, (2002), Simulations aux grandes échelles de la combustion instationnaire dans les systèmes partiellement prémélangés pauvres : 1er Colloque National sur la Recherche Aéronautique sur le Supersonique, Rapport contractuel CR/CFD/02/41, CERFACS.

[CFD97] G. Staffelbach, (2002), Calculs de flammes laminaires prémélangées, Rapport de stage WN/CFD/02/67, CERFACS.

[CFD98] X. Toussaint, (2002), Simulation instationnaire d'un écoulement transsonique turbulent autour d'un profil supercritique, Rapport de stage de D.E.A. WN/CFD/02/84, CERFACS.

[CFD99] K. Truffin and T. Poinsot, (2002), Projet ICLEAC : deliverable D4.4 - Measurements of transfer functions in cold flow using Large Eddy Simulations : theoretical framework and first tests., 24th month report CR/CFD/02/37, CERFACS.

[CFD100] B. Yerly, (2003), SImulation d'écoulements décollés subsoniques turbulents présentant des détachements tourbillonnaires, Rapport DEA WN/CFD/03/76, CERFACS.

3

Computational Electromagnetism

1 Overview Presentation

A. Bendali

The project “Computational Electromagnetism” addresses the difficulties encountered when solving large-scale problems in scattering and propagation of electromagnetic waves. Centimetric waves constitute the most used band of frequencies in several branches of engineering and industry: communications, remote sensing, defence, ... but asymptotic techniques are generally not effective for this range of frequencies. On the other hand, using ten unknowns per centimeter to correctly reproduce the variations of the electromagnetic field takes as much as one million of unknowns per m^2, that is, a few millions of unknowns for realistic problems. Two such problems (influence of an air-intake on the RADAR Cross Section (RCS) of an aircraft; effect of a satellite on the radiation of an inboard antenna) are presently studied under an active collaboration with MBDA-France and CNES.
The main progress achieved during the last two years concern both theoretical studies, algorithmic issues and implementation of codes well-adapted to massively parallel high-performance computers. For convenience, the description is structured along three main axes.

- **Boundary integral equations methods**
  - Use of the general theory of groups representation to take advantage of multiple symmetries in the geometry and material properties and to reduce as much as possible the size of the linear systems to be solved;
  - Shape reconstruction of an object from the knowledge of its RCS, in collaboration with INRIA, [CEM3];
  - Theoretical foundations of a new boundary integral formulation [CEM2].
- **Multi-levels Fast Multipole Method (MLFMM)**
  - Implementation of out-of-core and efficient Sparse Approximate Inverse (SPAI) preconditionners;
  - Implementation of a parallel version of the MLFMM;
  - Theoretical determination of some parameters, crucial for the stability and the accuracy of the method, for which only empirical estimates were previously available;
  - Reconstruction of the near field radiated by an antenna from the measurements of its far-field radiation patterns [CEM13].
- **Domain decomposition methods (DDM)**
  - Non-overlapping domain decomposition methods [CEM4];

- An efficient Schur's complement procedure in the frame of integral equations has been validated for large-scale cavity problems. In the same way, an overlapping domain decomposition method for boundary integral equations has been devised and validated in the 2D case [CEM5]. It has been used to couple a direct solution for the cavity problem to an asymptotic solution for the surrounding structure;
- Higher-order and robust effective boundary conditions for the scattering of an electromagnetic wave by a perfectly conducting metal coated by a thin dielectric layer [CEM1];
- Implementation of a parallel code for the coupling of a Finite Element (FE) and a Boundary Element (BE) method. Several studies targeting to do this coupling as efficiently as possible are currently conducted.

Collaborations take place with academic research institutions: MIP, INRIA (when N. Bartoli spent one year as a post-dosctoral fellow), ENAC (where the generalist code CESC has been installed to allow ENAC to undertake more realistic studies), KTH (three invited talks at the Workshop Inria-KTH in october 2003 at Stockholm), University of Uppsala (Sweden). A number of collaborations are also presently occuring with industrial partners (MBDA-France, CNES, Dassault-Aviation, CEA-CESTA).

2 Boundary Integral Equations Methods

2.1 CESC Code – Current state and short-term perspective

The acronym CESC stands for CERFACS Electromagnetic Solver Code. It solves Maxwell's equations in the frequency domain by means of a boundary integral formulation. After a rather difficult assembly process, the solution is reduced to that of a dense linear system by a direct method. The main characteristics of the code is its adaptation to massively parallel platforms. Currently, the code deals with problems which can involve at the same time: metallic surfaces, either closed or opened, multiple dielectric materials connected at general junctions, wires, even crossing an interface separating two dielectric media, imperfectly conducting surfaces. Also the code can use various formulations: Electric, Magnetic or Combined Field Integral Equations to achieve the determination of the solution.
The main difficulty of dealing with such general problems is to correctly express the currents, flowing across each edge of the meshes modeling the structure, in terms of the final unknowns. The current state of the code allows to deal with junctions involving several dielectrics, two of them being possibly separated by a metallic sheet, but it remains to develop a general approach.
CESC is a basic tool used for several studies to obtain reference solutions. For example, CESC has been used for preliminary tests before launching important research programs concerning

- substructuring methods for electrically-deep aircraft air-intakes;
- coupling of FE and BE methods;
- efficient solvers for imperfectly conducting surfaces.

CESC is based on the parallel solver SCALAPACK. As this solver cannot take advantage of a possible symmetry of the matrix, the "Parallel Algo" team is currently involved in the development of a similar solver without this drawback. The first results are satisfactory, and this solver will be added to the code once it will be fully validated.
During the last two years, CESC has been installed at MBDA-France, CNES and ENAC (Antennas Department). It is further aimed at becoming the production code of the Antennas department of CNES.

2.1.1 Accurate modeling of the feeding of a patch antenna by a coaxial cable

M. Fares, A. Bendali, F. Collino

The most critical and difficult part in the numerical simulation of the functioning of a patch antenna is related to the determination of its impedance, especially at the resonance frequency. Inside the coaxial cable and far enough from its junction with the patch, only the fundamental TEM mode is propagating. The determination of the reflection coefficient of this mode directly yields the impedance of the antenna. An impedance boundary condition is generally used as the boundary condition to truncate the cable, hence limiting the domain of computation. However, especially in the context of a BE solution, it is hard to take into account such kind of boundary condition. A new approach based on the expression of the boundary condition in terms of the fundamental TEM mode has been developed. Fig. 2.1 depicts the impedance obtained from measurements and from two codes, respectively obtained using this approach and through a more standard code based on the simplified model assuming an infinite ground plan.

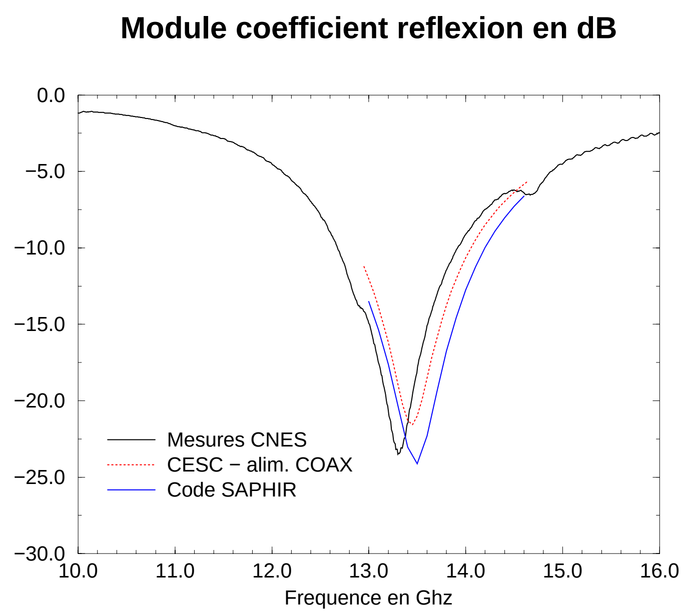

Figure 2.1: Impedance curve versus the frequency from measurements, code CESC and code SAPHIR

2.1.2 Systematic treatment of symmetries

F. Collino, M. Fares

The objective is to take advantage of symmetries to reduce the size of the linear system to be solved. For instance consider the case where the geometry and the material properties of the structure are symmetric relatively to a plan. In boundary integral formulations, the coefficient of the unknown at a point y in the equation set at a point x depends only on $(x-y)$. As a result, the related equations can be set as follows

$$\begin{cases} Zx_1 + Tx_2 = U_1 \\ Tx_1 + Zx_2 = U_2 \end{cases}$$

Clearly, the solution of this system can be obtained by solving two systems of half-order only

$$(Z+T)(x_1+x_2) = U_1 + U_2, \qquad (Z-T)(x_1-x_2) = U_1 - U_2.$$

Bossavit [1] has devised a general procedure to deal with such a reduction in the case of more general invariance properties, for which one has to use the theory of linear representation of groups.
Currently, CESC deals with such a reduction for perfectly conducting surfaces only. For instance, for the structure shown in Fig. 2.2 and for an arbitrary excitation, the only systems that are solved are those related to the small piece on the right of the figure.
The extension to structures involving dielectrics is planned for the next year. However this extension requiring quite deep changes in the code, it might be necessary to completely rewrite it.

2.2 Theoretical foundations for new boundary integral formulations

F. Collino, B. Després

This study concerns the analysis of a new system of integral equations for solving scattering problems related to a general impedance boundary condition. This new method presents some advantages with

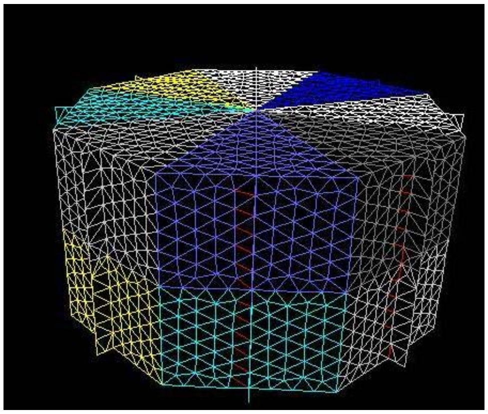

(a) Complete structure

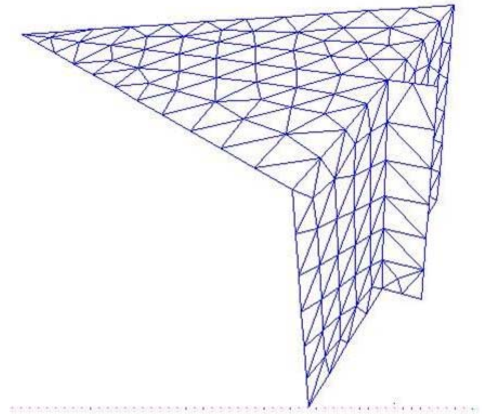

(b) Part characterizing the size of problems to be solved

Figure 2.2: Size reduction by exploiting symmetries

respect to more conventional approaches. The problem can be written as a penalized saddle point problem and, consequently, can be solved using iterative algorithms whose convergence is guaranteed *a priori*.
The method has been implemented successfully at CEA and has yielded very accurate discrete solutions. At CERFACS, this work has been conducted mainly from a theoretical point of view [CEM2].

2.3 Shape reconstruction from RCS observations

M. Fares, F. Collino, H. Haddar

The problem is to reconstruct the shape of a scatterer from multi-scattering RCS observations, that is, bistatic RCS with an illuminating plane wave for several directions of incidence.
The reconstruction is based on a technique, the linear sampling method, which has been devised by D. Colton [2]. It consists in computing an approximation of the indicator function of the scatterer, a "function" equal to $+\infty$ everywhere unless inside the scatterer where it is equal to 0. The quality of the reconstruction is quite impressive as depicted by Fig. iv in the appendix, illustrating the reconstruction of a plane [CEM3].

2.4 Internal references

[1] A. Bossavit, *Boundary-value problems with symmetry and their approximation by finite elements*, SIAM J. of Applied Math. **53** (1993) pp. 1352–1380.

[2] D. Colton, H. Haddar and P. Monk, *The linear sampling method for solving the electromagnetic inverse scattering problem*, SIAM J. Sci. Computing **24** (2002) pp. 719–731.

3 Fast Multipole Method in electromagnetic calculations

Electromagnetic scattering solutions by integral equations methods lead to dense systems of linear equations. When the characteristic size of the obstacle is about six times the wavelength, the solutions can be computed by direct methods, using high-performance and massively-parallel codes. However, if the size of the obstacle increases, the solutions can only be obtained by means of some iterative methods. The computation of the matrix-vector product then becomes the basic part of the iterative algorithm. It can be done efficiently by means of the Multilevel Fast Multipole Method.

3.1 Computer implementation aspects

F. Collino, **F. Millot**

The code has been coupled with various iterative solvers, as, e.g., with a flexible GMRES. As a result, it succeeds in solving large scale diffraction problems involving a cavity.
Work has been devoted to devising some preconditioning techniques [CEM17], exploiting the underlying mesh and extracting information to construct the preconditioner. Two types of information are available:

- When the geometries of the obstacle are smooth, only the neighboring edges are strongly coupled to each other. An effective preconditioning can be built by exploiting this topological information;
- When the geometries are not smooth, two edges far-away from each other can be strongly coupled. For each edge, all edges which are located at some given distance are selected, a geometric neighboring is defined, and the preconditioner is constructed by exploiting this information.

It is well known that the MLFMM technique allows to solve large-size problems. However, in order solve extremely large-scale problems, a highly parallel version of the MLFMM algorithm has to be developed. Such a parallel version using the Message Passing Interface for communication has been recently constructed, where angular directions are distributed on various processors.
The MLFMM code has been compared with other industrial codes using also the MLFMM method. In particular, results have been compared to those obtained at EADS and Dassault-Aviation, and good agreement has been observed [CEM14].
The out-of-core version of the code, allowing to solve large-scale diffraction problems, has been validated. It is used to solve both industrial and academic cases (the JINA test case "*Almond*" benchmark, and the Cobra cavity with a cap). Results have been compared to those obtained by industrial codes.

3.2 Theoretical aspects

3.2.1 A theoretical estimate of the accuracy of MLFMM for very high frequencies

F. Collino

The number of multipoles at a given level is a crucial parameter for the accuracy of the method. Some semi-empirical formulae have been proposed in previous studies. By means of theoretical estimates, some new formulae have been designed and validated, in collaboration with Dassault-Aviation.

3.2.2 Using the MLFMM algorithm to compute the radiated fields

N. Bartoli, F. Collino, F. Millot

A large-size obstacle can oftenly be decomposed into several items. The large-size problem can then be splitted into several small coupled problems. Consider for instance the case of two large-size and separated obstacles. The current located on a given obstacle creates a radiated field around it. This field changes the values of the current on the second obstacle. In turn, the current located on the second obstacle creates a field which changes the values of the current flowing on the first obstacle. The diffraction problem can hence be solved using an iterative process. One step of this iterative process is to compute the radiated field. It has been proposed to adapt the MLFMM algorithm to this task in order to decrease the computation time. The accuracy of this MLFMM computation has been studied. The influence of several parameters used in the MLFMM technique have been analyzed, and it has been found that the number of multipoles at a given level is a crucial parameter for the accuracy of the method. This method has been applied finally to more realistic cases. A factor 100 on the CPU time has been gained when using the MLFMM technique instead of an exact assembly process. This technique [CEM16] has also been implemented in an axisymetric code [3].

3.3 A MLFMM algorithm for solving imperfectly conducting problems

A. Bendali, F. Collino, F. Millot

A BE method is used to solve electromagnetic scattering problems in the frequency domain relative to an impedance boundary condition. A survey has been performed to investigate the different possibilities to solve such a problem [CEM20].
The total electromagnetic field is expressed in terms of the equivalent electric and magnetic currents on the surface of the scatterer to satisfy the boundary conditions. One possibility to solve the diffraction problem with an impedance condition is to keep the two currents as unknowns and to use an alternative form of the Combined Field Integral Equation. The equivalent currents are discretized by a BE method over a triangular mesh of the surface. The main drawback of this approach is that the order of the linear system is twice as large as in the perfect conductor case. This method has been implemented. Premilary results have been obtained and are compared with those obtained with an other formulation using a Lagrangian multiplier [CEM15].

3.4 A far-near field Transformation using the Fast Multipole Techniques

N. Bartoli, F. Collino, F. Dodu

The problem under consideration is to determine the coupling of an antenna with surrounding structures of large-size from the only knowledge of the antenna far-field measurements. The radiating properties of an antenna are often documented only by measurements in the far zone performed inside an anechoic chamber. The antenna designers are interested in the prediction of the coupling of the measured antenna with the surrounding elements in the near zone.
Two hypotheses are made to obtain the influence of a measured antenna on a surrounding satellite. First, only the influence of the antenna on the satellite structure is taken into account. Next, the satellite is illuminated by the far-field of the antenna measured in some given directions. The final system is hence uncoupled, and a single equation has to be solved for the current defined on the surface of the satellite. The associated right-hand side results from the illumination by the antenna. A classical approach consists

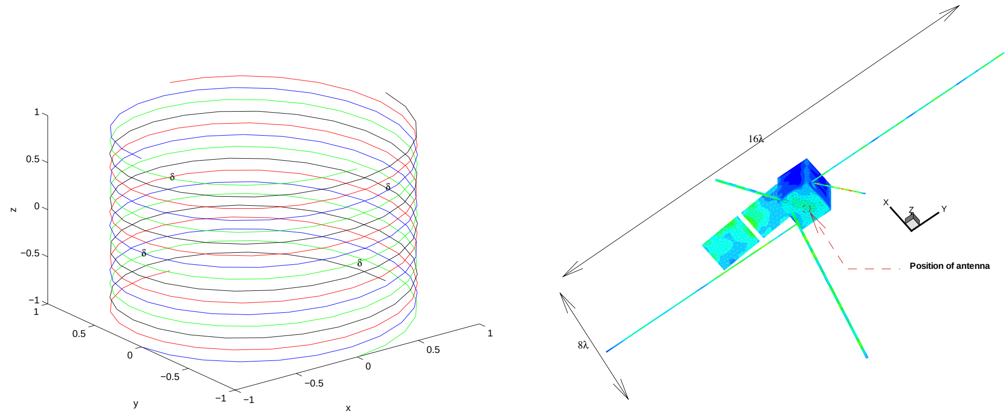

(a) Quadrifilar helicoidal antenna

(b) Satellite

Figure 3.1: Configuration antenna–satellite

Table 3.1: Relative quadratic error on the potential as a function of the distance antenna–satellite when the frequency equals 1.28GHz

Reference Potential = direct computation `CESC`			
distance antenna–satellite	$\lambda/4$	λ	10λ
`EXP` approach	56.60%	54.13%	35.31%
`FMM` approach	3.28%	2.08%	2.005%

then in using the far-field in a single direction. It is valid only if the satellite is set in the far zone of the antenna. In contrast, the new method is intended to determine the potential in the vicinity of the antenna from the knowledge of the far-field radiation pattern in all directions. The approach is based on a multipole expansion of the Green's kernel. An interpolation process of the far-field is also introduced. Some numerical experiments illustrate the efficiency and accuracy of the new approach. They also validate the main assumption: the current on the antenna is not too much perturbed by the presence of the satellite.
CNES has proposed a realistic case to validate the method. The antenna is defined by four helicoidal wires and each wire is fed in phase quadrature by a delta-gap as illustrated in figure 3.1-a. The dimensions of this antenna are 0.43λ in height and 0.3λ in diameter. The satellite "Demeter" is constituted by different perfectly conducting elements: a square box, some solar panels and cylindrical objects as shown in figure 3.1-b. The dimensions are about $8\lambda \times 16\lambda \times 12\lambda$. Three positions of the satellite are considered: $\lambda/4$, λ and 10λ from the antenna. Table 3.1 reports the relative quadratic error obtained with the two different approximations: `EXP` for exponential approach based on physical optic and `MLFMM` for the new approach ([CEM11], [CEM12], [CEM6], [CEM7], [CEM13])

3.5 Internal references

[3] N. Bartoli, *La méthode multiôle appliquée au calcul du champ proche* Rapport de Recherche INRIA, 4777, 2003.

4 Domain decomposition Methods

Several approaches exploiting the decomposition of the solution domain in two or more subdomains, overlapping or not, are considered. Such decompositions can be done to more adequately describe or solve the contribution of a particular region. Two examples are considered: the effect on the RCS of a structure of either a thin coating or a deep air-intake. The DDM approach can also be used to break a large-size problem into a system of small-size ones. It can be also used as an efficient preconditioning technique.

4.1 Higher-order and robust effective boundary conditions

N. Bartoli, A. Bendali

This theoretical study deals with the determination of the field scattered by a perfectly conducting metal coated by a thin dielectric layer. Direct numerical solutions of such kinds of problem leads to a large-size problem. Even when a large memory storage and enough computing power are available, such a solving can be affected by some numerical instabilities. Indeed some equations of the problem become nearly proportional for a too small thickness. The approach generally adopted is to take into account the effect of the thin coating through an effective boundary condition. This study has tackled the problem of defining some higher-order and robust instances of such boundary conditions. A rigorous justification of their accuracy has been also proved [CEM1].

4.2 Nonoverlapping DDM

Y. Boubendir, A. Bendali, M. Fares, F. Collino

The main results are [CEM4]:

- Depending on the availability of an efficient solver for the impedance boundary condition, this approach can be a powerful technique for coupling a FE in the area where the structure is made up of inhomogeneous dielectrics or too complicated to be solved through a BE and an integral equation formulation for the exterior. Indeed, at the algorithmic level, the FE and the BE solutions are completely uncoupled. Moreover this procedure suppresses the spurious modes which can corrupt the solution obtained by the usual coupling procedures;

- The initial radiation condition initially used by Després damps only the propagative part in the error at each iteration. A modification of this condition has been designed to deal also with the evanescent part of the error. This procedure has significantly improved the robustness of the method;

- As initially proposed, the method was able to deal only with mixed formulations, that is, with methods where a degree of freedom can be shared by at most two domains. A special procedure has been developed to overcome this drawback.

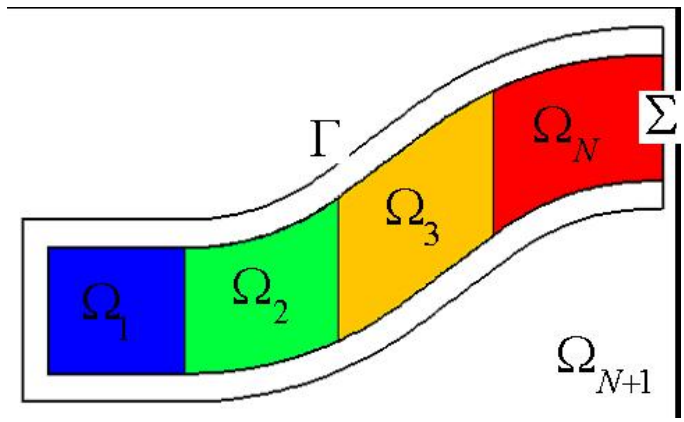

Figure 4.1: Decomposition of the cavity

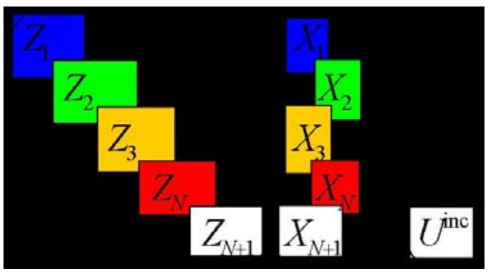

(a) Total system involving the currents at sectional interfaces

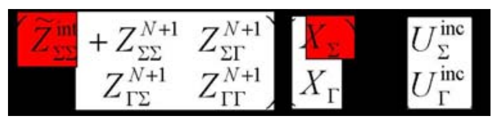

(b) Reduced system involving the exterior of the cavity only

Figure 4.2: Domain decomposition of the cavity

4.2.1 Scattering by an electrically deep cavity

N. Balin, A. Bendali, M. Fares, F. Collino

In the numerical calculation of an aircraft RCS, the determination of the contribution of the air-intake is likely the most difficult part to be solved. Standard approaches fail to deal with such a problem. Direct solutions cannot apply due to the huge computing time and memory storage they require. Fast methods like MLFMM become ineffective in this context because of the slowness of the convergence of the iterative solution procedure which has to be used then. This activity is the main theme of the collaboration with MBDA-France, following preliminary tests in 3D done by Fares with CESC. The main results obtained during the last two years are:

- Substructuring method for dealing with an electrically deep cavity: the geometry of the cavity is well-adapted to a substructuring procedure. Fig. 4.1 depicts how the cavity can be decomposed into small subdomains. The advantage of this decomposition comes from the fact that the equations and the unknowns of each subdomain are coupled only through the interfaces. So a Schur's complement technique can successively remove all the subdomains by solving small problems in each one of them at once (Fig. 4.2).

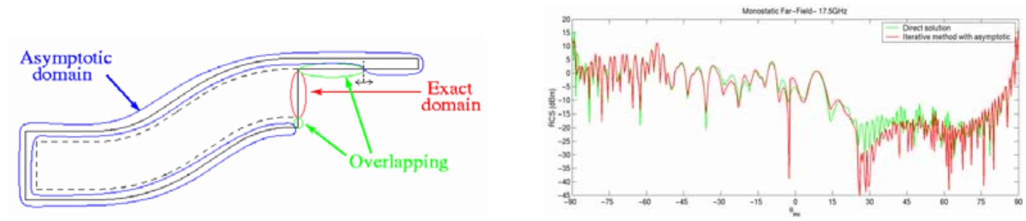

(a) Decomposition of the currents

(b) Exact and multi-methods solution

Figure 4.3: Coupling a BE and and asymptotic technique

The application of this technique to FE discretization is nothing else but the usual Irons's frontal method which has been adapted to this kind of problems in [5]. It has been also previously considered in the frame of an equivalent impedance boundary condition in [4]. However the dispersive drawbacks of the FE schemes make them not effective for this kind of problem unless using a high-degree method. In the same way, using an impedance boundary matrix at the discrete level may lead to a too strong constraint on the solution procedure for the exterior of the cavity. The solution which has been adopted is to do this substructuring in the context of a boundary integral formulation. The formulation has been fully validated in the 2D case. Some preliminary tests have shown that the method has the same efficiency in the 3D case;

- Overlapping Schwarz procedures in the context of boundary integral formulations: the boundary supporting the unknown currents is decomposed into several overlapping zones. Within each zone where two elements of the decomposition overlap, the currents are decomposed as the sum of two other currents, each of them attached to an element. The equations through the testing currents are decomposed accordingly. The problem is then reduced to a fixed-point problem which, if solved by a successive approximations procedure, results in a kind of block Jacobi method with overlapping. Instead this system is solved much more efficiently using a Krylov iterative method. The resulting method is as efficient as the powerful preconditioning techniques based on the construction of a Sparse Approximate Inverse (SPAI). Indeed the real advantage of this method is its ability to couple different methods of solution. Fig. 4.3 shows how a direct solution dealing with the interior of the cavity can be coupled to an asymptotic technique based on the Geometrical Theory of Diffraction.

4.3 Coupling FE and BE solutions

N. Zerbib, A. Bendali, N. Bartoli, F. Collino

The main application concerns the numerical modeling of the influence of a satellite on the radiation of an inboard antenna. The first achievements are:

- Parallel codes: a parallel code based on the library 'MUMPS' (see the "Algo" chapter) has allowed for the coupling of a FE with the BE solutions of CESC. This code can deal with middle-scale problems, that is, with a few millions of unknowns for the sparse matrices coupled to a few tens of thousands of unknowns for the dense matrices.

- Elimination of spurious modes in FE-BE coupling:

  a CFIE formulation has to be used to suppress spurious modes which can corrupt the solution at a resonance frequency for the cavity enclosed by the exterior surface on which is set the boundary integral equations. However, due to magnetic currents, the CFIE involves an integral operator which cannot be dealt with through a simple integration by parts. This study is presently in progress.

- Hybridization of Finite Element and Boundary Integral Methods:

  a new approach has been recently presented [6] for solving the time-harmonic Maxwell's equations relative to a dielectric object. If uses the FE method and proposes to truncate the computational domain by using an adaptive numerical absorbing boundary condition derived from the boundary integral equations. This new absorbing boundary condition depends on both the electric and magnetic fields at the surface of the object and is computed efficiently by using a mixed formulation. The proposed method presents several advantages. It produces an accurate solution, the truncation boundary can be placed very close to the object to minimize the computational domain, the final matrix is purely sparse, the system is free of interior resonance and the iterative solver requires few iterations to converge to an exact solution.

  This approach has been implemented in order to evaluate these properties in the 2D case. The first results are promising and the method seems to be a good candidate to deal with the interactions between a satellite and an inboard antenna.

4.4 Internal references

[4] A. Barka, P. Soudais and D. Volpert, *Scattering from 3-D Cavities with a Plug and Play Numerical Scheme Combining IE, PDE, and Modal Techniques* IEEE Transactions on Antennas and Propagation **48** (5) (2000) pp. 704–712.

[5] J. M. Jin, *Electromagnetic scattering from large, deep and arbitrarily shaped cavity*, Electromagnetics (1998) pp. 719–731.

[6] J. Liu and J. M. Jin, *A novel hybridization of higher order finite element and boundary integral methods for electromagnetic scattering and radiation problems*, IEEE Transactions on Antennas and Propagation **49** (2001) pp. 1794–1806.

5 Publications

5.1 Journal Publications

[CEM1] N. Bartoli and A. Bendali, (2002), Robust and High-Order Effective Boundary Conditions for Perfectly Conducting Scatterers Coated by a thin Dielectric Layer, *IMA Journal of Applied Mathematics*, **67**, 479–508.

[CEM2] F. Collino and B. Després, (2003), Integral equations via saddle point problems for time-harmonic Maxwell's equations, *Journal of Computational and Applied Mathematics*, **150**, 157–192.

[CEM3] F. Collino, M. Fares, and H. Haddar, (2003), Numerical and analytical studies of the linear sampling method in electromagnetic inverse scattering problems, *Inverse Problems*, **19**, 1279–1298.

5.2 Theses

[CEM4] Y. Boubendir, (2002), *Techniques de décomposition de domaine et méthode d'équations intégrales*, PhD thesis, CERFACS–INSA–MIP.

5.3 Conference Proceedings

[CEM5] N. Balin, A. Bendali, and F. Collino, (2002), Domain decomposition and additive Schwarz techniques in the solution of a TE model of the scattering by an electrically deep cavity, Berlin, Germany, 15th International conference on Domain Decomposition Methods, 149–156.

[CEM6] N. Bartoli and F. Collino, (2002), A Far to Near Interpolation, Cambridge, Massachusetts,USA, PIERS 2002, Progress In Electromagnetics Research Symposium, 297.

[CEM7] N. Bartoli, F. Collino, and F. Dodu, (2003), Using the Multipole Techniques for the Far to Near Field Transformation, In *Mathematical and Numerical Aspects of Wave Propagation*, Waves 2003, Jyväskylä, Finland, Springer, 662–668.

[CEM8] Y. Boubendir and A. Bendali, (2003), Dealing with Cross-Points in a Non-Overlapping Domain Decomposition Solution of the Helmholtz Equation, Jyväskylä, Finland, Waves 2003, 319–324.

[CEM9] F. Collino and F. Millot, (2002), A 2-components Algorithm for the Multilevel Fast Multipole Method for Solving Large scale Diffraction Problems, Toulouse, JEE02, European Symposium on Numerical Methods in Electromagnetics, 103–108.

[CEM10] F. Collino, M. Fares, and H. Haddar, (2003), On the validation of the linear sampling method in electromagnetic scattering problems, Jyväskylä, Finland, Waves 2003, 649–654.

5.4 Technical Reports

[CEM11] N. Bartoli and F. Collino, (2002), Etude de l'interaction d'une antenne et d'une structure métallique par la "Fast Multipole Method - Partie 2"., Contract Report CR/EMC/02/8, CERFACS.

[CEM12] N. Bartoli, F. Collino, and F. Dodu, (2002), Etude de l'interaction d'une antenne et d'une structure métallique par la "Fast Multipole Method - Partie 3"., Contract Report CR/EMC/02/101, CERFACS.

[CEM13] N. Bartoli, F.Collino, F. Dodu, and T.Koleck, (2003), A far-near field Transformation using the Fast Multipole Techniques, Technical Report TR/EMC/03/90, CERFACS.

[CEM14] Q. Carayol, F. Collino, F. Millot, and G. Sylvand, (2002), Comparaison de codes multipôles, Tech. Rep. CR/EMC/03/10, CERFACS.

[CEM15] O. Cellarier, (2002), Introduction d'une condition d'impédance dans un code d'électromagntisme, Tech. Rep. WN/EMC/03/54, CERFACS.

[CEM16] F. Collino and F. Millot, (2002), Analyse quantitative de la précision de la méthode multipolaire pour plusieurs objets diffractants, Tech. Rep. CR/EMC/03/134, CERFACS.

[CEM17] F. Collino and F. Millot, (2002), Mise en place d'un préconditionneur appliqué à un problème d'électromagnétisme, Tech. Rep. TR/EMC/02/122, CERFACS.

[CEM18] X. Lages, (2002), Approximation de la SER monostatique partir d'un nombre restreint d'incidences, Tech. Rep. WN/EMC/02/86, CERFACS.

[CEM19] M. Mensour, (2002), Mise en place d'un préconditionneur appliqué à un problème d'électromagnétisme, Tech. Rep. WN/EMC/02/86, CERFACS.

[CEM20] F. Silva, (2002), Résolution des problèmes de diffraction d'ondes électromagnétiques avec condition d'impédance par méthodes intégrales, Tech. Rep. WN/EMC/03/53, CERFACS.

4

Climate Modelling and Global Change

1 Introduction

Olivier Thual

Six projects are described in this report. The first three projects correspond to the new structuration of five former projects of the "Climate Modelling and Global Change" team. There are described in the three following sections and are entitled:

- Climate variability and predictability
- Ocean data assimilation for climate studies and seasonal prediction
- The PALM and OASIS couplers and applications

There are strong connections between these projects. The first project is characterized by a high level research on a large scope of actual topics on climate modelling. This expertise is very useful for the seasonal prediction experiments led in the second project. The numerical simulations of these experiments are strongly based on the ocean data assimilation methods which have been developped at a high scientific level. Both projects interact strongly with the software development project from which the PALM and OASIS couplers serve a large community of users in the world. This last project also contains other scientific activities strongly relying on these tools.

A project on "Synthetic Aperture Imaging" has recently merged the GLOBC team. It is described in the fifth section and is entitled:

- SMOS mission

The data that will be collected by the SMOS space mission, such as the sea surface salinity, will be of great interest for the climate studies.

The last project corresponds to development activities which are directly included in the MERCATOR project which deals with operational oceanography. The CERFACS contribution to this project is described in the last section and is entitled:

- The CERFACS contribution to the MERCATOR project

Another CERFACS project is connected to the activities of the "Climate Modelling and Global Change" team and is entitled:

- Environmental impact of aviation

Since it is also strongly connected with the activities of the "Computational Fluid Dynamics" team, it is described in the corresponding part of this scientific report.

2 Climate variability and predictability

2.1 Introduction

The world climate is currently changing due to the human-induced increase in the atmospheric concentrations of CO_2 and other greenhouse gases. In order to optimally define the adaptation and mitigation strategies needed to cope with the potential impacts of this expected climate change, a deeper understanding of the intrinsic variability of the climate system is needed to assess confidence in the detection, attribution and prediction of global and regional climate change due to anthropogenic causes.

Within this global framework, the scientific objectives of the Climate Variability and Predictability group are as follows:

- To improve the understanding of climate processes underlying the natural variability of the main climate modes, such as the North Atlantic Oscillation (NAO), the Atlantic Meridional Overturning Circulation (AMOC) and the El Nino Southern Oscillation (ENSO), and of the response of the NAO, AMOC and ENSO to climate change.

- To detect, attribute and describe anthropogenic climate change on global to regional scales with a focus upon Europe and West Africa, using high resolution atmospheric models and long-term, high quality, observations.

- To assess the impacts of anthropogenic climate change at regional scale with specific interest in the changes of extreme events distribution and hydrological cycle properties, with a focus upon Europe and West Africa, and to provide uncertainty bounds in future climate projections.

- To assess the risk of abrupt climate change, with emphasis upon the possible collapse of the thermohaline circulation and its regional impacts particularly over Europe.

For the past two years, work has concerned essentially the first objective. The main activity has been devoted to the continuation of work on the variability and predictability of low-frequency atmospheric fluctuations over the North Atlantic European sector. It has used extensively a methodology relying on the climate or weather regime paradigm and applied it to both Sea Surface Temperature (SST) and anthropogenically-forced variability. Coupled model experiments have also been performed to assess predictability of interannual to decadal variations in AMOC and associated Atlantic SST anomalies. Work has also been done on the decadal variability of the tropical Pacific and its links with the ENSO mode. Finally, a preliminary study of the origin of the decreasing trend in Sahelian rainfall during the 20^{th} century has also been performed.

2.2 Low frequency atmospheric variability and predictability over the North Atlantic European sector (C. Cassou, C. Delon, M.E. Demory, G. de Coetlogon, M. Déqué, C. Deser, M. Drévillon, A. Jouzeau, J. Hurrell, E. Maisonnave, L. Terray)

2.2.1 Circulation regime analysis for the North Atlantic European sector during the 20th century (C. Cassou, C. Deser, J. Hurrell, L. Terray)

The observed low frequency winter atmospheric variability of the North Atlantic-European region and its relationship with global surface oceanic conditions was investigated based on the climate and weather regimes paradigm. Cluster analyses are applied to monthly Sea Level Pressure (SLP) means from the NCEP-NCAR Reanalysis over 1950-2001. The statistical decomposition is performed for individual winter month (December/January/February) over the North Atlantic-European domain ($80^oW - 30^oE$/$20^oN - 80^oN$), where each month is considered an individual realization of the atmospheric states.

The clustering partition yields the optimal $k = 4$ number of significant winter climate regimes (Fig. 2.1). The first two clusters capture the negative and the positive phases of the NAO and are characterized by a zonally-elongated meridional pressure dipole between the Icelandic Low and the Azores High. The third cluster displays a strong anticyclonic ridge (RDG) off western Europe almost covering the entire basin. It is reminiscent of the positive phase of the East Atlantic (EA) teleconnection pattern which features the northward extension of the Azores High. The fourth cluster exhibits a zonal pressure dipole between Greenland and Scandinavia (GS), with a clear southeastward extension of low pressure anomalies towards the Iberian peninsula.

Asymmetries between the two phases of the NAO are found in the position of the Azores High and, to a weaker extent, the Icelandic Low. There is a significant eastward displacement or expansion towards Europe for the NAO$+$ climate regime compared to the NAO$-$ regime. This barotropic signal is found in different datasets and for two quasi-independent periods of record (1900-1960 and 1950-2001); hence, it appears to be intrinsic to the NAO+ phase. Strong spatial similarities between weather and climate regimes suggest that the latter, representing long timescale variability, can be interpreted as the time-averaging signature of much shorter timescale processes. Model results from the Météo-France ARPEGE Atmospheric General Circulation Model (AGCM) are used to validate observed findings. They confirm in particular the eastward shift of the Atlantic centers of action for the NAO$+$ phase, and strongly suggest a synoptic origin as it can be also extracted from daily analyses. These results bring together present-day climate variability and scenario studies where such a NAO shift was suggested, as the last three decades have been shown to be clearly dominated by the occurrence of NAO$+$ regimes when concentrations of greenhouse gases are rapidly increasing (Fig. 2.1). These findings highlight that the displacement of the North Atlantic centers of action should be treated as a dynamical property of the North Atlantic atmosphere, and not as a mean longitudinal shift of climatological entities in response to anthropogenic forcings.

The nonstationarity with time of the atmospheric variability has been documented. Late century decades differ from early ones by the predominance of NAO climate regimes versus others. Both tropical and extratropical SST anomalies alter the frequency distribution of the North Atlantic regimes [GLO3,GLO8]. Evidence is presented that the so-called Ridge regime is preferably excited during La Niña events, while the NAO regimes are associated with the North Atlantic SST tripole. The ARPEGE model results indicate that the tropical branch of the SST tripole affect the NAO regimes occurrence. Warm tropical SST anomalies are more efficient at exciting NAO$-$ regimes than cold anomalies are at forcing NAO$+$ regimes [GLO8]. The extratropical portion of the North Atlantic SST tripole also seems to play a significant role in the model, tending to counteract the dominant influence of the tropical Atlantic basin on NAO regimes [GLO3].

2.2.2 Relationships between early winter North Atlantic atmospheric variability and summer Atlantic SST (C. Cassou, C. Deser, J. Hurrell, M. Drévillon, L. Terray)

From both observations and models, the North Atlantic early wintertime atmospheric variability and its relationship with previous summer anomalous oceanic conditions have been investigated. The origin of the so-called summer North Atlantic Horseshoe (HS) SST mode, which is statistically linked to the next winter's NAO is first studied from data and CCM3 experiments. It is suggested that HS can be interpreted as the remote footprint of tropical atmospheric changes. Anomalous convective patterns corresponding to a displacement and/or reinforcement of the Atlantic Inter Tropical Convergence Zone (ITCZ) generate forced atmospheric Rossby waves that propagate northeastward from the Caribbean basin and lead to changes in trade wind intensity over the northern subtropical Atlantic. The perturbed turbulent and radiative fluxes at the surface associated with the teleconnection pattern would tend to imprint HS-shaped oceanic anomalies. The ARPEGE AGCM is then used to test if the persistence of HS anomalies from summer to late fall can feedback to the atmosphere and have an impact on the next winter's North Atlantic variability. A weak but coherent early winter response projecting on the NAO is obtained and reproduce the observed HS/NAO relationship obtained from lagged statistics. The role of the transients is hypothesized to be of central importance to explain the nature and the sign of the model response.

2.2.3 Decadal variability and predictability experiments with the ARPEGE/OASIS/ORCALIM model (C. Delon, A. Jouzeau, E. Maisonnave, L. Terray)

There is increasing evidence (from both observations and models) of decadal time-scale fluctuations in the circulation of the Atlantic Ocean. Variations in the meridional overturning circulation (MOC) may impact on the surface climate of both the ocean and the atmosphere through changes in the northward transport of heat by the ocean. Predictions of such decadal variations could bring considerable benefit to society, yet these remain unrealised partly because previous studies of predictability have revealed low levels of potential skill [GLO1]. This study, which was performed within the EC-FP5 PREDICATE project, represents an assessment of the potential predictability of variations in MOC and associated Atlantic SST anomalies with the ARPEGE/OASIS/ORCALIM coupled atmosphere-ocean-sea-ice model. The experimental design is as follows: the coupled model experiments are of the form of ”perfect ensemble” experiments, in which ocean initial conditions are fixed and the ensemble is generated by taking different atmospheric initial states. Thus the ensemble spread represents that which would be obtained in a hypothetical operational forecast system in which the ocean state is exactly known and the model is perfect. Thus it provides an upper limit on the estimate of predictability. The experiments were initiated from a long control integration, with an ensemble size of 6 and the length of the experiments being 25 years. An attempt was made to initiate experiments from high and low values of the strength of the MOC.

The model has a magnitude of natural internal decadal variability in its control integration of the order of 3-4 Sverdrups for the MOC. Empirical Orthogonal Function (EOF) analysis of the MOC suggests two different timescales for the ocean thermohaline circulation variations. The first EOF depicts a basin-wide cell with a maximum between 30N and 50N at a depth of about 2000 meters. The principal component (PC) of this mode shows low frequency fluctuations at a period between 30 and 50 years. This mode is related to density anomalies in the Nordic seas and seems to be driven by salinity in the Labrador Sea and by temperature further south. The second EOF mode depicts two cells of opposite sign, extending from the surface to the bottom of the ocean, resembling the Ekman response to the surface wind forcing of the ocean. The PC of this mode has a nearly white spectrum with significant fluctuations at the decadal time scale. Lagged correlation between this PC and the NAO index shows a maximum at lag 0. The regression, at lag 0, of surface zonal wind stress and SST on the second PC depicts the well-known tripole pattern for

SSTs and NAO-like pattern for the wind stress. Hence, the decadal mode of the MOC seems to be driven by fluctuations in the NAO.

Potential predictability in the ensemble experiments has been identified, when either the ensemble spread is small with respect to the background levels of natural variability, or when the ensemble mean is shifted with respect to the climatological average value, indicating a bias in the probability of greater or less than average conditions. The results indicate the existence of interannual to decadal potential predictability in the MOC. Moreover, the predictability is higher for the ensemble starting from a high MOC phase. For the North Atlantic SSTs, the potential predictability does not exceed two years in the annual mean for both ensembles. Over Europe, surface air temperature does not seem to be predictable more than one year in advance. Moreover, there is no evidence of any sensitivity to the phase of the MOC. It was also found in PREDICATE that, while different models do produce different estimates of predictability, some models show high levels of potential skill on time-scales of decades and longer that may, one day, be exploited for climate forecasts.

2.2.4 Influence of anthropogenic forcing upon winter atmospheric circulation over the North Atlantic European sector (M.E. Demory, G. de Coetlogon, M. Déqué, E. Maisonnave, L. Terray)

Analyses of both the observed record and transient integrations with climate models forced by scenarios of increasing greenhouse gases concentrations have suggested that anthropogenic climate change may project onto pre-existing modes of natural variability. In this study, an ensemble of climate change scenarios performed with a global general circulation model of the atmosphere with high horizontal resolution over Europe is used to investigate the possible influence of anthropogenic greenhouse forcing on the North Atlantic European climate. The global AGCM used in this study is the variable resolution new version of the ARPEGE climate model. It has a T106 spectral truncation and 31 vertical levels. The maximum horizontal resolution is about 0.5^o and stays fairly high over the North Atlantic and European sectors. The high-resolution AGCM is used to obtain an improved regional level simulation over specific periods of interest or time slices from fully coupled coarse resolution climate models. A first ensemble of three time-slice experiments has been used for the current climate (1960-1999), where the model is forced by monthly mean observed SST and historical greenhouse gas and sulphate aerosol concentrations. A second ensemble of eight time-slice climate change (2070-2099) experiments has been used using various matching combinations of SST forcing and IPCC A2 and B2 SRES scenarios of future greenhouse gas and sulphur emissions. The SST boundary forcing are combinations of observed SSTs and mean SST changes in response to the radiative forcing such as the observed 1960-1989 SST interannual variability is maintained for the 2070-2099 period. The mean SST changes are derived from transient simulations with the ARPEGE-OPA [GLO5] and HadCM3 coupled general circulation models (CGCM), which have been both forced by the A2 and B2 SRES scenarios. Clustering analyses based on the k-means partitioning algorithm are then used to describe possible changes in the NAE winter atmospheric circulation due to anthropogenic influence. The algorithm seeks preferred or recurrent atmospheric patterns (or climate regimes) in the atmospheric state space. The simulated regimes for the current climate compare very well with the observed ones in terms of spatial structure and frequency of occurence.

It is found that the end-of-century climate change strongly projects onto the positive phase of the North Atlantic Oscillation during the wintertime. It reflects in the doubling in the residence frequency of the climate system in the associated circulation regime, in agreement with the non-linear climate perspective (Fig. ixa in the appendix). Analysis also indicates the robustness of the anthropogenic regime shift against internal atmospheric variability, as well as uncertainty in prescribed boundary conditions. The strong increase in amplitude response, compared to coarse resolution coupled models studies [GLO5] (Fig. ixb in the appendix) , suggests that improved model representation of regional climate is needed to achieve more reliable projections of anthropogenic climate change on European climate.

2.3 Study of the relationship between tropical Pacific decadal variability and the low-frequency modulation of ENSO activity (C. Cibot, B. De Witte, E. Maisonnave, L. Terray)

In this study, spatial and temporal structures of interannual to decadal variability in the tropical Pacific Ocean are investigated using results from a long control integration using a global atmosphere-ocean coupled general circulation model. The model is the ARPEGE/OASIS/ORCALIM CGCM which was assembled for the PREDICATE project. The model produces quite realistic mean state characteristics, despite a SST climatology too cold and a thermocline shallower than observations in the western Pacific. The periodicity and spatial patterns of the modelled ENSO compare well with those observed over the last 100 years although the quasi-biennial timescale is dominant. Lag-regression analysis between the mean zonal wind stress and the 20^{o}C isotherm depth suggests that the recently proposed recharge-oscillator paradigm is operating in the model. Decadal thermocline variability is characterized by enhanced variance over the western tropical South Pacific (7^{o}S). The associated subsurface temperature variability is primarily due to adiabatic displacements of the thermocline as a whole due to Ekman pumping anomalies located in the central Pacific south of the equator. These wind anomalies appear to be caused by SST anomalies in the eastern equatorial Pacific. Further analysis shows the existence of a coupled mechanism where the off-equatorial sub-surface temperature anomalies move northwestward to the western equatorial Pacific and modify the equatorial coupled dynamics in such a way that the original SST anomaly is reversed in the east. This quasi-decadal variability has a period of roughly 11 years. The possible relationships between this decadal tropical mode and the low-frequency modulation of ENSO variance was also investigated: it was found that the decadal tropical mode is highly correlated to the low frequency modulations of ENSO, as recently found in other coupled models. It questions the commonly accepted hypothesis that low frequency modulations of ENSO are due to decadal changes of the mean state characteristics. In the model, the anomaly patterns associated with the low frequency modulations of ENSO (highly similar to the decadal mode patterns) are not consistent with this hypothesis. They are more likely the result of the ENSO nonlinearities (asymmetric spatial structure between El Niño and La Niña events). These nonlinearities (also found in observations) can strongly act in the model, because they are favoured by stronger and more regular than observed ENSO events. So the other mechanisms which operate in observations and influence the decadal variability are less visible in the model, dominated by the influence of modelled ENSO variability.

2.4 Influence of global ocean SST forcing upon the low frequency variability of the West African Monsoon (C. Caminade, E. Maisonnave, L. Terray)

The interannual and decadal variability of July-September regional rainfall over the Sahel is studied using an ensemble of 8 SST-forced simulations with the ARPEGE AGCM, integrated from 1948 until 1997. The simulated variability of Sahel rainfall can be separated into an internal part (noise) and an external part (signal forced by SST) using the traditional analysis of variance method. At interannual time scales, the SST-forced fraction of variability is about 30% in average and slightly more for decadal fluctuations. The model has good skill at decadal scale as it reproduces the observed opposition between the wet $1950-60$s and the dry $1970-90$s periods. The SST pattern associated to the simulated rainfall decreasing trend is remarkably similar to the one deduced from the observed precipitation data. It is very close to the so-called global extra-tropical mode (with weak amplitude in the tropical band and opposite sign anomalies in the Northern and Southern extra-tropics). This provides indirect evidence that the recent anomalously dry rainy seasons are mainly due to low-frequency changes in global SSTs. More detailed statistical analysis suggests that the Indian ocean may play the leading role in the simulated teleconnection over the Sahel region at these long time scales. In particular, the south eastern Indian ocean, which has also been shown to be a major player for the Indian Monsoon [GLO9], seems to be a key region. The skill at interannual time scale is more modest mostly due to the strong model underestimation of the links between Sahel rainfall and ENSO events after 1970.

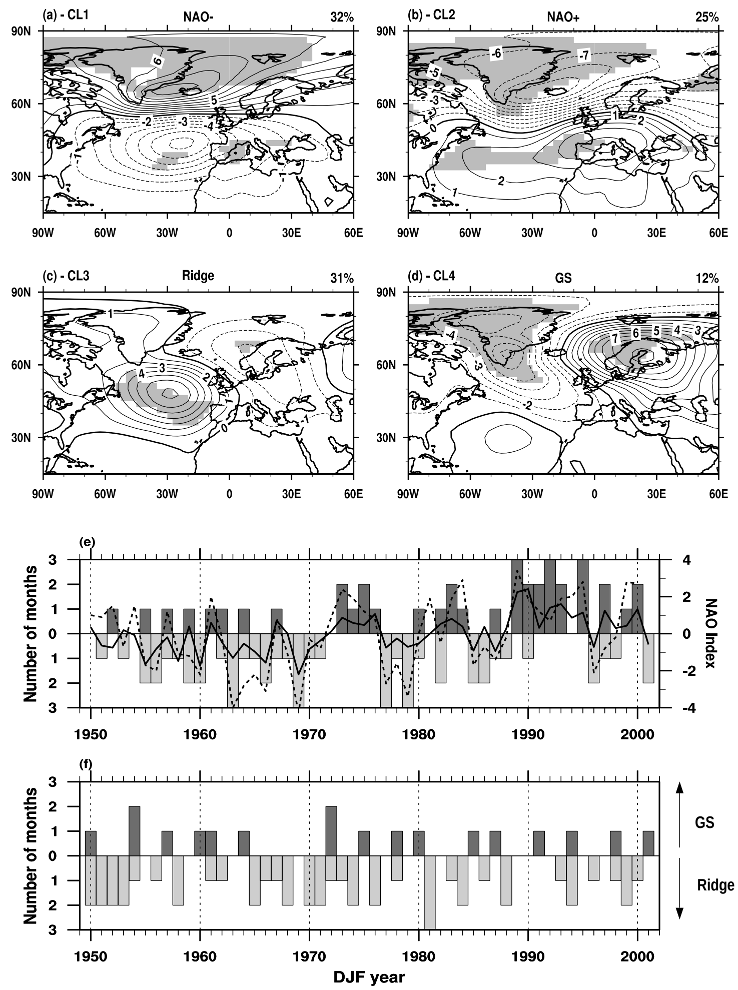

Figure 2.1: **(abcd)** 1949-2001 Winter Sea Level Pressure regimes $[hPa]$ over the North Atlantic sector from NCEP Reanalysis. Shaded areas exceed the 95% confidence level. Contour interval is every $1hPa$. **(ef)** Time history of the occurrence of the NAO and Ridge/GS regimes . The vertical bars indicate the number of months relative to each winter where the given regime is present. Solid line stands for the standardized expansion coefficient of the leading DJF SLP EOF. The dashed line is the NAO index based on Hurrell dataset.

3 Oceanic data assimilation for climate studies and seasonal prediction

The ocean data assimilation project at CERFACS spans three main research activities: (1) the development of a variational data assimilation system (OPA_VAR) for the OPA ocean general circulation model; (2) the application of OPA_VAR to produce ocean analyses over extensive periods and the evaluation of these analyses to examine key features of the ocean mean state and variability; (3) the application of the ocean analyses to initialize coupled models for climate prediction and predictability studies on seasonal time scales.

The EC-FP5 project ENACT on enhanced ocean data assimilation and climate prediction (2002–2005) is providing a coordinated European framework for developing and evaluating the OPA_VAR system. The complementary EC-FP5 project DEMETER (2001–2004) has been the focus of the seasonal prediction activities at CERFACS, in particular for assembling the coupled model OPA-OASIS-ARPEGE and for evaluating its forecast performance initiated from non-assimilated (control) ocean analyses.

This chapter summarizes the main developments in each of the three areas mentioned above.

3.1 Development of an ocean data assimilation system

3.1.1 Development of 3D-Var and 4D-Var systems for OPA (A. Weaver, N. Daget, E. Machu, A. Piacentini, S. Ricci)

The OPA_VAR developments are separated into two main streams: incremental versions of (1) three-dimensional variational assimilation (3D-Var - FGAT) and (2) four-dimensional variational assimilation (4D-Var). The incremental 3D-Var and 4D-Var systems are complementary since the basic elements used in 3D-Var are also needed in 4D-Var. The principal difference between the 3D-Var and 4D-Var is in the linear model used to describe how the increments to the model state at initial time evolve within the assimilation window. In 3D-Var the approximation is made that changes in the model initial state persist for the duration of the assimilation window, while in 4D-Var changes at initial time are translated to changes at later times in the window by the tangent-linear model. The other elements of the OPA_VAR system (i.e., observation operators, background- and observation-error covariance matrices, etc.) are shared by both 3D-Var and 4D-Var. The 3D-Var is computationally much less expensive than 4D-Var and therefore is potentially more practical for global and/or high resolution applications such as those being developed for MERCATOR. 3D-Var also provides an important reference for evaluating the cost benefits of 4D-Var.

The OPA_VAR has been developed for the global (ORCA2) configuration of OPA version 8.2. The global system has been built from prototype 3D-Var and 4D-Var systems that were originally developed and extensively validated for a tropical Pacific configuration of OPA version 8.1 ([GLO13], [GLO11]). The tropical Pacific configuration has also been made available with the new source code. This simpler configuration has been an invaluable tool for testing many of the new developments to the system before their implementation in the global model.

During the last two years, major improvements were made in the representation of the background error covariances. These are described separately in the next section. Improvements to the assimilation system were also made in other areas. A digital filter has been included as a weak constraint in the 4D-Var cost function in order to penalize high frequency oscillations (internal gravity waves) in the solution trajectory [GLO56]. A more efficient minimization algorithm based on a preconditioned conjugate gradient method has been implemented in collaboration with the ALGO team. The observation interface has been generalized to allow for the assimilation of salinity data, altimeter data and SST data [GLO38] and to enable the observations to be identified by instrument type (buoy, XBT, floats,...) and geographical position so that they can be assimilated with possibly different observation operators (e.g., daily mean or point measurements) and error characteristics. Significant effort has also been devoted to adapting the assimilation system and job scripts to run on different platforms (IBM at ECMWF; Compaq at CERFACS) and to produce various diagnostics and output required for ENACT. The innovations (observation-minus-background) and residuals (observation-minus-analysis) generated by the assimilation system are now stored directly in the original ENACT *in situ* data file to facilitate the evaluation and inter-comparison of the assimilation products. All model fields are stored as averages over calendar months and selected fields are stored at higher frequency for more detailed analysis as required by the ENACT common diagnostics procedure. Also, model restart files can be stored at the end of each calendar month for initializing seasonal forecasts.

3.1.2 Background-error covariance modelling (A. Weaver, E. Machu, S. Ricci)

The background-error covariances play a vital role in both 3D-Var and 4D-Var. They are important for determining how information is effectively extracted from the data and for ensuring that the analysis increments are both smooth and balanced. This an area of the data assimilation system where important theoretical and practical advances have been made in the last two years.

In particular, the development of a very general framework for constructing auto-correlation models that are practical for high-dimensional ($> 10^6$ elements) variational assimilation systems has been continued. The basic algorithm is based on the application of a generalized diffusion (GD) operator ([5]) to effect the smoothing action of a correlation operator. The GD operator can be used to generate very general correlation structures (inhomogeneous, anisotropic, nonseparable). Both “time”-explicit and “time”-implicit versions of the algorithm have been developed and tested ([GLO33], [3]). Implicit schemes have the advantage of extending the range of functional forms permitted by the correlation model and of potentially significantly reducing the numerical cost of the algorithm. In collaboration with the ALGO team, the use of iterative techniques as an efficient way of applying an implicit GD operator is being explored.

Other major improvements to the covariances were made by including multivariate constraints between background errors in temperature (T) and salinity (S) [GLO68], sea surface height (SSH) and density, and density and currents. The constraints encompass linear or linearized (state-dependent) relationships based on T-S conservation, the hydrostatic approximation, dynamic height and geostrophy (with a high-order geostrophic relation applied near the equator). An example of the multivariate covariance structures between SSH and the other state variables is given in Fig. 3.1. These covariance structures can be interpreted as the analysis increment (up to a proportionality constant) that would be generated by assimilating a single altimeter observation using 3D-Var. The increment is physically sensible: a positive SSH innovation (observation-minus-background) is associated with a positive T increment in the thermocline, a dipole-like S increment centred at the depth of the background salinity maximum, and an eastward geostrophic current increment.

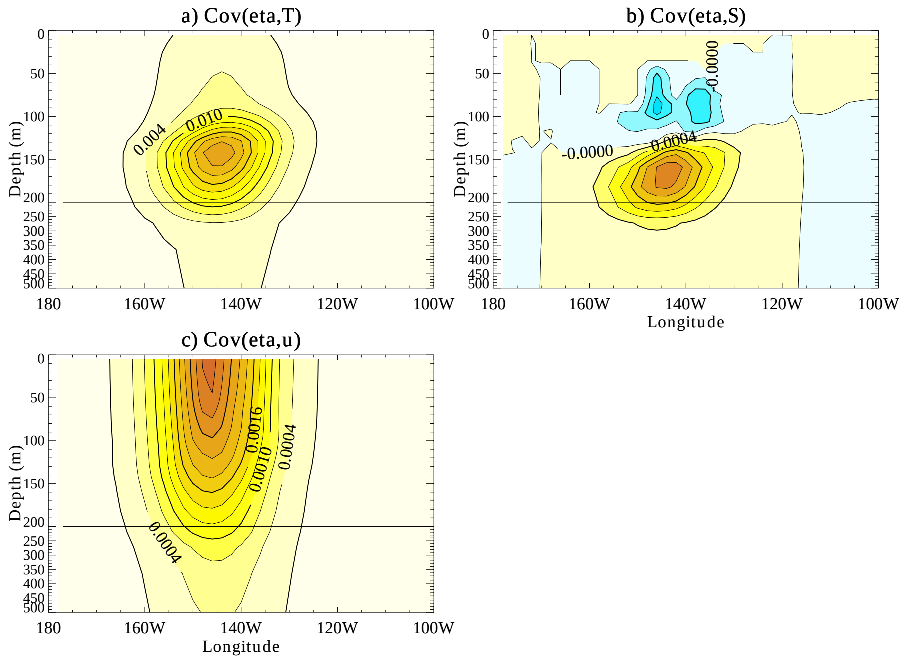

Figure 3.1: Depth section at the equator of the background error covariance between SSH and temperature (upper left panel), SSH and salinity (upper right panel), and SSH and the zonal component of velocity (lower left panel).

A state-dependent parameterization of the background temperature error variances has also been derived to allow the largest variances to be focussed in regions where the local thermal variability is strongest. This parameterization was inspired from earlier 4D-Var experiments ([GLO13]) where the dynamically-evolved background-error standard deviations in 4D-Var tended to be largest near the level of the thermocline where vertical temperature gradients are a maximum (Fig. 3.2).

3.2 Production and evaluation of ocean analyses

3.2.1 Tropical Pacific ocean analyses (A. Weaver, S. Ricci)

Extensive sets of analyses over the period 1993-98 have been produced routinely with different versions of the 3D-Var and 4D-Var systems for the tropical Pacific configuration ([GLO13], [GLO11], [GLO68]). In these experiments *in situ* temperature data from an ECMWF quality-controlled version of the GTSPP data-set were assimilated. Figure 3.3d illustrates the impact of the improved multivariate, flow-dependent covariance model in 3D-Var on the climatology of the equatorial surface currents. For comparison, Fig. 3.3c shows the same climatology for a 3D-Var experiment with the original univariate, flow-independent covariance model, and Fig. 3.3a shows the observed climatology from [2]. A notable feature in Fig. 3.3c is a large eastward bias in the equatorial surface currents that develops in the univariate analyses (although the model temperature state - the assimilated variable - is greatly improved by assimilation). The main impact of the improved covariances in 3D-Var is to eliminate this eastward bias and bring the currents much closer to the observed climatology. It is interesting to note that the surface currents in a 4D-Var experiment (Fig. 3.3b) with the original (univariate) covariance model are also much improved over the corresponding (univariate) 3D-Var experiment, illustrating the benefits of employing the tangent-linear model as a dynamical constraint

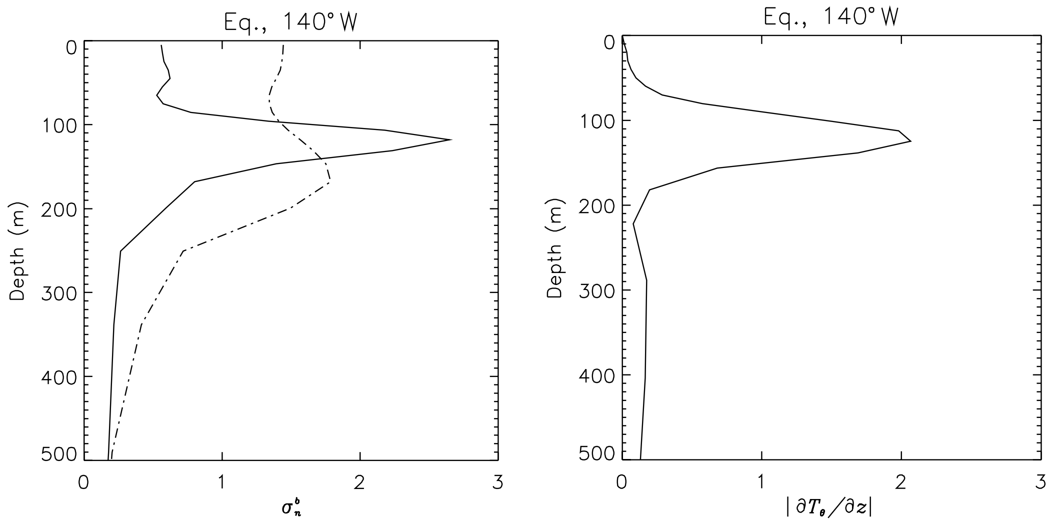

Figure 3.2: Left panel: vertical profiles of the background-error standard deviations (in $^\circ$C) used in 3D-Var and 4D-Var at the equator at 140°W. The dashed-dotted curve corresponds to the standard deviations specified at the beginning of the assimilation window. In 3D-Var, these are also the effective standard deviations used at all future times within the window. The solid curve corresponds to the effective standard deviations used implicitly in 4D-Var at the end of the 30-day window in a particular cycle of 4D-Var. Right panel: the corresponding profile of the background $|\partial T/\partial z|$ at this location. The values of $|\partial T/\partial z|$ have been multiplied by a factor of ten in order to be plotted with the same horizontal scale as in panel a.

in the analysis step. The impact of the improved (multivariate, flow-dependent) covariance model in 4D-Var remains to be evaluated, but one can anticipate even greater improvements than those seen in Figs. 3.3b and 3.3d.

3.2.2 Global ocean analyses (Ph. Rogel, A. Weaver, N. Daget, S. Ricci)

A 10-year set of 3D-Var global ocean analyses (1990-99) has been produced with the DEMETER version of the ORCA2 configuration used at CERFACS. The assimilated data-set is the ECMWF GTSPP *in situ* temperature observations and the surface forcing fields are from ERA-40. As expected, the variance of interannual temperature anomalies is significantly improved compared to that of the control (no data assimilation) experiment, leading to a better agreement with *in situ* observations. In the Pacific, the variability patterns are similar to those in the control but the amplitude is increased, partly because the mean temperature state has a steeper thermocline gradient. Furthermore, substantial improvements in the temperature variability in the tropical Atlantic Ocean and, to a lesser extent, in the tropical Indian Ocean are observed.

The new developments to the background error covariances have also been shown to have had a significant positive impact on the quality of the global ocean analyses, particularly in the representation of salinity and equatorial currents (model fields not directly constrained by the data), compared to analyses produced using the previous univariate, state-independent covariance formulation ([3]). This is clearly illustrated in Fig 3.4, which shows a depth section along the equator of the 1990-99 mean salinity state in the global

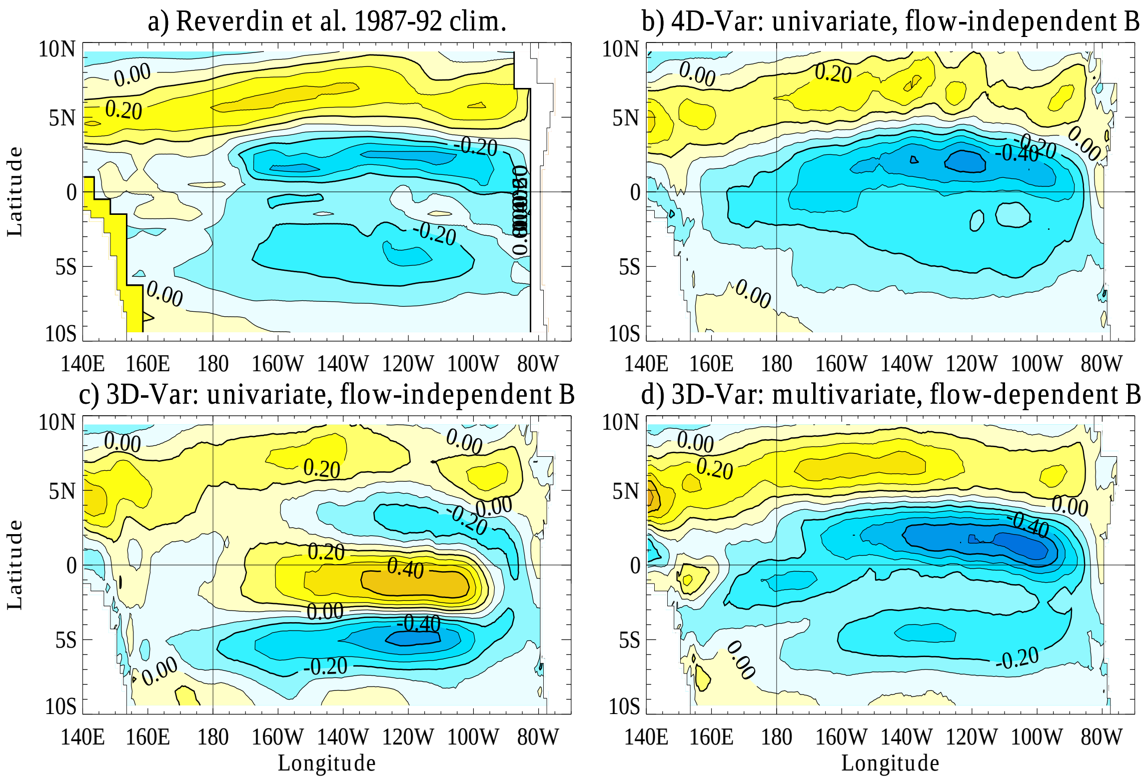

Figure 3.3: a) Observed climatology [2]. Climatologies from assimilation experiments with the tropical Pacific model using existing and improved formulations of the background error covariances: b) 4D-Var with univariate, flow-independent covariances; c) 3D-Var with univariate, flow-independent covariances; d) 3D-Var with multivariate, flow-dependent covariances. The contour interval is $0.1\mathrm{ms}^{-1}$, and the shaded blue (yellow) regions indicate westward (eastward) currents.

model from two experiments with 3D-Var assimilation of *in situ* temperature data: one experiment employs a univariate, state-independent covariance matrix while the other employs a multivariate, state-dependent covariance matrix. The effect of the improved covariances is to maintain realistic vertical salinity gradients while conserving the improvements to the temperature state brought by assimilating the *in situ* temperature data.

The main ocean analysis production for the global model is being carried out within the ENACT framework. ENACT employs input fields and a spin-up and climatological relaxation strategy different from those used above within the DEMETER framework (higher quality and additional observational data-sets, different ERA-40 products,...), and which is common to all partners in the project. Analysis production with 3D-Var and 4D-Var versions of the assimilation system has recently started for the period 1987-2001.

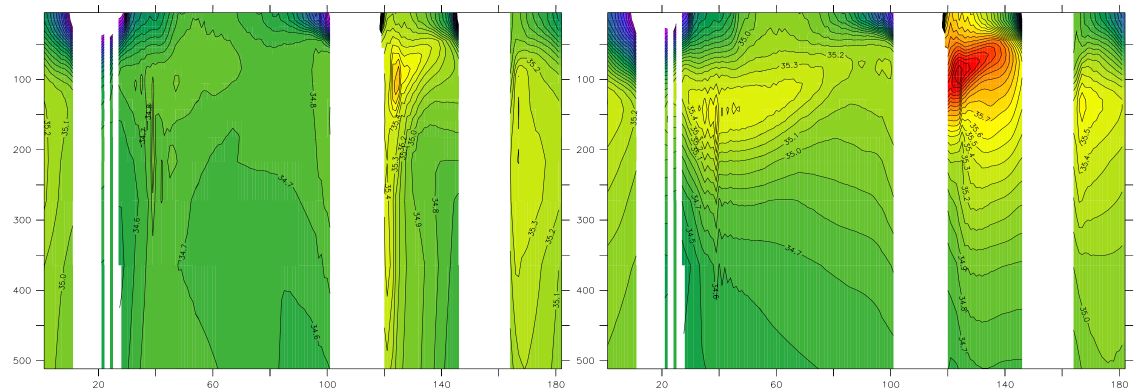

Figure 3.4: Depth section at the equator of the 1993-99 mean salinity state in the global OPA model (ORCA2) produced from 3D-Var assimilation of *in situ* temperature data. Left panel: 3D-Var with univariate, flow-independent covariances; Right panel: 3D-Var with multivariate, flow-dependent covariances.

3.3 Seasonal Prediction

3.3.1 Introduction

Seasonal prediction aims at taking advantage of possibly predictable statistical properties of the atmosphere at seasonal time scales. An important part of this predictability is potentially due to interactions with slow varying components of the climate system, in particular the upper ocean whose thermal inertia and dynamical time scales can influence the atmosphere. They can at least partially explain some climate anomalies, in the tropics, but also at mid-latitudes and over the European area, such as a colder-than-usual winter, or a warm summer.

3.3.2 The coupled seasonal climate prediction system (Ph. Rogel, E. Maisonnave, N. Daget)

A series of coupled seasonal hindcasts has been produced and archived at ECMWF for the period 1980-2001. The ocean initial conditions (ICs) have been obtained by running the ORCA2 model in forced mode. After a spin-up, during which the model remained close to climatology, the model was forced with ERA40 daily fluxes, winds, and with a 200 W/m^2/°C restoring SST term. The strategy used to produce perturbed ensembles of ocean ICs uses one set of daily wind perturbations and four sets of SST perturbations provided by ECMWF.

Additional developments have been carried out to produce ensembles of global ocean initial conditions in the presence of ocean data assimilation. In particular, in order to preserve the same general procedure for perturbing the ocean state, and also to avoid inconsistencies between the perturbed SST and the observed temperature in the subsurface, sets of perturbed observations were constructed that preserve the shape of the mixed layer by interpolating the SST perturbations onto the observed locations. From these sets of perturbed observations, ensembles of perturbed ocean 3D-Var analyses have been produced. This strategy was shown to create higher amplitude perturbations even at the thermocline level.

The forecast model couples the atmosphere model from CNRM (ARPEGE), the ocean model from LODyC (ORCA2) through the OASIS coupler. ARPEGE is initialised from ERA40.

Hindcasts have been produced from 1980 to 2001 following the DEMETER standards (6-month lead, 9 members, initialised in February, May, August and November). More details of the system developed for DEMETER can be found in [GLO69] and [GLO70], see also [1].

3.3.3 Some results of the system (Ph. Rogel)

3.3.3.1 The tropics

As an illustration of the model's ability to predict important climate features, Fig. vii (in the appendix) shows the prediction i of the peak phase of the 1997 ENSO event. The maximum phase is correctly simulated, though its amplitude is slightly underestimated. Figure viii (in the appendix) shows the prediction of the season-averaged temperature one month in advance, and shows that the ensemble almost always includes the actual anomaly, especially during the 1997 event. The ability of the model to predict the major interannual phenomenon is also confirmed by looking at other time-scales (monthly anomalies), other variables (especially atmospheric pressure and precipitation in the tropics), but also subsurface temperature anomaly.

3.3.3.2 The extratropics

In general, a good tropical skill is necessary for improving seasonal prediction over the globe, but not sufficient. It appears, as shown in Fig. x in the appendix, that winter prediction (e.g. temperature, but also precipitations) over Northern Hemisphere, and particularly over Europe, is one strength of the CERFACS model. Indeed, RPSS (shown in Fig. x in the appendix), which represents a rather rigorous test over these regions, is positive, which is not the case for all models (except for the multi-model). This is confirmed by all other scores (ACC, ROC, Value). On the other hand, summer predictions over the same region are clearly a weakness of the model. Again, RPSS corroborate results obtained with other scores, and results over the whole northern subtropics are in agreement.

3.3.4 Contribution of the CERFACS prediction system to the DEMETER multi-model (Ph. Rogel)

In the framework of DEMETER, comparison of several models is possible. In particular, comparison of CERFACS, CNRM and LODyC results brings some interesting features as theses models have common components. For example, in the tropics, CERFACS and CNRM results are rather close, with slightly better ACC scores for CERFACS during the first 4 months, and the reverse for months 5 and 6. A possible explanation is the smoother process by which perturbations in SST are introduced. In the northern subtropics, scores favour significantly CERFACS versus CNRM, though the atmosphere model (which is thought to be the most important component for these regions) is rigorously the same, as well as the atmospheric initial conditions. It is possible that the coupled model drift, which is significantly different between models, may have a substantial impact on the variability.

[1] T. N. Palmer and co authors, (2004), Development of a European Multi-Model Ensemble System for Seasonal to Inter-Annual Prediction (DEMETER), *Bull. Amer. Meteorol. Soc.*, **In press**.

[2] G. Reverdin, C. Frankignoul, E. Kestenare, and M. J. McPhaden, (1994), Seasonal variability in the surface currents of the equatorial Pacific, *J. Geophys. Res.*, **99**, 20323–20344.

[3] S. Ricci, (2004), *Assimilation variationnelle océanique: modélisation multivariée de la matrice de covariance d'erreur d'ébauche*, PhD thesis, Université Paul Sabatier (Toulouse III).

[4] A. T. Weaver and P. Courtier, (2001), Correlation modelling on the sphere using a generalized diffusion equation, *Q.J.R. Meteorol. Soc.*, **127**, 1815–1846.

4 OASIS and PALM couplers and applications

Coupling numerical models is a central issue in the climate research community and in other research fields such as electromagnetism and computational fluid dynamics.

The OASIS coupleur has been designed to exchange coupling fields between climate component models and to perform the transformations and 2D interpolations needed to express, on the grid of the target model, the coupling fields produced by the source model.

The PALM coupleur has been designed to implement a general tool allowing to easily integrate high-performance computing applications in a flexible and extensible way. This dynamic coupler has originally been designed for oceanographic data assimilation algorithms, but its application domain extends to every kind of scientific applications.

4.1 The OASIS coupler

Most of the developments on the OASIS coupler have been done within the framework of the EC-FP5 PRISM project. During PRISM first year, CERFACS coupler OASIS 2.4 has been improved and a new version, OASIS3, has been released. The development of a new coupler, OASIS4, involving a global rewriting of the coupler, started in parallel.

4.1.1 Development of the OASIS3 coupler (S. Valcke, D. Declat)

The main improvements of the OASIS3 coupler [GLO80] are the following:

- A global rewritting of the memory management using F90 dynamic allocation;
- A new communication library based on MPI1;
- New interpolation functionality, based on the Los Alamos National Laboratory SCRIP 1.4 library;
- A flexible PRISM System Model Interface Library (PSMILe) for coupling and I/O. The coupling functionality is based on the OASIS communication library using MPI1 or MPI2. PSMILe allows a standard parallel communication with OASIS3 or directly between models having same decomposition and same grid. PSMILe also offers I/O functionality (inputs/outputs from/to disk files) and automatically behaves according to the user's choices specified in OASIS3 configuration text file *namcouple* (coupling or I/O mode, coupling or I/O frequency, local transformations, etc.).

OASIS3 has been adapted to PRISM common directory structure and standard compilation environment. OASIS3 was presented and ready for hand-on exercises in 2003.

4.1.2 Development of the OASIS4 coupler (S. Valcke, D. Declat)

During PRISM second year, the rewriting of the coupler to produce OASIS4, which specifications were established in 2003 [GLO81], summoned up the greatest part of coupler development efforts. The following aspects have been developed:

- A new PSMILe library, for coupling and I/O, now including parallel repartitioning between models having the same grid but different decompositions. A new aspect is the inclusion in the PSMILe of the interpolation neighbour search, based on an efficient parallel multigrid 3D algorithm; the results of the search are transferred to the Transformer;
- A Driver, handling the process management and the coupled model monitoring;
- A Transformer, acting as a buffer and performing the interpolation *per se*;
- An XML (Extensible Markup Language) environment. Each model comes with its "Application Description" (AD) and with the Potential Model Input and Output Description (PMIOD) of its model component(s). In the composition phase, the user generates the Specific Coupling Configuration (SCC) file and, for each component model, the Specific Model Input and Output Configuration (SMIOC). At run-time, the different parts of the system act accordingly to the user specifications provided in the SCC and SMIOCs XML files.

An OASIS4 prototype, including the main parts of the coupler, is now available. The OASIS4 final version, which will offer more sophisticated interpolation schemes, improvement in the PSMILe parallel neighborhood search, and parallelisation of the Transformer, is due at the end of PRISM in December 2004.

4.1.3 Users and applications

Today, OASIS is used regularly by about 20 research groups for ocean-atmosphere coupling in Europe (France, Germany, UK, Belgium, Sweden, Norway) but also in the USA, Japan and Australia. OASIS3 will be used in the PRISM demonstration runs, which will imply about 10 different coupling configurations based on a number of state-of-art atmosphere, ocean, sea ice, atmospheric chemistry, and marine bio-geochemistry component models, and 4 different computing platforms (NEC SX6, SGI IRIX64, Fujitsu VPP5000, IBM Power4).

4.2 The PALM coupler

4.2.1 Support and Training for the PALM_RESEARCH product (S. Buis, T. Morel, A. Piacentini)

The PALM_RESEARCH sofware (Fortran 90 programming, SPMD - Single Program Multiple Data paradigm, MPI1 message passing library) has been delivered at the end of 2001. This product is used in the MERCATOR project. Its use is free for research purposes and is encouraged for the MERCATOR-related assimilation activities.
The PALM project is thoroughly presented on the web site: `http://www.cerfacs.fr/~globc`.
The software is provided with an installation guide and a user guide. The user guide includes a tutorial to go progressively through all the features of the PALM prototype and of its graphical interface PrePALM.
A three day training session can be provided if necessary. Four sessions were organized in 2002 and 2003 for a total of forty trained people.
The PALM team provides a constant user support for the PALM products. The mail address `palmhelp@cerfacs.fr` can be used by all users to contact the PALM team.

PALM_RESEARCH release is still improved. In particular spatial interpolation tools for geophysical data and the possibility to combinate boxes have been added to the algebra tool box [GLO51] [GLO64]. The PALM users' community is now spured to use the PALM_MP release instead of PALM_RESEARCH to take advantage of the new functionalities and the improvements on memory management. The change to this new release is transparent for the source developped by the users, due to an upward compatibility of the latest release of PALM.

4.2.2 Implementation of the final version (E. Gondet,S. Buis, T. Morel, D. Déclat, N. Barriquand)

The last two years main activity of the PALM team was the development of a MPMD release of the coupling software PALM called PALM_MP. This one is based on MPI2 which provides communications between independant processes. On the contrary of the MPI1 standard which is used on the SPMD release of PALM, the MPI2 standard, now available on most common platforms using native or public implementation such LAM, allows a better memory management and leads to an higher and clearer independence between sources which have to be coupled. In concrete terms, although some main parts of the previous PALM kernel as the management of the distributed objects have been re-used, PALM_MP Kernel was largely rewritten. The crucial part of this new kernel is the scheduler which manages and allows the good behaviour of simultaneous and independant processes. The scheduler is based on the MPI2 ports and a new scheme of communication have been set in order to improve performances [GLO90]. The main PALM_MP new features are the introduction of the sub-object concept which allows to pick up only a part of an object, the possibility for the users to use C/C++ languages as well as FORTRAN77 and 90 to develop their own PALM units, and a more flexible temporal management of objects. At the same time, tools for real-time supervision has been developped. At present, the first tests on concrete assimilation data cases are in progress.

4.2.3 Development of a PALM breadboard (A. Piacentini, S. Buis, T. Morel, S. Massart, A. ElAkkraoui, N. Chapelon, O. Pannekoucke)

The development activity was accompanied by an extensive testing of the new code. With the aim of testing the flexibility, the performances and the portability of the PALM software and of its interface PrePALM, a bench case has been designed. It is based on a 2D shallow water nonlinear model and it makes use of its linear tangent and adjoint versions. The models have been developed and set into the PALM formalism. These models have been used to implement a 3D-Var and a 4D-Var assimilation scheme. Starting from these assimilation schemes, the bench case has been improved and it includes now twelve different cases implementing the 3D-Var, the 3D-FGAT, the 3D-PSAS, the 4D-Var, the incremental 4D-Var methods with different minimizers. This bench case is the base of the development of an advanced tutorial for the PALM applications in data assimilation [GLO52].

4.3 Applications

4.3.1 PALM applications

4.3.1.1 Data assimilation for atmospheric chemistry (S. Massart, T. Morel, D. Cariolle)

The EC-FP5 ASSET project brings the atmospheric chemistry community together around chemical data assimilation issues. The first step was to develop an incremental variational assimilation scheme called 3DFGAT, that takes into account the time of observations but does not consider the dynamic of the phenomenon. The analysis of such method depends largely on the description of background and observations error covariance matrix. The use of an univariate analysis (no correlation between ozone fields

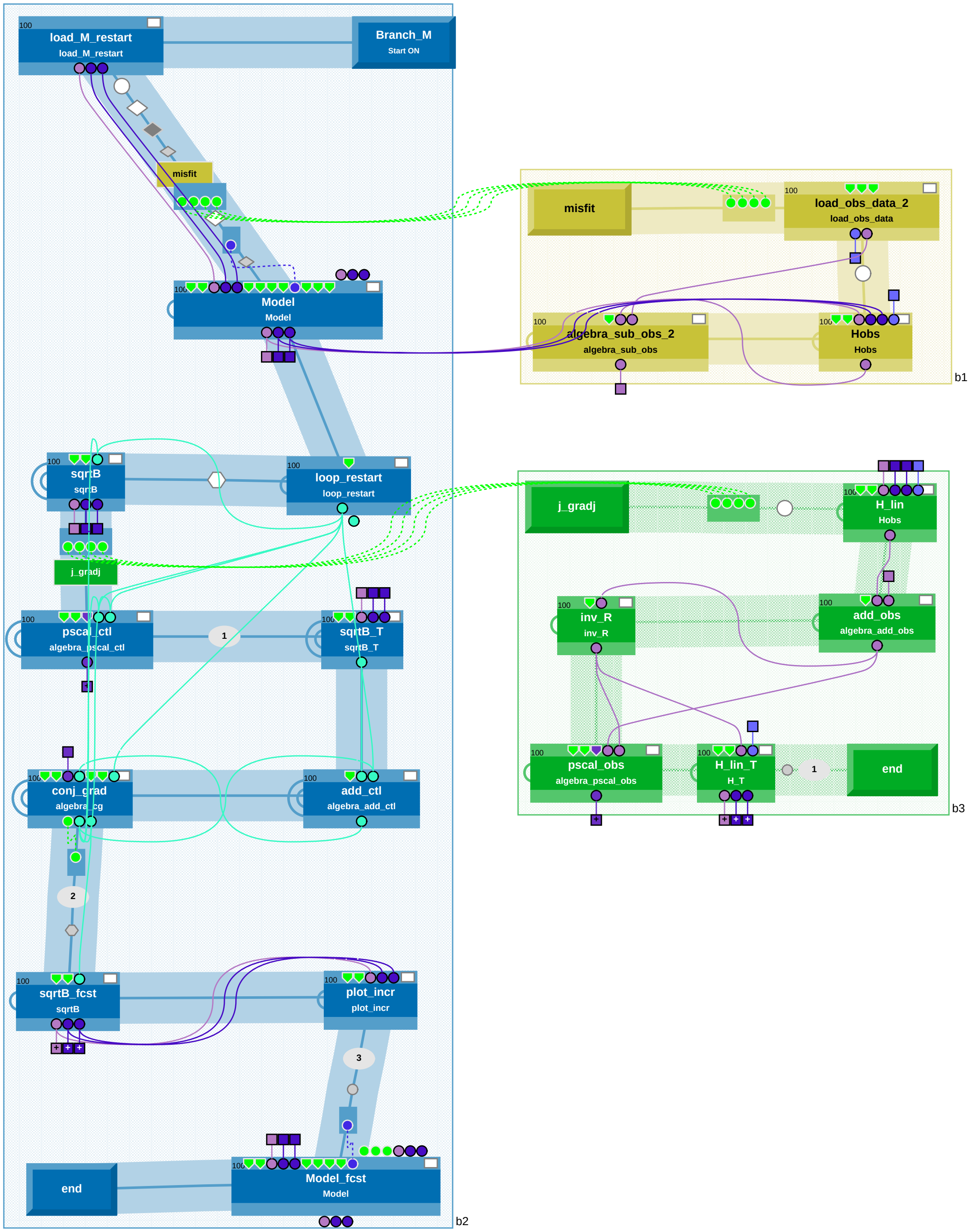

Figure 4.1: The 3D-FGAT method as seen through the PrePALM_MP interface

and other species or meteorological fields) provides an increment of ozone that is spread with a diffusion equation included in the background error covariance matrix [5].
Beyond these achievements, prospective efforts have been made, through several meetings, in order to have PALM recognized as a standard tool for atmospheric chemistry data assimilation.

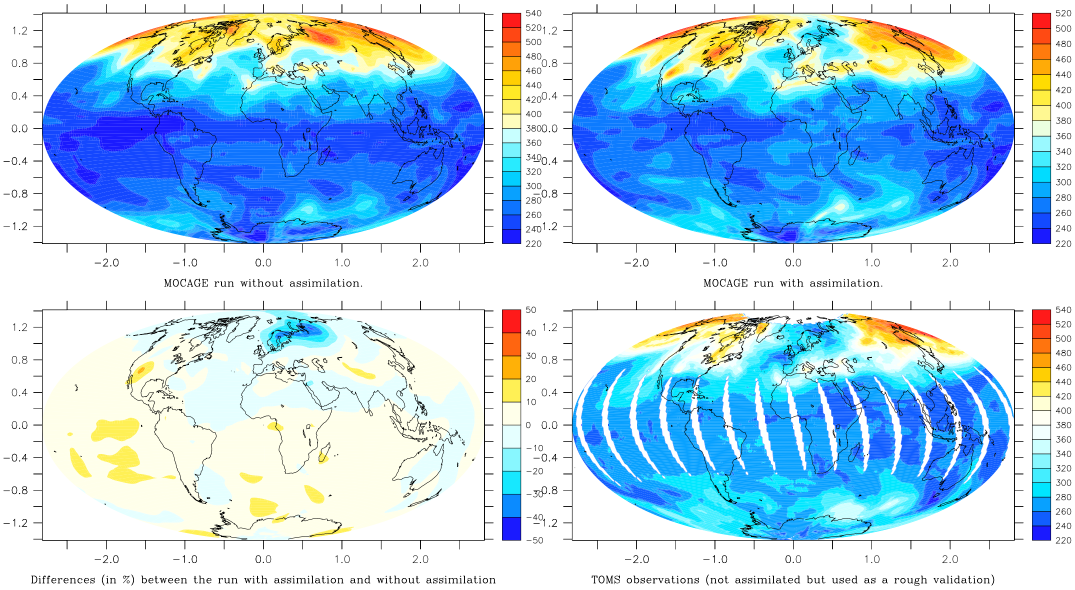

Figure 4.2: Total ozone field on March 2nd, 2000, 0 UT : (a) simulated by MOCAGE, without assimilation ; (b) simulated by MOCAGE with assimilation of March 1st, 2000, GOME ozone profiles. (c) Total ozone column relative differences (in %) between the MOCAGE run with assimilation and without assimilation of the GOME ozone profiles. The differences are produced after one day of assimilation, for March 2nd , 2000, at 0 UT. (d) Total ozone column measured by TOMS at local noon on March 1st, 2000. TOMS observations are not assimilated but used as a rough validation of the assimilating algorithm.

4.3.1.2 Data assimilation for neutronics (S. Buis, S. Massart)

Since a few years, EDF is interested in data assimilation in different fields, such as atmospheric chemistry or concrete delayed behaviors of nuclear power plants [GLO16]. The ADONIS project, created in January 2004, is aimed at evaluating the interest of data assimilation methods in neutronic simulation. Models for simulating the nuclear core of nuclear plants, and observations of the state of this core such as neutron flux or water temperature, both provided by EDF, are being complemented by assimilation methods developed by CERFACS using the PALM software.

4.3.1.3 Data assimilation in MERCATOR project (S. Buis, T. Morel)

PALM is the platform which has been chosen by MERCATOR in order to perform data assimilation. One of the advantage of PALM is that it allows for easy changes or connections of schemes in different configurations. These configurations, PSY1 and PSY2, are compatible, and use the same PALM interface. PALM units have been split in order to optimize the treatments.

4.3.1.4 Application to Numerical Weather Prediction (S. Buis, T. Morel)

The PALM group is involved in a scientific and technical collaboration with SMC (Service Météorologique du Canada) aimed to set the basis for the use of PALM in the next operational forecast/assimilation suite. As a counterpart, SMC will take part in some specific development of the final versions of PALM and will insure the porting to the supercomputers installed at SMC.

[5] A. T. Weaver and P. Courtier, (2001), Correlation modelling on the sphere using a generalized diffusion equation, *Q.J.R. Meteorol. Soc.*, **127**, 1815–1846.

5 SMOS Mission

E. Anterrieu, B. Picard

5.1 Introduction

Synthetic Aperture Imaging Radiometers (SAIR) are powerful instruments for high-resolution observation of planetary surfaces at low microwave frequencies. Within the frame of the SMOS space mission, a project led by the European Space Agency and devoted to the remote sensing of Soil Moisture and Ocean Salinity from a low orbit platform, the work was focussed on the reconstruction of radiometric brightness temperature maps from interferometric measurements. It has been demonstrated that the corresponding inverse problem is not well-posed, unless a regularizing constraint is introduced in order to provide a unique and stable solution. Three methods for the regularization of the inverse problem have been proposed. The corresponding solutions have been analyzed and the links between their physical and mathematical meanings established.

5.2 Direct problem

SAIR devoted to Earth observation measure the correlation between the signals collected by pairs of spatially separated antennae A_k and A_l which have overlapping fields of view, yielding samples of the visibility function $V(\mathbf{u})$, also termed complex visibilities, of the brightness temperature map $T(\xi)$ of the observed scene. The relationship between $V(\mathbf{u})$ and $T(\xi)$ is given by a spatial Fourier-like integral:

$$V(\mathbf{u}_{kl}) \propto \frac{1}{\sqrt{\Omega_k \Omega_l}} \iint\limits_{\|\xi\|\leq 1} F_k(\xi)\overline{F}_l(\xi)T(\xi)\widetilde{r}_{kl}(\frac{-\mathbf{u}_{kl}\xi}{f_o})\,\mathrm{e}^{-2\mathrm{j}\pi\mathbf{u}_{kl}\xi}\,\frac{\mathrm{d}\xi}{\sqrt{1-\|\xi\|2}}\,. \tag{5.1}$$

The components $\xi_1 = \sin\theta\cos\phi$ and $\xi_2 = \sin\theta\sin\phi$ of the angular position variable ξ are direction cosines (θ and ϕ are the traditional spherical coordinates), $\mathbf{u}_{kl}$ is the spatial frequency associated with the two antennae A_k and A_l, $F_k(\xi)$ and $F_l(\xi)$ are the normalized voltage patterns of the antennae with equivalent solid angles Ω_k and Ω_l, $\widetilde{r}_{kl}(t)$ is the fringe-wash function which accounts for spatial decorrelation effects, $t = \mathbf{u}_{kl}\xi/f_o$ is the spatial delay and f_o is the central frequency of observation.
Denoting by ℓ the number of antennae of the instrument, the number of complex visibilities provided by the interferometer is equal to $\ell(\ell-1)/2$ when accounting for the hermitian property of Equation (5.1). Since SAIR have limited dimensions, the spatial frequencies $\mathbf{u}_{kl}$ sampled by an interferometer are confined to a limited region of the Fourier domain: the experimental frequency coverage H. In the case of SMOS the visibility samples are obtained from raw data inside a star-shaped window over an hexagonally sampled grid $\mathbb{G}_\mathrm{u}$ in the Fourier domain. For computation purposes, numerical quadrature is used to represent integral (5.1) as a summation over n^2 integrand samples, here the n^2 pixels of the spatial grid $\mathbb{G}_\xi$ (the dual grid of $\mathbb{G}_\mathrm{u}$).

5.3 Inverse problem

The inverse problem aims at inverting the discrete version of relation (5.1) to retrieve a brightness temperature map T from the complex visibilities V, i.e. solving the linear system:

$$\mathbf{G}T = V, \tag{5.2}$$

where $\mathbf{G}$ is the discrete linear operator from the object space E into the data space F describing the basic relation (5.1). Since the direct problem is stated via an integral equation, the inverse problem does not usually have a straightforward solution. Moreover, since the dimension of the object space E (here the n^2 pixels used to sample T) is often larger than the dimension of the data space F (the $\ell(\ell-1)/2$ samples of V), the linear system (5.2) is an underconstrained problem with multiple solutions for T. The minimum of the least-square criterion

$$\min_{T\in E} \|V - \mathbf{G}T\|_F^2, \tag{5.3}$$

which is also the solution of the normal equation $\mathbf{G}^*\mathbf{G}T = \mathbf{G}^*V$, is therefore not unique because the square matrix $\mathbf{G}^*\mathbf{G}$ is singular. Thus, the inverse problem is ill-posed and has to be regularized in order to provide a unique and stable solution for T.

5.3.1 Tikhonov regularization

A standard approach is to find the brightness temperature map T_r that realizes the minimum of the quadratic functionnal

$$\min_{\substack{T\in E\\ \mu\in\mathbb{R}}} \|V - \mathbf{G}T\|_F^2 + \mu\|T\|_E^2 \tag{5.4}$$

where μ is a Lagrange parameter to be determined. The unique solution of (5.4) is the solution of the Euler equation $(\mathbf{G}^*\mathbf{G} + \mu\mathbf{I})T = \mathbf{G}^*V$. This map could be obtained through the computation of the inverse of the non singular square matrix $\mathbf{G}^*\mathbf{G} + \mu\mathbf{I}$:

$$T_r = \mathbf{G}_\mu^+ V, \tag{5.5}$$

where $\mathbf{G}_\mu^+ = (\mathbf{G}^*\mathbf{G}+\mu\mathbf{I})^{-1}\mathbf{G}^*$. The drawback of this numerical approach is the regularization parameter μ because the determination of its optimal value may raise some difficulties.

5.3.2 Minimum-norm regularization

A second standard approach is to find the minimum-norm solution of (5.2) by means of computing the temperature map T_r that realizes the minimum of the constrained optimization problem

$$\begin{cases} \min\limits_{T\in E} \|T\|_E^2 \\ \mathbf{G}T = V \end{cases} \tag{5.6}$$

This map could be obtained through the computation of the More-Penrose pseudo-inverse $\mathbf{G}^+$ of the rectangular matrix $\mathbf{G}$: $T_r = \mathbf{G}^+V$. Owing to the particular role played by the smallest singular values of $\mathbf{G}$ in the computation of $\mathbf{G}^+$, it is preferable to compute it with the aid of a truncated singular value decomposition rather than with a standard one, so that the regularized minimum-norm solution is now given by:

$$T_r = \mathbf{G}_m^+ V, \tag{5.7}$$

where m indicates the number of singular values discarded prior to inversion. Here again, the drawback of this approach is the choice of the optimal value for m which plays the role of a numerical regularization parameter.

5.3.3 Band-limited regularization

Referring now to a physical concept, namely the limited resolution of SAIR, another approach is to find the temperature map T_r which has its Fourier transform confined to the experimental frequency coverage H. This band-limited solution realizes the minimum of the constrained optimization problem

$$\begin{cases} \min_{T \in E} \|V - \mathbf{G}T\|_F^2 \\ (\mathbf{I} - \mathbf{P}_H)T = 0 \end{cases} \tag{5.8}$$

where $\mathbf{P}_H$ is the projector onto the subspace $\mathcal{E}$ (of E) of the H-band limited functions. The unique solution of (5.8) is given by:

$$T_r = \mathbf{U}^* \mathbf{Z} \mathbf{A}^+ V, \tag{5.9}$$

where $\mathbf{A}^+ = (\mathbf{A}^*\mathbf{A})^{-1}\mathbf{A}^*$ is the More-Penrose pseudo-inverse of the rectangular matrix $\mathbf{A} = \mathbf{G}\mathbf{U}^*\mathbf{Z}$, $\mathbf{U}$ is the Fourier transform operator and $\mathbf{Z}$ is the zero-padding operator beyond H.

5.4 Results

Simulations have been performed for for a Y-shaped array equipped with 3 antennae per arm in addition to the central one, leading to a total number of antennae and receivers $\ell = 10$. The dimension of the hexagonally sampled grids $\mathbb{G}_\xi$ and $\mathbb{G}_\mathrm{u}$ has been fixed to $n^2 = 256$ so that the size of the real-valued matrices $\mathbf{G}$ and $\mathbf{A}$ are 91×256 and 91×73. Provided that the optimal values for μ and m are used, it turns out that the three methods have the same behaviour with regards to the stability of the reconstruction process whatever the amount of input radiometric noise. The main results are summarized in Fig. 1 and concern the links between these three methods.

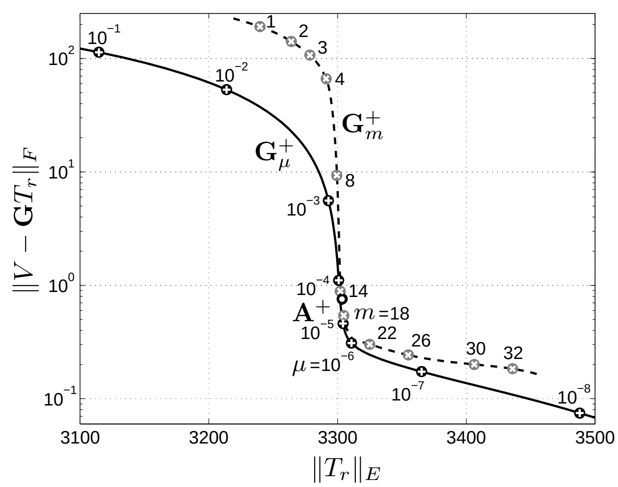

Figure 5.1: Variations of $\|V - \mathbf{G}T_r\|_F$ with $\|T_r\|_E$ for the Tikhonov solution (5.5) with $10^{-8} \leq \mu \leq 10^{-1}$ *(solid line and ⊕)*, the regularized minimum-norm solution (5.7) with $1 \leq m \leq 32$ *(dashed line and ⊗)* and the band-limited solution (5.9) *(○ marker)*.

As predicted by the theory, the plot of $\|V - \mathbf{G}T_r\|_F$ versus $\|T_r\|_E$ for the Tikhonov solution (5.5) with $10^{-8} \leq \mu \leq 10^{-1}$has the shape of the letter L (hence the name of “L-curve”). The optimal value for μ corresponds to the point with maximum curvature because it is the best compromise between approximation error and noise propagation. Here it is about 10^{-6}, however this value may depend on the amount of input noise. The same variations have been reported for the minimum-norm solution (5.7) with $1 \leq m \leq 32$. It is worthy to note that the plot has also a L-shaped behaviour and the maximum curvature point corresponds here to $m = 18$. The number of singular values kept in the inversion is therefore equal to $91 - 18 = 73$ which is exactly the number of non-redundant frequency points in the experimental frequency coverage H. Finally, the same quantities have been reported for the band-limited solution (5.9). It can be observed that this point is also very close to the points corresponding to the optimal values for μ and m, which confirms the link between the three approaches, this one having the advantage to have a physical meaning and to be independant from any regularizing parameter. Moreover, the dimension of the system to be solved is here reduced to the minimum number of unknowns (or degrees of freedom), the number of frequencies in the experimental frequency coverage, while taking into account, in the least-square sense, all the available complex visibilities without averaging the potentially redundant ones.

6 CERFACS contribution to the MERCATOR project

This report, summarizing CERFACS' contributions to the MERCATOR project, appears also as such in the MERCATOR activity report prepared by the Groupement d'Intérêt Public (GIP) MERCATOR-OCEAN.

6.1 Introduction

The Mercator project develops several ocean circulation-modelling and assimilation systems to both serve the international Global Ocean Data Assimilation Experiment (GODAE) and the future French 'Centre d'Océanographie Opérationnelle'. Three main research axis have been selected. The 'Système d'Assimilation Mercator' (SAM) is an essential component of the different ocean prediction systems or prototype systems. The 'Prototype Atlantique et Méditerranée' (PAM) is designed to investigate very high resolution forecasting feasability over a region that has already been widely studied. The 'Prototype Océan Global' (POG) addresses the global objective of *GODAE* and benefits from the previous PAM implementation.

6.2 The Assimilation System SAM (J.M. Lellouche, E. Rémy and B. Tranchant)

The Mercator project adopted a strategy for incremental improvement of data assimilation schemes, i.e., first starting with a well-known method (Optimal Interpolation) and progressively using of more advanced techniques such as SEEK or 4D-VAR [19]. That is why the main characteristic of the Mercator Assimilation Systems (SAM) is the use of the PALM software [GLO28] which is a modular tool for coupling and running ocean configurations and various data assimilation schemes such as OI, SEEK, 3D-VAR or 4D-VAR [19]. Actualy, it provides a general structure for a modular implementation of a data assimilation system.

6.2.1 SAM-1

The first System of Assimilation Mercator (SAM-1) is the reduced-order optimal interpolation scheme SOFA [14] which is able to incorporate both altimeter and *in situ* observations.

6.2.1.1 SAM-1-v1

This first version SAM-1-v1 developped in the Mercator project allows the assimilation of anomalies of the sea level (altimetry) and it is an univariate scheme. It is adapted to the constraints of the scientific computation multiprocessors for the configurations of great dimension like PAM and ORCA-025 (see 6.3 and 6.4).
There are two types of data used in the first system. The assimilated data are altimetric tracks from JASON, ERS and GFO and also a pseudo-data of Mean Sea Surface Height (MSSH) as a reference level for the Sea

Surface Height (SSH) based on the work of [26]. Following [13], for Optimal Interpolation an approximate background error covariance matrix B^f is used, such as:

$$B^f = D^{f^{\frac{1}{2}}} C D^{f^{\frac{1}{2}}} \tag{6.1}$$

where D^f is a background error variances matrix and C a correlation matrix. In SAM-1-v1, a constant 7 cm background error variance has been chosen and the correlation structure for the background (C matrix) has the form of a spatio-temporal bell which varies in shape according to the geographical position [GLO59]. Observation errors are assumed to be decorrelated in space and time. The observation error variances are specified according to the knowledge of instrumental characteristics. So, a 3 cm error is used for JASON and a 4.5 cm error is used for ERS-2 and GFO [GLO59].
The model initialisation is realized by converting the 2D SLA analysis increments into 3D increments of pronostic variables using an algorithm based on the lifting-lowering method [12]. Now, three prototypes (three different ocean model configurations) use this system and run operationaly: PSY1v1 (MNATL 1/3^o), PSY2v1 (PAM 1/15^o), PSY2Gv1 (MiniPOG: ORCA2^o). One prototype is being developped: PSY3v1(POG:ORCA025^o).

6.2.1.2 SAM-1-v2

A second version of SAM-1 has been developped [14], which allows to use multivariate modes on the vertical (1D EOFs). This approach was first explored by [15]. The background error covariance matrix is modelled as:

$$B^f = S^T Br^f S \tag{6.2}$$

The Br^f matrix contains the background error covariances in the reduced space and S^T are the eigenvectors of B^f with S the reduced space simplication operator. Br^f is block diagonal and organized in mode-based block where each one modelled using the OI parametrisation 6.1 [14]. The *estimation* state vector is x=(ψ: barotropic streamfunction, T: temperature, S: salinity), so vertical EOFs are trivariate in these variables. Compared to the previous system, this multivariate scheme assimilates both altimeter data from satellites, *in-situ* (T,S) data from the CORIOLIS database, but also weekly SST and SSS climatology. Since 2003, this multivariate scheme is used operationaly for the MNATL (1/3^o) configuration, named PSY1v2 prototype. It is also being implemented in the PAM (1/15^o) configuration and should be operational in 2004 (PSY2-V2), see section 6.2.2. It should also be implemented into the ORCA2^o configuration (PSY2Gv2) in 2004.

6.2.2 SAM-2

The incremental improvement of data assimilation schemes lead to upgrade the 3D background error modelisation from a sequential point of view. Therefore one needs to use advanced estimation techniques, adapted to the high resolution, using coherent multivariate covariances of error with dynamics.
One of the first step was to use SAM-1-v2, which is built from a simplified algorithm based on OI (observation space) with multivariate **1D** modes. The next generation, named SAM-2, began in 2003 with two main objectives: the development of a multivariate tool built from a SEEK algorithm (modal space) and the use of **3D** multivariate modes. The SEEK (Singular Evolutive Extended Kalman) filter algorithm ([24],[28]), it is a Reduced Order Kalman Filter designed to assimilate altimeter, *in-situ* profile and high resolution surface temperature data.
Because both SAM-1-v2 and SAM-2 are based on the ROEKF (Reduced-Order Extended Kalman Filter) equation, it was interesting to build a tool able to drive both SAM-1-V2 and SAM-2. So,the first step was to develop a software platform (Figure 6.1) able to use both 1D and 3D multivariate modes by using the Reduced Order Optimal Interpolation (ROOI1D and ROOI3D). This ROOI3D case is the first version of SAM-2 and is called SAM-2-v0. This first version uses a global 3D EOFs basis, with a R constant diagonal

matrix. The next step will be to use the SEEK algorithm by using 3D modes from a local 3D EOFs basis, a R non diagonal matrix and an adaptative scheme. To illustrate the first SAM-2-V0 analysis, Figure 6.2 shows the barotropic streamfunction increment calculated after the assimilation of Sea Level Anomalies (SLA) during one week forecast with an *estimation* state vector (ψ,T,S).

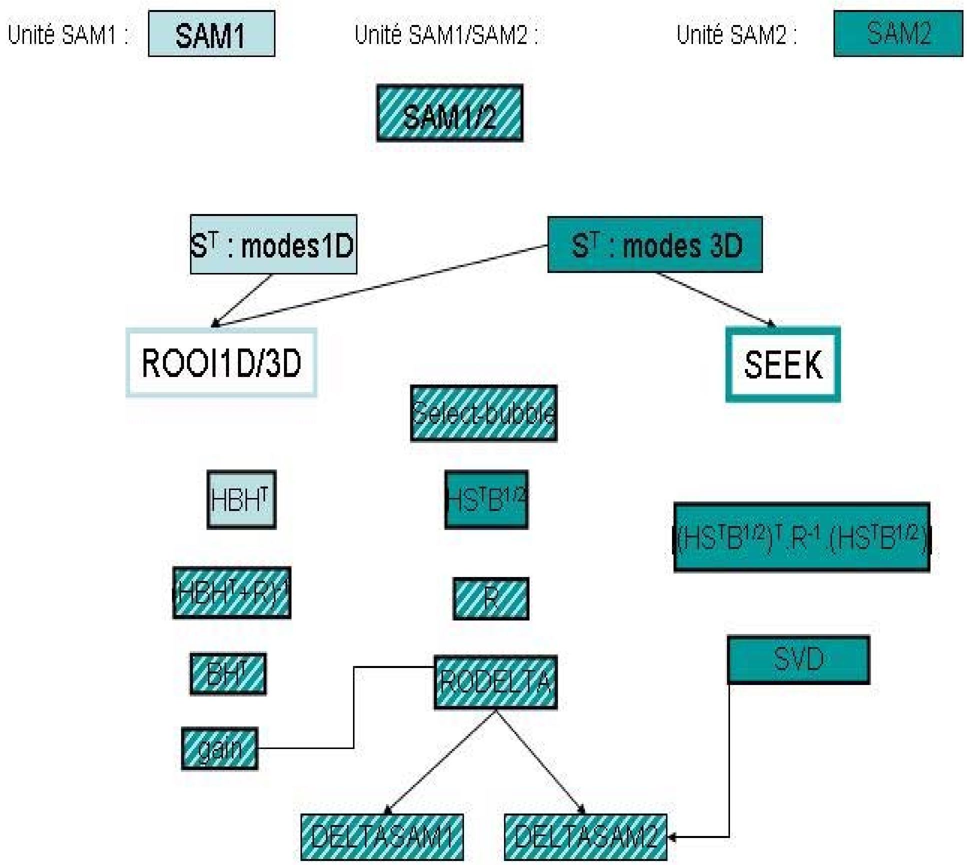

Figure 6.1: Schematic representation of the software platform SAM1/SAM2. SAM1 units (1D background error) and SAM2 (3D background error) are respectively shown in dark green and light green. Common units SAM1/SAM2 are bi-color. Two kinds of algorithm (OI or SEEK) are available depending on the activation of units

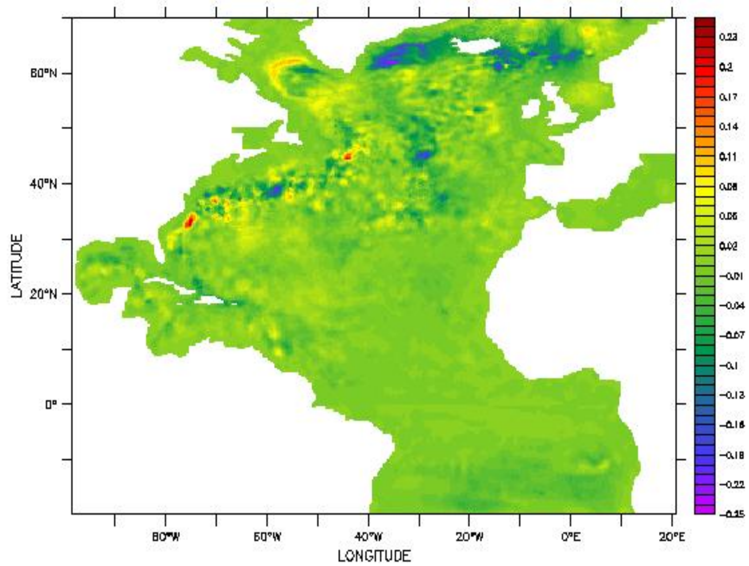

Figure 6.2: Barotropic stream function increment (m) from a multivariate SAM-2-v0 analysis

6.3 The North Atlantic and Mediterranean model configuration PAM and the first operational Prototype System PSY2 (Romain Bourdallé-Badie, Nicolas Daget, Yann Drillet, Jean-Michel Lellouche, Benoît Tranchant and Laure Siefridt)

.

6.3.1 Introduction

The North Atlantic and Mediterranean Mercator configuration PAM is a very high resolution (5 to 7 km) model based on the OPA-8.1 ocean general circulation model [23]. The PAM configuration benefited from the experience gained with the lower resolution (1/3^o) MNATL configuration which has been inherited from the CLIPPER project [11] aiming at simulating the Atlantic basin circulation. MNATL is used as a handy research and development tool and is part of the first Mercator operational system which is used for real time analysis and forecasts since January 17^{th} 2001.

The PAM model configuration was designed in 1998, implemented and tuned in 1999 and 2000. Sensitivity tests have been conducted during the years 2000 and 2001 which are described in [GLO14]. During 2002-2003, PAM model has been improved with the implementation of new parameterizations. Validatation and quantification of the gain between several experiments were also performed , as well as scientific studies about the meso scale and the transport trough North Atlantic straits. At this time around 40 years of simulation with the PAM model have been realized, which represent 10000 h CPU on the Fujitsu VPP5000 and 50 To of output files.

The analysis and forecasting system PSY2 (Prototype SYstem 2) uses the PAM model and the SAM-1-v1 system (see section 6.2.1.1).

6.3.2 Improvements of the PAM model : PAM2 configuration

6.3.2.1 Open boundary condition

MERCATOR develops for GODAE two analysis and forecast ocean systems. The first one is global and has a coarse resolution (1/4°), the second one is regional and has a fine resolution (1/15°). Communication between the global model and the regional one takes place at the southern boundary. The open boundary conditions (OBC) developed in the OPA code by the CLIPPER project allow the evolution of the temperature, salinity and velocity boundaries. The low resolution configuration (MNATL, 1/3°) is useful for performing several experiments with an open boundary condition and for extracting data for the 9° North boundary condition. The results obtained with a low and a high resolution north Atlantic domain show the influence of the open boundary conditions. Nevertheless the results obtained with the low and the high resolution domain are not consistent. Indeed, the overturning and eddy kinetic energy of the low resolution model are clearly improved, which is not so obvious for the high-resolution domain. The use of the open boundary conditions gives much larger improvements to the low resolution simulation than to the higher one. Consequently, horizontal resolution of the boundary conditions seems to play the dominant part. The implementation of a temporal evolution of the boundary conditions improves the variability in the domain and particularly in the Caribbean Sea.

6.3.2.2 Bottom Boundary Layer (BBL)

The Beckmann and Dorsher parameterization [7] was implemented in OPA model. The implementation of this parameterization in the PAM configuration leads to comparable results to those obtained in several CLIPPER configurations. The goal of this parameterization is to simulate the flow of dense water after a sill with a better realism. In the North Atlantic basin, two areas are particularly concerned: the Mediterranean Water (MW) outflow after the Gibraltar Strait and the dense water circulation through the Denmark Strait and Iceland Scotland Ridge. In these two cases BBL has a positive impact with a better depth for the MW and more cold water in the bottom of the two Nordic straits. Nevertheless this is not enough to obtain a realistic water mass in these areas where a temperature and a salinity relaxation in the Gulf of Cadiz is always useful. For the Nordic straits several solutions will be considered like another advection scheme or an open boundary condition in the northern part of the domain allowing the introduction of fresh water.

6.3.2.3 The lateral friction scheme

First experiments were done with MNATL (1/3° resolution model) during the year 2001. The lateral friction scheme has a very imprtant influence in this model. The results of this preliminary study have induced several tests with the high resolution model PAM. Due to the cost of PAM model, short tests (7 months) have been led with several parameterizations:

- free-slip test (control simulation);
- partial no-slip condition;
- mixing parameterization of the diffusion (laplacian/bilaplacian) according to the coastal distance;
- partial slip condition proportional to the instability of the simulated coastal currents.

The impact of these different parameterizations on the Gulf Stream separation is small, the Gulf Stream overshooting for all simulations after the Cape Hatteras. In the control simulation (free slip) a single gyre in Alboran Sea is simulated. A no-slip boundary condition is needed for the formation of the two observed gyres in this region. This parameterization has also an impact on the Meddies formation, described in section 6.3.4.1.

6.3.2.4 Impact of the forcing fluxes

Two studies concerning the impact of the surface forcing on the North Atlantic ocean have been carried. The first one was the implementation of a new parameterization of the temperature retroaction term [10]. The experiments were realized using the MNATL 1/3^o model and a temperature retroaction term computed with the 1998 ECMWF analyses using the Barnier formulation [6].
The second one concerns the interannual variability in the North Atlantic area [20]. The experiments were also realized using MNATL model with a salinity relaxation coefficient without interannual variability.
The impact of the wind variability and principally the NAO influence was also studied.
These two studies show the large influence of the surface forcing field and particularly the relaxation formulation in the forcing function. The Labrador Sea, which is a region of great interest, is the more sensitive area and seems really important to constraint the surface in the Labrador Sea for reducing the large temperature and salinity drift in the model.

6.3.2.5 Sub grid parameterization of the re-stratification.

The Gent and Mc Williams parameterization (GM90) [17] is a subgridscale parameterization which allows the re-stratification of the water column during the summer when the model is not eddy-resolving. In the case of the Labrador Sea, re-stratification during the summer is due to the atmospherics fluxes but also to some warm eddies detaching from the North Atlantic current and from the Greenland current. These eddies are advected in the centre of the Labrador Sea where they diffuse and warm the upper layers. In the case of MNATL model, the 1/3^o of degree horizontal resolution is not sufficient to simulate this re-stratification, while it is possible to simulate the re-stratification with a 1/15^o of degree model. The simulation of such events can however be reproduced with a good realism with the GM90 parameterization in the 1/3^o of degree model, which acts in the model like a diffusion operator. The aim being to have the best compromise between the representations of the current (intensity, turbulence) and the water mass (salinity, temperature, vertical stratification) in the PAM model, experiments with a regionalization of the GM90 parameterization in PAM model have been carried. The summer re-stratification is clearly better with GM90.

6.3.2.6 Advective scheme

In the OPA-8.1 code, the advection of temperature and salinity is computed with a spatial centred scheme. Stability is ensured with a diffusion operator. But a decrease of the meso-scale activity and the creation of local extrema are induced by this scheme. The goal of the study was to quantify the impact of a monotone and conservative advective scheme (MUSCL) [8]. The fronts and the mixed layer depth are indeed more realistic, but a strong decrease of the currents intensity and of the transports are observed. Some adjustments are needed before this advective scheme can be used.

6.3.3 The first operational Prototype System PSY2

6.3.3.1 Main PSY2v1 developments in year 2002

The assimilation of altimetric data in MNATL provides, in an operational mode, oceanic forecasts every week since January 17th 2001 (PSY1v1). The switch from MNATL to the high resolution model PAM needed some adaptations also usable by the other configurations ORCA2 and ORCA025.
Two important modifications due to the PAM computational cost and to the complexity of the PAM grid have been done:

- The sequential assimilation scheme has been parallelized. Analysis unit is distributed over several processors. PSY2v1 uses now the last PALM version which made easier the assimilation algorithm parallelization;

- The data selection has been adapted. In particular, a canvas grid has been introduced so that model and analysis grid points are located on the same reference system, with no need of an additional interpolation, wich is an advantage for the calculation of the innovation vector.

Others modifications have been performed :

- The assimilation parameters have been adjusted. In particular, Atlantic background error covariances uses zonal and meridional correlation radii issuing from the PSY1v1 2001 analysed SLA. For the Mediterranean Sea, radii are constant in space (150 km) and in time (30 days);
- The Inverse Simplification lifting-lowering stage has been completed by a vertical mode of displacement that evolves with time and space, depending on the vertical stratification [16];
- The correction takes into account the specific PAM bathymetry and buffer zones.

Many problems appeared before real-time operations could be achieved. The more important was the MPI library behaviour on the VPP5000 at Météo France. MPI fonctions *mpi_gather* and *mpi_scatter* did not work correctly. So, these functions have been reprogrammed using MPI basis functions *mpi_send* and *mpi_recv*.
Finally, real time could be reached after a little more than one year of integration starting from the climatology. The assimilated data were altimetric tracks from JASON and ERS-2 satellites. In the last four months, the GFO (Geosat Follow One) data have been taken into account by the assimilation algorithm.
Globally speaking, comparison between PSY1v1 and PSY2v1 of the analysed and forecasted Sea Surface Height shows the positive impact of high resolution. The Gulf Stream is slightly more both south and the North Atlantic current and the Azores front are more pronounced. In the region of the Gulf of Mexico and Caribbean Sea, numerous eddies observed by satellites are better represented in PSY2v1. In this region, the diagnostics of assimilation for PSY1v1 and PSY2v1 are similar. The ratio RMS(misfit) / RMS(data) is less than unity, which means that the assimilation performs well in this region where eddies are numerous. A section from New-York to Brest shows that PSY2v1 is able to better restore the fresh water tongue visible in the climatology around 50°W and 41.7°N, which corresponds to the southern penetration of the Labrador current. The diagnostics of assimilation corroborate this result, and are indeed better for PSY2v1 than for PSY1v1 in the region of the Gulf Stream.

6.3.3.2 PSY2v1 corrective maintenance

The analysis and forecasting system PSY2v1 runs in real-time mode since January 8^{th} 2003. The system behaviour has been carefully scrutinized in 2003. Some problems have been identified particularly during the Prestige pollution in November 2002 in the Bay of Biscay, and for the exceptional Mediterranean strong temperature in summer 2003 [GLO94].
The followings points have been modified:

- Bathymetry abnormalities have been corrected in the Bay of Biscay, the Western Brittany and the English Channel;
- The free-slip lateral friction condition has been replaced with a partial no-slip condition to improve the Mediterranean circulation;
- The minimal vertical diffusivity has been reduced in the surface layers to allow a more important stratification during summer warming;
- The interpolation technique (OASIS 3) allows now to use the high resolution of the ECMWF forcings;

- The Mean Sea Surface Height (MSSH) has been modified (correction on the continental shelf and raising over the domain). This has been done to reduce the gap with the climatology due to a 30 meters isopycnes lifting and to correct currents along continental shelfs and the Mediterranean Water outflow;
- The barotropic velocity increments were too strong compared with PSY1v2 (beta version of Multivariate Multi-data assimilation system). They have been reduced at the Inverse Simplification lifting-lowering stage.

6.3.4 Validation, oceanographic studies

6.3.4.1 The Meddies in the PAM model

The present generation of high-resolution ocean model offers a new way to investigate the characteristics and evolution of the ocean meso-scale. An analysis of the simulated Mediterranean eddies, the so called Meddies, has been performed [GLO93]. The model used is the Mercator North Atlantic [9°N, 70°N] and Mediterranean Sea Prototype PAM. The Meddies are coherent structures of warm and salt Mediterranean Water advected in the North East Atlantic. A 5-years experiment performed with PAM reproduced the main observed characteristics of the Meddies: thermohaline properties (11.8°C, 36 psu), sizes (radius between 25 and 110 km), thickness (between 500 and 1000 m), westward advection velocities (1.4 cm.s^{-1}), angular velocities (a period of 20 days), a good estimate of the number of Meddies in the north-east Atlantic (around 22) and their realistic geographical distribution (80% southern of 40°N). Furthermore and in agreement with a previous study based on an observation cruise, these modeled Meddies represent half of the westward salinity transport of MW. A sensitivity experiment shows the Meddies formation is highly sensitive to the lateral boundary friction condition. Using a no-slip condition, instead of the free-slip condition used in the previous experiment, the main Meddies birthplace is displaced at St Vincent Cape instead of Tejo Plato, in agreement with observations, and the spatial distribution of the Meddies becomes then more realistic.

6.3.4.2 Oceanic transport through

Straits play a special role in ocean circulation. They transform water masses, form currents and allow water to flow from one basin to another. In the North Atlantic and Mediterranean area simulated using the PSY2v1 analysis and forecasting system, there are numerous straits more or less determining large-scale circulation throughout the basin. The study focused on straits in two areas: the Caribbean Sea, where the Gulf Stream is formed, and the North-East Atlantic where the North Atlantic bottom waters and Greenland current are formed. This study is based on the transport of water masses computed by PSY2v1 from October 2001 to June 2003 after having divided up the areas into sections [9].
During 2003, the mean transport in the Caribbean as well as its variations agree with previous results. On the other hand, there is no apparent correlation in barotropic transport between water flowing from the Caribbean Sea and the intensity of the Florida current. The PSY2v1 system predicts the Florida current reasonably accurately. There is quite a significant difference, however, between the analysis and forecasts for the entrance to the Caribbean Sea. This may be due to proximity to the buffer zone and a badly represented Brazil current. The PSY2v1 system greatly underestimates the intensity of currents flowing over the Iceland-Scotland Ridge and through the Denmark Strait compared with actual measurements. This is true for both surface waters defined herein as having a density below 27.8 kg/m^3 and bottom waters, which have a density above 27.8 kg/m^3. This bias already exists in simulations without data assimilation using PAM, but it is even stronger in analyses using PSY2v1. The PSY2v1 system also exaggerates transport variability compared with actual measurements. The quantity of dense water coming through the two straits is 14.1 Sv (annual mean), which indicates an intense bottom water current from the Atlantic along the American coastline. The sub-polar gyre formed by the Greenland current has intense but realistic transport values.

6.3.5 Perspectives

Next step will concern the realization of a long experiment over the last decade period with the PAM2 configuration including all the new parameterizations. This experiment will be useful to study :

- The variability of the mixed layer in the North Atlantic and in the Mediterranean Sea with a particular attention in the deep water formation;
- The intensity and the variability of the transport through the principal straits and currents;
- The meso scale activity, the formation, thermohaline characteristics and dynamics of the eddies.

For PSY2, next step will concern the implementation of the new assimilation system SAM name SAM-1-v2 (see 6.2.1.2) using fully multivariate Empirical Orthogonal Functions (EOFs) of ψ $T(z)$ and $S(z)$. This new system (PSY2v2) will allow to assimilate simultaneously altimeter SLA, *in situ* temperature and salinity profiles and surface observation such as the Sea Surface Temperature (SST) and Sea Surface Salinity (SSS).

6.4 The global configuration models(C. Derval, L. Fleury, G. Garric and E. Rémy)

This work concerns the development of a global ocean model configuration at medium resolution. This component will be part of a global ocean forecasting system of MERCATOR for the end of 2004. The set-up of the configuration began in 2001 with the choice of the horizontal and vertical resolution, taking into account the future computer capacities. The numerical model is the ocean general circulation model OPA8.2 ([23]) with a diagnostic-only sea-ice component. The horizontal grid is an ORCA-type grid, with two poles on land in the Northern Hemisphere to avoid singularities at the north geographic Pole. The ORCA025 configuration, with a free-surface formulation, corresponds to a $1/4°$ resolution, e.g. with 1042x1021 horizontal grid points, and, in agreement with the DRAKKAR project, has 46 vertical levels, from 6 meters layer depths at surface to 250 meters layer depth at the bottom. The use of the NetCDF format for input and output files was chosen for easy-sharing purpose. Developments were done to extend the use of this format to multi-processors environment.
Year 2002 was dedicated to the preparation of input fields and to performing tests on the two multi-processor computers of METEO-FRANCE and ECMWF. A first two-year experiment was achieved at the end of this year; the spin-up period was analysed and allowed to improve the dynamical part of the model configuration before launching a longer experiment. Online and offline diagnostics routines were developed to analyse results and compare them to observations.

6.4.1 ORCA025 - Glace if

The model starts at rest with the global temperature and salinity Levitus climatology ([22]). The extrapolation of the $1°$x $1°$ Levitus'98 data set on the $1/4°$ grid caused the blow-up of the model in the Mediterranean and the Red Seas. The extrapolated Levitus data were replaced by the Medatlas climatology in the Mediterranean basin and by a mean profile in the Red Sea. An ERA-15 climatology forcing fields, a re-analysis product of the ECMWF, are used for the first experiments. For the experiment analysis, online diagnostic routines as mass transports through user-defined vertical sections, inherited from the PAM configuration, were adapted to the multi- basin case. Numerous technical works were accomplished to run the model, to archive easily the results via UNIX scripts shells and to visualize the diagnostics with the IDL software.

6.4.1.1 2-year simulation POG-03

This first climatological simulation was used to diagnose strong biases, to test both the input-output procedure in the multi-processors/NetCdf configuration and the online diagnostics ([GLO72]). It reveals some weaknesses in the large-scale oceanic circulation:
- Mediterranean and Red seas outflows are to shallow compared with observations;
- The equatorial undercurrent are too strong, especially in the Pacific Ocean where its expansion is too far east.

6.4.1.2 Improvements of the model configuration

As the number of vertical levels changed in agreement with the Drakkar configurations, we used more recent bathymetric ([GLO67]) data were used, Etopo2 and BedMap for latitudes lower than 20°S. Their interpolation on the new grid was done using the median of the data falling into each grid cell, to not bias the depth by bathymetric structures smaller than the grid-cell size. The time-step was also changed to reduce the CPU cost by tuning the diffusion coefficient and limit the smaller grid size.

From what was learned with the POG-03 simulation, different improvements of the internal parameterization were done during the first semester of 2003:

- The horizontal eddy viscosity in the equatorial band is enhanced by adding a second order viscosity parameterization ([GLO50]);
- Restoring zones to Levitus climatology are implemented around the Mediterranean and Red seas outflows to constrain the dense water to flow at the right depth;
- River runoffs are also prescribed as well as a term to close the freshwater budget. A relaxation term to Levitus Sea Surface Climatology is also used to compute the freshwater fluxes.

6.4.1.3 The 3-year climatological simulation: POG-04

A 3-year climatological simulation, POG-04, using the same forcing fields that the POG-03 experiment apart the evaporation flux which was multiplied by 0.6 to equilibrate the freshwater budget, have been performed ([GLO66]). The main circulation features, as the gyres, are well- represented, but the usual problems in z-coordinates eddy- permitting configuration are also present like the wrong position of the Gulf Stream. A first analysis of the experiment was done per ocean basin, compared to Levitus salinity and temperature fields used to initialize the simulation. Due to the resolution, strong and narrow western boundary currents are present, mass transports through major straits and between oceans basins are coherent with the observations. At the equator a cold bias is observed, especially in the eastern site of the Atlantic and Pacific basin, this being probably due the forcing fields. The amplitude of the undercurrent is comparable to the observed one (Figure 6.3). The variability of the Indian Ocean due to the monsoon is well represented. At high latitudes, water mass properties are not satisfactory, but this should change with the use of the LIM model ([18]). The spatial resolution permits the explicit representation of some eddy activity, for example in the Aghulas region. The eddy kinetic energy computed over 1 year shows the area of strong variability represented by the model (Figure 6.4).

6.4.2 The ORCA-LIM configuration

6.4.2.1 The ORCA025-LIM configuration

In 2002, an effort was done to begin the parallelisation of the LIM ice model. The problems encountered in the setup of the LIM model in his parallel configuration were solved, so that a first 3-month experiment with the ORCA025-LIM configuration could be performed in late 2003.

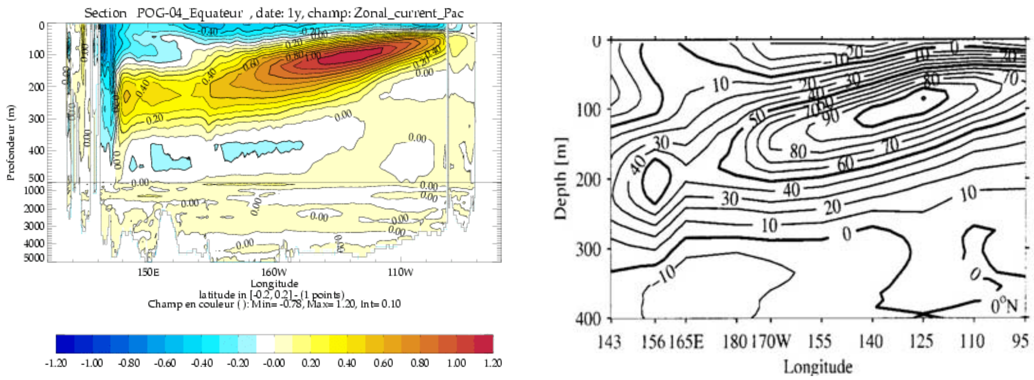

Figure 6.3: Pacific equatorial undercurrent : in the left panel, the yearly mean of the zonal velocity field at the equator in POG-04 experiment, in the right panel, the zonal velocity field issued from hydrological data CTD/ADCP data, (Johnson et al, Oct. 2001).

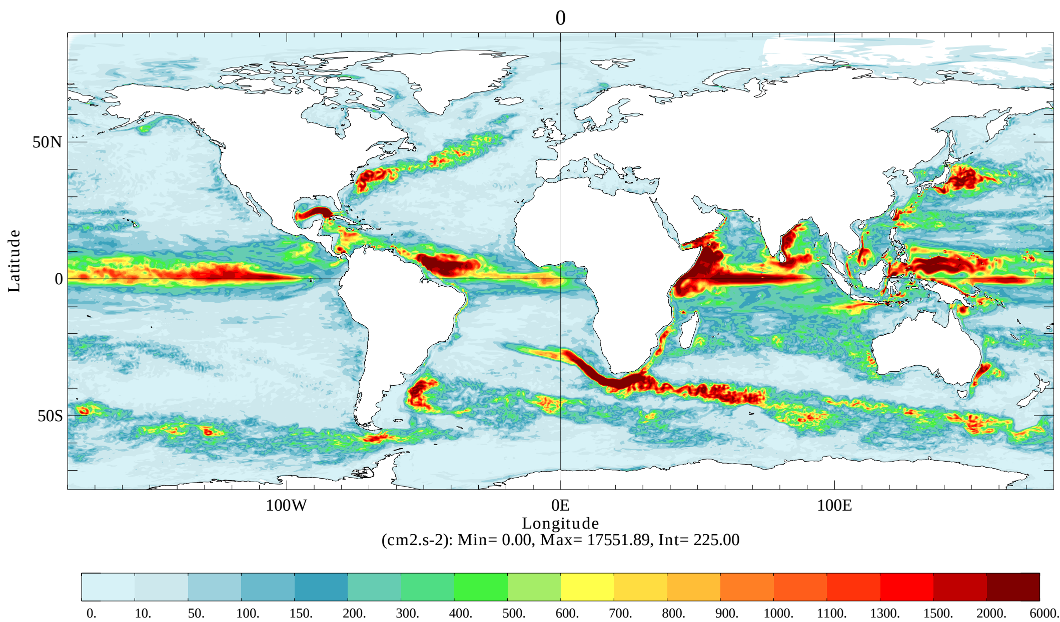

Figure 6.4: Eddy Kinetic Energy computed over the third year of the POG-04 experiment.

6.4.2.2 The ORCA2-LIM experiments

Various sentivity interannual experiments (1993-2002) concerning the atmospheric forcing in the 'bulk' framework have been performed with the ORCA2-LIM model. As the atmospheric forcing is supposed to have his major deficiencies at high latitudes, these experiments focused on the systematic biases exhibited by the ECMWF analysis and their potential impact on the sea-ice simulation. The choice of the ECMWF analysis as atmospheric forcing have been promoted by the need to test the future atmospheric forcing (i.e; ECMWF forecasts) in the operational mode.

One of the experiment used different observed atmospheric climatology (tagged 'CLIO' package) to get a control simulation. The simulated sea-ice in this experiment has a realistic mean state, and particularly the ice thickness. The simulated sea-ice extension was compared with the sea-ice concentration SSM/I (Special Sensor Microwave/Imager) dataset from the NSIDC (National Snow Ice Data Center). With a 25km horizontal resolution over the entire 1978-2002 period, this dataset represents a unique and homogeneous large scale sea-ice observed dataset. For higher-resolution evaluation purpose at high latitudes, collaborations were initiated with the CERSAT (Centre ERS d'Archivage et de Traitement) at IFREMER (Institut Franccais de Recherches et d'Exploitation de la MER), the Institute of Environmental Physics at Bremen University (Germany) and the NERSC (Nansen Environmental and Remote Sensing Center) at Bergen University (Norway).

Comparisons made between different experiments forced either solely by ECMWF analysis (experiment ORC1 hereafter), or combining ECMWF analysis and 'CLIO' hydrological cycle (precipitations, cloudiness and air surface humidity) or combining ECMWF analysis and part of the 'CLIO' hydrological cycle (cloudiness and air surface humidity) allowed to conclude partially for the Arctic Ocean. Due to the relative atmospheric dryness of the Arctic climate, impacts of precipitations and air surface humidity on the simulated arctic sea ice seem less important that those initiated by the cloudiness. For example, a mean cloudiness difference of about 8% over the Arctic Basin produced a sea ice thickness anomaly of around 1.5m in this area. The increase of the cloudy 'blanket' during winter decreased the surface cooling. This relative winter warming prevailed the filtering role of the solar radiance played by the clouds during summer, and results in a general decrease of the sea ice mass.

Nevertheless, the analysis of the CMAP precipitations used in the 'CLIO' package at high latitudes revealed spurious small- scales patterns and raised the need to get more reliable observed rainfall data in polar areas. Thanks to the incorporation of the TOVS (TIROS Operationnal Satellite) data beyond 40 latitude, various studies showed a better quality of the rainfall GPCP (Global Precipitation Climatology Project) Version 2 dataset at high latitudes. The GPCP dataset (1979-1992) was then used and compared with the ECMWF analysis rainfall datasets over the entire 1993-2002 period for the Southern Hemisphere. The main pattern is the polar shift of the circumpolar through in the ECMWF analysis compared to the GPCP one. A dipole pattern can be observed where GPCP precipitations exceed generally (tenths of mm/day) the ECMWF analysis north of the $60°$S latitude. This comparison raised the question of the right spatial position of the austral circumpolar through in the ECMWF model and, more generally, in the atmospheric GCM. Another experiment combining the GPCP precipitations data and the ECMWF analysis (experiment ORC4 hereafter) was performed to analyse the impact on simulated sea ice. The general increase of precipitations over sea ice in the ECMWF rainfall field results obviously in a general zonal pattern snow-thickness positive anomaly in the ORC1 experiment compared to the ORC4 experiment. The transformation of snow in ice together with the large spread out of the divergent thicker ice results in a large increase of the total sea ice mass during winter in the ORC1 experiment. Furthermore, the effect of an increased albedo together with a thicker ice delayed the onset of the melt season. Large and localised differences between the GPCP and ECMWF rainfall datasets occur in areas where the storm tracks interact strongly with the orography (South America, Antarctica peninsula and New Zealand Island). This bias is commonly observed in spectral models as the sharp orography (as the Antarctica Peninsula and the Andes Cordillera) are crudely represented by the spectral truncations in finite numbers of waves. More (resp. less) precipitation in the ECMWF analysis downstream (resp. upstream) of the flow beyond (resp. ahead) the orography were observed, as compared to the GPCP estimates. The impact on the sea ice simulation is illustrated downstream the Antarctica Peninsula in the Weddell Sea. East of the peninsula, the excess of snowy precipitation leads to snow accumulation locally over the sea ice cover, the sea ice drift contributes to transporting this snow thickness anomaly downstream into the Weddell Sea and beyond. Generally, the positive anomaly of precipitations in the ECMWF analysis localised in the Antarctic Peninsula and the coast of Ross Sea have a weak and localised effect on the sea ice thickness (few centimetres).

Focused firstly on the hydrological cycle, an analysis of the ECMWF analysis dynamical forcing (wind stress) exhibited an important bias in the Central Arctic Basin. A persistent cyclonic circulation in this area during summer prevented the sea ice outflow and produced a non-realistic strong piling up of ice ($>$ 10m) in the Arctic Basin. An experiment in which the wind stress is computed from the wind components at 10m height did not remove this strong summer cyclonic gyre. Another experiment in which the turning angle between the wind stress and the wind at 10m has been fixed to $20°$ (initially set to $0°$) reduced the ice accumulation ($<$ 8m) but did not erase the abnormal sea ice thickness distribution in the Arctic Basin. This major problem is still under investigations and needs to be solved taking into account the final set up of the ORCA025- LIM atmospheric forcing in operational mode.

It has to be noted that the initial sea ice thickness newly formed at the leads surface has been fixed to 1.0m instead of the initial 0.3m value. This change induced a better seasonal cycle of the sea ice mass, and particularly for the antarctica sea ice.

A more detailed report is actually in preparation to discuss the surface ECMWF analysis at high latitudes and their impacts on the sea ice simulation with the ORCA2-LIM model.

[6] B. Barnier, L. Siefridt, and P. Marchesiello, (1995), Thermal forcing for global ocean circulation model using a three-year climatology of ECMWF analyses, *J. Marine Syst.*, **6**, 363–380.

[7] A. Beckmann and D. Dörscher, (1997), A method for improved representation of dense water spreading over topography in geopotential-coordinate models, *J. Phys. Oceanogr.*, **27**, 581–591.

[8] L. Bessières, (2002), Comparaison des schémas d'advection MUSCL et ARAKAWA, dans le cadre de la modélisation de l'oéan Nord Atlantique avec la configuration MNATL, *Rapport de stage INSA*.

[9] R. Bourdallé-Badie, Y. Drillet, and K. Béranger, (2004), Oceanic transport through Atlantic straits in PSY2V1 prototype, *Newsletter Mercator*, **11**.

[10] S. Chêne, (2002), Etude d'une nouvelle paramétrisation du rappel en surface à la température dans un modèle océanique à moyenne résolution, *Rapport de stage IM1*.

[11] P. CLIPPER, (2000), Modélisation à haute résolution de la circulation dans l'océan Atlantique forcée et couplée océan-atmosphère, *Rapport Scientifique et Technique 1998*, **CLIPPER-R3-2000**.

[12] M. Cooper and K. Haines, (1996), Data assimilation with water property conservation, *J. Geophys. Res.*, **101**, 1059–1077.

[13] R. Daley, (1991), Atmospheric Data Analysis, *Cambridge University Press, England*, 457 pp.

[14] P. De Mey and M. Benkiran, (1991), A multivariate reduced-order optimal interpolation method and its application to the Mediterranean basin-scale circulation, *Ocean Forecasting: Conceptual basis and applications,N. Pinardi Ed., Springer-Verlag*, 281–303.

[15] P. De Mey and A. Robinson, (1987), Assimilation of altimeter Eddy Fields in a Limited-Area Quasi-Geostrophic Model, *J. Phys. Oceanogr.*, **17**, 2280–2293.

[16] P. Faucher, (2001), *Description de la variabilité verticale de l'Atlantique Nord en coordonnées isopycnales. Application à l'assimilation de donnés altimétriques dans un modèle aux équations primitives*, PhD thesis, Université Toulouse III).

[17] P. Gent and J. C. Mc Williams, (1990), Isopycnal mixing in ocean circulation models, *J. Phys. Oceanogr.*, **20**, 150–155.

[18] H. Goosse, J.-M. Campin, E. Deleersnijder, T. Fichefet, P.-P. Mathieu, M. A. Morales Maqueda, and B. Tartinville, (2001), Description of the CLIO model version 3.0.

[19] K. Ide, P. Courtier, P. Ghil, and A. Lorenc, (1997), Unified Notation for Data Assimilation: Operational, Sequential and Variational, *J. Meteorol. Soc. Japan (Special issue)*, **75-1B**, 181–189.

[20] S. Korabi, (2003), Etude de la variabilité interannuelle de l'océan Atlantique Nord : Processus océaniques et rôle du forçage atmosphérique, *Rapport de stage IENM/IMCLI*.

[21] W. Large, (1998), Modeling and parameterization ocean planetary boundary layers, *E.P. Chassignet and J. Verron (Eds), Ocean Modeling and Parameterization, Kluwer Academic Publishers*, 81–120.

[22] S. Levitus, (1982), Climatological Atlas of the World Ocean, *NOAA Professional Paper 13*.

[23] G. Madec, P. Delecluse, M. Imbard, and C. Levy, (1998), OPA8.1: Ocean general circulation model reference manual, *Notes du pole de modélistaion, Institut Pierre-Simon Laplace (IPSL)*.

[24] D. Pham, J. Verron, and M. Roubaud, (1998), A Singular Evolutive Extended Kalman Filter for data assimilation in oceanography, *J. Marine Syst.*, **16(3-4)**, 323–340.

[25] A. Piacentini, (2002), PALM. A dynamic parallel coupler, VECPAR 2002, Porto, Portugal, 26–28 June.

[26] M. H. Rio and F. Hernandez, (2002), Estimation d'une topographie dynamique moyenne sur l'Atlantique Nord et Tropical, *Rapport n CLS/DOS/NT/02.515*, pp. 48.

[27] O. Talagrand, (1998), A posteriori evaluation and verification of analysis and assimilation algorithms, *Proceedings of Workshop on Diagnosis of Data Assimilation Systems, Reading, England*.

[28] C.-E. Testut, (2000), *Assimilation de données satellitales avec un filtre de Kalman de rang réduit dans un modèle aux Equations Primitives de l'océan Atlantique*, PhD thesis, Université Joseph Fourier (Grenoble I).

7 Publications

7.1 Journal Publications

[GLO1] J. C. André, J. Y. Caneill, M. Déqué, P. Rogel, L. Terray, and Y. Tourre, (2002), La prévision du climat de l'échelle saisonnière à l'échelle décennale, *C. R. Géoscience*, **334**, 1115–1127.

[GLO2] J. C. André, (2003), Sur la crédibilité des conséquences de l'effet de serre, *C. R. Géoscience*, **335**, 503–507.

[GLO3] M. Davey, M. Huddleston, K. Sperber, P. Braconnot, F. Bryan, D. Chen, A. Colman, C. Cooper, U. Cubasch, P. Delecluse, D. DeWitt, L. Fairhead, G. Flato, C. Gordon, T. Hogan, M. Ji, M. Kimoto, A. Kitoh, T. Knutson, M. Latif, H. Le Treut, T. Li, S. Manabe, C. Mechoso, G. Meehl, S. Power, E. Roeckner, L. Terray, A. Vintzileos, R. Voss, B. Wang, W. Washington, I. Yoshikawa, J. Wu, S. Yukimoto, and S. Zebiak, (2002), STOIC: a study of coupled model climatology and variability in tropical ocean regions, *Clim. Dyn.*, **18**, 403–420.

[GLO4] M. Drévillon, C. Cassou, and L. Terray, (2003), Model study of the wintertime atmospheric response to autumn tropical Atlantic sea-surface-temperature anomalies., *Quart. J. Roy. Meteor. Soc.*, **129**, 2591–2611.

[GLO5] G. Garric and M. Huber, (2003), Quasi-decadal variability in paleoclimate records: Sunspot cycles or intrinsic oscillations?, *Paleoceanography*, **18**, 1068 – 10.1029/2002PA000869.

[GLO6] A. M. Moore, J. Vialard, A. T. Weaver, D. L. T. Anderson, R. Kleeman, and J. Johnson, (2003), The role of air-sea interaction in controlling the optimal perturbations of low-frequency tropical coupled ocean-atmosphere modes., *J. Climate.*, **16**, 951–968.

[GLO7] J. Royer, D. Cariolle, F. Chauvin, M. Déqué, H. Douville, R. M. Hu, A. Planton, S. Rascol, J. L. Ricard, D. Salas y Mélia, F. Sevault, P. Simon, S. Somot, S. Tyteca, L. Terray, and S. Valcke, (2002), Simulation des changements climatiques au cours du XXI-e siècle incluant l'ozone stratosphérique (Simulation of climate changes during the 21st century including stratospheric ozone), *C. R. Géoscience*, **334 (3)**, 147–154.

[GLO8] Y. Tang, R. Kleeman, A. M. Moore, A. T. Weaver, and J. Vialard, (2003), The role of air-sea interaction in controlling the optimal perturbations of low-frequency tropical coupled ocean-atmosphere modes., *Geophys. Res. Lett.*, **30(13)**, 1694, doi:10.1029/2003GL017664.

[GLO9] L. Terray and C. Cassou, (2002), Tropical Atlantic sea surface temperature forcing of quasi-decadal variability over the North Atlantic European region, *J. Climate*, **22**, 3170–3187.

[GLO10] P. Terray, P. Delecluse, L. Terray, and S. Labattu, (2003), Sea surface temperature forcing of the Indian summer monsoon., *Clim. Dyn.*, **21**, 593–618.

[GLO11] J. Vialard, A. T. Weaver, D. L. T. Anderson, and P. Delecluse, (2003), Three- and four-dimensional variational assimilation with an ocean general circulation model of the tropical Pacific Ocean. Part 2: physical validation., *Mon. Wea. Rev.*, **131**, 1379–1395.

[GLO12] A. Vidard, F. X. Le Dimet, and A. Piacentini, (2003), Determination of Optimal Nudging Coefficients., *Tellus*, **55A**, 1–15.

[GLO13] A. T. Weaver, J. Vialard, and D. L. T. Anderson, (2003), Three- and four-dimensional variational assimilation with an ocean general circulation model of the tropical Pacific Ocean. Part 1: formulation, internal diagnostics and consistency checks., *Mon. Wea. Rev.*, **131**, 1360–1378.

[GLO14] R. B.-B. Y. Drillet and L. Siefridt, (2002), Tests de sensibilité dans le modèle haute résolution Mercator, *Annales Mathématiques Blaise Pascal*, **9**, 283–298.

7.2 PhD and HdR Thesis

[GLO15] M. Drevillon, (2002), *Interaction océan-atmosphère à l'échelle saisonnière sur la région Atlantique Nord-Europe : rôle des routes dépressionnaires et mécanismes associés sur la variabilité climatique*, PhD thesis, Université Paul Sabatier (Toulouse III).

[GLO16] S. Massart, (2003), *Méthodologies de l'assimilation de données. Application à la chimie atmosphérique et à la mécanique des structures*, PhD thesis, Institut National Polytechnique de Toulouse.

[GLO17] L. Terray, (2002), *Les mécanismes de la variabilité climatique aux échelles saisonnière à décennale sur la région Europe Atlantique Nord*, "Habilitation à Diriger des Recherches", Institut National Polytechnique de Toulouse.

7.3 Conference Proceedings and Book Chapters

[GLO18] P. Bahurel, I. Charron, P. De Mey, T. De Prada, E. Dombrosky, L. Fleury, E. Gondet, C. Le Provost, P. Le Traon, H. Mercier, A. Piacentini, and L. Siefridt, (2002), MERCATOR, French GODAE assimilation center; project overview, Biarritz, 13-15 June,, International Symposium ”En route to GODAE”, 293–294.

[GLO19] R. Bahurel, I. Charron, P. De Mey, T. De Prada, E. Dombrowsky, L. Fleury, E. Gondet, C. Le Provost, P.-Y. Le Traon, H. Mercier, A. Piacentini, and L. Siefridt, (2002), MERCATOR, French GODAE assimilation center: project overview, International symposium ”En route to GODAE”,, Biarritz, France, 13–15 June.

[GLO20] R. Bourdallé-Badie, D. Y., and L. Siefridt, (2002), The Mercator Assimilation System: The North Atlantic and Mediterranean MERCATOR project, Biarritz, 13-15 June,, International Symposium ”En route to GODAE”, 287–288.

[GLO21] P. DeMey, T. Awaji, M. J. Bell, A. F. Bennett, P. Brasseur, G. Evensen, I. Fukumori, H. Hurlburt, D. Stammer, and A. T. Weaver, (2002), Approaches to data assimilation within GODA, International symposium ”En route to GODAE”,, Biarritz, France, 13–15 June.

[GLO22] E. Guilyardi, R. G. Budich, and S. Valcke, (2003), PRISM and ENES: European Approaches to Earth System Modelling, the 10th ECMWF Workshop on the Use of High Performance Computing in Meteorology 2002, Reading, U.K, 19 pp.

[GLO23] J. Lellouche and Tranchant, (2003), Les diagnostics d'assimilation dans PSY2, *Mercator Newsletter*, **9**, pp 15–23, Avril 2003.

[GLO24] J. Lellouche, B. Tranchant, N. L., and T. Morel, (2002), The Mercator Assimilation System: A modular approach to drive modeling, assimilation and data components together, Biarritz, 13-15 June,, International Symposium ”En route to GODAE”, 265–266.

[GLO25] J. Lellouche, B. Tranchant, N. L., M. Benkiran, and E. Greiner, (2002), Operational Data Assimilation in the Mercator North Atlantic and Mediterranean High Resolution Prototype PAM, AGU Fall Meeting, San Francisco, 6–10 December.

[GLO26] S. Massart, J. P. Argaud, and S. Ghavamian, (2002), Propagation des erreurs a posteriori pour l'évolution non-linéaire des propriétés physico-chimiques du béton, CANUM 2002 Actes du 34eme congrès national d'analyse numérique, 27–31 May.

[GLO27] S. Massart, J. P. Argaud, A. Piacentini, and O. Thual, (2002), Identification of chemical species emission and sensitivity analysis with variational assimilation of restricted artificial observations, In *Monitoring and Management of Environmental Problems*, 9th International Conference on The Modelling, Bergen, Norway, 6-8 May, p 79–88.

[GLO28] A. Piacentini, (2002), PALM. A dynamic parallel coupler, VECPAR 2002, Porto, Portugal, 26–28 June.

[GLO29] B. Tranchant, B. Benkiran, P. De Mey, E. Greiner, J. Lellouche, and C.-E. Testut, (2003), A modular assimilation system for operational oceanography, Roger Daley Memorial Symposium, 28 Sept.–01 Oct., Montral (QC), Canada.

[GLO30] B. Tranchant, J. Lellouche, Y. Drillet, L. Siefridt, Bourdallé-Badie, B. Benkiran, E. Greiner, P. Brasseur, C.-E. Testut, and J. Branckart, (2002), The Mercator Data Assimilation system, Operational Oceanography and Remote Sensing Symposium, London, 5–7 March.

[GLO31] B. Tranchant, J. Lellouche, N. L., M. Benkiran, E. Greiner, and E. Dombrowsky, (2002), Assimilation de données en mode opérationnel avec le modèle haute résolution PAM (Prototype Atlantique nord et Méditerranée,Toulouse, 17-19 December), Atelier de Modélisation de l'Atmosphère, Météo-France, 35–38.

[GLO32] N. Verbrugge, B. Tranchant, C. Le Provost, E. Greiner, L. Fleury, Y. Drillet, R. Bourdallé-Badie, and B. Benkiran, (2002), The MERCATOR Tropical and North Atlantic Prototype: Comparison of the 1993-98 ocean reanalysis to WOCE data, World Ocean Circulation Experiment (WOCE) and Beyond, San Antonio, USA. November 18–22.

[GLO33] A. T. Weaver and S. Ricci, (2003), Constructing a background-error correlation model using generalized diffusion operators, 8 -12 September, ECMWF Seminar on "Recent developments in atmospheric and ocean data assimilation", ECMWF, Reading, U. K., 327 – 339.

[GLO34] A. T. Weaver, (2003), 3D-Var and 4D-Var approaches to ocean data assimilation, 13 - 15 November, ECMWF Workshop on the "Role of the Upper Ocean In Medium Range And Extended-Range Forecasting", ECMWF, Reading, U., p 57–66.

7.4 Technical Reports

[GLO35] The PALM group, (2002), PALM and PrePALM Research QuickStart Guide for version 2.2.0, Technical Report TR/CMGC/02/107, CERFACS. available on Global Change web.

[GLO36] J. C. André, M. Déqué, P. Rogel, and S. Planton, (2003), La vague de chaleur de l'été 2003 et sa prévision saisonnière, Working Notes WN/CMGC/03/126, CERFACS. available on Global Change web.

[GLO37] E. Anterieu, (2003), Stabilized image reconstruction algorithm for synthetic aperture imaging radiometers, Working Notes WN/CMGC/03/42, CERFACS. available on Global Change web.

[GLO38] D. Bari and P. Rogel, (2003), Assimilation variationnelle de la température de surface dans l'océan global, Technical Report TR/CMGC/03/51, CERFACS. available on Global Change web.

[GLO39] M.-B. Benticha, (2003), Couplage Océan-Atmosphère avec PALM et OASIS, Technical Report TR/CMGC/03/68, CERFACS. available on Global Change web.

[GLO40] S. Buis, (2002), First study on a communication model for PALM-MP, Working Notes WN/CMGC/02/79, CERFACS. available on Global Change web.

[GLO41] S. Buis, (2002), Sub-objects in PALM-MP, Working Notes WN/CMGC/02/80, CERFACS. available on Global Change web.

[GLO42] C. Cibot, L. Terray, B. Dewitte, and E. Maisonnave, (2003), Mechanisms of tropical Pacific interannual-to-decadal variability in the ARPEGE/ORCA global coupled model, *Climate Dynamics*, Submitted.

[GLO43] C. Cilly, (2003), Implémentation de méthodes d'interpolations 3D pour le coupleur OASIS, Technical Report TR/CMGC/03/67, CERFACS. available on Global Change web.

[GLO44] N. Daget, (2003), Location of observation points on a grid and Test of different interpolation schemes, Technical Report TR/CMGC/03/79, CERFACS. available on Global Change web.

[GLO45] D. Déclat and the PALM group, (2002), The Coding Conventions for the PALM-MP, Technical Report TR/CMGC/02/9, CERFACS. available on Global Change web.

[GLO46] D. Declat and the PALM group, (2002), Creation of a context of communications between two executables using MPI ports, Working Notes WN/CMGC/02/75, CERFACS. available on Global Change web.

[GLO47] D. Déclat, (2002), Development of PINT: a Parallel and scalable INTerpolation library for global coupled climate model, Technical Report TR/CMGC/02/25, CERFACS. available on Global Change web.

[GLO48] D. Declat, (2003), Interaction between the transformer and the PSMILe library, Technical Report TR/CMGC/03/103, CERFACS. available on Global Change web.

[GLO49] E. Demory, (2003), Influence du réchauffement climatique dû à l'augmentation de la concentration des gaz à effet de serre sur le climat de la région Europe Atlantique Nord, Technical Report TR/CMGC/03/66, CERFACS. available on Global Change web.

[GLO50] C. Derval, (2003), Paramétrisation de la viscosité dans la bande équatoriale pour la configuration ORCA025, Oct. 2003, tech. rep.

[GLO51] S. Dion, (2002), Création d'une interface graphique pour la manipulation d'opérations algébriques dans le coupler de codes parallèles PALM, Technical Report TR/CMGC/02/90, CERFACS. available on PALM web.

[GLO52] A. El Akkraoui, N. Chapelon, and N. Pannekoucke, (2003), Implémentation de nouvelles méthodes d'assimilation variationnelle dans un modèle océanique simplifié, Technical Report TR/CMGC/03/36, CERFACS. available on Global Change web.

[GLO53] D. Fenieys, (2002), La variabilité de l'océan Atlantique Tropical: Origines et impacts sur les régions continentales adjacentes, Working Notes WN/CMGC/02/82, CERFACS. available on Global Change web.

[GLO54] M. Frouvelle, (2003), Treatment of particular points in SCRIP, Technical Report TR/CMGC/03/55, CERFACS. available on Global Change web.

[GLO55] C. Halluitte, (2002), Etude de l'influence d'El Nino sur les precipitations en Inde, Technical Report TR/CMGC/02/76, CERFACS. available on Global Change web.

[GLO56] C. Jauffret, (2003), Mise en place de l'initialisation par filtrage numérique dans le système d'assimilation 4D-Var du modèle de circulation générale océanique OPA, IENM Rapport de stage no. 867, Meteo-France.

[GLO57] A. Jouzeau, E. Maisonnave, V. S., and L. Terray, (2003), Climatology and Interannual to Decadal Variability diagnosed from a 200-year Global Coupled Experiment, Technical Report TR/CMGC/03/30, CERFACS. available on Global Change web.

[GLO58] A. Jouzeau, E. Maisonnave, V. S., and L. Terray, (2003), Decadal Predictability Study using a Global Coupled Model, Technical Report TR/CMGC/03/83, CERFACS. available on Global Change web.

[GLO59] J. M. Lellouche and B. Tranchant, (to be submitted in 2004), The Mercator Assimilation System: A modular approach to drive modelling, assimilation and data components together, *J. Atmos. Ocean. Technol.*

[GLO60] E. Maisonnave, C. Cibot, C. Delon, M. Drévillon, and A. Piacentini, (2002), SIBYLLE: Visualisation Ferret des grilles ORCA et ARPEGE (Guide d'utilisation), Technical Report TR/CMGC/02/81, CERFACS. available on Global Change web.

[GLO61] E. Maisonnave, C. Cibot, C. Delon, M. Drevillon, A. Piacentini, and D. Bari, (2003), Sibylle 1.2: Guide d'utilisation, Working Notes WN/CMGC/03/94, CERFACS. available on Global Change web.

[GLO62] E. Maisonnave, (2002), persona: utilitaire de cration et de retouche de masques Netcdf, Working Notes WN/CMGC/02/117, CERFACS. available on Global Change web.

[GLO63] E. Maisonnave, (2002), vair2cdf: convertisseur Vairmer/Netcdf de fichiers de donnes, Technical Report TR/CMGC/02/113, CERFACS. available on Global Change web.

[GLO64] M. Monteillet, (2003), Création d'unités d'interpolation pré-définies pour le coupleur PALM, Technical Report TR/CMGC/03/81, CERFACS. available on Global Change web.

[GLO65] A. Piacentini and the PALM group, (2002), Dynamic Features of PALM MP. Part I: design., Technical Report TR/CMGC/02/110, CERFACS. Restricted diffusion.

[GLO66] POG-Team, (2003), Dossier d'expérimentation ORCA025, édition 01, avril 2003, tech. rep.

[GLO67] E. Rémy, L. Siefridt, L. Fleury, and M. Bremond, (2003), Construction de la bathymétrie pour la configuration modèle ORCA025, Mai 2003, tech. rep.

[GLO68] S. Ricci, A. T. Weaver, J. Vialard, and P. Rogel, (2003), Incorporating state-dependent temperature-salinity constraints in the background-error covariance of variational ocean data assimilation, *Mon. Wea. Rev.*, Submitted.

[GLO69] P. Rogel and E. Maisonnave, (2003), CERFACS ocean analysis and seasonal forecasting system: unassimilated reference hindcast experiments, Technical Report TR/CMGC/03/87, CERFACS. available on Global Change web.

[GLO70] P. Rogel and E. Maisonnave, (2003), Quelques résultats des prévisions couplées DEMETER effectuées au CERFACS, Technical Report TR/CMGC/03/88, CERFACS. available on Global Change web.

[GLO71] P. Rogel, (2003), Global ocean analysis and diagnostics for seasonal prediction, Technical Report TR/CMGC/03/86, CERFACS. available on Global Change web.

[GLO72] P. team, (2003), Dossier de définition de l'outil ORCA025, édition 03, octobre 2003, tech. rep.

[GLO73] The PALM group, (2002), A coding norm for PALM, Technical Report TR/CMGC/02/10, CERFACS. available on Global Change web.

[GLO74] The PALM group, (2002), PALM and PrePALM Research Installation and Configuration Guide for version 2.1.0, Technical Report TR/CMGC/02/39, CERFACS. available on Global Change web.

[GLO75] The PALM group:, (2002), PALM and PrePALM Research Installation and Configuration Guide for version 2.2.0, Technical Report TR/CMGC/02/108, CERFACS. available on Global Change web.

[GLO76] The PALM group, (2002), PALM and PrePALM Research QuickStart Guide for version 2.1.0, Technical Report TR/CMGC/02/38, CERFACS. available on Global Change web.

[GLO77] The PALM group, (2002), Sample Data Assimilation Applications with PALM Research, Technical Report TR/CMGC/02/32, CERFACS. available on Global Change web.

[GLO78] The PALM group, (2002), Sample Data Assimilation Applications with PALM Research version 2.1.0, Technical Report TR/CMGC/02/40, CERFACS. available on Global Change web.

[GLO79] J. I. Tshimanga, (2002), Comparaison de deux implmentations de la mthode quasi Newton Mmoire limite utilises dans un problme d'assimilation de donnes en ocanographie, Technical Report TR/CMGC/02/71, CERFACS. available on Global Change web.

[GLO80] S. Valcke, A. Caubel, D. Declat, and L. Terray, (2003), OASIS3 Ocean Atmosphere Sea Ice Soil User's Guide, Technical Report TR/CMGC/03/69, CERFACS. available on Global Change web.

[GLO81] S. Valcke, (2002), High Level Architecture Choices and Design for the PRISM Coupler and I/O Library (ARCDI 2.2), Working Notes WN/CMGC/02/47, CERFACS. available on Global Change web.

[GLO82] S. Valcke, (2002), Minutes of the May 21st 2002 WP3a/WP4a meeting in Toulouse, Working Notes WN/CMGC/02/59, CERFACS. available on Global Change web.

[GLO83] S. Valcke, (2002), Minutes of the PSMILe development meetings (Paris, September 18-19, 2002), Working Notes WN/CMGC/02/128, CERFACS. available on Global Change web.

[GLO84] S. Valcke, (2002), Minutes of the WP3a Sankt-Augustin meeting (14-15/03/2002), Working Notes WN/CMGC/02/42, CERFACS. available on Global Change web.

[GLO85] S. Valcke, (2002), Minutes of the WP3a Toulouse meeting (16-17/04/2002), Working Notes WN/CMGC/02/43, CERFACS. available on Global Change web.

[GLO86] S. Valcke, (2002), Minutes of the WP3a-WP4a Hamburg meeting (21/02/2002), Working Notes WN/CMGC/02/44, CERFACS. available on Global Change web.

[GLO87] S. Valcke, (2002), PRISM - Minutes of the WP3a-WP4a Toulouse meeting (19/04/2002), Working Notes WN/CMGC/02/45, CERFACS. available on Global Change web.

[GLO88] S. Valcke, (2002), Requirements and Design Options for the PRISM Coupler (REDOC II.2), Working Notes WN/CMGC/02/46, CERFACS. available on Global Change web.

[GLO89] S. Valcke, (2003), Minutes of the Sankt-Augustin WP3a meeting and other issues raised during the PRISM workshop (February 24-27, 2003), Working Notes WN/CMGC/03/28, CERFACS. available on Global Change web.

[GLO90] S. Valcke, (2003), Minutes of WP3a meeting, Sankt-Augustin, 26/11/2003, Working Notes WN/CMGC/03/121, CERFACS. available on Global Change web.

[GLO91] F. Vossepoel, A. T. Weaver, J. Vialard, and P. Delecluse, (2003), Adjustment of near-equatorial wind stress with four-dimensional variational data assimilation in a model of the Pacific Ocean, *Mon. Wea. Rev.*, Submitted in 2003.

[GLO92] A. T. Weaver, J. Vialard, D. L. T. Anderson, and P. Delecluse, (2002), Three- and four-dimensional variational assimilation with an ocean general circulation model of the tropical Pacific Ocean, Technical Memorandum Volume 165, 74 pp, ECMWF.

[GLO93] C. L. P. Y. Drillet, R. Bourdallé-Badie and L. Siefridt, (submitted in 2003), The Meddies in the Mercator North Atlantic and Mediterranean Sea eddy r esolving model, *J. Geophys. Res.*

[GLO94] J. L. Y. Drillet, E. Greiner and N. Verbrugge, (2004), Saut qualitatif dans le modèle Atlantique Nord et Méditerranée ha ute résolution (PSY2V1), *Newsletter Mercator*, **12**.

5

ENScube Group

1 Introduction

Pierre-Henri Cros

During the period the N'S^3 group has focused its activity on the deployment of its results toward new sectors. The objective was to promote numerical simulation, and more particularly CFD simulation, toward industrial activities for which this technology is not well implemented yet.

In order to convince the targeted industries of the benefits of this technology, the N'S^3 group decided to emphasize the means that should help them to appropriate its results:

- by making the results more accessible thanks to advanced visualisation;
- by favouring continuous exchanges thanks to collaborative tools.

Implementing such a new approach requires firstly to gain credibility. During the period the N'S^3 group adopted a step-by-step approach, aiming at gaining credibility in three different technologies (numerical simulation, advanced visualization, collaborative tools), and at progressively increasing the awareness and acquaintance of its customers with numerical simulation.

When possible, the N'S^3 group proposed to use their advanced tools in the framework of on-going contracts dealing with CFD simulation (e.g., ventilation in an aircraft cabin, ASICA).

Projects focusing purely on advanced visualisation, but requiring no numerical simulations, were also achieved. The purpose was to increase confidence in numerical objects, before possibly starting numerical simulations aimed at improving them. Correspondingly, the results obtained for the AéroConstellation A380 assembly plant virtual mock-up opened discussions for a work on the simulation of the AIRBUS painting-hall ventilation.

The N'S^3 group adopted the same progressive approach for collaborative tools. A project was launched with a multi-site Airbus group to validate the ergonomics of the N'S^3 solution and the N'S3 workflow proposed to shorten the validation cycle of results.The first results gave the N'S^3 group the opportunity to prepare working with one of the Airbus subcontractor involved in this field.
Thanks to the above activities and results, the N'S^3 group can now continue on a stronger basis to fulfil its objectives, which are to take advantage of CERFACS know-how for developing new activities toward new customers.

2 Numerical simulation projects

2.1 Aircraft Cabin Heating Ventilation and Air Conditioning (P. Moinat, G. Jonville)

In the frame of the ASICA project, CERFACS' contribution was to provide numerical models to analyse criteria of comfort and health in an aircraft cabin. When the industrial partner did choose a commercial solver to develop these models, the project was transferred to the N'S^3 group, who took in charge its realization but worked in collaboration with the CFD team for expertise.
The aim of the ASICA project was to enhance cabin air quality through Environmental Control Systems (ECS) improvement. Cabin air quality in civil aircraft becomes more important due to longer flights, higher flight levels, more passengers per aircraft and higher recirculated air rates. It is important to maintain a high standard and to further improve cabin air quality to meet future requirements and in order to avoid passenger and crew complaints.
The numerical simulation of Heating Ventilation and Air Conditioning (HVAC) in aircraft cabin has been realised by the N'S^3 group. A CFD model was developed using the structured multi-block flow solver Numeca/FineTurbo. In the ventilation domain, the Mach number regime is low. A density-based formulation was applied, and a preconditioning method based on pseudo compressibility approach was used to handle low speed and incompressible flows. Steady computations were performed with a k-epsilon turbulence model in several operation points of the ventilation system. Adiabatic and heated passenger model cases were investigated. The convection and diffusion of the heat generated by passengers were simulated and modelled by a heat flux imposed on the skin.
A high quality structured mesh was required to capture the fine structures of the flow. The convergence of the computations is becoming slow when all heat loads are activated, due to the unsteady tendency of physical phenomena. To reduce the cost of the computations, the Full-Multi-Grid technique was used with four grid levels. The validation of the model was realised thanks to physical measurements obtained during the project in a real mock-up of a representative cabin section with mannequins. Experimental and numerical results were compared and both improved. The CFD techniques and tools helped in the development of the cabin mock-up during the project. Validations showed that the model could be used as a predictive tool for preliminary design purpose. A practical industrial use of CFD for ventilation design is foreseen.

The capability of the CFD simulations to capture the process of diffusion of a pollutant in a ventilated cabin was also evaluated (see Fig. xi in the appendix). Normally, thanks to the efficient filters placed in the ECS, only very small quantities of pollutants enter the cabin through the air supply. In such conditions, the passive scalar approximation remains valid. A multi-species approach is however required if higher concentrations contaminate the cabin, for example from a localized source. In any cases, one is interested in the time-scale information related to the ventilation efficiency, e.g. the time required for a pollutant to reach a given location in a room, the time required to remove all pollutants from a room, the time a pollutant will stay with a significant concentration at a given location (and identification of the stagnation regions). It was shown that the CFD approach is able to provide these data.

In the frame of this project, N'S^3 group also provided his industrial partners with collaborative review stations. The objective was to use video-conferencing between the 3 partners as a support for their collaboration in the project. N'S^3 group organized this task, defined the networking solution and performed the installation (the configuration of the 3 stations on the 3 sites and their maintenance was sub-contracted to Vircinity IT Consulting Gmbh).

The system has been quite intensively used to complete the specifications of the experimental conditions and to solve several misunderstandings; the shared visualisation functionality was used to present and discuss the CFD results. The system was also used to review the progress of N'S^3-group work, and to define the templates of numerical simulation summaries and of results presentation.

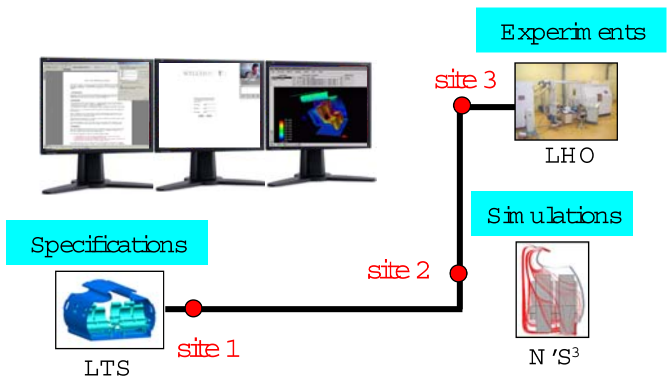

Figure 2.1: Multisite collaborative review between N'S^3 group and its industrial partners thanks to the N'S3 solution

2.2 Flow Field around a Hypersonic Missile (G. Jonville, consultant D. Darracq)

During the preceding period, the CFD team validated the NSMB code to compute the flow around complex 3D geometries in hypersonic flight conditions, assuming the gas to be perfect or considering the gas to be real. For real-gas effects, the code was adapted to predict flows at chemical and thermal equilibrium based on Park's model.

In 2002, the N'S^3 group applied these validated algorithms by using NSMB code to carry out a numerical investigation of the flow field around a hypersonic forebody missile (see Fig. xii in the appendix). The goal was to optimise the design of the missile and to compute the aerodynamic field for aero-optic distortion concerns.

Three kinds of structured multi-block meshes were generated, depending on the free-stream Mach number. Adapted numerical schemes, specific physical modelling of turbulence, and computational strategies, were selected to perform simulations for several hypersonic flight conditions and, depending on the case, with or without real-gas effects. In a first step, a 2D parametric study was realised by computing several configurations to quantify the effect of the nose-tip shape and of the flight conditions on the aerodynamic field. In a second step, 3D numerical simulations were performed for several shapes, with two nose-tip shapes and two optic-window shapes, for several flight scenarios.

The parametric results and the comparison of the aerodynamic fields around different 3D geometries allowed to identify the most favourable shape to reduce the shock-wave intensity and to decrease the temperature over the optic window. The computed aerodynamic field around this optimised shape was provided as input data for an optic study to deduce the optic distortion above the window.

2.3 Aerodynamic Expertise on a Sound Damping Facility (P. Moinat, G. Jonville, consultant T. Schönfeld

The N'S^3 group provided aerodynamics expertise on a future sound-damping facility. A Ground Run-up Enclosure is intended to absorb the sound or deflect its propagation, in order to significantly reduce the noise pollution in the neighborhood. The design of the facility is therefore mainly driven by acoustic concerns, and also additionally by aerodynamic constraints. To check the engines, good operating conditions are required, without any blockage of the upstream air or perturbation of the outflow-jet due to the enclosure. The N'S^3 group provided the appropriate expertise in aerodynamics and CFD to analyze proposals and to recommend an optimized solution.

3 Virtual reality projects

F. Crouzet, P. Moinat, G. Jonville, consultant C. Garrigue

Relying on its experience in scientific visualization using an advanced stereoscopic visualisation equipment, the N'S^3 group has developed a consulting activity in 3D computer graphics and advanced visualisation.

The N'S^3 group Reality CentreTM is an active stereoscopic visualization facility (see Fig. xiii in the appendix) equipped with

- Sgi Onyx2 computer with 2 Infinite 2 graphic pipes;
- $4m1.2m$ flat screen;
- 3 Barco 1209 CRT projectors with an optical mirror system enabling rear projection;
- Stereographics Crystal Eyes active glasses + E2 emitter for synchronization;
- Flock of Bird tracking system.

Two software's offering 3D stereoscopic projection capabilities are used for scientific visualizations: Ensight Gold from CEI, and Covise from Vircinity.
Apart from the N'S^3 group, several CERFACS teams used the advanced visualization centre:

- The Mercator group for 3D visualizations of the Gulf Stream vortices;
- The Algo team for 3D visualizations of homotopic deviation;
- The CFD team for the presentation of its results to various partners..

The stereoscopic 3D visualization on a large display facilitates the analysis of complex data by the expert. Such an advanced visualization system is also very helpful to enhance the communication of the results:

- images facilitate understanding, and therefore multidisciplinary collaboration;
- impressive visualizations have a strong impact and add value to the results.

These benefits are however not limited to scientific visualization, but can be exploited to optimise industrial-design processes and, ultimately, the quality of products:

- visualization helps detecting design errors early in the design cycle;
- visualization facilitates the multidisciplinary exchange and the integration of the constraints due to the product environment.

As part of its technology transfer objectives, the N'S^3 group devoted efforts to promote these possibilities to targeted industries, including several Airbus services.

In this frame, the N'S^3 group has been involved in the exploitation of a virtual mock-up of the A380 assembly site (the STAR project). The N'S^3 group assisted Airbus in this realization by contributing to the specifications of the virtual mock-up and continuously supervising its development (see Fig. xiv in the appendix). In addition, the N'S^3 group took the lead of several complementary contributions to this virtual mock-up: the gas station, the energy production unit, the landscaping, roads and parking lots, the fences, gates and guards posts.
After delivery of the new assembly site, the N'S^3 group foresees that the virtual mock-up can continue to be exploited, in particular to support the operation and the maintenance of the site. This exploitation may involve numerical simulation studies.

The N'S^3 group also assisted Airbus Communication to rationalize the production and the use of the 3D computer graphics. N'S^3 group made a review of Airbus Communication subcontractors in order to draw a clear picture of their competencies and to facilitate the choice of the provider for each needs in 3D graphics. In addition, N'S^3 group helped Airbus to define the procedure of supplying 3D CAD data to the 3D computer graphics subcontractors. The objective is to minimize the work of integration and the cost of the realizations.

Another project requiring sophisticated communication has been the A380 ”Grand Itinéraire” road between Langon and Toulouse. The N'S^3 group provided a 3D numerical mock-up, allowing to visualize the impressive lorry carrying the Airbus A380 sections when crossing two villages along this road. The virtual mock-up included:

- the 3D model of the road and houses along the road;
- photo-realistic textures applied on the houses fronts;
- the 3D model of the lorry and its load;
- the complex trajectory of the lorry parts along the road obtained from a separate study.

4 Development of collaborative working solutions

M. Larive

The N'S^3 solution is a computer supported collaborative working tool designed to ease the co-operation between remote partners in the context of numerical simulations projects. In its current state it is not targeting the desktop work place of the engineer, but is designed to replace a real meeting room in a distributed working environment. The N'S^3 solution allows the user to exploit all the classical conference tools as the audio/video system, the sharing applications, the whiteboard and the chat, but also to co-visualize and co-manipulate 3-dimensional data with his partners.

The N'S^3 solution is designed to be of very intuitive use: most of the functionalities can be activated with simple mouse clicks. A particular effort was also made to develop a clear ergonomic interface. The strategy is to use three monitors. Each has a specific role. The central screen contains the tools for controlling the conference. On the left screen, the usual office applications can be shared for interactive and collaborative editing. The right screen is devoted to the 3D co-visualization.

The specificity of the N'S^3 solution is the possibility for the user to :

- launch the presentation of his numerical simulation results directly out of PowerPoint;
- cut and paste a snapshot of the 3D data onto the whiteboard and add comments;
- save the whiteboard content as a basis for the minutes.

In order to permit these processes, developments in software adaptation and integration were realised. The integrated software are :

- IBM for the audio/video conferencing customized with Java development;
- Microsoft for application sharing, whiteboard and chat, encapsulated with C++ development;
- Covise, the N'S^3 collaborative visualisation software for numerical simulation 3D data.

All these applications are communicating via N'S^3 scripts and applets, which manage the roles and the actions of each of them.

For an N'S^3 meeting, the user needs only to :

1. Define a date and an agenda, as for a normal meeting;
2. Prepare the documents to be presented, as for a normal meeting;
3. Prepare his 3D data by converting them via the N'S^3 solution, transfer the data from the user system to the N'S^3 solution via a USB mobile hard disk in order to keep the N'S^3 solution clearly separated from the internal network;

4. Send his 3D data to his partners by email or by ftp, according to the data size;
5. Choose a virtual room for the meeting and define a password;
6. Host a session and manage the guest coming;
7. co-visualize and co-manipulate the documents.

The benefits obtained from the use of the N'S^3 solution are clear:

- Virtual meetings can be planned quicker and more frequently;
- Co-manipulating of the simulations results by sharing visualizations;
- Easier comprehension by commenting snapshots of specified viewpoints of the results;
- Shortening delays to reach final objectives;
- More efficient work.

6

Computer Support Group

1 Introduction

Nicolas Monnier

1.1 Key responsibilities

Key responsibilities of CERFACS' "Computer Support Group" are :

- To define CERFACS' Computer and Network architectures and perspectives for their upgrade and evolution;
- To provide, integrate and maintain all necessary and selected CERFACS' hardware and software solutions;
- To address CERFACS teams' needs with integrated solutions and services;
- To assist researchers, providing them technical and application expertise including assistance with programming and optimisation;
- To spread all necessary practical information advising CERFACS' users in their main areas of interest.

This support activity is the responsability of a five people team.

1.2 General strategy

General strategy is :

- Listening to the users' needs, federating them to benefit from scaling factors;
- With the help of HPCN suppliers, allow CERFACS' researchers to work in an up-to-date software and hardware HPCN environment (Storage capacities, Computing power, Post-processing and Networking);
- Ensure developments portability through the access to a wide range of architectures;
- Establish partnership for accessibility to high-end configurations.

2 Architecture and Actions.

Isabelle d'Ast, Gerard Dejean, Fabrice Fleury, Patrick Laporte

2.1 CERFACS' computing resources (As of Dec 03).

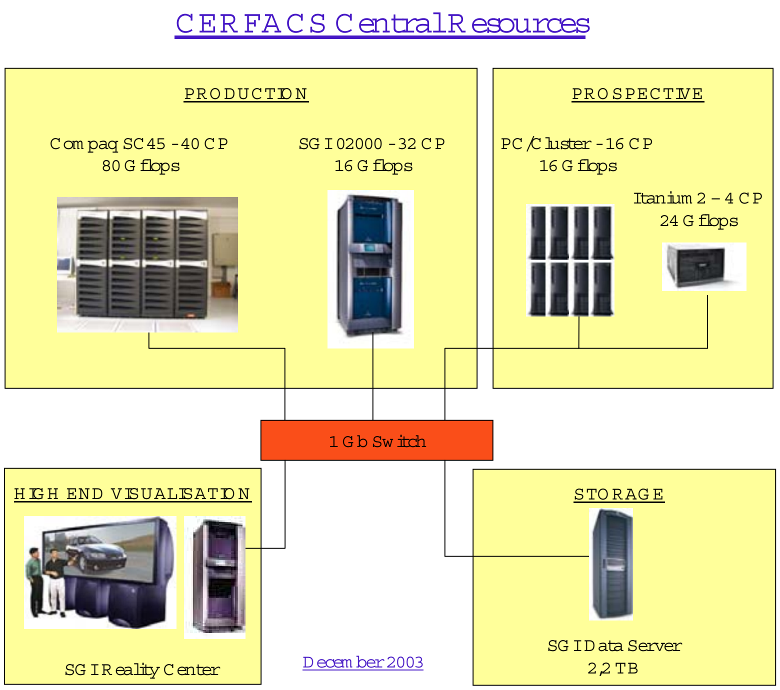

Figure 2.1: CERFACS' computing resources

During the period CERFACS' computer resources have seen three main improvements :

- Computing power : 2.5 times faster with the HP Alpha-Server upgrade : from 32 to 80 GFlops peak performance in 2002;
- Network Bandwidth : 10 times larger with a 1 Gb/sec backbone and 100 Mb switched network in 2003;
- New prospective hardware : Intel Itanium Servers.

2.2 Software environment and Support.

CERFACS' software environment covers three domains :

- Scientific development tools : CERFACS' users need a whole array of tools which allow them to create, test, debug and exploit their computational simulations. In this frame, one looks for availability of a wide range of scientific tools (compilers, profilers, debuggers, scientifical libraries, and parallelization tools) and their associated documentation. The availability of several Operating Systems associated with their scientifical development environment guarantes portability of developments on a wide range of Unix machines;
- Job and data management tools : giving users a complete set of tools is not enough. One has to provide a job management environment on the central computers, including batch queues, rules of usage and accounting means to optimise global throughput of CERFACS' computers (LSF and PBS batch systems are currently in use). On the other hand, the "Computer Support Group" provides data backup / restore (Time Navigator);
- Dedicated applications servers : in addition to development and management tools, several dedicated application servers are essential to complete a high-level software environment. These application servers are either an extension of computing facilities (Visualization servers, Data Management Server, MatLab servers) or an integral part of CERFACS' infrastructure (Web servers, Mail server, printer server, NIS, ...).

2.3 Prospective on Itanium Servers

During the period the Group helped CERFACS' developpers to port their solvers on new Itanium architectures.

In 2002 a first Itanium server (IBM xseries 3300) was installed and the codes AVBP (CFD), CESC (EMC) and MUMPS (Algo) were ported on this server. Next, two configurations HP rx5670 (quadriprocessor Itanium2 McKinley 1Ghz, then quadriprocessor Itanium2 Madison 1,5 Ghz) completed the installation. As shown in the performance chart below (fig 1), Madison quadriprocessor outperforms one node of the Alphaserver (EV68 1Ghz quadriprocessor), and achieves performance which can be compared to the best superscalar chips and architecture available at the time.

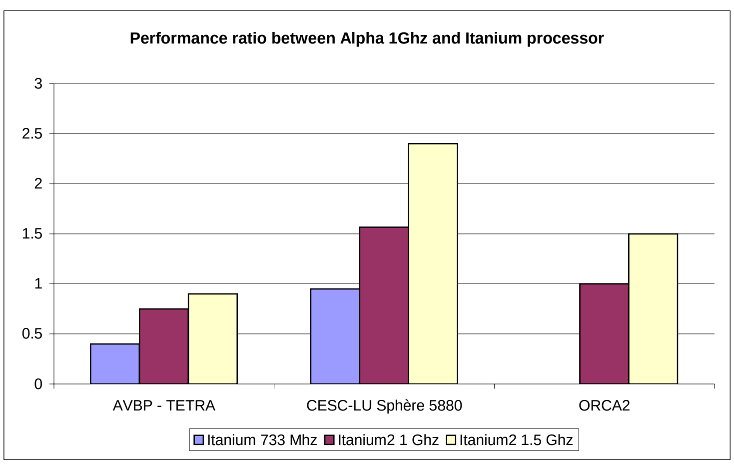

Figure 2.2: Performance ration between Alpha 1 Ghz and Itanium Processor

ORCA2 is 1.5 times faster on a quadriprocessor Itanium2 1.5 Ghz than on a quadriprocessor Alpha EV68 1Ghz (see Fig. 2.2).

2.4 Prospective on grid computing

Two testbeds have been prepared during the period, to better assess the performance of grid computing technologies.

The first one allowed to interconnect two computers, one at CERFACS and one at ID-IMAG, through Globus toolkit, and to launch runs from one computer to the other. The second one merged CERFACS' and LAAS' clusters into one single grid, allowing a parallel application to run without additional burden on either resource center.

2.5 Remote visualisation

The continual increase in processing power available at national computing centers allows researchers to run more complex numerical simulations and to obtain more accurate results. However, increase in complexity and accuracy leads to huge results files that are difficult to process : management of many large pre- and post-processing files is now a major difficulty that slows the development of more realistic numerical simulations.

As an example it may take between one and two days to transfer results files from CINES to CERFACS. A remote visualisation was developed with CINES, where visualisation is done on CINES visualisation server and remotly displayed on a local CERFACS' client, more than 200 km away. In this way, post-processing can be done through the network without transfering any detailed data but only compressed images (see also Sec. 2.4 in the CFD chapter).

Appendix

Color illustrations

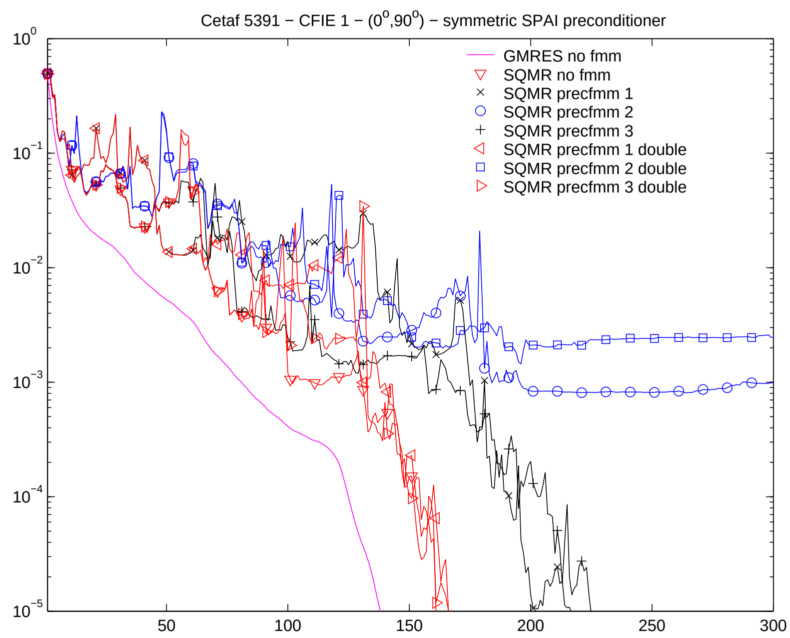

Figure iii: Convergence behaviour of GMRES and SQMR with various fast multipole calcultations.

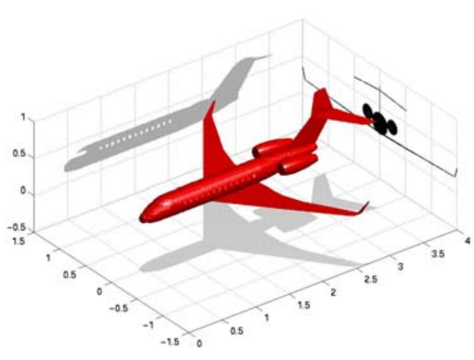

(a) Exact geometry

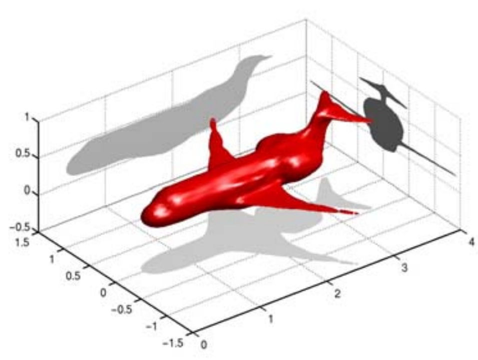

(b) Reconstructed geometry

Figure iv: Reconstruction of an airplane

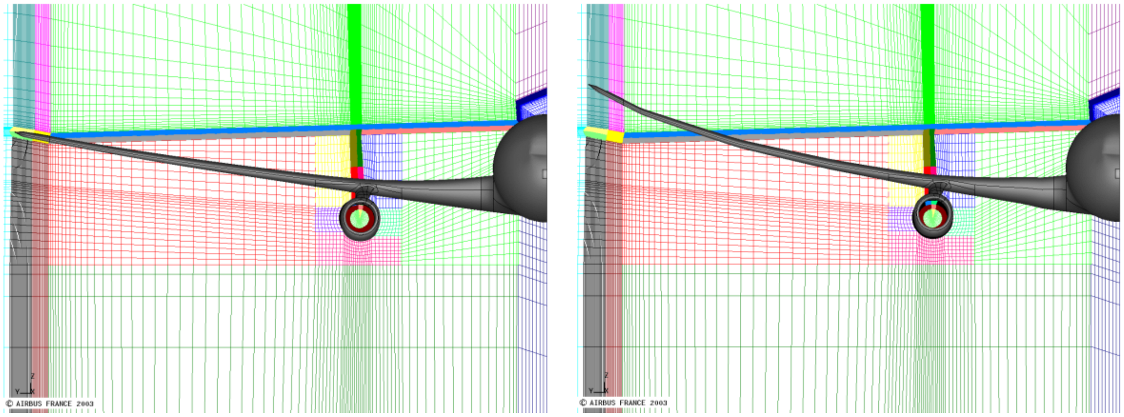

Figure v: Shape deformation of a structural mode

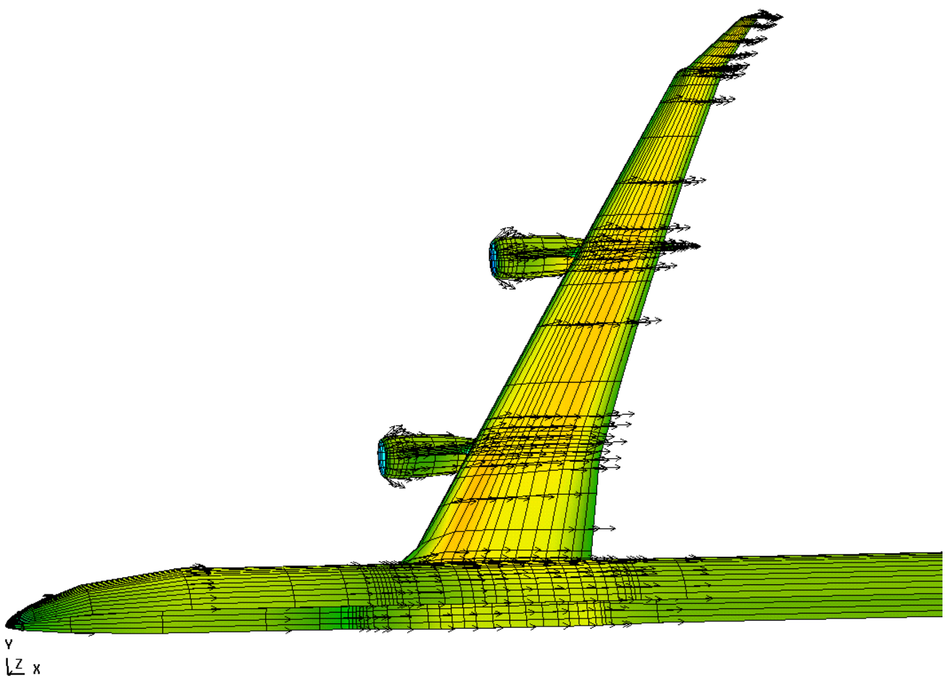

Figure vi: A340 MSR1 configuration.

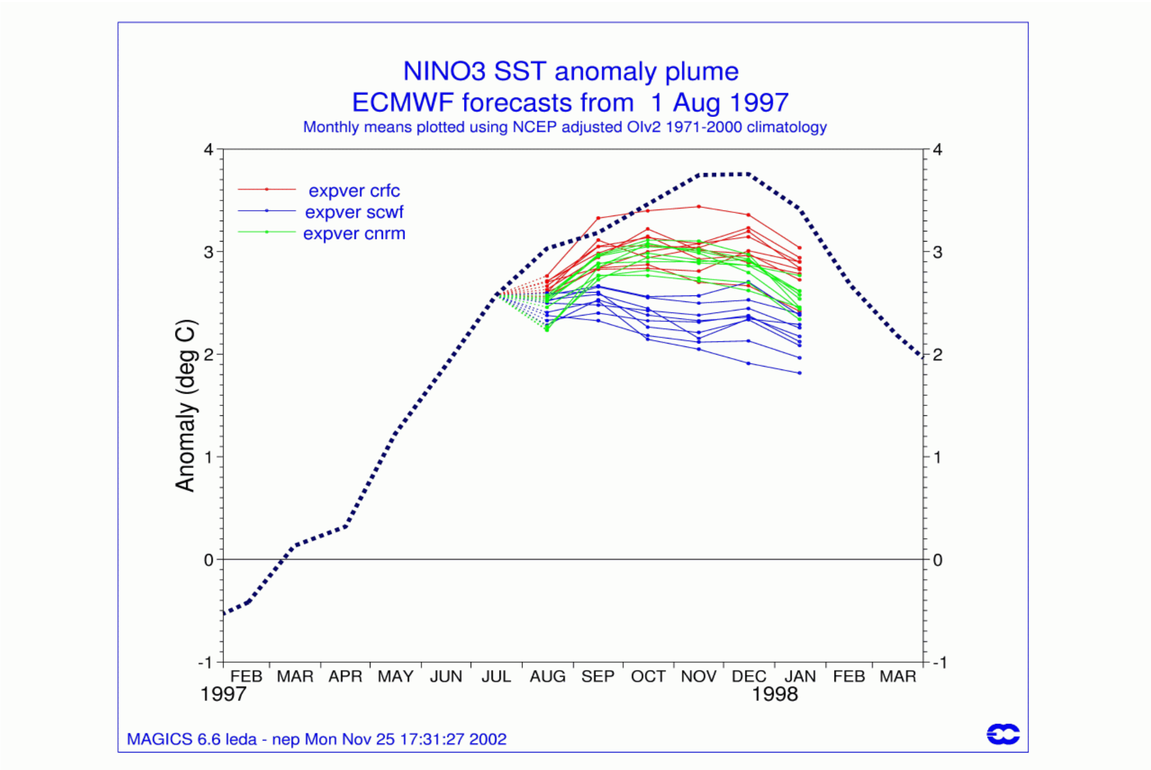

Figure vii: CERFACS prediction of the Niño3 temperature anomaly peak of late 1997 (in red) along with other models results.

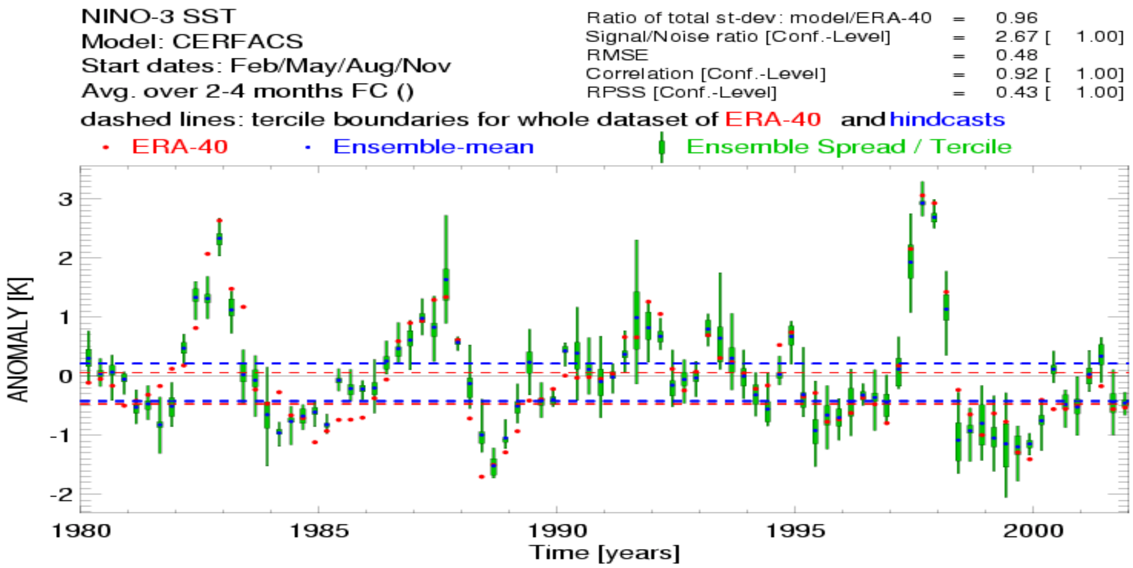

Figure viii: Seasonal prediction one month in advance of Niño3 and season-averaged indices of surface temperature, as produced by the CERFACS system.

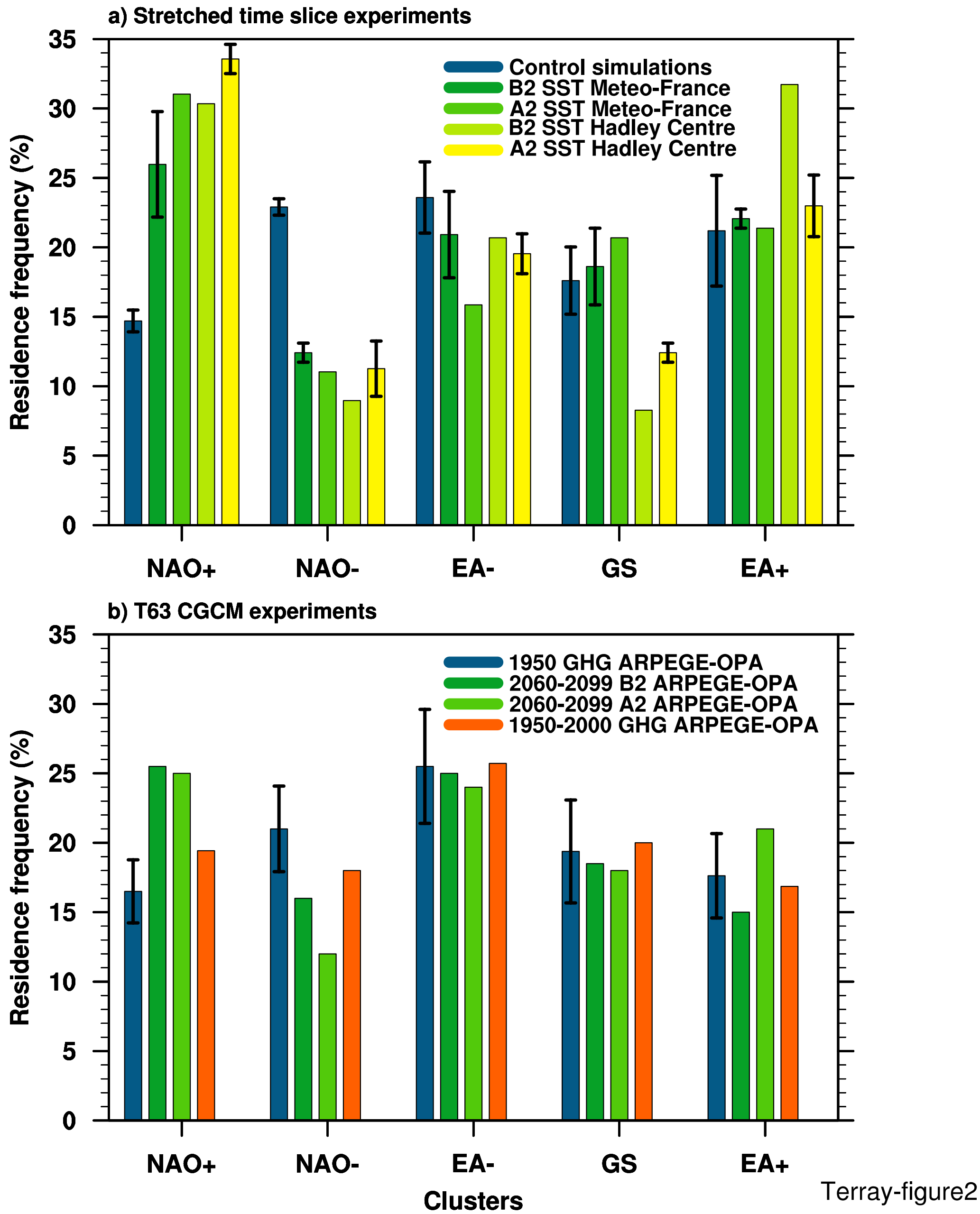

Figure ix: **(a)** Changes in regime residence frequency (in %) between the present climate and the four time-slice scenarios of the late 21st century as simulated by the variable resolution ARPEGE AGCM. **(b)** Changes in regime residence frequency (in %) between the control integration (GHG fixed at their 1950 values), the present and future climate (given by the 1950-2000 and 2060-2099 periods of the two transient scenarios, respectively) as simulated by the ARPEGE-OPA CGCM. The black arrows indicate the range of uncertainty due to internal atmospheric variability as given by one standard deviation of the within-ensemble variability.

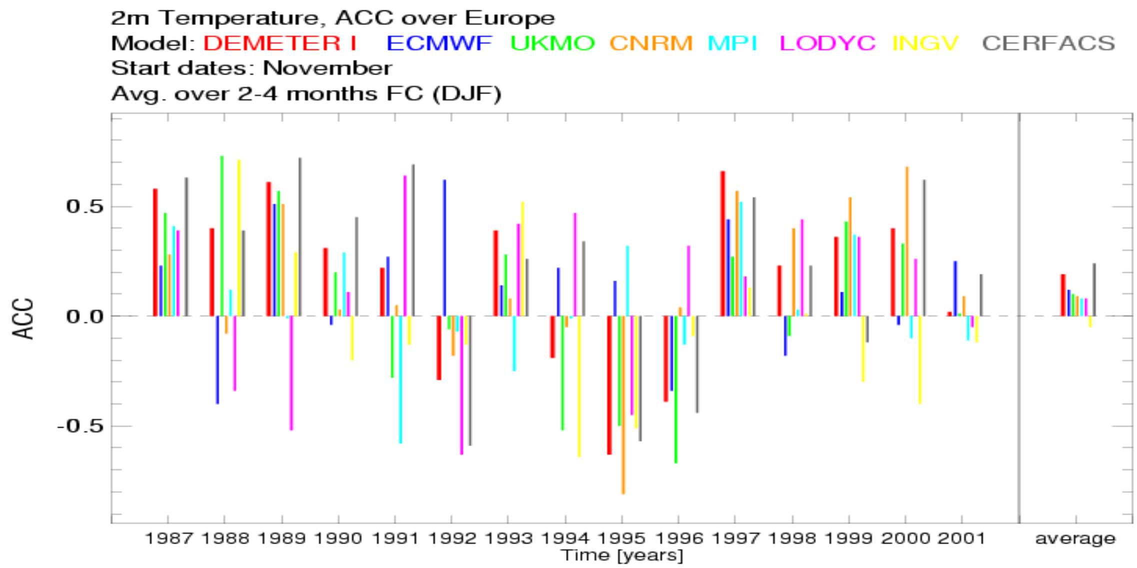

Figure x: Ranked Probability Skill Scores of winter temperature predictions over Europe one month in advance; CERFACS is in black.

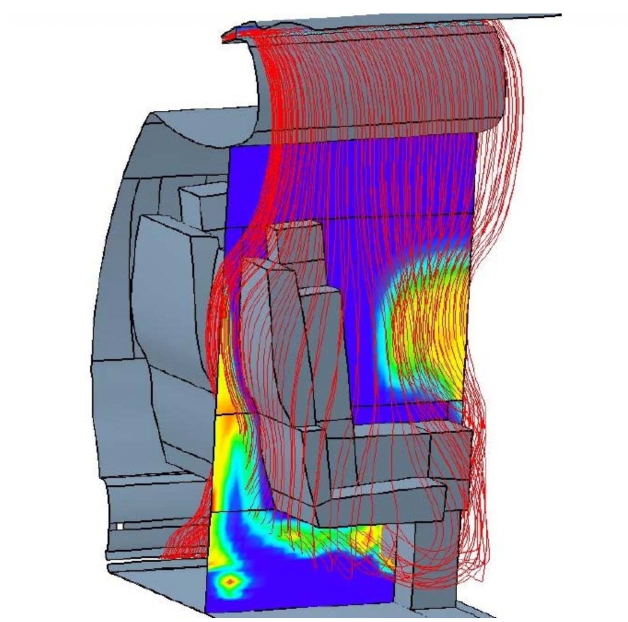

Figure xi: Path and concentration of lagrangian particles released through the air supply

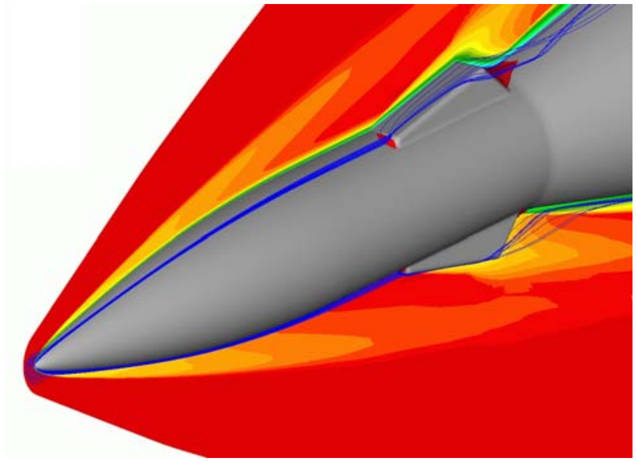

Figure xii: Flow simulation around a hypersonic missile - Mach number field

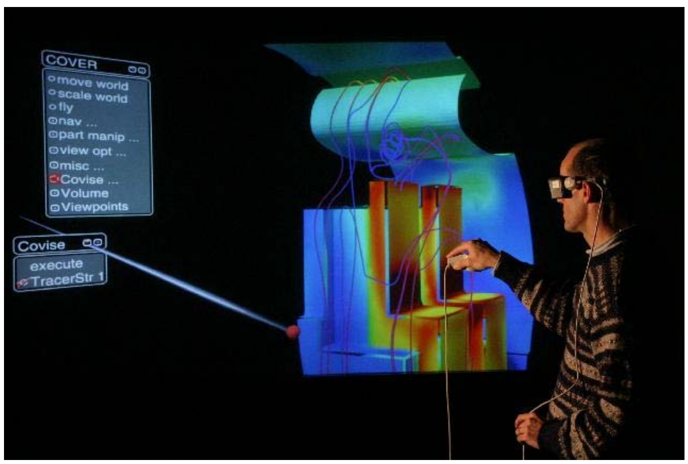

Figure xiii: 3D visualization of CFD results in the N'S^3 group Reality Centre

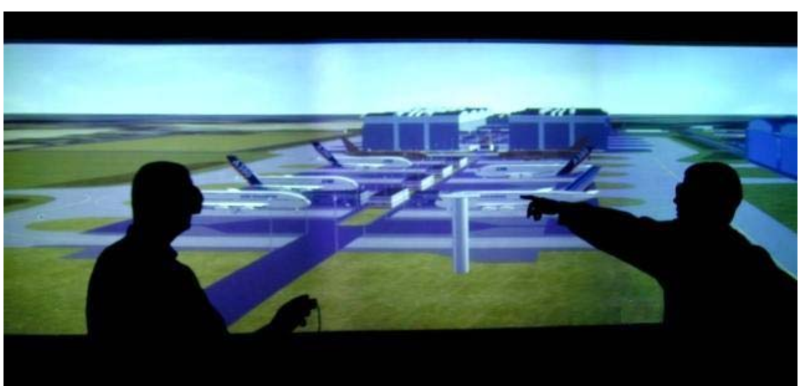

Figure xiv: Visit of the Airbus STAR virtual mock-up